$CD8^+$ T CELLS ARE IMPAIRED DURING VIRAL ACUTE RESPIRATORY INFECTION BY COORDINATED INHIBITORY PATHWAYS

By

John Joseph Erickson

Dissertation

Submitted to the Faculty of the

Graduate School of Vanderbilt University

in partial fulfillment of the requirements

for the degree of

DOCTOR OF PHILOSOPHY

in

Microbiology and Immunology

December, 2013

Nashville, Tennessee

Approved:

Sebastian Joyce

James Crowe

Terry Dermody

R. Stokes Peebles

John Williams

To my wonderful wife Lauren,

Your love and support are blessings that know no bounds

ACKNOWLEDGEMENTS

This work was financially supported by Public Health Service grants AI-85062 and AI-082417 from the National Institute of Allergy and Infectious Diseases, and T32 GM-007347 for the Vanderbilt Medical Scientist Training Program. Additional support was provided by the Elizabeth B. Lamb Center for Pediatric Research and a Dissertation Enhancement Grant from the Vanderbilt University Graduate School. The Vanderbilt Medical Center Flow Cytometry Shared Resource is supported by the Vanderbilt Ingram Cancer Center (NIH P30 CA-68485) and the Vanderbilt Digestive Disease Research Center (NIH DK-58404). I thank all these funding sources for their support, without which this work would not have been possible.

The pronoun “we” is used throughout the three data chapters of this thesis (Chapters II, III, IV) to reflect the collegial and collaborative nature of the work I have been privileged to engage in throughout my graduate students. While I performed the majority of the experiments described hereafter, several individuals provided technical assistance, performed data analysis or contributed scientifically to the work. I acknowledge these individuals with extreme gratitude in the coming pages. The introductory and concluding chapters utilize the pronoun “I”, as these sections contain my own thoughts and ideas. Of course, these ideas are based on the work of those that came before me and I acknowledge the great work of the giants upon whose shoulders I attempt to stand.

I must first express my deep and sincere thanks to my mentor, John Williams. John has fostered my development as a scientist since the first day I walked into his office. He is an exemplary teacher and an enthusiastic mentor. His enthusiasm for science is palpable, contagious and always a source of motivation. John allowed me the freedom to pursue essentially any project I wanted, a task that at first seemed daunting

when considering the broad fields of virology and immunology. I ultimately settled on a project studying $CD8^+$ T cells. John never batted an eye at this decision and encouraged me to read the literature and talk to the experts at Vanderbilt to learn the techniques to study these cells. I do not know of many people willing to take such a chance on a new project and I thank him for allowing me to pursue this. In such a way, my graduate career has taken the course favored by Robert Frost, down the road less-traveled, but it has paid dividends to my scientific training and none of it would have been possible without the constant support of John Williams. Mentor, teacher, and friend, I will always reflect on my time in his lab with gratitude and contentment.

Training in the Williams laboratory has been exciting and fun. John has assembled an excellent and diverse team and it has been a pleasure to work with them on a daily basis. Each laboratory member has contributed to my scientific development and I thank them for their friendship, scientific advice, critiques, and encouragement. I thank Sharon Tollefson, master of all things virology, for sharing her wisdom and teaching me everything I know about viral culture. I especially thank her for never saying "no" when I ask her to perform titrations for "just one more experiment." I thank Monika Johnson for her help with RT-PCR and her constant support of my science. I thank Drew Hastings for assistance with animal experiments, scientific guidance and most of all his friendship and daily discussions of all things science and non-science. Additionally, Drew mapped the epitopes in wildtype mice that I use frequently in my studies. I also thank Jennifer Schuster for her expertise on clinical infectious disease, knowledge of HMPV epidemiology and friendship, I extend special thanks to former lab member Reagan Cox for her scientific mentorship, guidance, friendship and perfect example of hard work and dedication to science.

At the beginning of my graduate career I knew what a T cell was but I had no idea how to study them. I extend my deepest gratitude to Dr. Michael Rock and Sandra

Yoder for getting me started on this adventure. Without their support and guidance I would have floundered. I especially thank Sandy for teaching me much of what she knows about the art of flow cytometry. I also thank my committee chair Dr. Sebastian Joyce, who not only provided mice and reagents, but also mentored me early during graduate school and challenged me to be the best, most rigorous scientist possible. From his lab, I thank Charles Spencer for providing mice used in my studies and for teaching me mouse irradiation. Also, my deepest thanks go to Pavlo Gilchuk, who has been my partner in crime in studying $CD8^+$ T cells. His scientific advice has been absolutely critical to my career and helped guide me during my graduate studies. He unselfishly put my needs ahead of his own on several occasions. No one else in the world is capable of delivering a high quality tetramer in 48-hours with a smile on his face.

I thank the Department of Pathology, Microbiology and Immunology, the former Department of Microbiology and Immunology, and the Graduate Education Committee for the Graduate Program in Microbiology and Immunology for their dedication to training students. I would also like to thank the Boothby, Crowe, Denison, and Dermody labs for their help, reagents, and friendship. Special thanks go to Dr. Mark Boothby for collaboration and support of my growth as a scientist.

The Vanderbilt Medical Scientist Training Program made my training possible. I first thank Dr. Terry Dermody, program director and member of my thesis committee, for his constant scientific and career support, plus his unyielding commitment to mentoring and training the next generation of scientists. I have learned much from his excellent example of leadership. I also thank Assistant Director Larry Swift for his support and conversation at many MSTP events. In addition, I thank the MSTP support team, especially Mellissa Krasnove and Jim Bills, for their constant attention to detail and assistance during my time in the program. I also thank the Canby Robinson Society for supporting the Vanderbilt MSTP and my training.

I had the pleasure to work with great collaborators at Vanderbilt. I especially thank Kevin Weller, Dave Flaherty and Brittany Matlock in the Flow Cytometry Shared Resource for their assistance and advice with flow cytometry experiments. I thank Dr. Kelli Boyd and Mellissa Downing in the Translational Pathology Shared Resource for performing histopathology and slide analysis of stained mouse lungs. Much thanks also go to Drs. Joyce Johnson and Annette Kim for help with procuring and staining human pathology specimens for PD-1. Vicky Amann in the Genome Science Resource was invaluable for her guidance with microarray experimental design and execution. Finally, I thank Drs. Yu Shyr and Pengcheng Lu for extensive data analysis and statistical support for microarray experiments.

My thesis committee has been invaluable for steering my graduate studies. I thank Dr. Sebastian Joyce, committee chair, for his advice, encouragement and the rigor he brought to my scientific endeavors. I thank Dr. James Crowe for thinking outside the box and pushing my science forward. I am grateful to Dr. Stokes Peebles for consistently engaging in my project and offering helpful suggestions. And again I thank Dr. Terry Dermody, who always asks penetrating questions at meetings and helped move my project to the next level. I also thank Dr. Chris Aiken for filling in on my committee at a critical juncture.

I would not be where I am today without the encouragement of Dr. Peter Zimmerman at Case Western Reserve University. Pete took a chance on a young undergraduate with no scientific background and gave me a place in his lab. His enthusiasm and support of a fellow swimmer launched my scientific career. He also encouraged me to apply to MSTP programs, of which I knew nothing when I started working in his lab. Dr. Brian Grimberg from his laboratory was the first to teach me about science and I am forever indebted to him for his training.

Equally important in my graduate school career are the people who have supported me outside of the laboratory. Late in June 2007, long before the arrival of 90% of my medical school class, ten naive, wet-behind-the-ears, young scientists arrived at Vanderbilt eager to start an eight-year training program. My MSTP class has been described as “unusually close”, but it is the friendships I have made with these individuals that I will value more than anything when I leave this phase of my training. Eric, Tanner, Brian, Liz, Frances and Caroline, I thank you for your friendship and support throughout this journey. “TDSG for life!”

I would not be where I am today without the love and support of my family. My mother has always encouraged me. She raised me to be the man that I am today and she always pushed me to better myself. My father inspired me to pursue a career in medicine through his own love of and devotion to the field. He has always been a steadfast encourager and has helped me in innumerable ways. I also give special thanks to the Preyss family for their love and support over the last six years.

To my wife, Lauren, I owe the greatest thanks of all. Day in and day out she has loved and encouraged me. About 10% of the time when experiments would work, she was there to celebrate with me and tell me how proud she was of me. The 90% of the time when experiments would fail or give uninterpretable results, she was even more supportive and helped me to stay positive. She has an unwavering spirit and the uncanny ability to help me see through problems and find new solutions. She daily put my needs ahead of her own, unselfishly loving me. She did all this while also completing her own graduate training as a physician assistant. She is a truly remarkable woman and I am a blessed man to call her my wife. No matter the highs and lows that the life of a physician-scientist will bring, I know she will always be there for me. I am so thankful that “God gave me you.”

TABLE OF CONTENTS

LIST OF TABLES

LIST OF FIGURES

LIST OF ABBREVIATIONS

Ab	Antibody
Ag	Antigen
ANOVA	Analysis of variance
APC	Antigen presenting cell
BSA	Bovine serum albumin
B7tg	HLA-B7**0702* transgenic mice
D^b	Murine MHC class I molecule H2-D^b
DC	Dendritic cell
ELISPOT	Enzyme-linked immunosorbent spot assay
FACS	Fluorescence-activated cell sorting
F	Fusion protein (HMPV)
FBS	Fetal bovine serum
HIV	Human immunodeficiency virus
Hr	Hour
HMPV	Human metapneumovirus
IAV	Influenza virus
IFNγ	Interferon-gamma
IL-#	Interleukin-#
K^b	Murine MHC class I molecule H2-K^b
LAG-3	Lymphocyte activation gene 3
LCMV	Lymphocytic choriomeningitis virus
LRI	Lower respiratory infection
M	Matrix protein (HMPV)

MIN	Minute
N	Nucleoprotein (N)
PBS	Phosphate-buffered saline
PCR	Polymerase chain reaction
PD-1	Programmed Death-1
PD-L1	Programmed Death Ligand-1
PD-L2	Programmed Death Ligand-2
PFU	Plaque forming unit
P.I.	Post-infection
PIV5	Parainfluenza virus 5
RSV	Human respiratory syncytial virus
RT	Room temperature
RT-PCR	Reverse transcription polymerase chain reaction
S.D.	Standard deviation
S.E.M.	Standard error of the mean
T_{CD8}	$CD8^+$ T cell
TCR	T cell receptor
TET	Tetramer (MHC class I)
TIM-3	T-cell immunoglobulin domain and mucin domain 3
TNF	Tumor necrosis factor alpha
VACV	Vaccinia virus
WT	Wildtype

CHAPTER I

Introduction

Thesis Overview

The experiments described in this thesis define mechanisms controlling $CD8^+$ T cell (T_{CD8}) impairment in the respiratory tract during viral acute lower respiratory infection (LRI). In Chapter I, I provide background on the purpose, phenotypes and functions of T_{CD8} during acute and chronic viral infections in the context of understanding potential mechanisms controlling impairment during viral LRI. In Chapter II, I present data defining the extent of lung T_{CD8} impairment during viral LRI and identify the first known mechanism controlling this process. I define T cell receptor (TCR) signaling as necessary for impairment and the inhibitory receptor programmed death-1 (PD-1) as a key mediator. Therapeutic blockade of PD-1 restores T_{CD8} effector functions and enhances viral clearance. I further show that the PD-1 pathway is activated in humans with severe viral LRI. In Chapter III, I explore whether PD-1 contributes to lung T_{CD8} impairment during reinfection by utilizing B cell deficient mice as well as a T cell vaccination strategy. In Chapter IV, I use global gene expression analysis to profile impaired lung T_{CD8}. From this work, I identify additional inhibitory receptors, including lymphocyte-activation gene 3 (LAG-3), that regulate lung T_{CD8} during LRI and can compensate for loss of PD-1 signaling. I show data defining an overlapping, redundant network of inhibitory receptors that limit T_{CD8} effector functions in the respiratory tract. In Chapter V, I summarize my thesis studies and offer future experiments for continuation of this work.

Viruses that Cause Acute Lower Respiratory Infection

Paramyxoviruses and HMPV Infection: The paramyxovirus family encompasses a diverse group of viruses that cause a variety of human diseases. Respiratory syncytial virus (RSV), parainfluenza virus (PIV) and human metapneumovirus (HMPV) are significant human pathogens that cause acute LRI. HMPV, the main focus of my studies, is a paramyxovirus identified in 2001 that is a major cause of upper and lower respiratory tract infections in children and the immunocompromised worldwide (van den Hoogen et al., 2001b; Williams et al., 2004; Williams et al., 2006). Paramyxoviruses are enveloped, negative-sense, single-stranded RNA viruses that cause significant bronchiolitis and pneumonia in infancy and early childhood (Hall, 2001). HMPV causes hospitalization in previously healthy infants or high-risk groups at rates similar to other respiratory viruses (Deffrasnes et al., 2007; Edwards et al., 2013; Williams et al., 2004). These viruses cause indistinguishable clinical disease and represent a significant health threat (Deffrasnes et al., 2007; Langley and Anderson, 2011; Pavia, 2011; Williams et al., 2004).

Despite the frequency of infection with these viruses and minimal antigenic drift, protective immunity is poorly established, as individuals can be repeatedly reinfected throughout life (Hall et al., 1991; Johnson et al., 1961; Kroll and Weinberg, 2011). This may be due to waning immunity in the respiratory tract in some cases, but reinfection is possible even at just a few weeks post-infection (Hall et al., 1991; Johnson et al., 1961). The proclivity of paramyxoviruses to cause serious disease in high-risk populations and also reinfect otherwise healthy individuals is likely due to their ability to evade the host immune response. There are several well-defined viral mechanisms for evading *innate* immunity. For example, many paramyxoviruses encode a V protein that targets signal transducer and activator of transcription (STAT) family members to inhibit type I

interferon production, a potent arm of the innate immune response (Horvath, 2004). Respiratory syncytial virus (RSV) encodes proteins NS1 and NS2, which not only inhibit STAT2 but also interfere with RIG-I, a sensor of viral RNA (Ling et al., 2009). However, innate immune evasion does not adequately explain the high frequency of reinfection.

The ability to reinfect individuals, plus the lack of effective vaccines against these viruses, suggest that *adaptive* immune responses in the respiratory tract are compromised. There is some evidence for this, but the precise mechanisms of impairment are not well understood. Measles virus, another paramyxovirus, causes lymphopenia and immunosuppression via FasL-mediated death of lymphocytes (Griffin, 2010), while RSV is thought to promote a T helper 2 (Th2)-biased cytokine response (e.g., IL-4 and IL-5), leading to ineffective immunity (Bueno et al., 2008). As discussed below, T_{CD8} are functionally impaired in the respiratory tract, but mechanisms governing this phenomenon are unknown.

Influenza virus: Influenza A virus (IAV) is member of the orthomyxovirus family and consists of a segmented, single-stranded, negative-sense RNA genome. Owing to its segmented genome, IAV can rapidly generate novel reassortant viruses that extend its host range to new populations lacking neutralizing antibodies directed against its surface hemagglutinin protein. Such is the case during pandemics like the recent H1N1 pandemic in 2009. Annually, IAV causes nearly half a million fatalities (WHO, 2012), making it a significant public health threat. Like paramyxoviruses, IAV also possesses well-defined mechanisms for evading innate immune responses (van de Sandt et al., 2012), but evidence for specific mechanisms governing adaptive immune evasion are sparse. The best evidence in humans comes from studies showing that T_{CD8} epitopes are under selective pressure (Berkhoff et al., 2005). However, this cannot be the case for all T cell epitopes, as many epitopes exist in crucial segments of viral structural

proteins that if mutated significantly reduce viral fitness (van de Sandt et al., 2012). Therefore, the severity of infections with novel pandemic strains, the ability of seasonal IAV strains to re-infect and an inconsistent annual vaccination all highlight that identification of IAV adaptive immunity evasion strategies are of utmost priority. Characterization of the mechanisms causing poor immunity to viral LRI is necessary to design effective therapeutics or novel vaccines against these viruses.

$CD8^+$ T Cells – Purpose, Activation and Function

T_{CD8} provide protective immunity against viruses, intracellular bacteria and tumors. They have the unique ability to react to pathogens by massive clonal expansion and differentiation into cytotoxic effector cells capable of homing to infected tissues to clear the infection. Their activation, differentiation and ultimate fate are tightly regulated to prevent bystander tissue damage to the host. Additionally, T_{CD8} can form long-lived memory cells that are rapidly reactivated and expanded to protect against the same pathogen if re-encountered. My thesis work is primarily concerned with the phenotype and function of T_{CD8} at the peak of respiratory virus infection, so I will first briefly explain the steps leading up to this point.

T cell responses to most acute infections occur in three stages: (1) intense clonal expansion and effector T cell differentiation, (2) contraction (death of most effectors via apoptosis) and (3) formation of long-lived memory cells (Figure 1-2A) (Kaech and Wherry, 2007). Pathogen-specific T_{CD8} begin as only 100-200 naïve precursors that then expand 10^4- to 10^5-fold (Blattman et al., 2002). Naïve T_{CD8} are primed by antigen presenting cells (APCs) in secondary lymphoid organs like the spleen and lymph nodes draining the site of infection (Zhang and Bevan, 2011). Dendritic cells (DCs) are the most efficient APC for priming T_{CD8} owing to their high expression of co-stimulatory ligands and efficient ability to migrate away from the site of infection to lymphoid tissues

where naïve T_{CD8} await. DCs load foreign peptides of 8-10 amino acids onto MHC class I molecules and present them at their cell surface. Naïve T_{CD8} recognize the peptide:MHC complex (i.e., Ag) via the TCR, which sends the first signals necessary for activation and proliferation. Signal two is delivered by CD28 on the T cell surface interacting with the costimulatory ligands CD80 and CD86 on the APC. CD28 induces signaling through the PI3K-Akt-mTOR pathway, which supplements TCR-mediated signaling through mTOR and MAPK pathways (Salmond et al., 2009). Without costimulation, T cells become anergic (i.e., in a state of unresponsiveness), a key mechanism ensuring maintenance of peripheral tolerance to prevent development of autoimmunity. Inflammatory cytokines provide the third signal necessary to fully differentiate and expand T_{CD8} (discussed later).

Activated T_{CD8} migrate to sites of infection where they recognize Ag presented by MHC class I molecules on the surface of infected cells (Figure 1-1). They possess lytic granules containing perforin and granzymes that are released upon Ag recognition to kill the infected cell. Perforin is a pore-forming molecule that is required for clearance of many viral infections (Sad et al., 1996), while granzymes are serine-proteases that activate cytoplasmic caspases to induce apoptosis (Hoves et al., 2010). T_{CD8} can also secrete a variety of cytokines, such as tumor necrosis factor alpha (TNF) and interferon-gamma (IFNγ) that recruit or activate other immune cells as well as cause cellular injury. Polyfunctional T_{CD8} that secrete IFNγ, TNF and IL-2 and rapidly proliferate upon Ag exposure represent the subset of cells best able to provide protective antiviral immunity (Betts et al., 2006). During acute viral LRI, T_{CD8} help clear the infection by elaboration of cytokines and direct lysis of infected cells (Bruder et al., 2006).

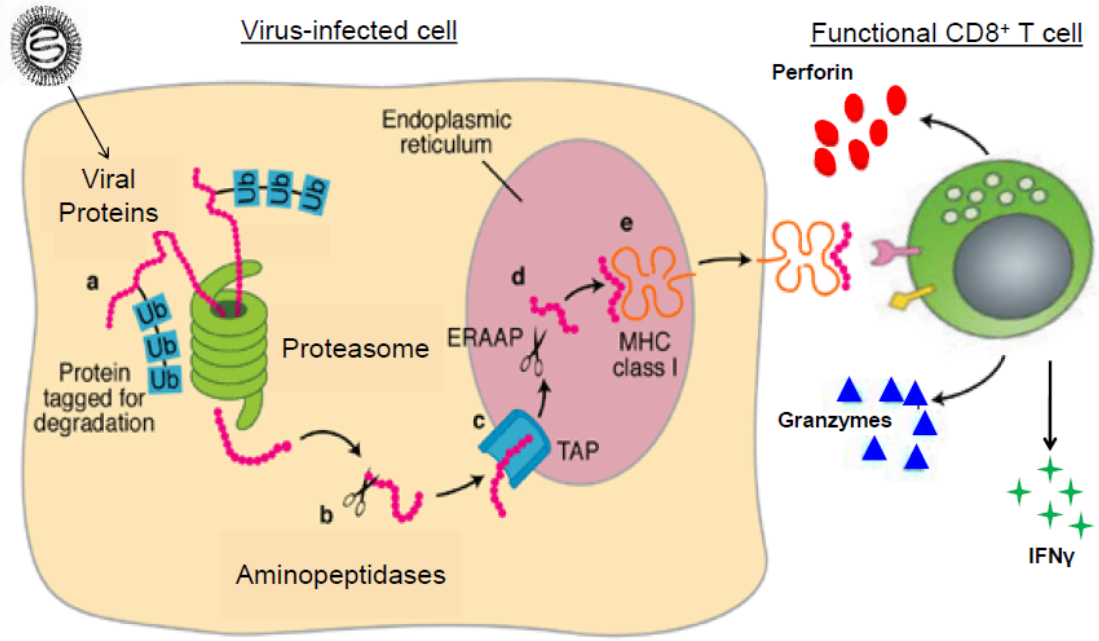

Figure 1-1: T_{CD8} recognition of infected cells and effector mechanisms. Misfolded viral proteins are ubiquitylated and then cleaved by the proteasomes into smaller peptides, followed by TAP-mediated transported into the ER. 8-10 amino acid peptides are loaded onto MHC class I molecules for presentation at the cell surface. T_{CD8} possess a unique T cell receptor (TCR) recognizing a specific antigenic peptide in the context of MHC class I, which leads to the release of perforin and granzyme via degranulation of preformed vesicles, ultimately leading to death of the infected cell.

CD8$^+$ T Cells – Impairment During Acute Viral LRI

Despite the contribution of T_{CD8} to respiratory virus clearance, additional evidence suggests that lung T_{CD8} are largely impaired in their ability to execute the effector functions mentioned previously. A landmark study published in 2002 by Chang and Braciale laid the groundwork for my thesis studies by describing T_{CD8} impairment during RSV infection in mice (Chang and Braciale, 2002). In this study, they performed parallel analysis of MHC-tetramer staining, which quantifies total Ag-specific T_{CD8}, with intracellular cytokine staining for IFNγ, which measures T_{CD8} effector function, to show that only a fraction of lung RSV-specific T_{CD8} in BALB/c mice are capable of responding to antigenic stimulation. This finding was corroborated by a study employing C57BL/6 mice demonstrating that both lung tissue and airway T_{CD8} were unresponsive during

RSV infection (Lukens et al., 2006). Similar results were also obtained during PIV-5 infection (Gray et al., 2005). In all three studies, neither spleen nor lymph node-resident virus-specific T_{CD8} were impaired. Additional analysis revealed that lung T_{CD8} also lose the ability to make TNF and lyse infected cells due to a reduced ability to mobilize lytic granules with decreased granzyme B content (Vallbracht et al., 2006). The results of these studies are summarized in Table 1-1.

Initially, Chang and Braciale showed that infection with an H2N2 strain of IAV resulted in fully functional lung T_{CD8} (Chang and Braciale, 2002), suggesting that pulmonary impairment may be paramyxovirus-specific. However, subsequent studies do not support this notion. First, RSV-specific genes with known immunomodulatory effects (NS1 and NS2) did not affect impairment (Kotelkin et al., 2006). Another group found that IAV infection did cause decreased cytotoxic ability of airway virus-specific T_{CD8} (Vallbracht et al., 2006). Additionally, intranasal infection with either H1N1 IAV or vaccinia virus (VACV) caused profound T_{CD8} impairment (DiNapoli et al., 2008). The specific molecular mechanisms governing T_{CD8} impairment during acute viral LRI are completely unknown and are therefore the topic of study for my thesis research.

Virus	Day	Functional T_{CD8} (%)	Outcome	Reference
RSV	8	47	Impairment	(Chang and Braciale, 2002)
RSV	21	58	Impairment	(Lukens et al., 2006)
PIV-5	12	46	Impairment	(Gray et al., 2005)
Influenza (H2N2)	8	>100	No Impairment	(Chang and Braciale, 2002)
Influenza (H1N1)	8	19	Impairment	(DiNapoli et al., 2008)

Table 1-1. Summary of lung T_{CD8} impairment during acute viral LRI. The percentage of functional T_{CD8} was calculated by dividing the percentage tetramer-positive $CD8^+$ T cells by the percentage IFNγ-positive $CD8^+$ T cells for a given virus-specific epitope.

$CD8^+$ T Cells – Effector versus Memory Phenotypes

Effector T_{CD8}: To assess what potentially goes awry with T_{CD8} during acute viral LRI, it is important to discuss what is known about effector and memory T_{CD8} differentiation in other settings. During most acute infections, functional, non-impaired effector T_{CD8} are generated that help clear the pathogen. This is not the case for chronic infections, which will be discussed later. Much of the literature describing T_{CD8} during acute infections involves the model mouse pathogen lymphocytic choriomeningitis virus (LCMV) or the intracellular bacteria *Listeria monocytogenes*. At the peak of the primary response to these pathogens, effector T_{CD8} are functionally and phenotypically heterogeneous (Figure 1-2A). The majority of these are short-lived effector cells (SLEC) that will undergo apoptosis once the infection is cleared, while a small percentage of memory precursor effector cells (MPEC) survive to become bona fide memory cells (Figure 1-2B) (Parish and Kaech, 2009). At the individual cell level, each naïve T_{CD8} is capable of differentiating into both effector and memory T_{CD8} populations (Gerlach et al., 2010). Some work suggests that clonal heterogeneity develops as early as the first cell division due to asymmetric distribution of the transcription factor T-bet (Chang et al., 2011). T-bet drives T helper 1 (Th1) $CD4^+$ T cell development and is also critical for effector T_{CD8} differentiation (Naito et al., 2011). Small increases in T-bet, even as low as two-fold, favor early SLEC development (Joshi et al., 2007).

Despite this very early T_{CD8} heterogeneity, later signals play a significant role in differentiation. For instance, TCR stimulation and cytokine signaling expand and enforce SLEC development. Effector T cells progressively lose memory potential and terminally differentiate in proportion to TCR signaling strength (Ahmed and Gray, 1996). IL-12 directly induces T-bet (Joshi et al., 2007) via the mTOR pathway (Rao et al., 2010) while IL-2 signaling drives effector differentiation and acquisition of cytolytic functions (Pipkin et al., 2010) via the transcriptional repressor Blimp-1 (Malek and Castro, 2010). Blimp-1

promotes SLEC development during acute infection and specifically upregulates granzyme B and perforin (Rutishauser et al., 2009). During IAV infection, it supports T_{CD8} migration to the lung through CCR5 expression (Kallies et al., 2009). Blimp-1 upregulates transcription factors associated with effector cell differentiation, such as T-bet and ID2, while inhibiting factors that promote memory development, such as Tcf-1 and Eomes (Kaech and Cui, 2012). Blimp-1 and Bcl-6 oppose one another at the transcriptional level, as Bcl-6 promotes memory differentiation (Crotty et al., 2010; Ichii et al., 2007; Ichii et al., 2002). Besides Blimp-1's role, Runx3, Notch2 and Wnt signaling all promote effector T_{CD8} functions (Cruz-Guilloty et al., 2009; Jeannet et al., 2010; Maekawa et al., 2008; Zhou et al., 2010). Additionally, other inflammatory signals, costimulation, immunomodulatory receptors and encounters with different APC subsets all shape the specific T_{CD8} response to an infection.

It is important to note that SLEC are a functional subset of T_{CD8} that play a key role in the elimination of infection with certain intracellular pathogens. They generally display enhanced cytolytic functions compared to MPEC due to greater perforin and granzyme levels and degranulation ability (Lefrancois and Obar, 2010). Large numbers of effectors are also important for controlling viral replication. The forces that drive them to differentiate to this state, however, result in a decreased lifespan due to enforced terminal differentiation. However, as discussed below, acquisition of an effector phenotype may actually be necessary for eventual T cell memory development, as all memory T_{CD8} at some point in their differentiation express the gene for granzyme B (Bannard et al., 2009).

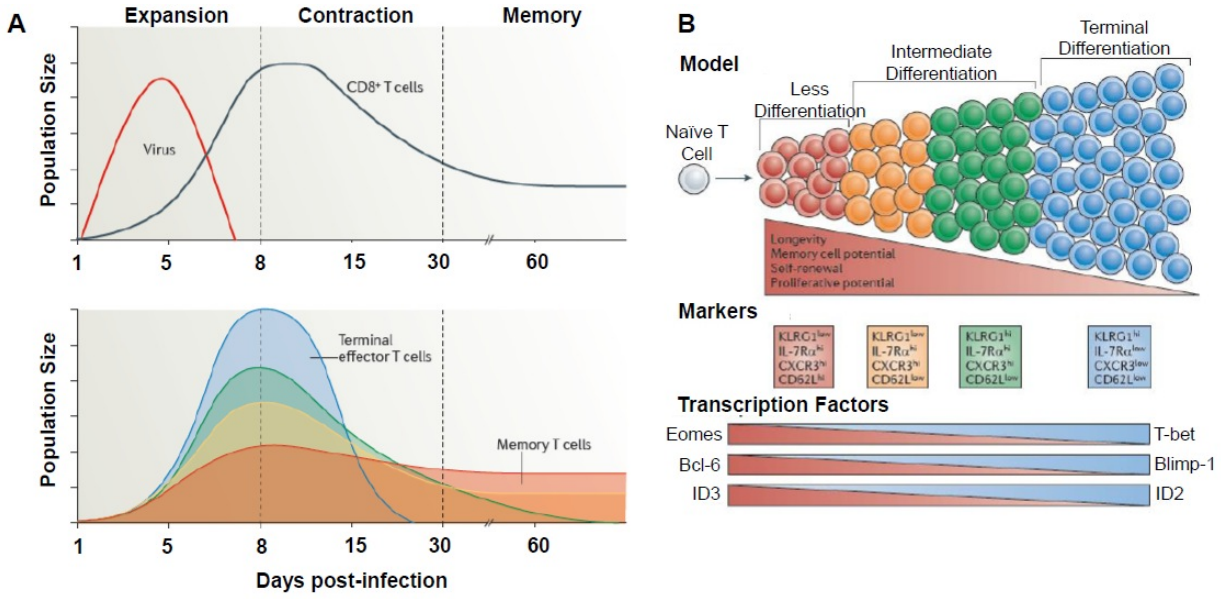

Figure 1-2. T_{CD8} heterogeneity during acute infections. (**A**) During an acute viral infection, Ag-specific T_{CD8} rapidly proliferate (expansion phase) and differentiate into cytotoxic T lymphocytes that kill infected cells. Most effector T_{CD8} then die (contraction phase). 5–10% survive and mature into memory T_{CD8} capable of rapid reactivation upon reinfection. (**B**) The T_{CD8} response at the peak of infection is heterogeneous, consisting of diverse cellular subsets based on differences in gene and protein expression, effector functions, migratory patterns, proliferative capacity and long-term fate. Terminal effector T cells (shown in blue) are KLRG1^{hi}IL-7R^{low}CD27^{low} and memory precursor cells (shown in red) are KLRG1^{low}IL-7R^{hi}CD27^{hi}. The functional and phenotypic state of each subset is governed by certain transcription factors. Eomes, Bcl-6 and ID3 all promote memory development, while their counterparts T-bet, Blimp-1 and ID2, respectively, drive effector differentiation. Adapted from (Kaech and Cui, 2012).

Memory T_{CD8}: After the clearance of an acute infection, most effector T_{CD8} die during the contraction phase, but some MPEC survive to become long-lived memory T cells that are multipotent, self-renewing and capable of rapid proliferation. Several models exist of how memory T_{CD8} develop, but using the SLEC/MPEC theory described above, both subsets develop early during infection and the resulting inflammatory milieu and strength of TCR signaling determine the fate commitment of each individual cell (Kaech and Wherry, 2007). In this model, SLEC are terminally differentiated, while MPEC retain the plasticity to become SLEC if they encounter persisting Ag or inflammation. Therefore, in this model, it is the strength of the inflammatory signals discussed previously that

determine the fate of memory T_{CD8}. As an example that I take advantage of later in my thesis work, during DC vaccination, where DCs rapidly present Ag and deliver co-stimulation to naïve T_{CD8} in the absence of overt inflammation, the majority of T_{CD8} become memory cells (Badovinac et al., 2005a). This pathway can be deflected by inflammation to produce more effector T_{CD8} (Pham et al., 2009).

Not surprisingly, since effector T cell differentiation is intimately tied to strength of TCR signaling (i.e., signal one), then blunting this pathway by either shortening the infection length or reducing the duration of stimulation leads to enhanced memory T_{CD8} development (Badovinac and Harty, 2007; Joshi et al., 2007). The intensity of signal two through the costimulatory receptors CD28, CD40, 4-1BB, ICOS and OX40 all impact the size of the effector and memory T cell populations. Of these, OX40 directly promotes the MPEC to memory cell transition (Mousavi et al., 2008). Additionally, 4-1BB signaling significantly impacts the size of the memory response to IAV infection (Bertram et al., 2002) and collective signaling through OX40 and 4-1BB during IAV priming imprints memory T_{CD8} with a capacity for re-expansion upon challenge (Hendriks et al., 2005). Signal three is delivered by inflammatory cytokines and also critically effects memory development. For a constant amount of Ag, increasing inflammatory signals (e.g., IFN and IL-12) deflect MPEC to SLEC development through the induction of T-bet (Joshi et al., 2007).

IL-7R is a marker for MPEC and later full-fledged memory cells. SLEC possess a KLRG1^{hi}IL-7R^{low} phenotype, while MPEC are KLRG1^{low}IL-7R^{hi}. While examination of these markers has yielded valuable insights during infection with model pathogens, they are not exclusive or universally true markers for memory formation. The frequency of IL7R and KLRG1 expression varies substantially between different infections or vaccination strategies. First, the expression of these markers can differ widely based upon proinflammatory cytokine expression (e.g., IL-12) as discussed previously (Joshi et

al., 2007). During IAV infection, the expression of IL-7R and KLRG1 were more closely linked with antigen encounter and did not reflect ability to form memory cells, especially as lung T_{CD8} were IL-7R^{hi}, IL-7R^{hi}CD62L^{hi} or IL7R^{hi}KLRG1^{lo}, suggesting a MPEC phenotype (Croom et al., 2011). Greater consistency for these markers in predicting memory potential during IAV infection was found in the draining LN, suggesting a unique phenotype exists for the front line T_{CD8} engaging infected cells in the respiratory tract. Additionally, direct comparison of Listeria infection to vesicular stomatitis virus (VSV) revealed T_{CD8} in the VSV-infected spleens expressed more IL-7R and less KLRG1 and this ratio could be reversed by administration of CpG oligonucleotides that induce IL-12 (Obar et al., 2011). Finally, during IAV infection, both KLRG1^{hi} and KLRGI1^{low} effectors develop and these subsets exhibit developmental plasticity through the SLEC and MPEC phenotypes (Ye et al., 2012). Thus, there is significant variability in the SLEC/MPEC paradigm and the utility of these definitions for lung T_{CD8} during respiratory virus infection is incompletely defined.

Once the transition from MPEC to memory cell is complete, different subsets of memory T_{CD8} form. These cells persist independently of TCR signaling and mainly depend on the cytokines IL-7 and IL-15 (Surh et al., 2006), which do not program T_{CD8} for memory generation, but rather provide survival signals (Hand et al., 2007; Sun et al., 2006). Effector memory (T_{EM}) cells, owing to their lack of LN homing receptors (e.g., CD62L^{lo}, CCR7^{lo}), exist outside of the lymphatic system and recirculate through potential portals of pathogen entry. In general, they respond rapidly but have reduced proliferative capacity. Central memory (T_{CM}) cells (CD62L^{hi}, CCR7^{hi}) persist mainly in LN, mount robust secondary responses and establish effector functions upon restimulation (Kaech and Wherry, 2007). More recently, resident memory (T_{RM}) cells (CD103^{hi}, CD69^{hi}, CD62L^{lo}, CD27^{lo}) have been described that are retained within previously infected tissues and do not recirculate (Kaech and Wherry, 2007). Repetitive boosting of

memory T_{CD8} augments the effector-like quality of resulting T_{EM} (Nolz and Harty, 2011; Wirth et al., 2010). The type of memory cell require for protection against a pathogen depends on the route of infection, replication kinetics and pathogenesis of the organism. For respiratory virus infections, local T_{EM} tend to be more protective than T_{CM} (Liang et al., 1994). T_{EM} persist in the lung for several months post-IAV or Sendai virus infections (Hogan et al., 2002; Hogan et al., 2001) and the lung environment itself maintains these cells in an activated state (i.e., independent of Ag) (Kohlmeier et al., 2007). However, circulating memory T_{CD8} also help with protection against IAV challenge by rapid recruitment in a CCR5-dependent manner (Kohlmeier et al., 2008) and reacquisition of effector functions through IFN signaling (Kohlmeier et al., 2010).

To summarize the background presented thus far, T_{CD8} possess diverse effector functions and substantial flexibility in their developmental program depending on the nature of the infection. The factors driving effector differentiation will be important as we begin to discuss when this process goes awry. Most of the work elucidating T_{CD8} development and memory differentiation have been done using model systems or model Ag. The data I present later will apply these concepts to acute viral LRI with human pathogens.

$CD8^+$ T Cells – Exhaustion

T cell exhaustion is a unique state of T_{CD8} differentiation that occurs during chronic infections and cancer. Because exhausted T cells are dysfunctional, they more closely resemble the functional status of impaired lung T_{CD8} during acute viral LRI than the effector T_{CD8} produced during other acute infections. Therefore, T cell exhaustion will be considered as a model for how T_{CD8} can become functionally impaired. Despite the acute nature of viral LRI, T_{CD8} become impaired and fail to degranulate or produce cytokines upon Ag stimulation. This indicates that the normal T_{CD8} developmental

program into functional effector cells is compromised, either from the outset or occurring rapidly during the course of infection.

Exhaustion is a state of extreme T cell impairment that arises during periods of prolonged Ag exposure (Figure 1-3A). Unlike the characteristics of T cells in acute infections discussed previously, exhausted T_{CD8} have poor effector functions, upregulate numerous inhibitory receptors and possess a transcriptional profile distinct from either effector or memory T_{CD8}. Exhaustion was first described during chronic LCMV infection of mice (Gallimore et al., 1998), but has subsequently been observed during chronic viral, bacterial and parasitic infections of mice and humans as well as during cancer (Virgin et al., 2009). As we will see, negative regulatory pathways that are both extrinsic (IL-10) and intrinsic (PD-1) to the cell drive this process. Exhaustion is deserving of considerable attention due to potential therapeutic applications for reversing this state to help clear established infections, treat refractory malignancies and boost vaccine responses.

Experimentally, exhaustion refers to tetramer-positive T_{CD8} that fail to produce cytokines when stimulated. This process has been most thoroughly examined during chronic LCMV clone-13 infection of mice, where T_{CD8} progressively lose effector functions in a step-wise and time-dependent process. IL-2 production, proliferative capacity and cytolytic killing are lost first, followed by TNF production, and finally IFNγ weeks after initial infection (Wherry et al., 2003). In the final stages, T cells are physically deleted (Figure 1-3B). The most important factor impacting exhaustion is viral load: epitopes presented to a higher degree are more exhausted (Wherry et al., 2003) and T_{CD8} in infected tissues with higher viral burdens or more exhausted (Blackburn et al., 2009; Mueller and Ahmed, 2009). Viral escape mutations that ablate T_{CD8} epitopes result in down-regulation of inhibitory receptors in the T_{CD8} that no longer recognize Ag

(Blattman et al., 2009). In addition to viral load, a long duration of infection and loss of $CD4^+$ T cell help also exacerbate exhaustion (Wherry et al., 2003).

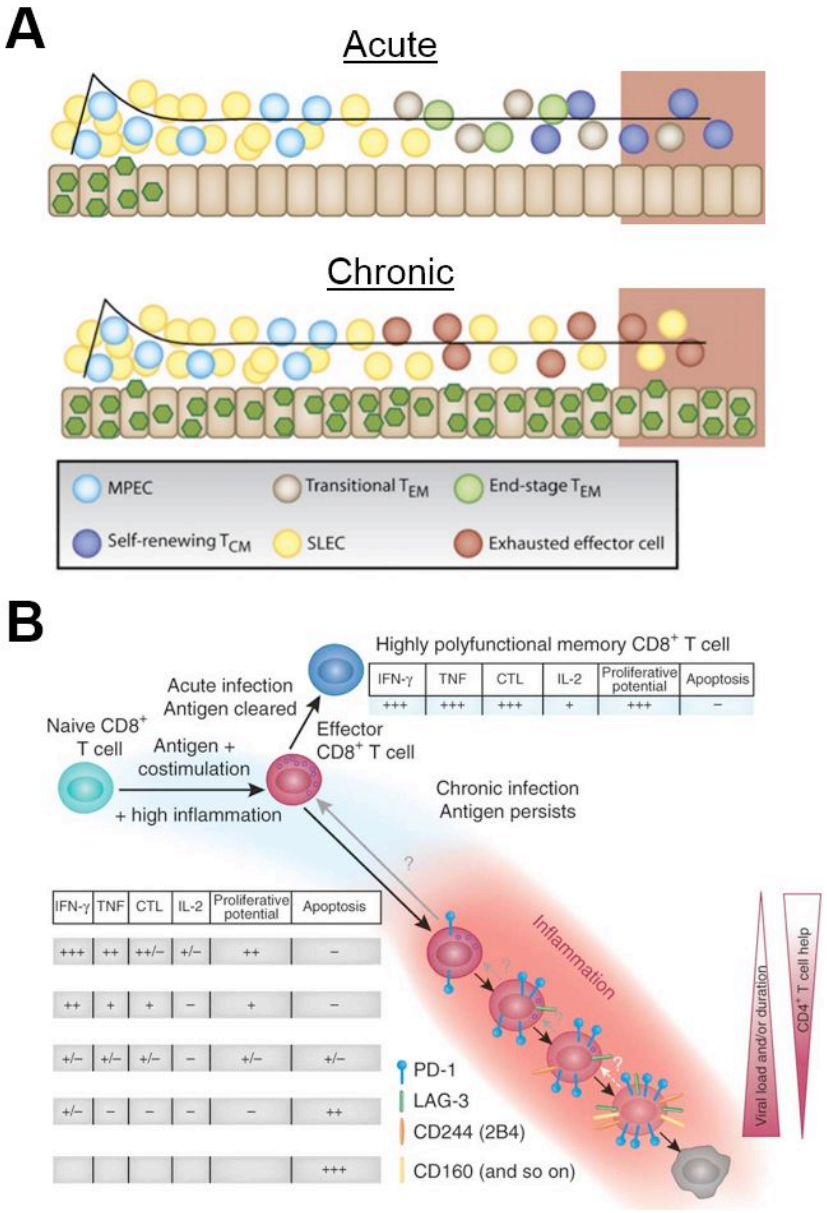

Figure 1-3. T_{CD8} exhaustion. (**A**) During acute infections, SLEC (yellow cells) and MPEC (aqua cells) develop early, with SLEC dying soon after viral clearance. MPEC transition into functional memory cells (purple cells) over time. During chronic infections, this same process takes place early. However, Ag persistence and high inflammation lead to T cell exhaustion. Recent data, though, suggests that even amongst exhausted cells are those with memory-like potential. Adapted from (Kaech and Wherry, 2007). (**B**) Acute infection generates polyfunctional memory T_{CD8} upon pathogen clearance. During chronic infection, Ag persistence and continued inflammation drive exhaustion, where T_{CD8} lose effector functions in a step-wise manner due to the concerted actions of inhibitory receptors such as PD-1. Adapted from (Wherry, 2011).

T_{CD8} exhaustion occurs in a similar fashion in humans during chronic infections with HIV, HBV and HCV (Virgin et al., 2009). Important differences exist, though, such as during HIV infection, where virus-specific T_{CD8} rarely lose the ability to make IFNγ but do lose other cytokines and cytotoxicity (Betts et al., 2006). However, exhaustion in mice and humans share many similarities. During HCV infection, T_{CD8} lose IFNγ production (Lechner et al., 2000) and peripheral virus-specific T_{CD8} are deleted (Bowen and Walker, 2005). Additionally, highly active retroviral therapy during HIV infection or epitope escape mutations both lead to the eventual loss of virus-specific T_{CD8}, indicating Ag-dependent TCR signaling is required for maintenance of these cells (Shin and Wherry, 2007).

During normal memory development, TCR signaling is no longer necessary and IL-7/IL-15 maintain homeostatic self-renewal of these cells (discussed previously). Exhausted T_{CD8} do not express the receptors for either IL-7 or IL-15 (Shin and Wherry, 2007) and so during chronic infections T_{CD8} become dependent on TCR signaling for survival. The loss of virus-specific T_{CD8} upon Ag withdrawal or viral mutation does not restart memory T cell development (Wherry et al., 2004) unless it occurs very early (Blattman et al., 2009), suggesting that T cell exhaustion is a uniquely differentiated state.

Indeed, this has been verified experimentally. First, exhausted T_{CD8} at day 30 post-clone-13 infection transferred into mice acutely infected with LCMV strain Armstrong fail to persist and form memory cells, whereas if day 8 T_{CD8} are transferred they retain the ability to form memory (Angelosanto et al., 2012). Indeed, the cells that persist into the memory phase come from KLRG1^{lo} memory precursors that still exist before the establishment of chronic infection, suggesting that exhaustion is a developmental process that takes time to be fully established. Second, transfer of fully

exhausted T_{CD8} into naïve mice that are subsequently challenged with acute LCMV results in viral control due to re-expansion of a population of memory-like cells (Utzschneider et al., 2013). These memory-like cells retain their exhaustion phenotype (i.e., PD-1^{hi}, limited ability to make cytokines), indicating stable transmission of exhaustion to the resulting daughter cells. Third, epigenetic modifications of genes associated with impairment may be a potential mechanism explaining the encoding and heritability of the exhausted state. TCR signaling drives demethylation of the promoter for *Pdcd1* (the gene encoding the inhibitory receptor PD-1) that is maintained even after Ag clearance, poising the cell for rapid re-expression of PD-1 (Youngblood et al., 2011). Finally, the transcriptional profile of exhausted cells is vastly different than effector or memory T_{CD8} (Wherry et al., 2007), indicating that at a global gene expression level exhaustion is a unique state governed by unique transcriptional networks (Doering et al., 2012). These results, along with those demonstrating partial reversal of exhaustion via inhibitory receptor blockade (discussed later), collectively demonstrate that T cell exhaustion is not simply extreme terminal differentiation of effector T_{CD8}, but rather a unique and adaptive state that balances attempts to control viral replication while placing limits on immune-mediated pathology.

T cell exhaustion is unique from anergy or senescence, two other states of T cell dysfunction. As mentioned previously, anergy results when initial TCR signals are received in the absence of adequate costimulation, leading to a state of hyporesponsiveness (Schwartz, 2003). Genes associated with anergy (e.g., Ikaros, Caspase 3, SOCS2, 4-1BBL) are not upregulated by exhausted cells and a gene set enrichment analysis of these two conditions did not reveal any relatedness (Wherry et al., 2007). Indeed, while anergy appears to be regulated at the level of the TCR, exhaustion represents more of a globally reprogrammed state. Using engineered T cells expressing two TCR (one specific for a tolerizing or exhausting Ag and the other for a

foreign, unrelated Ag), the same group of researchers found that anergic T cells were rescued via immunization through the second TCR (Teague et al., 2008) while this was not the case for exhausted T celles (Jackson et al., 2013). These results indicate that anergy is regulated in a membrane proximal manner through alterations in TCR signaling, while exhaustion is controlled downstream of the TCR. As for senescence, KLRG1 is a marker for senescent cells that exhausted cells simply do not express (Wherry et al., 2007). Additionally, as discussed previously, in most other settings, $KLRG1^{+}$ cells can still carry out effector functions, unlike exhausted cells. Therefore, T cell exhaustion appears to be unique from other states of T cell dysfunction.

Inhibitory Pathways During Chronic Infection

The immune system contains numerous regulatory mechanisms to limit damage from an over exuberant response. These inhibitory pathways constitute cell surface inhibitory receptors, soluble factors and immunoregulatory cells (i.e., regulatory T cells). Of these, the best understood is the role of inhibitory receptors. These receptors play key roles in inducing self-tolerance to prevent autoimmunity (Kasagi et al., 2011), suggesting they may have either evolved independently or been co-opted to function during T cell exhaustion or impairment. It has been suggested that functional effector T_{CD8} can transiently express these receptors during activation but then rapidly down-regulate them (Virgin et al., 2009). However, my own research will challenge this notion.

Programmed Death-1 and Its Ligands: PD-1 (CD279) is a CD28-family member that was originally identified on cells undergoing programmed cell death (Ishida et al., 1992). It is a 288 amino acid type I transmembrane glycoprotein that contains a single IgV-like domain that is expressed on activated T cells, B cells and monocytes (Agata et al., 1996a). It is closely related to CTLA-4 (Lin et al., 2008), another inhibitory receptor, but

functions via a distinct mechanism. PD-1 directly antagonizes TCR stimulation to exert its inhibitory effects. Ligation results in recruitment of src homology 2 domain-containing tyrosine phosphatase 2 (SHP-2) to a C-terminal tyrosine residue present in an immunoreceptor tyrosine-based switch motif (ITSM) on PD-1's cytoplasmic tail. SHP-2 then dephosphorylates the TCR-associated proteins CD3ζ and ZAP70, blocking activation of PI3K and hence inhibiting the PI3K/Akt pathway (Figure 1-4) (Chemnitz et al., 2004b; Okazaki et al., 2001; Pages et al., 1994; Sheppard et al., 2004). PD-1 signaling subsequently inhibits production of the pro-survival factor Bcl-xL (Chemnitz et al., 2004a), as well as transcription factors associated with effector function, such as T-bet and Eomes (Nurieva et al., 2006).

PD-1 expression has been linked to signaling through the TCR as a result of Ag exposure. CD3 stimulation induces PD-1 (Agata et al., 1996b) and increased Ag load leads to greater dysfunction during LCMV infection (Wherry et al., 2003). Early viral epitope escape mutations result in decreased PD-1 expression on virus-specific T_{CD8} that no longer see Ag (Blattman et al., 2009) and T_{CD8} in tissues with higher viral loads have increased PD-1 expression (Blackburn et al., 2009). During human infections, PD-1 expression is greatest in HIV patients with the highest viral loads (Trautmann et al., 2006), while long-term nonprogressors (who control virus without antiviral therapy) have T cells expressing relatively little PD-1 (Zhang et al., 2007). However, until recently, a direct relationship between the amount of surface expressed PD-1 and the degree of impairment has been unclear. While all exhausted T_{CD8} express PD-1, not all cells expressing PD-1 are exhausted (Duraiswamy et al., 2011). By specifically controlling the amount of PD-1 expressed, Wei *et. al* demonstrated that high levels of PD-1 are necessary to inhibit MIP-1β production, moderate levels block cytotoxicity and IFNγ production and very low levels impair TNF and IL-2 production as well as proliferation (Wei et al., 2013). These results recapitulate the loss of T cell functions observed during

chronic viral infection (Wherry et al., 2003) and indicate that PD-1 expression directly correlates with T cell impairment.

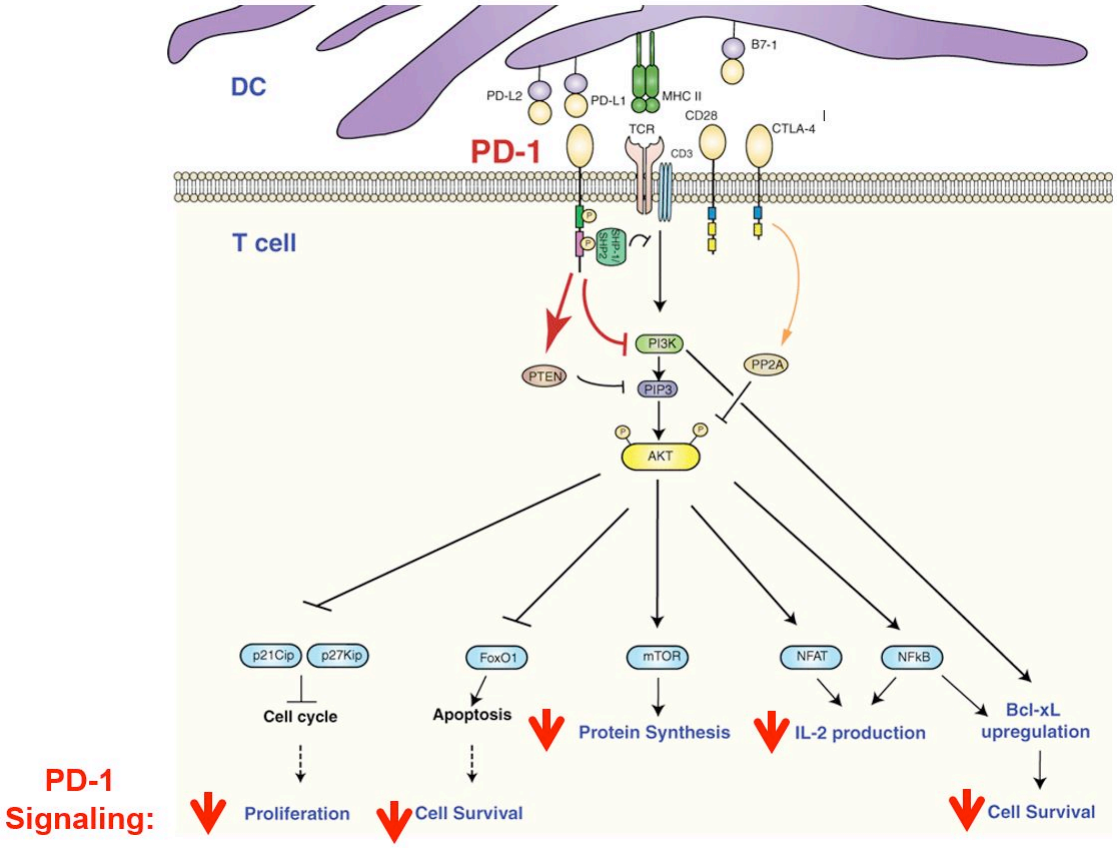

Figure 1-4. PD-1 signaling. Binding of the ITSM on PD-1's cytoplasmic tail by SHP-1 or SHP-2 results in the dephosphorylation of proximal TCR signaling molecules (CD3ζ and ZAP-70) and augmentation of PTEN expression, which blocks PIP_3. PD-1 signaling effectively attenuates the activation of the PI3K/Akt pathways and results in decreased T cell proliferation, survival, protein synthesis and IL-2 production. Note that PD-1 signals differently than CTLA-4, another inhibitory receptor. Adapted from (Francisco et al., 2010).

PD-1 is upregulated during acute LCMV infection but then rapidly suppressed following viral clearance (Barber et al., 2006). Exhausted T_{CD8} maintain expression and blockade of the PD-1 pathway restores function to these cells leading to enhanced clearance of ongoing chronic infection (Barber et al., 2006). These results established PD-1 as a major inhibitory pathway in T cell exhaustion and raised the possibility that

exhaustion is an active process that can be targeted to reverse T cell dysfunction and improve viral control. This theory has yet to be tested for human infections, but a significant amount of data indicate its potential therapeutic value. PD-1 impairs T cells during HIV infection (Day et al., 2006; Freeman et al., 2006; Trautmann et al., 2006), although this has only been tested *in vitro*. However, *in vivo* PD-1 blockade during simian immunodeficiency virus (SIV) infection resulted in improved T_{CD8} responses, greater neutralizing antibody levels and enhanced survival (Velu et al., 2009). PD-1 also impairs T cells during cancer (Jung et al., 2010) and recent clinical trials indicate that anti-PD-1 monoclonal antibody therapy is safe and at least partially effective against both refractory hematological malignancies (Berger et al., 2008) and solid tumors (Brahmer et al., 2010). These results indicate that targeting PD-1 may prove to be a viable new immunotherapeutic option in the treatment of cancer and chronic infections. Whether therapeutic PD-1 blockade could prove useful during acute viral LRI will be addressed by my thesis work (Figure 1-5).

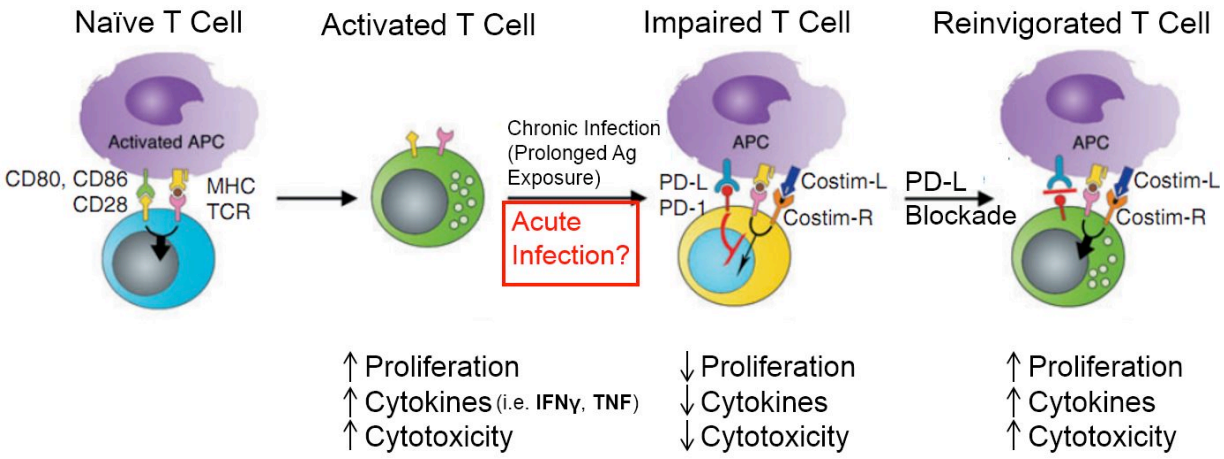

Figure 1-5. Therapeutic targeting of PD-1. Prolonged antigen exposure, previously described in the context of chronic infection, leads to upregulation of PD-1, which counteracts TCR signaling and CD28 co-stimulation, resulting in diminished T cell effector functions. PD-L blockade is being explored clinically as a possible way to reinvigorate impaired T cells. By therapeutically targeting PD-1, productive TCR signaling can be restored and effector functions brought back online. This strategy has proved successful in restoring T_{CD8} functions during chronic infections in mice and in human cancer patients. PD-1's role in mediating T cell impairment during acute respiratory infection is unknown. Adapted from (Sharpe et al., 2007).

The two ligands for PD-1 are the B7-family members PD-L1 (Freeman et al., 2000) and PD-L2 (Latchman et al., 2001). PD-L1 (B7-H1, CD274) is the most crucial PD-1 ligand for regulating T_{CD8} in autoimmunity (Greenwald et al., 2005) and exhaustion (Barber et al., 2006; Blackburn et al., 2009; Butler et al., 2012a; Jin et al., 2010b). PD-L1 is constitutively expressed on the surface of T and B cells, DCs, and macrophages (Yamazaki et al., 2002). PD-L1 transcript is expressed by a wide range of nonhematopoietic cells (including the lung parenchymal cells) (Freeman et al., 2000), but surface expression only follows activation (Dong et al., 2002). PD-L1 is also expressed on many tumor types, where it inhibits tumor-infiltrating T_{CD8} to promote malignancy immune evasion (Curiel et al., 2003; Dong et al., 2002; Iwai et al., 2002). Both type I and type II IFNs upregulate PD-L1 (Eppihimer et al., 2002; Schreiner et al., 2004), as the promoter region contains two interferon regulatory factor-1 (IRF-1) sites (Lee et al., 2006). IFNγ represses microRNA-513, which normally prevents PD-L1

protein from being expressed on the cell surface (Gong et al., 2009). IFNγ is required for PD-L1-mediated suppression of T_{CD8} during experimental autoimmune encephalitis (Cheng et al., 2007). Finally, dsRNA and LPS induce PD-L1 on DCs in a TLR3- and TLR4-dependent manner, respectively (Groschel et al., 2008). Taken together, these results indicate that PD-L1 is non-specifically upregulated by inflammation during infection, whereas T cell PD-1 expression is controlled by the specific interaction of the TCR with cognate Ag. The role of PD-1 in impairing lung T_{CD8} during acute viral LRI will be discussed in Chapter II.

Other Inhibitory Pathways: In addition to PD-1, exhausted T_{CD8} co-express TIM-3, LAG-3, CD160, 2B4, CTLA-4 and other inhibitory receptors (Figure 1-5) (Crawford and Wherry, 2009b). The combinations of inhibitory receptors and total number expressed affect the severity of dysfunction (Blackburn et al., 2009). PD-1 is a master regulator of exhaustion, so single blockade of these other receptors has minimal impact (Barber et al., 2006; Blackburn et al., 2009; Jin et al., 2010b). However, combined blockade of PD-1 and TIM-3 (Jin et al., 2010b), PD-1 and LAG-3 (Blackburn et al., 2009; Butler et al., 2012a) or PD-1 and CTLA-4 (Kaufmann et al., 2007; Nakamoto et al., 2009) all considerably enhance T cell functionality over PD-1 blockade alone. Whether all these receptors collaborate to impair TCR signaling or they have distinct, non-overlapping functions remains to be determined and will be a focus of Chapter IV of my work.

The signaling mechanisms for TIM-3, LAG-3 and CD160 are poorly understood, as they lack classic motifs associated with T cell signaling (e.g., ITIM or ITAM). As discussed previously, PD-1 and CTLA-4 both antagonize TCR signaling, albeit by different mechanisms of action. However, PD-1 signaling also induces the transcription factor BATF, which further inhibits effector functions (Quigley et al., 2010). Therefore, inhibitory receptors may also function by upregulation of other genes involved in

controlling T cell functions. A final additional consideration for the role of various inhibitory receptors in exhaustion and T cell impairment is the expression of their ligands. TIM-3 binds Galectin-9, a secreted molecule, while LAG-3 binds MHC class II molecules with higher affinity than CD4 (Odorizzi and Wherry, 2012). The environment of the T_{CD8} then becomes important as the availability of different ligands could fine tune the functionality of these cells. How these receptors and their ligands shape lung T_{CD8} impairment during acute viral LRI will be discussed further in Chapter IV.

In addition to the cell-intrinsic role of inhibitory receptors in T cell exhaustion, cell-extrinsic cues also play a part. IL-10 is highly expressed during chronic infections by APCs (Wilson et al., 2012) and blockade of this inhibitory cytokine enhances viral control by improving T cell responses (Blackburn and Wherry, 2007; Brooks et al., 2006; Ejrnaes et al., 2006). Similarly, blocking TGF-β signaling also improves T_{CD8} functions during chronic LCMV infection (Tinoco et al., 2009). Additional cytokines, such as IL-2, IL-7 and IL-21 help to maintain the limited effector functions that do exist during chronic infections (Wherry, 2011).

Finally, several transcriptional pathways have been implicated in T cell exhaustion. As discussed previously concerning the differentiation of functional effector T_{CD8} during acute infection, Blimp-1 is a transcriptional repressor that promotes terminal differentiation. Blimp-1 is highly expressed by exhausted T_{CD8} and promotes upregulation of many inhibitory receptors (Shin et al., 2009). Interestingly, Blimp-1 haploinsufficiency balances promotion of T_{CD8} effector functions with reversal of exhaustion (Shin et al., 2009). Therefore, low Blimp-1 expression favors memory development, intermediate levels promote effector differentiation, while high expression drives exhaustion. T-bet, another promoter of effector T_{CD8} differentiation, actually sustains T_{CD8} functions during exhaustion by repressing PD-1 expression (Kao et al., 2011). Eomes, in contrast, which has been linked with functional memory generation, is

more highly expressed by terminally exhausted T_{CD8} progeny. Finally, BATF is a transcription factor upregulated via PD-1 signaling that dimerizes with c-Jun, displacing c-Fos, therefore impairing AP-1 mediated transcription (Quigley et al., 2010). These results suggest that the same transcription factors differentially regulate effector versus memory versus exhausted T_{CD8} states depending on expression level and cooperation with other impairment related genes.

Inhibitory Receptors During Acute Infection

I now return to the driving question behind my thesis studies, which is what causes lung T_{CD8} impairment during acute viral LRI? Given the similarities between impaired lung T_{CD8} and exhausted T cells, I reasoned that inhibitory receptors may be mediating this process. Specifically, I hypothesized that the PD-1/PD-L1 pathway impairs lung T_{CD8} during acute viral LRI.

While the role of PD-1 in promoting T cell exhaustion during chronic infections is well established, the functions of PD-1 during acute infections are much less clear. Mice acutely infected with lymphocytic choriomeningitis virus (LCMV) possess functional T_{CD8} that rapidly downregulate PD-1 in the spleen (Barber et al., 2006; Wherry et al., 2003), while mice acutely infected with Friend retrovirus possess T_{CD8} that express high levels of PD-1 yet remain cytotoxic (Zelinskyy et al., 2011). *PD-L1*$^{-/-}$ mice infected with rabies virus (Lafon et al., 2008) or a neurotropic coronavirus (Phares et al., 2009) exhibited enhanced pathology but increased virus clearance. These studies suggest that PD-1 negatively impacts immune responses to acute viral infections, but whether PD-1 specifically affectsT_{CD8} is unknown.

As for the functions of PD-1 during acute viral LRI, even less is known. Indirect evidence suggested a potential role, as IL-2 rescues T_{CD8} impairment during RSV infection of mice (Chang et al., 2004) as it does during chronic infection (Blattman et al.,

2003). RSV infection also upregulates PD-L1 expression on bronchial epithelial cells (Stanciu et al., 2006) leading to inhibition of non-specific T_{CD8} activity (Telcian et al., 2011). PD-L expression by respiratory epithelial cells represents an attractive model for how signals could be delivered to inhibitory receptors on the cell surface of lung T_{CD8}. Lung epithelial cells are capable of acting as APCs and express MHC class I, CD80 and CD86 and these molecules are upregulated by infection (Kim et al., 2005; Papi et al., 2000).

Limited data also exists for the roles of other inhibitory receptors in acute viral LRI. LAG-3 negative regulates T_{CD8} memory development during Sendai virus infection (Workman et al., 2004), while TIM-3 limits T_{CD8} effector functions during acute HSV-1 infection (Sehrawat et al., 2010) and IAV infection (Sharma et al., 2011). More work has been done exploring the role of the immunoregulatory cytokine IL-10. T_{CD8} themselves secrete IL-10 to limit immune pathology (Palmer et al., 2010; Sun et al., 2011a; Sun et al., 2009). Effector T_{CD8} are the primary producers of IL-10 in the lung during IAV and RSV infections (Sun et al., 2011a). IL-10 expressing cells are surprisingly the most potent effectors, producing higher amounts of IFNγ, TNF and granzyme B than IL-10$^-$ counterparts. IL-2 produced by CD4 T cells and IL-27 from neutrophils are both required for the development of IL-10 producing T_{CD8} via activation of Blimp-1 (Sun et al., 2011b). During RSV infection, IL-10-producing T_{CD8} also express the IL-10 receptor, suggesting the possibility of an auto-regulatory pathway for repression of T_{CD8} effector functions (Sun et al., 2009).

In summary, numerous pathways tightly regulate T_{CD8} development, phenotype and functions. Most acute infections generate functional T_{CD8} that aid in viral clearance. During acute viral LRI, that is not the case, as lung T_{CD8} rapidly become impaired. T_{CD8} impairment may be better understood in the context of T cell exhaustion that is observed during chronic viral infections and cancer. It is unknown what mechanisms govern lung

T_{CD8} impairment. Many co-stimulatory and inhibitory receptors may play a role in fine-tuning the overall lung T_{CD8} response (Figure 1-6). My thesis is concerned with identification of these mechanisms and in more fully elucidating where in the grand scheme of T_{CD8} differentiation lung T_{CD8} exist. It is only through a more complete understanding of this process that novel therapeutics and effective vaccination strategies can be developed.

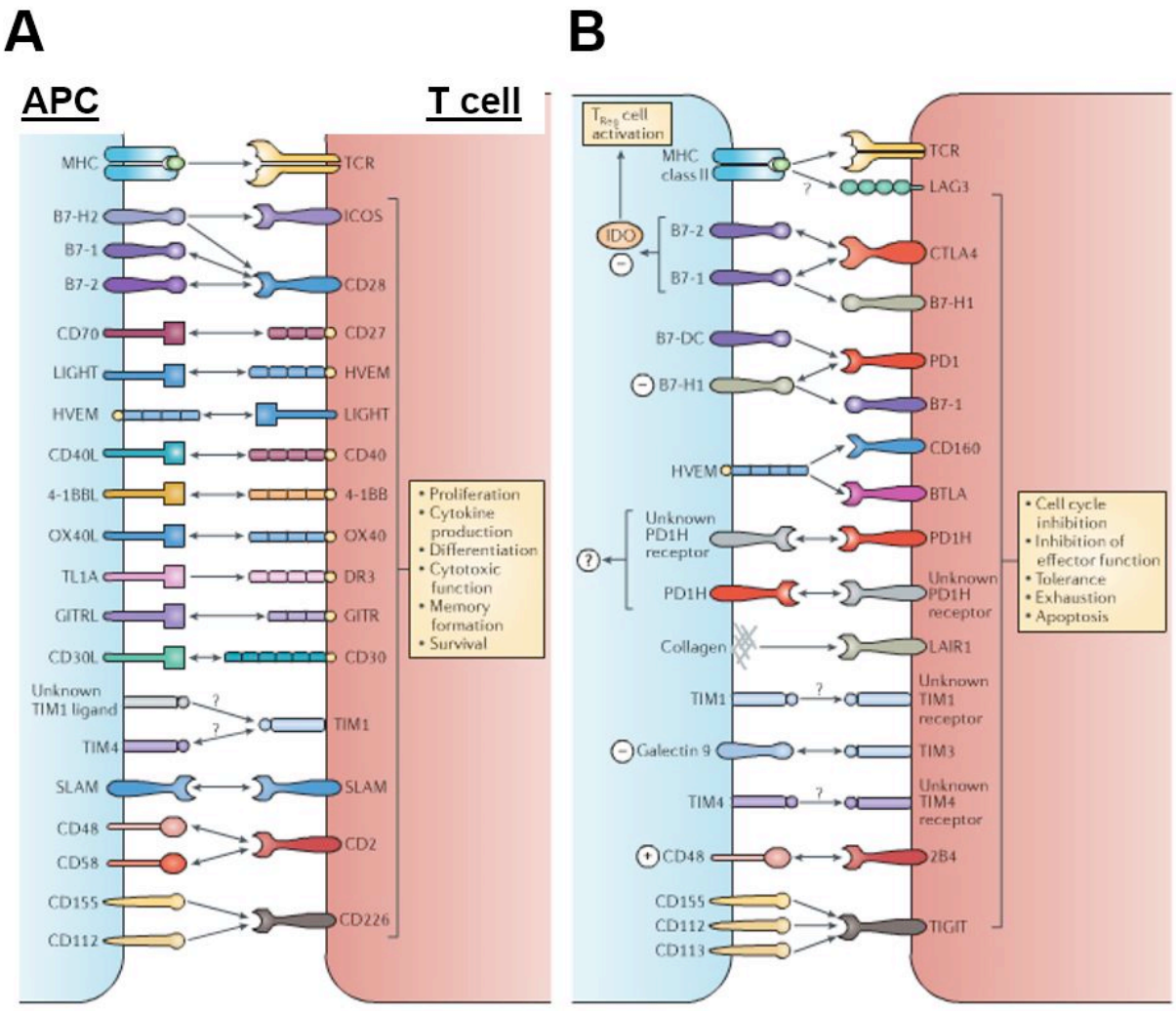

Figure 1-6. Co-signaling pathways in T cells. (**A**) Co-stimulatory molecules enhance T cell activation by supplementing TCR signaling. CD28 provides strong co-stimulation and is required to fully activate T cells and prevent anergy. Additional receptors help shape the magnitude and quality of the T cell response. (**B**) Inhibitory receptors antagonize TCR signaling and other positive signals. PD-1, TIM-3, LAG-3, 2B4 and CTLA-4 all play a defined role in T cell exhaustion. From (Chen and Flies, 2013).

CHAPTER II

Viral Acute Lower Respiratory Infections Impair $CD8^+$ T Cells through PD-1

INTRODUCTION

Human metapneumovirus (HMPV), respiratory syncytial virus (RSV) and influenza A virus (IAV) are leading causes of acute lower respiratory infection (LRI) worldwide, especially in infants, the elderly and the immunocompromised (Deffrasnes et al., 2007; Langley and Anderson, 2011; Pavia, 2011; Williams et al., 2004). No effective vaccines or therapeutics exist for either HMPV or RSV and influenza vaccine must be re-administered annually. Despite the frequency of infection with these viruses and minimal antigenic drift of HMPV and RSV, protective immunity is poorly established, as individuals can be repeatedly reinfected throughout life (Hall et al., 1991; Johnson et al., 1961; Kroll and Weinberg, 2011). An ineffective adaptive immune response might account for this susceptibility, as recent studies have demonstrated infection of mice with RSV (Chang and Braciale, 2002; DiNapoli et al., 2008; Lukens et al., 2006; Vallbracht et al., 2006), IAV (DiNapoli et al., 2008) or parainfluenza virus 5 (PIV-5) (Gray et al., 2005) results in impaired pulmonary $CD8^+$ cytotoxic T lymphocytes (T_{CD8}), cells that normally mediate recovery from LRI by elaboration of cytokines and direct lysis of infected cells (Bruder et al., 2006). Specific mechanisms governing pulmonary T_{CD8} functional impairment during acute viral LRI remain incompletely defined and represent a potential avenue for therapeutic intervention and design of more effective vaccines.

T_{CD8} functions are tightly regulated by a variety of stimulatory and inhibitory receptors (Blackburn et al., 2009; Crawford and Wherry, 2009a; Jin et al., 2010b). During chronic infections (Barber et al., 2006; Blattman et al., 2009; Velu et al., 2007; Wherry et al., 2003; Zhang et al., 2007) and cancer (Inman et al., 2007; Sakuishi et al.,

2010b; Zhou et al., 2011), programmed death-1 (PD-1) has a well-defined role in mediating T_{CD8} exhaustion, where prolonged T cell receptor (TCR) stimulation by persistent viral or tumor antigens maintains PD-1 expression. PD-L1, a ligand for PD-1, is constitutively expressed by many hematopoietic cells and inducible on most other cell types by pro-inflammatory cytokines (Cheng et al., 2007; Stanciu et al., 2006; Yamazaki et al., 2002), including respiratory epithelial cells (Stanciu et al., 2006). PD-L1 ligation of PD-1 antagonizes TCR signaling by blocking PI3K/Akt activation, leading to decreased protein synthesis, cytokine production, proliferation and survival (Francisco et al., 2010). Blocking PD-1 ligation restores function to exhausted T_{CD8} during HIV infection (Barber et al., 2006; Trautmann et al., 2006) and recent clinical trials indicate that anti-PD-1 monoclonal antibody therapy is safe and at least partially effective against both refractory hematological malignancies (Berger et al., 2008) and solid tumors (Brahmer et al., 2010). Direct modulation of the PD-1/PD-L1 pathway therefore possesses significant therapeutic potential.

A role for PD-1 in mediating T_{CD8} impairment during acute infections is unclear. Mice acutely infected with lymphocytic choriomeningitis virus (LCMV) possess functional T_{CD8} that rapidly downregulate PD-1 in the infected spleen (Barber et al., 2006; Wherry et al., 2003), while mice acutely infected with Friend retrovirus possess T_{CD8} that express high levels of PD-1 yet remain cytotoxic (Zelinskyy et al., 2011). In humans during acute hepatitis B virus infection, high T_{CD8} PD-1 levels correlate with a positive clinical outcome, presumably due to reduced T_{CD8}-mediated liver damage (Zhang et al., 2008). However, during acute hepatitis C virus infection, high PD-1 expression is associated with T_{CD8} impairment and progression to chronic infection (Rutebemberwa et al., 2008). More recent studies have suggested that PD-1 plays an inhibitory role during some acute infections, such as viral central nervous system infection (Lafon et al., 2008; Phares et al., 2009), pulmonary fungal infection (Lazar-Molnar et al., 2008) or bacterial

sepsis (Huang et al., 2009; Yao et al., 2009). However, mechanisms governing PD-1 regulation in these settings and the specific impact of PD-1 signaling on T_{CD8} functional impairment during acute viral infections are unknown.

We hypothesized that viruses causing acute LRI induce PD-1-mediated T_{CD8} functional impairment in the infected lung where both viral antigen to drive PD-1 upregulation and PD-L1 to ligate PD-1 are present. We report that PD-1 signaling rapidly induced pulmonary T_{CD8} impairment during HMPV and IAV infections. Using intranasal delivery of peptide-loaded dendritic cells (DCs) to elicit a T_{CD8} response in the absence of viral replication, we demonstrate that cognate viral antigen is necessary and sufficient to induce PD-1 upregulation, but that infection-induced PD-L1 is also required for T_{CD8} impairment. Importantly, therapeutic inhibition of PD-1 ligation using monoclonal antibody blockade prevented impairment and reduced viral titers without exacerbating lung histopathology, though mild airway dysfunction was observed. T_{CD8} impairment was more pronounced during secondary infection, as memory T_{CD8} were severely impaired and expressed more PD-1 than T_{CD8} during primary infection. PD-1 signaling blockade during challenge infection of immunized mice restored function to pulmonary T_{CD8} and significantly augmented their protective capacity resulting in reduced viral titers. Finally, PD-1 and PD-L1 were expressed in the lungs of patients with severe acute viral LRI, suggesting that modulation of the PD-1/PD-L1 pathway could enhance anti-viral T_{CD8} functions in these patients, a population for which limited treatment options currently exist.

RESULTS

HMPV T_{CD8} epitope mapping in C57BL/6 and HLA-B*0702 transgenic mice

Since previous studies of HMPV disease in small animals utilized BALB/c mice (Alvarez and Tripp, 2005; Melendi et al., 2007) or cotton rats (Williams et al., 2005), we first characterized HMPV infection of C57BL/6 (B6) mice. Viral titers peaked in the lungs at day 5 post-infection, declined at day 7 and were undetectable by day 10 (Figure 2-1A), consistent with an acute infection (Deffrasnes et al., 2007). Viral genome was still detectable in the lungs up to 6 weeks post-infection (Figure 2-1B). Lower airway histopathology was consistent with peribronchiolitis and perivasculitis (Figure 2-1C).

To more specifically study the anti-HMPV T_{CD8} response, we mapped epitopes in B6 mice as well as B6-Kb^0Db^0;B7.2 transgenic (B7tg) mice, which can only recognize T_{CD8} epitopes restricted by human HLA-B*0702 (Rohrlich et al., 2003b). In B6 mice, 11 epitopes were identified with similar frequencies of IFNγ-secreting HMPV-immune splenocytes at day 10 post-infection (Figure 2-2A and not shown). To determine which epitope-specific T_{CD8} targeted the primary site of HMPV infection, we further screened B6 epitopes in lung lymphocytes and determined that H2-$D^b/F_{528-536}$ (F528) and H2-K^b/N_{11-19} (N11) resulted in the highest responses (Figure 2-2A). In B7tg mice, 6 T_{CD8} epitopes were identified (Supplementary Figure 2-1B and not shown). Stimulation with $M_{195-203}$ (M195) and to a lesser extent $N_{198-206}$ (N198) peptides produced a large fraction of HMPV-immune splenocytes releasing IFNγ at day 10 post-infection (Figure 2-2B). HMPV replication kinetics and lung pathology in B7tg mice were similar to B6 mice (not shown).

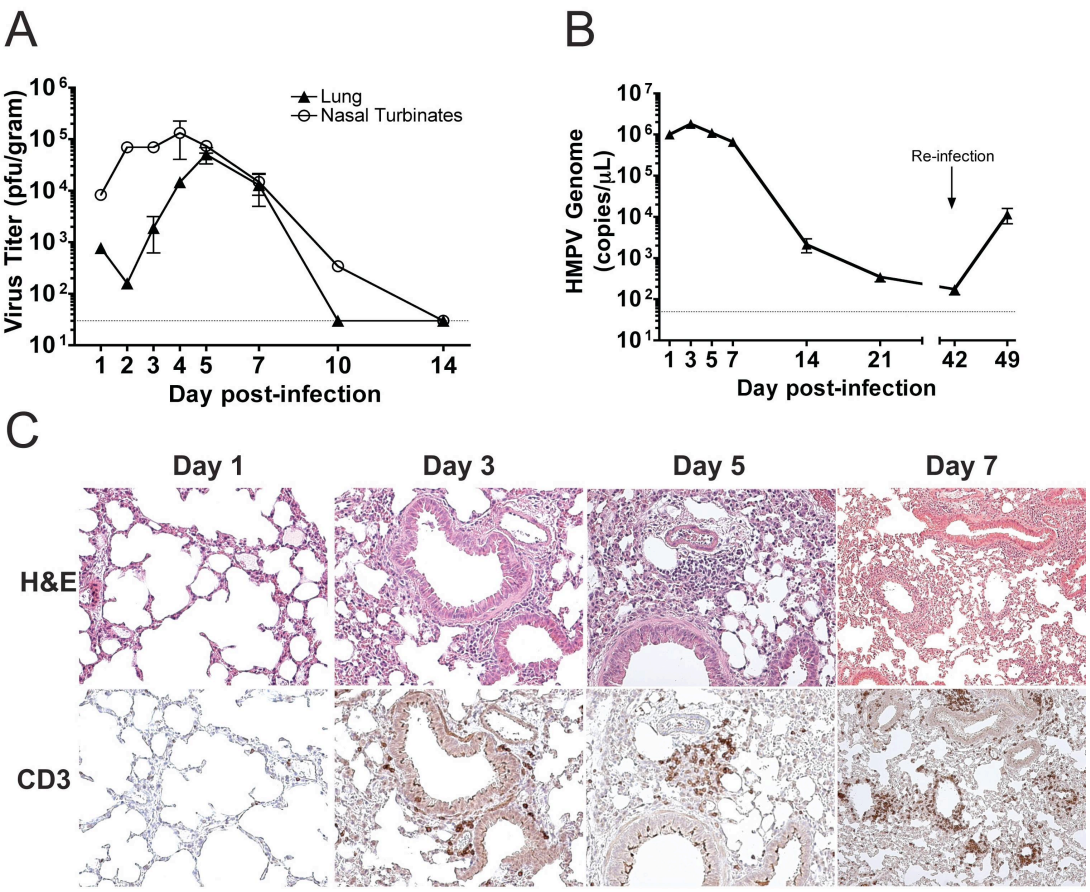

Figure 2-1. Kinetics of HMPV viral replication and lower airway pathology. (**A**) C57BL/6 (B6) mice were infected intranasally (i.n.) with HMPV and viral titers were quantified for the lungs (closed triangles) and nasal turbinates (open circles) in plaque forming units (pfu) per gram of tissue (n=3-6 mice per time point). Dotted line indicates the limit of viral detection. (**B**) Real-time RT-PCR targeting the HMPV N gene was used to quantify genome levels in the lungs of infected mice at the indicated times post-infection (n=5-10 mice per time point). Arrow indicates time at which mice were challenged with HMPV. (**C**) Images represent serially cut lung sections stained with hematoxylin and eosin (H&E) (top panels) or anti-CD3 (bottom panels) and are representative of 3-5 individual mice per time point for which viral titers were determined to confirm infection. Days 1-5 magnification = 200X. Day 7 magnification =100X. Representative data from several experiments are shown.

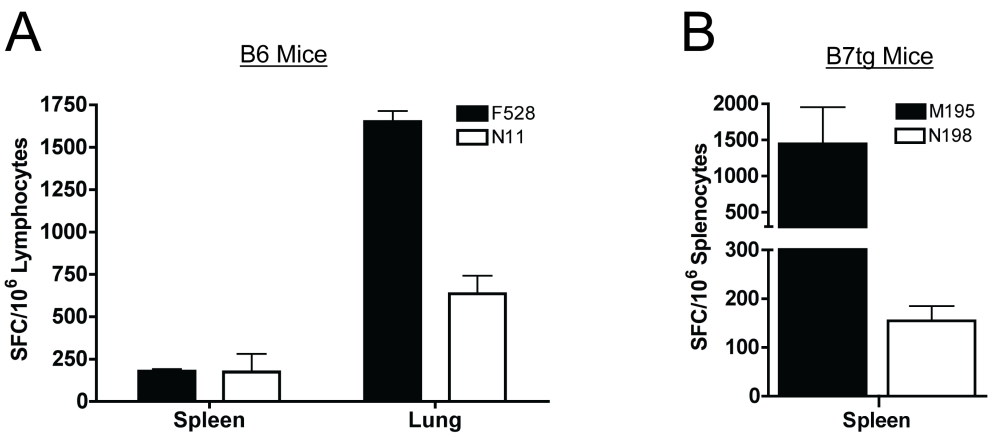

Figure 2-2. Identification of HMPV T_{CD8} epitopes. C57BL/6 (B6) (**A**) or B6-Kb0Db0;B7.2 transgenic (B7tg) (**B**) mice were infected with HMPV and then spleen or lung lymphocytes were isolated 10 days post-infection. HMPV immune cells were screened for IFNγ release via ELISPOT assay using H2-Db/H2-Kb (**A)** or HLA-B**0702* predictopes (**B**).Results indicate spot forming cells (SFC) per 10^6 splenocytes or lung lymphocytes following stimulation with the indicated peptide (background subtracted). Results for only the top two epitopes are shown. Data in (**A**) are combined from at least 2 independent experiments with 3-5 individual mice per experiment while data in **(B)** are combined from 3 independent experiments with 5 pooled mouse spleens per experiment.

Pulmonary T_{CD8} are impaired and upregulate PD-1 during HMPV infection

HMPV-specific T_{CD8} were quantified using two separate assays performed in parallel: MHC class I tetramer staining enumerates total epitope-specific T_{CD8} directly *ex vivo*, while epitope restimulation followed by intracellular cytokine staining (ICS) for IFNγ, a direct correlate of cytolytic activity (Horton et al., 2004), and surface staining for CD107a, an indicator of cytotoxic granule release (Betts et al., 2003), quantifies effector functions (Figure 2-3). In the spleen, we observed a high concordance between tetramer staining and CD107a mobilization or IFNγ production in T_{CD8} at all time points (Figure 2-4A,B). However, by day 7 post-infection11.8% of lung-infiltrating T_{CD8} were detected with M195 tetramer, while only 3.5% produced IFNγ or degranulated when restimulated with M195 peptide (Figure 2-4C,D). Pulmonary T_{CD8} function continued to decline over time, with less than 10% functional by week 6 (Figure 2-4D and 2-4E). Thus, a large fraction

of pulmonary HMPV-specific T_{CD8} failed to respond to antigen, and this impairment persisted for several weeks beyond viral clearance.

During chronic infections or cancer, T_{CD8} become exhausted with progressive loss of effector functions in the order IL-2>TNFα>IFNγ>CD107a, followed by clonal deletion (Wherry et al., 2003). To define the extent of impairment during HMPV infection, we quantified other effector functions at the peak of the T_{CD8} response. Thirty-six percent of lung-infiltrating T_{CD8} expressed granzyme B (GzmB), which were predominantly M195 tetramer$^+$ (Figure 2-5A). While about two-thirds of M195-specific T_{CD8} were GzmB$^+$, far fewer produced IFNγ and even less produced TNFα or IL-2 (Figure 2-5B,C). Strikingly, lung M195-specific T_{CD8} were more severely impaired during secondary infection, where neutralizing antibody completely blocks viral replication in the lungs (Figure 2-4E and data not shown). Since M195 epitope-specific cells account for such a high percentage of virus-activated lung T_{CD8} during primary and secondary infection, we questioned whether T_{CD8} impairment was restricted to the immunodominant response. This was not the case, as subdominant N198-specific T_{CD8} were functionally impaired to a similar degree (Figure 2-4F), as were other epitopes tested (not shown). Thus, pulmonary HMPV-specific T_{CD8} were impaired in multiple key effector functions.

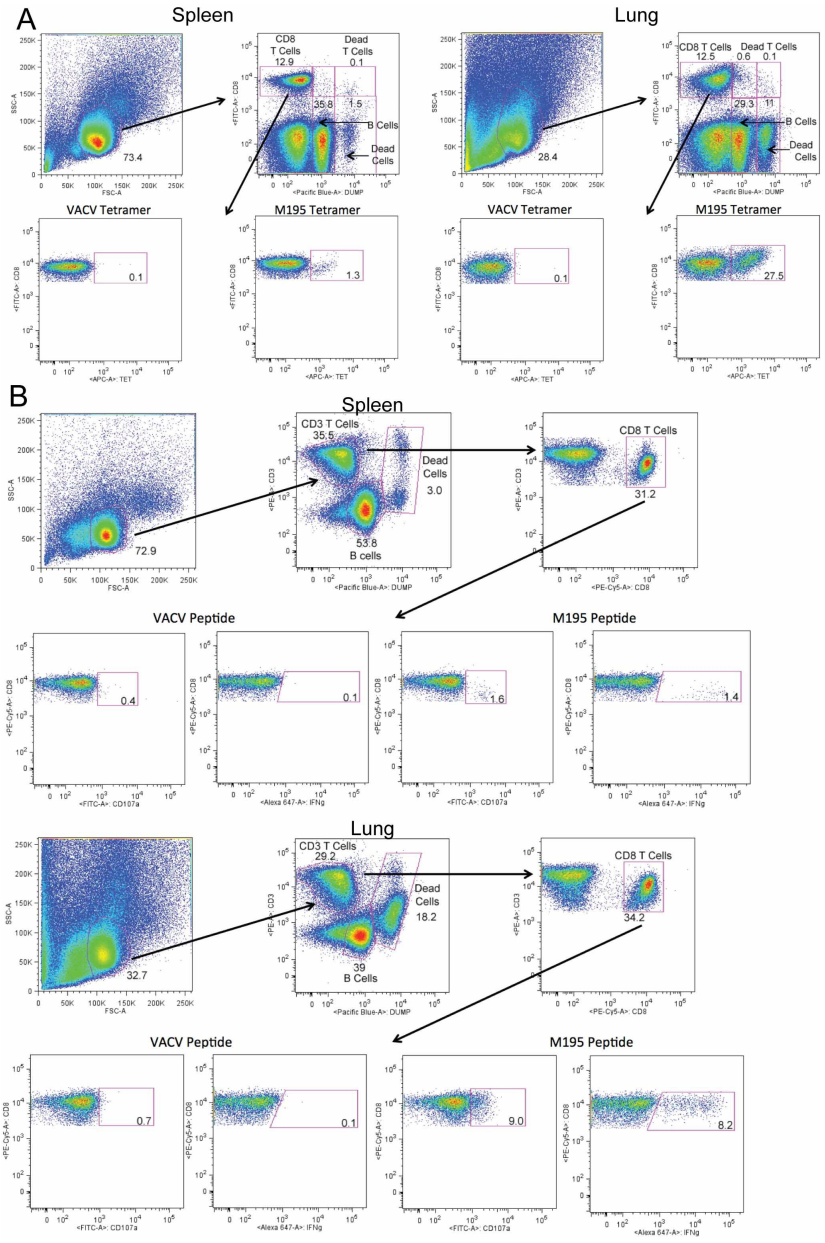

Figure 2-3. Flow cytometry gating strategy. For both tetramer staining **(A)** and intracellular cytokine staining (ICS) **(B)**, lung or spleen cells were surface stained for CD8 and CD19. For ICS, cells were also stained for CD3. Dead cells were excluded using an amine reactive dye. For tetramer analysis, cells were stained directly *ex vivo*. For ICS, cells were first restimulated for 6 hours with 10μM peptide in the presence of anti-CD107a antibody and the protein transport inhibitors brefeldin A and monensin before surface and intracellular staining for IFNγ. For B7tg mice, background values obtained from staining with an irrelevant VACV-specific tetramer or restimulation with the same VACV peptide (A34R$_{82\text{-}90}$, the immunodominant epitope for VACV in B7tg mice) were subtracted. For B6 mice, background values obtained from staining with IAV NP366 tetramer or restimulation with the same peptide were subtracted. 10,000-20,000 CD8$^+$ T cells were counted per lung or spleen.

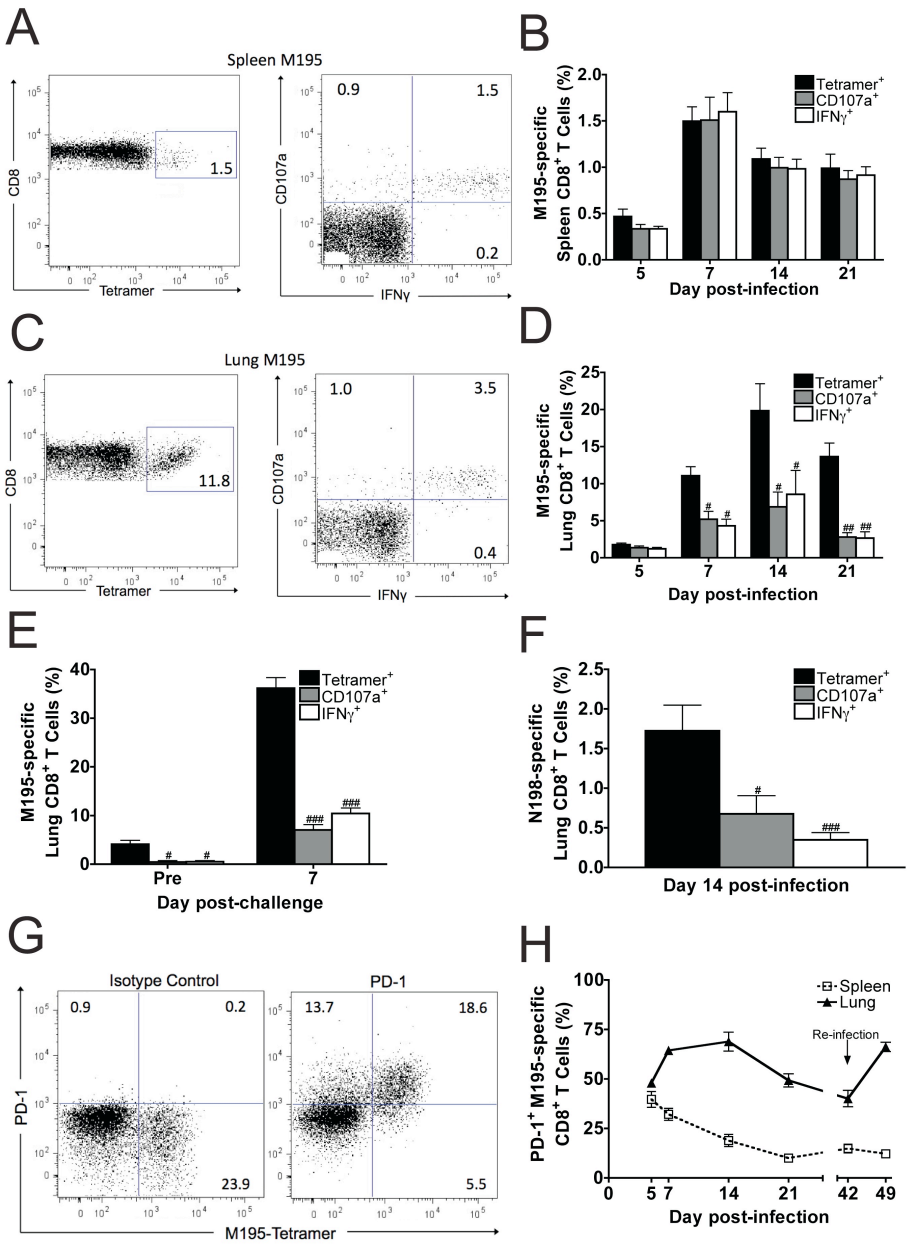

Figure 2-4. Pulmonary T_{CD8} are impaired and upregulate PD-1 during HMPV LRI. (**A-D**) Spleen (**A** and **B**) and lung (**C** and **D**) lymphocytes were isolated from B7tg mice at the indicated times post-HMPV infection. Representative histograms from day 7 post-infection (**A** and **C**) and combined data from several time points (**B** and **D**) enumerate the T_{CD8} response directed against the $M_{195-203}$ (M195) epitope. Numbers in flow plots indicate the percentage of $CD8^+$ T cells that either bind to M195 tetramer or respond to restimulation with M195 peptide by mobilizing CD107a to the cell surface (i.e. degranulating) or producing IFNγ. # indicates statistically different $CD107a^+$ (gray bars) or $IFN\gamma^+$ (white bars) $CD8^+$ T cells compared to $tetramer^+$ cells (black bars) analyzed in parallel from the same mice at the same time point. (**E**) M195-specific T_{CD8} response at day 42 post-primary infection (Pre) and then at day 7 post-challenge. (**F**) $N_{198-206}$ (N198) specific T_{CD8} response at day 14 post-infection. (**G**) Representative flow cytometry plots demonstrating PD-1 expression versus M195 tetramer staining at day 14 post-infection

in the lung. Numbers in each quadrant indicate the percentage of $CD8^+$ T cells. (**H**) Kinetics of PD-1 expression on spleen (open squares) or lung (closed triangles) M195-specific $CD8^+$ T cells. Arrow indicates time at which mice were challenged with HMPV (day 42 post-primary infection). Data are representative of at least two independent experiments with 4-5 individual mice per time point. Twenty-thousand $CD8^+$ T cells were counted for the spleen and 10,000 for the lung. $^{\#}$ $p<0.05$, $^{\#\#}$ $p<0.005$, $^{\#\#\#}$ $p<0.0005$ (two-tailed, paired t-test).

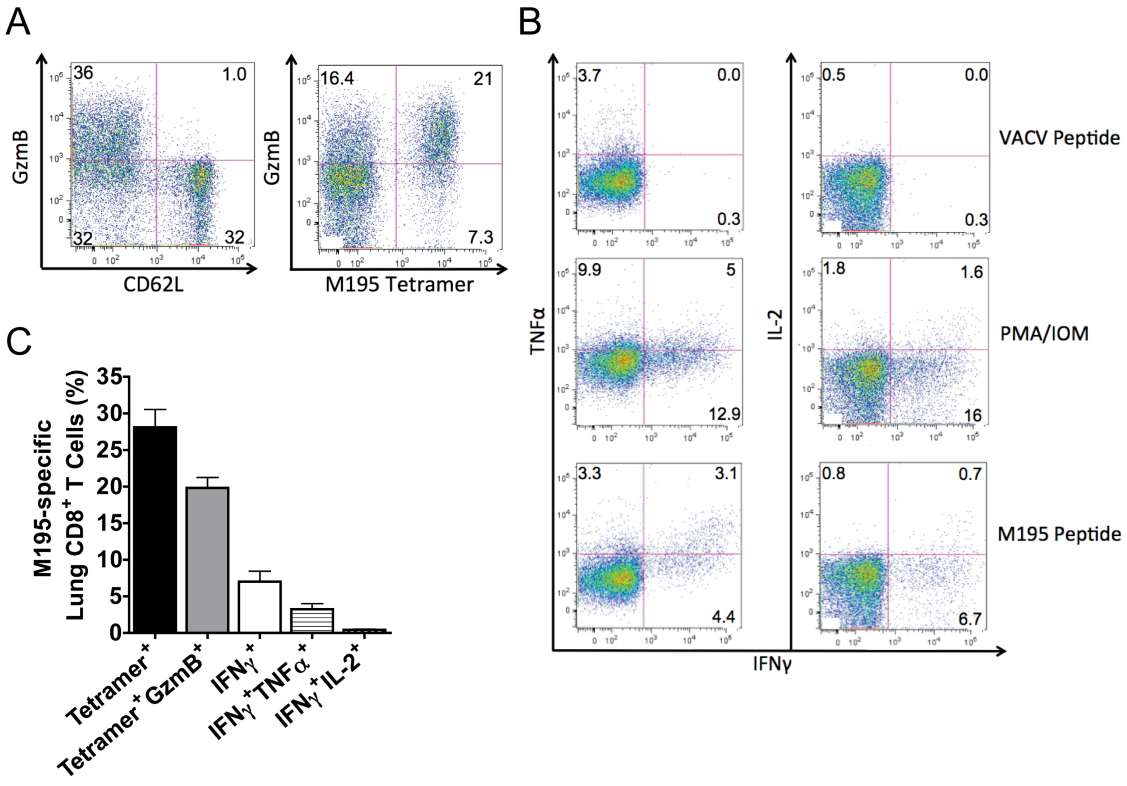

Figure 2-5. HMPV-specific pulmonary T_{CD8s} are impaired for multiple key effector functions. B7tg mice were infected with HMPV and lung lymphocytes were isolated 10 days post-infection. (**A**) Lung lymphocytes were stained directly *ex vivo* with M195 tetramer and anti-CD62L followed by intracellular staining for granzyme B (GzmB). $GzmB^+$ T_{CD8s} were identified by exclusionary gating from the $CD62L^+$ population, which are $GzmB^-$ naïve or central memory cells (left flow plot). The same GzmB electronic gate was applied to M195 $tetramer^+$ cells in order to identify $GzmB^+$ M195-specific T_{CD8s} (right flow plot). (**B**) Lung lymphocytes from the same mice were restimulated with an irrelevant VACV peptide, mitogen (PMA/ionomycin) or M195 peptide. Flow plots are gated on $CD8^+$ T cells and display IFNγ versus TNFα (left column) or IFNγ versus IL-2 (right column). (**C**) Summary of all lung T_{CD8} functions examined in (**A**) and (**B**). One representative experiment of two independent experiments with 5 individual mice per experiment is shown.

Given the progressive degree of functional impairment observed in pulmonary HMPV-specific T_{CD8}, we wondered whether these cells expressed the inhibitory receptor PD-1, a marker of impaired T cells. In naïve mice, <5% of lung or spleen T_{CD8} expressed PD-1 (not shown). In contrast, during HMPV infection PD-1 was rapidly upregulated on M195-specific T_{CD8} by day 5 and reached maximum expression in the lungs between days 7 and 14 (Figure 2-4G,H). Over half of pulmonary T_{CD8} remained PD-1^+ several weeks after viral clearance. Upon reinfection, PD-1 levels returned to those observed during primary infection (Figure 2-4H), despite undetectable lung virus replication (not shown). In contrast, M195-specific T_{CD8} in the uninfected spleen upregulated PD-1 early during infection but steadily decreased expression over time, which did not increase upon challenge infection. PD-1 expression was not restricted to a limited TCR repertoire as the M195-specific population was polyclonal, primarily representing the Vβ2 and Vβ9 families (Figure 2-6A). PD-1 expression between different TCR Vβ families (Figure 2-6B) and different epitopes (Figure 2-6C) was indistinguishable. Thus, prolonged PD-1 expression by a polyclonal lung T_{CD8} population was associated with impairment.

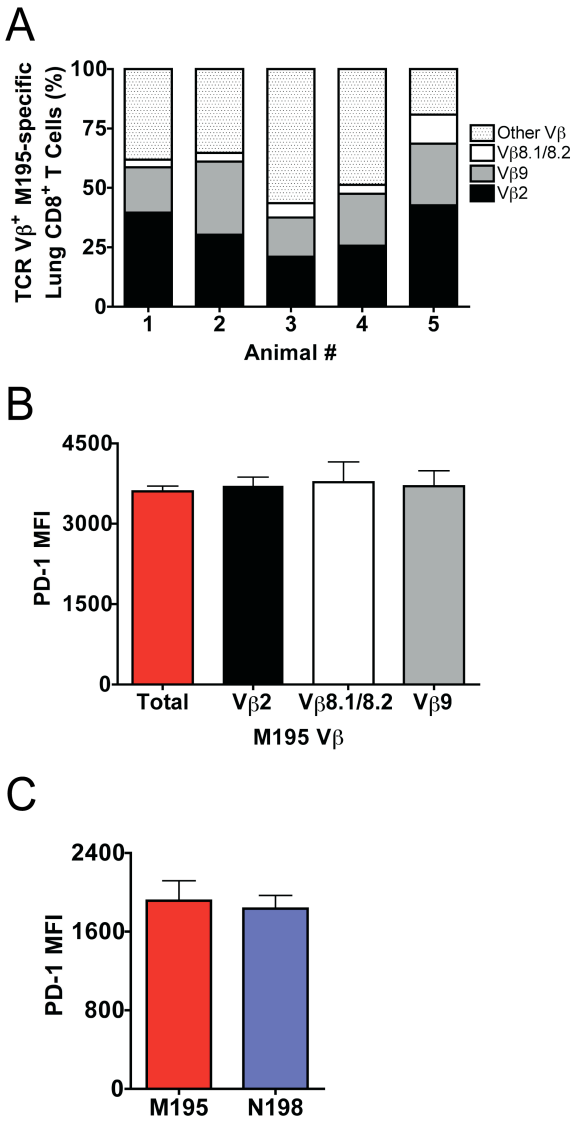

Figure 2-6. HMPV-specific T_{CD8s} are polyclonal with indistinguishable PD-1 expression between different TCR Vβ families and different epitopes. B7tg mice were infected with HMPV and lung lymphocytes were isolated 10 days post-infection. (**A**) Lung cells were stained with M195 tetramer and a panel of Vβ-specific antibodies. The three most common TCR Vβ chains are shown for each individual mouse. (**B**) PD-1 mean fluorescence intensity (MFI) for total M195-specifc T_{CD8s} (red bars) is displayed alongside the MFI for individual Vβ families. (**C**) PD-1 MFI is shown for either M195- (red bar) or N198- (blue bar) specific T_{CD8s}. One representative experiment of two independent experiments with 5 individual mice per experiment is shown.

Viral infection is required for pulmonary T_{CD8} impairment and PD-1 upregulation

To determine whether T_{CD8} upregulate PD-1 in response to other acute viral LRI, we infected B6 mice with influenza virus (strain A/34/PR/8) and measured lung T_{CD8} responses to the immunodominant H2-D^b/$NP_{366-374}$ (NP366) epitope (Flynn et al., 1998) (Figure 2-7A). As previously described (Chang and Braciale, 2002), we observed no impairment at day 7 post-infection. However, there was substantial impairment of both IFNγ production and degranulation by day 14, with the majority of pulmonary NP366-specific T_{CD8} expressing PD-1 at both time points (Figure 2-7B). Intranasal infection of B7tg mice with vaccinia virus (VACV) also resulted in T_{CD8} impairment and PD-1 upregulation for the immunodominant epitopes $A34R_{82-90}$ and $D1R_{808-817}$ (not shown). These data indicate that functional impairment of pulmonary PD-1^{hi} T_{CD8} is a common host response to different virus families capable of causing acute LRI.

Since several human viruses are capable of eliciting pulmonary T_{CD8} impairment, we wondered whether this was a consequence of T_{CD8} trafficking to the unique lung microenvironment. To address this, we employed peptide-loaded, LPS-matured bone marrow-derived dendritic cells (DCs), which are potent antigen presenting cells that, once administered, traffic to draining LNs to prime naïve T_{CD8} (Badovinac et al., 2005b; Hamilton and Harty, 2002). Matured DCs were $CD11b^+$ and upregulated MHC molecules, costimulatory CD86 and the LN homing receptor CCR7 (Figure 2-8A). DCs were loaded with M195 peptide and administered intranasally (i.n.) to recapitulate the route of infection utilized by respiratory viruses and to elicit epitope-specific T_{CD8} in the absence of viral replication. M195-specific T_{CD8} were detectable in the lung by day 5 post-immunization (Figure 2-8B), the same time HMPV-specific T_{CD8} arrive in the lung following HMPV infection. Interestingly, lung-infiltrating M195-specific T_{CD8} elicited by DCs were not impaired at either day 7 or 14 post-immunization (Figure 2-7C) and expressed low levels of PD-1 (~25%, Figure 2-7D) as compared to infection (~75%,

Figure 2-4H). Furthermore, DC-elicited M195-specific T_{CD8} were polyfunctional, with most containing GzmB and producing TNFα and IL-2 in addition to IFNγ (Figure 2-8C). Next, mice were DC immunized either subcutaneously (s.c.) or i.n. to determine if DC-elicited T_{CD8} provide protection against subsequent challenge infection. Following challenge of s.c. immunized mice, only M195-DCs decreased lung viral titers at the peak of virus replication (Figure 2-8D). In contrast, i.n. immunization with mock-DCs loaded with a VACV epitope or N198-DCs resulted in an 8- to 10-fold reduction in viral titers (Figure 2-8E), suggesting that either residual DCs present in the lung or non-specific pulmonary T_{CD8} provide some degree of protection. Importantly, i.n. immunization with M195-DCs resulted in an even greater 35-fold reduction in viral titers as compared to unimmunized mice. Interestingly, mice infected with HMPV and then challenged i.n. with M195-DCs several weeks later exhibited the same degree of T_{CD8} impairment (Figure 2-7E) and PD-1 upregulation (Figure 2-7F) as mice undergoing secondary viral infection, suggesting that the impairment program is maintained in antigen-experienced peripheral memory T_{CD8}, a population that accounts for much of the recall response to secondary viral LRI (Roberts and Woodland, 2004).

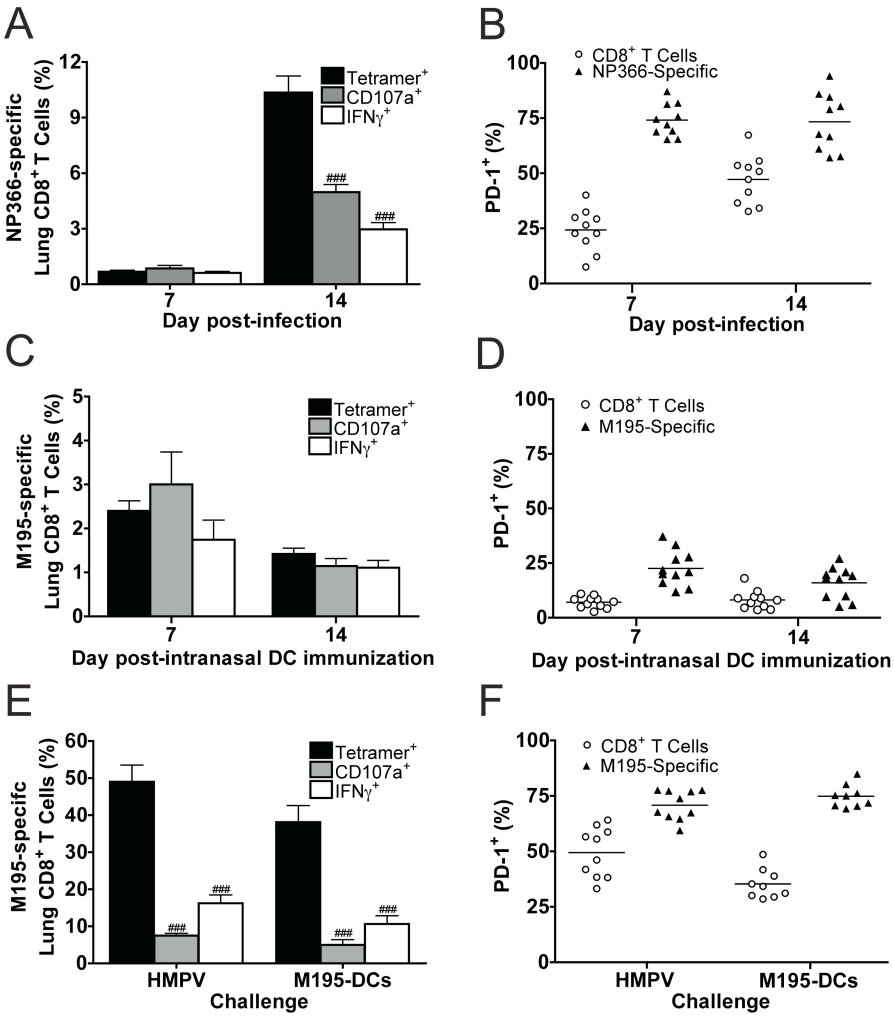

Figure 2-7. Viral infection is required for pulmonary T_{CD8} impairment and PD-1 upregulation. (**A** and **B**) B6 mice were infected with IAV (strain A/34/PR/8) and the lung T_{CD8} response (**A**) and PD-1 expression (**B**) were assessed at days 7 and 14 post-infection for the H2-D^b/$NP_{366-374}$ (NP366) epitope. (**C** and **D**) B7tg mice were immunized i.n. with M195 peptide-loaded, LPS-matured DCs and the lung M195-specific T_{CD8} response (**C**) and PD-1 expression (**D**) were quantified. (**E** and **F)** B7tg mice were infected with HMPV and then challenged at least 50 days later with either virus (HMPV) or M195-loaded DCs (M195-DCs) delivered i.n. Lung lymphocytes were harvested at day 7 post-challenge and the T_{CD8} response (**E**) and PD-1 expression (**F**) were quantified. PD-1 expression on total lung $CD8^+$ lymphocytes (open circles) and epitope-specific $CD8^+$ T cells (closed triangles) are shown (**B**,**D**,**F**). Each symbol represents an individual mouse, while horizontal lines denote the mean for each group. Data are combined from two independent experiments with 5 individual mice per time point per experiment. $^{\#}$ $p<0.05$, $^{\#\#}$ $p<0.005$, $^{\#\#\#}$ $p<0.0005$ (two-tailed, paired t-test).

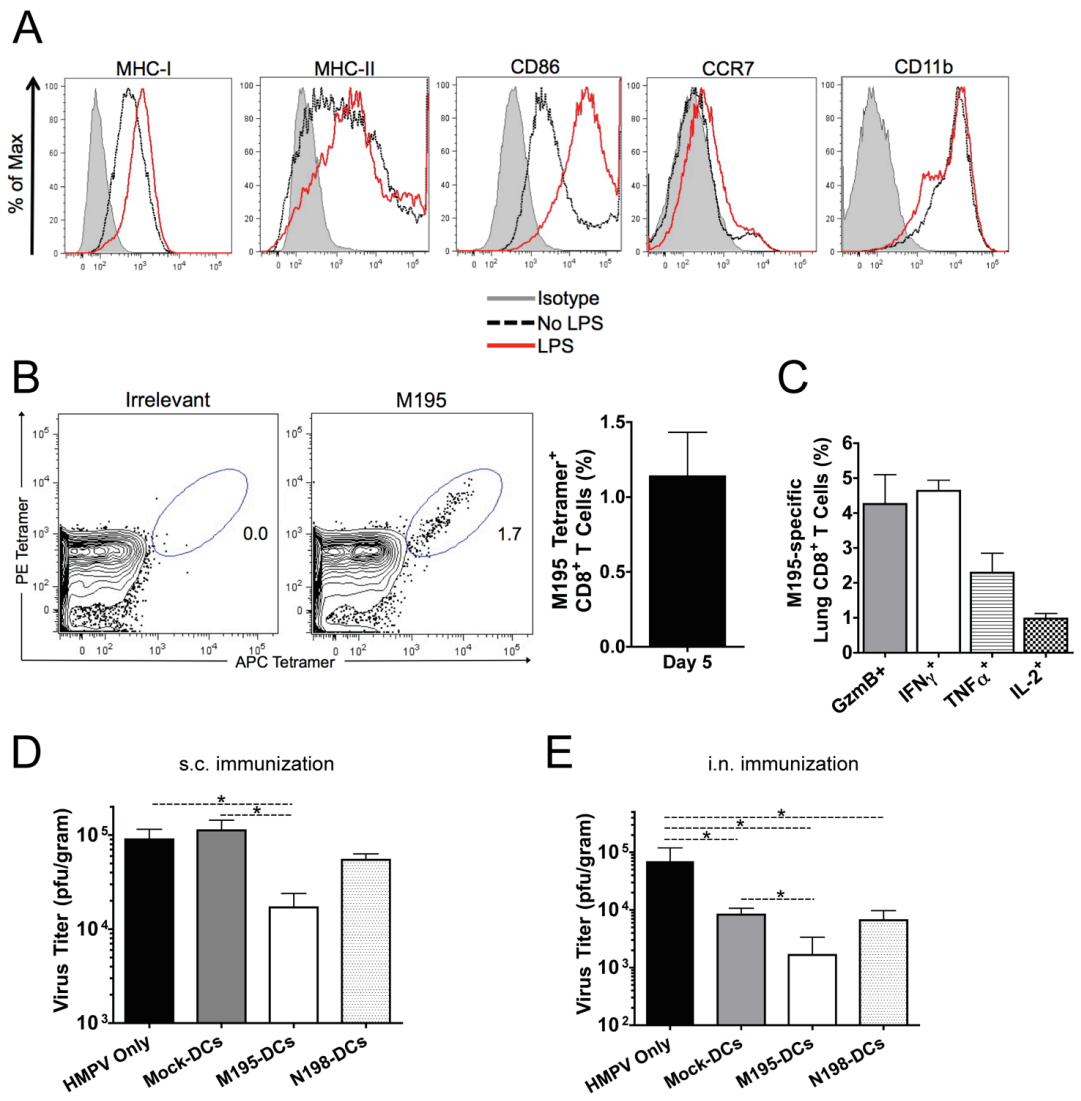

Figure 2-8. Intranasal DC immunization elicits polyfunctional T_{CD8s} capable of protecting mice from challenge infection. (**A**) Bone marrow-derived DCs were either not matured (dotted black line) or matured with LPS (solid red line) and then stained for several maturation markers. (**B** and **C**) B7tg mice were immunized intranasally with M195-loaded, LPS-matured DCs. (**B**) At day 5 post-immunization, lung lymphocytes were isolated and stained with either dual color irrelevant (left flow plot) or M195 (right plot) tetramers to increase the sensitivity of detection. Bar graph displays combined data from several individual mice. (**C**) At day 7 post-immunization, lung lymphocytes were isolated and stained for intracellular GzmB or restimulated with M195 peptide and stained for intracellular IFNγ, TNFα and IL-2. (**D** and **E**) B7tg mice were immunized subcutaneously (s.c.) (**D**) or i.n. (**E**) with DCs loaded with M195 (M195-DCs), N198 (N198-DCs) or an irrelevant vaccinia virus peptide (Mock-DCs). Control animals were unimmunized (HMPV Only). At day 14 post-immunization, mice were challenged with HMPV and 5 days later lungs were harvested for viral titration. Data in (**A** and **B**) are representative of at least two independent experiments. Data in (**C-E**) are combined from 2 or 3 independent experiments with 4-5 individual mice per group per experiment. * $p<0.05$ (one-way ANOVA with Bonferroni post-test)

Cognate viral antigen in the presence of active LRI is required for PD-1 induction and T_{CD8} impairment

Antigen-dependent TCR signaling is associated with PD-1 upregulation during chronic infections (Barber et al., 2006; Blattman et al., 2009; Trautmann et al., 2006; Zhang et al., 2007), but a variety of cytokines can also induce PD-1 independently of antigen exposure (Keir et al., 2008; Kinter et al., 2008). To determine whether viral antigen present at the site of infection is the primary cause of both pulmonary T_{CD8} impairment and PD-1 upregulation, we took advantage of the fact that i.n. DC immunization elicits unimpaired, PD-1^{lo} T_{CD8} directly in the lung environment (Figure 2-7C,D). Therefore, we DC immunized mice i.n. with either the VACV epitope $A34R_{82-90}$ (A34R) or the HMPV epitope M195. There is no cross-reactivity between A34R and any HMPV epitopes as A34R-tetramer fails to stain HMPV-immune splenocytes or lung lymphocytes. A34R-immunized mice were either unchallenged or HMPV challenged, while M195-immunized mice were HMPV challenged (Figure 2-9A). A34R-specific T_{CD8} in unchallenged mice were not impaired (Figure 2-9B), consistent with M195-specific T_{CD8} following M195-DC immunization (Figure 2-7C). Importantly, during HMPV challenge, A34R-specific T_{CD8} were not substantially impaired for either degranulation (Figure 2-9B, Figure 2-10A) or IFNγ production (Figure 2-9B, Figure 2-10B), while M195-specific T_{CD8} in the same infected lungs were severely impaired as during primary infection. Thus, HMPV infection does not impair the functionality of heterologous VACV-specific T_{CD8}. M195-immunized HMPV challenged mice mounted a robust secondary response to the M195 epitope, but were the most severely impaired (Figure 2-9B, Figure 2-10A,B), suggesting that antigen-experienced T_{CD8} are more susceptible to functional exhaustion than T_{CD8} responding to primary infection. The degree of impairment in each group correlated with PD-1 levels: PD-1 expression on A34R-specific T_{CD8} was similarly

low between unchallenged and challenged mice (Figure 2-9C). In M195-immunized HMPV challenged mice, almost 100% of M195-specific T_{CD8} were PD-1^+ (Figure 2-9C) and there was a 60% increase in mean fluorescence intensity (MFI) over that of M195-specific T_{CD8} in A34R-immunized mice (Figure 2-9C), indicating that PD-1 is more highly expressed during secondary immune responses.

During chronic infections, persistent viral antigen causes PD-1-mediated T_{CD8} exhaustion through continuous stimulation of the TCR (Blattman et al., 2009; Keir et al., 2008; Mueller and Ahmed, 2009; Wherry et al., 2003). To determine whether antigen exposure alone is capable of inducing PD-1 expression and functional impairment in the respiratory tract, mice were immunized i.n. with M195-loaded DCs and then administered either an irrelevant peptide or M195 peptide i.n. to provide cognate antigen for TCR stimulation. After re-exposure to cognate antigen, M195-specific T_{CD8} remained fully functional (Figure 2-9D) but significantly upregulated PD-1 (Figure 2-9E), indicating that antigen-dependent TCR signaling is sufficient for PD-1 upregulation but not functional impairment in the acute setting.

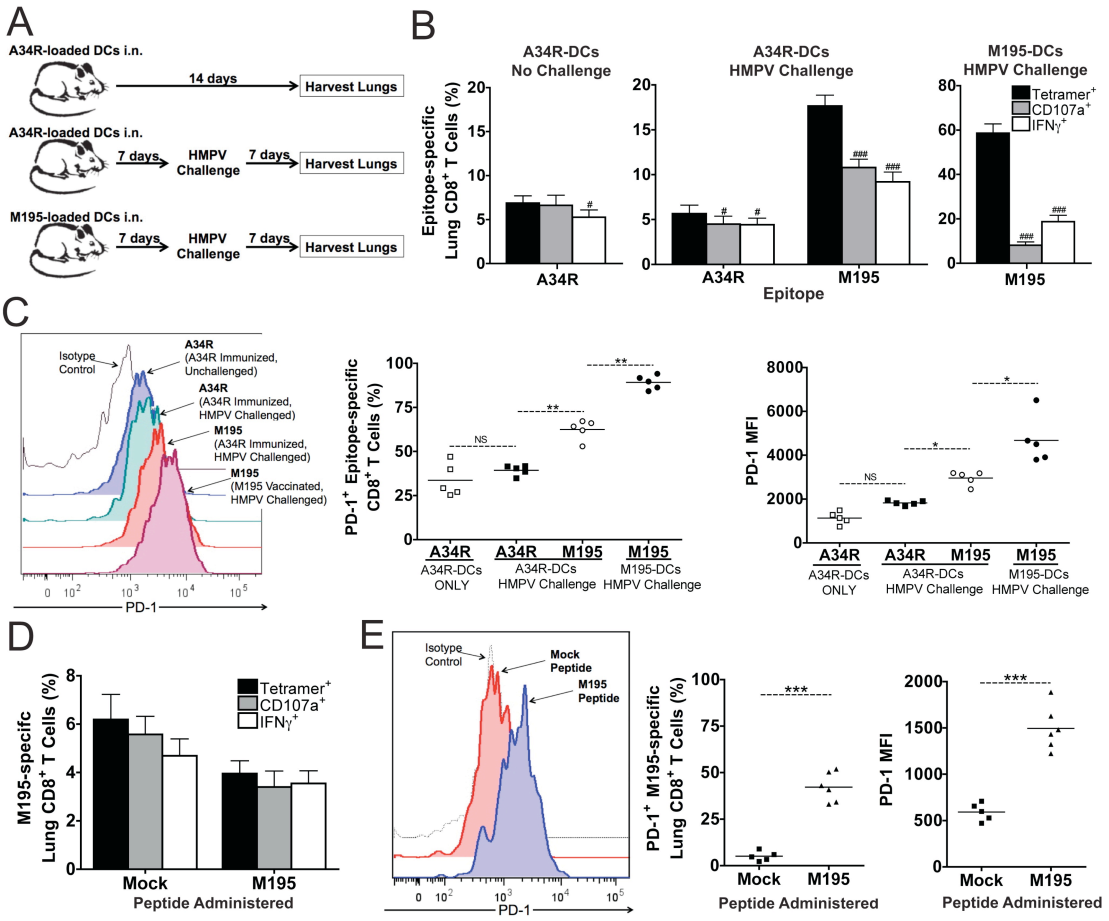

Figure 2-9. Cognate viral antigen in the presence of active LRI is required for PD-1 induction and T_{CD8} impairment. (**A**) Experimental strategy for (**B** and **C**): B7tg mice were immunized i.n. with VACV $A34R_{82-90}$ (A34R)-loaded or HMPV M195-loaded DCs and lung lymphocytes were harvested at either day 14 post-immunization (A34R immunization) or day 7 post-HMPV challenge (both A34R and M195 immunizations). (**B**) The A34R- and M195-specific T_{CD8} responses were quantified in each group of mice as indicated. (**C**) PD-1 expression is shown as either representative histograms, % positive or mean fluorescence intensity (MFI). (**D** and **E**) Mice were immunized i.n. with M195-loaded DCs and then 50µg of either an irrelevant peptide (Mock) or M195 peptide (M195) were administered daily i.n. for 7 days. The M195-specific T_{CD8} response (**D**) and PD-1 expression (**E**) following repeated peptide administration were quantified. Data in (**B**) are combined from three independent experiments while data in (**C-E**) are representative of at least two independent experiments with 4-6 individual mice per group per experiment. $^{\#}$ $p<0.05$, $^{\#\#}$ $p<0.005$, $^{\#\#\#}$ $p<0.0005$ (two-tailed, paired t-test). ^{NS} $p>0.05$, * $p<0.05$, ** $p<0.005$ (one-way ANOVA with Bonferroni post-test [**C**] or two-tailed Student's t-test [**E**]).

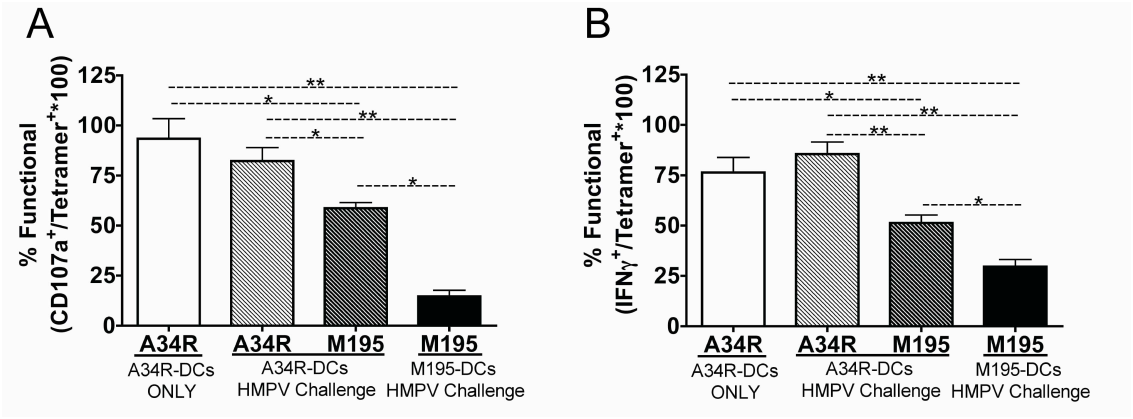

Figure 2-10. Cognate viral antigen is required for pulmonary T_{CD8} functional impairment (continued). From the same experiment in Figure 2-9, the percentage of functional epitope-specific T_{CD8s} was calculated by dividing the percentage of $CD8^+$ T cells that are either $CD107a^+$ **(A)** or $IFN\gamma^+$ **(B)** by the percentage of $CD8^+$ T cells that are $tetramer^+$ for the same epitope. * $p<0.05$, ** $p<0.005$ (one-way ANOVA with Bonferroni post-test).

Taken together, the preceding data suggested that both cognate viral antigen and active LRI are required for PD-1 induction and T_{CD8} impairment. Since cognate antigen alone failed to induce impairment in the absence of infection, we hypothesized that upregulation of the PD-1 ligand PD-L1 was also required. HMPV or IAV infection of human bronchial epithelial cells upregulated PD-L1 in a dose-dependent manner (Figure 2-11), consistent with previous findings for RSV (Stanciu et al., 2006). HMPV also induced PD-L1 upregulation in the lungs of infected mice: PD-L1 gene expression increased 4-fold by day 5 post-infection, 10-fold by day 7, and decreased rapidly by day 14 (Figure 2-12A). In contrast, PD-L1 expression was unchanged on day 7 post-DC immunization and increased slightly by day 14 (Figure 2-12B). Thus, PD-L1 expression increased early during viral infection in association with $PD\text{-}1^{hi}$ T_{CD8}, but not during DC immunization where T_{CD8} are $PD\text{-}1^{lo}$.

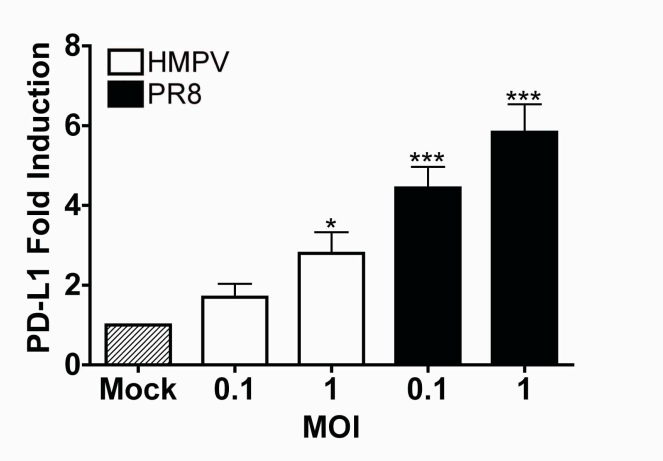

Figure 2-11. Viral infection of human bronchial epithelial cells induces PD-L1 upregulation. Human bronchial epithelial cells (BEAS-2b line) were either mock infected or infected with the given multiplicities of infection (MOI) for HMPV or IAV (strain A/34/PR/8). 48 hours later cells were surface stained for PD-L1 and analyzed by flow cytometry. The fold induction of PD-L1 MFI over mock infection is shown. Data are combined from 4 independent experiments. Asterisks indicate statistically higher PD-L1 levels compared to mock infected cells. * $p<0.05$, *** $p<0.0005$ (two-tailed, Student's t-test).

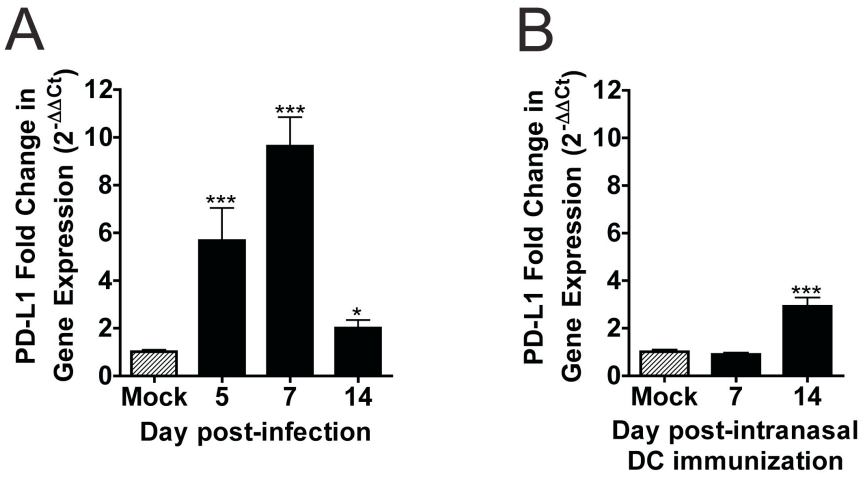

Figure 2-12. PD-L1 expression increases in lungs upon viral infection but not DC immunization. B7tg mice were either infected with HMPV (**A**) or immunized i.n. with M195-loaded DCs (**B**). At the indicated times post-inoculation lung RNA was extracted for quantification of PD-L1 gene expression using real-time RT-PCR. PD-L1 levels were normalized to the housekeeping gene HPRT and the relative gene expression compared to mock infected animals is shown ($2^{-\Delta\Delta Ct}$ method). Data are combined from two independent experiments with 4-6 individual mice per time point per experiment.

Asterisks indicate statistically higher PD-L1 levels compared to mock-infected mice. * $p<0.05$, *** $p<0.0005$ (two-tailed, Student's t-test).

Blockade or ablation of PD-1 signaling prevents pulmonary T_{CD8} functional impairment during acute viral LRI

To prevent PD-1 ligation and determine whether pulmonary T_{CD8} impairment requires infection-induced PD-L1, we injected mice with blocking antibodies against PD-1 ligands (Anti-PD-L) prior to infection and then every two days following infection. Anti-PD-L resulted in a greater percentage of M195-specific T_{CD8} in the spleens of infected animals, but more importantly improved function of pulmonary T_{CD8} compared to mice treated with isotype control antibody (Figure 2-13A). The percentage of functional M195-specific cells increased from 65% to 95% $CD107a^+$ and from 45% to 71% $IFN\gamma^+$ in anti-PD-L mice compared to control mice (Figure 2-13B). Anti-PD-L also augmented the amount of IFNγ synthesized in spleen and lung M195-specific T_{CD8} (Figure 2-13C). The percentage of $PD\text{-}1^+$ M195-specific T_{CD8} increased in both the spleen and lung of anti-PD-L treated mice (Figure 2-13D), again indicating that PD-1 upregulation alone is insufficient to induce T_{CD8} impairment and that ligation by PD-L1 is also required. To gauge the broader immunomodulatory effects of blocking PD-1 signaling, we quantified total cytokine levels in HMPV infected lungs. Anti-PD-L resulted in increased pro-inflammatory cytokines IFNγ, TNFα and IL-6, while IL-17A and the anti-inflammatory cytokines IL-10 and TGFβ were unchanged (Figure 2-13E). Both IL-2 and IL-4 were below the limit of detection (not shown). Importantly, prevention of pulmonary T_{CD8} impairment and augmentation of cytokine levels resulted in enhanced viral clearance, as anti-PD-L reduced lung viral titers 2-fold on day 5 post-infection and greater than 30-fold on day 7 (Figure 2-13F).

Despite the increased level of pro-inflammatory cytokines and functional T_{CD8}, anti-PD-L was not associated with increased lung histopathology (Figure 2-14). However, to gauge more relevant clinical outcomes in live mice, we utilized a mouse oximeter to quantify airway dysfunction, a key feature of severe LRI in humans (Hartert et al., 1999). Airway dysfunction and subsequent air trapping leads to pulsus paradoxus, an exaggeration in the pulse volume during respiration as a result of increased breathing effort (Rebuck and Pengelly, 1973). HMPV infection alone did not increase breathing effort as compared to mock infection (Figure 2-13G). However, anti-PD-L resulted in double the breathing effort of that observed in isotype control treated animals. Thus, anti-PD-L reduced functional impairment in a population of protective HMPV-specific T_{CD8}, but did, to some degree, increase airway dysfunction.

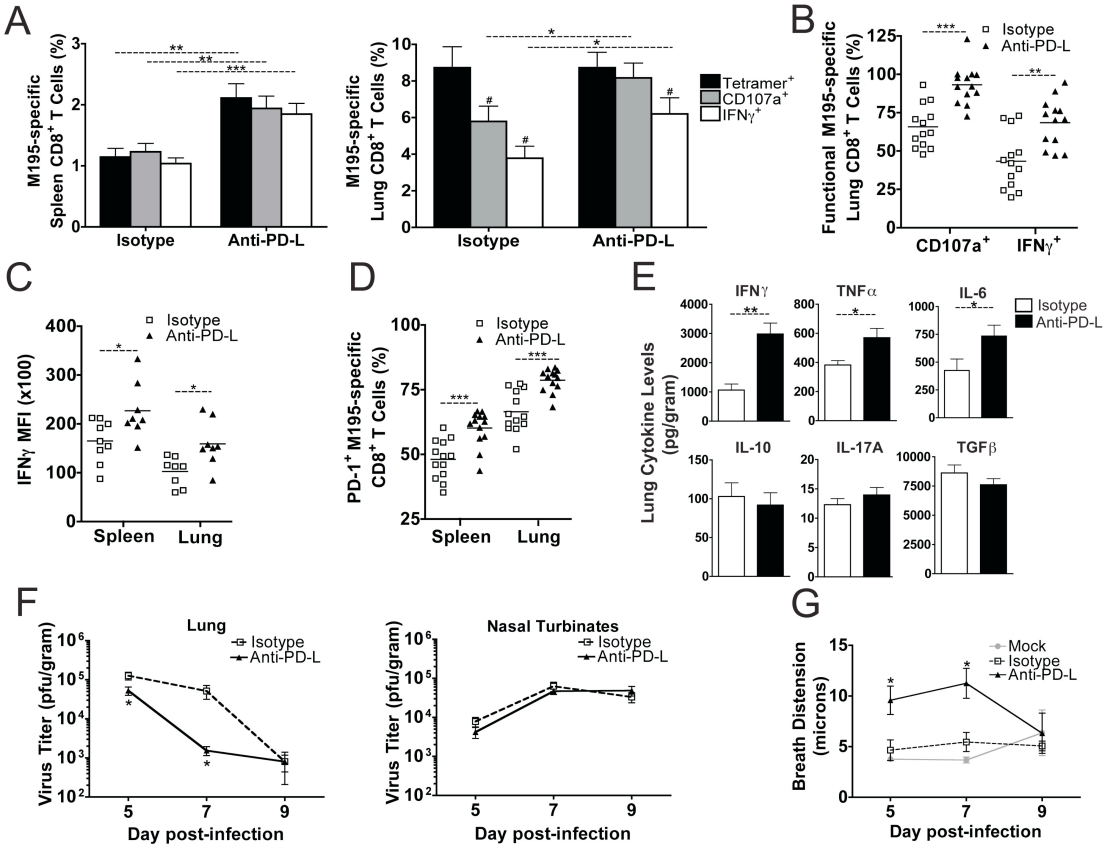

Figure 2-13. Blocking PD-1 ligation prevents functional impairment of pulmonary T_{CD8} during HMPV infection. B7tg mice were injected i.p. with 200µg of isotype control antibody (Isotype) or both anti-PD-L1 and anti-PD-L2 blocking antibodies (Anti-PD-L) for two days prior to infection and then every other day during HMPV infection. (**A**) The M195-specific T_{CD8} response was quantified in the spleen and lung at day 7 post-infection. (**B**) The percentage of functional M195-specific pulmonary T_{CD8} was calculated by dividing the percentage of $CD8^+$ T cells that are either $CD107a^+$ or $IFN\gamma^+$ by the percentage of cells that are $tetramer^+$ for both isotype (open squares) and anti-PD-L (closed triangles) treated mice. (**C**) IFNγ MFI from M195 stimulated cells is shown. (**D**) PD-1 expression on spleen and lung M195-specific $CD8^+$ T cells. (**E**) Lung cytokines were quantified by cytometric bead array at day 7 post-infection. (Note: IL-2 and IL-4 levels were below the limit of detection). (**F**) Lung and nasal turbinate viral titers were quantified via plaque assay on days 5, 7 and 9 post-infection. (**G**) Breath distension of peripheral arteries, a measure of pulsus paradoxus and airway dysfunction, was quantified noninvasively by pulse oximetry as described in Methods. Mock indicates mice that were mock infected. Data in (**A-E**) are combined from two or three independent experiments with 4-5 individual mice per group per experiment, while data in (**F** and **G**) are representative of two independent experiments with 5 mice per group. # $p<0.05$ (two-tailed, paired t-test); * $p<0.05$, ** $p<0.005$, *** $p<0.0005$ (two-tailed, Student's t-test).

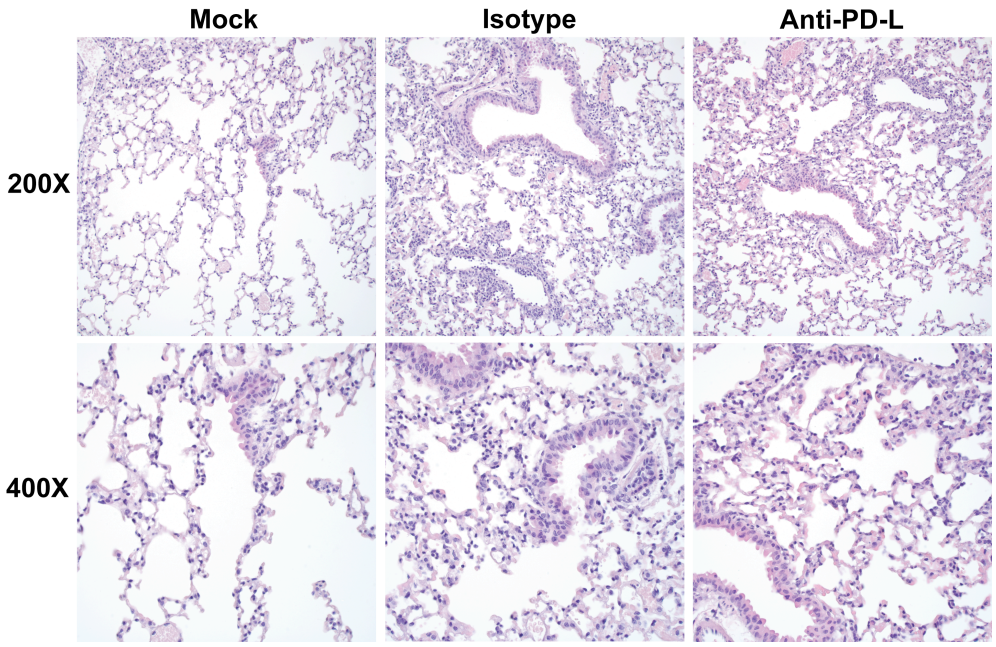

Figure 2-14. Anti-PD-L treatment does not exacerbate lower airway pathology. Mice were treated and infected as described in Figure 2-13. Lung sections from Isotype or Anti-PD-L treated mice were H&E stained. Images are representative of 4-5 individual mice per group. Original magnifications as indicated.

We next employed *PD-1*$^{-/-}$ mice (Nishimura et al., 1998) to completely abolish PD-1 signaling and confirm that results from anti-PD-L treatment were due to inhibition of PD-1 signaling and not reverse signaling through PD-L1 (Keir et al., 2008). *PD-1*$^{-/-}$ mice were maintained on the B6 background, so we examined the HMPV-specific T_{CD8} response directed against the F528 and N11 epitopes. Similarly to anti-PD-L, *PD-1*$^{-/-}$ mice possessed a higher percentage of splenic HMPV-specific T_{CD8} (Figure 2-15A), as well as a greater percentage of lung F528- and N11-specific T_{CD8} that degranulated and produced IFNγ as compared to wildtype (WT) mice (Figure 2-15B). This translated to a greater percentage of functional pulmonary HMPV-specific T_{CD8} in *PD-1*$^{-/-}$ mice (Figure 2-15C). Unlike anti-PD-L, we also observed a 3-to-4-fold increase in the absolute

number of both tetramer^{+} (Figure 2-15D) and IFNγ^{+} (Figure 2-15E) T_{CD8} in *PD-1*$^{-/-}$ mice over WT mice (Figure 2-15E). IFNγ and TNFα cytokine levels were significantly elevated in the lungs of *PD-1*$^{-/-}$ animals, while IL-10 and IL-17A were trending upwards and IL-6 and TGFβ were unchanged (Figure 2-15F). Given both the increased number of HMPV-specific T_{CD8} and their increased functionality in *PD-1*$^{-/-}$ mice, we asked whether PD-1 signaling functions to prevent immunopathology during acute viral LRI. Both WT and *PD-1*$^{-/-}$ mice exhibited the same pattern of peribronchiolitis and perivasculitis with similar numbers of CD3^{+} mononuclear cells infiltrating each of these spaces (Figure 2-15G), suggesting that abrogation of PD-1 signaling in the setting of acute LRI does not exacerbate lower airway histopathology.

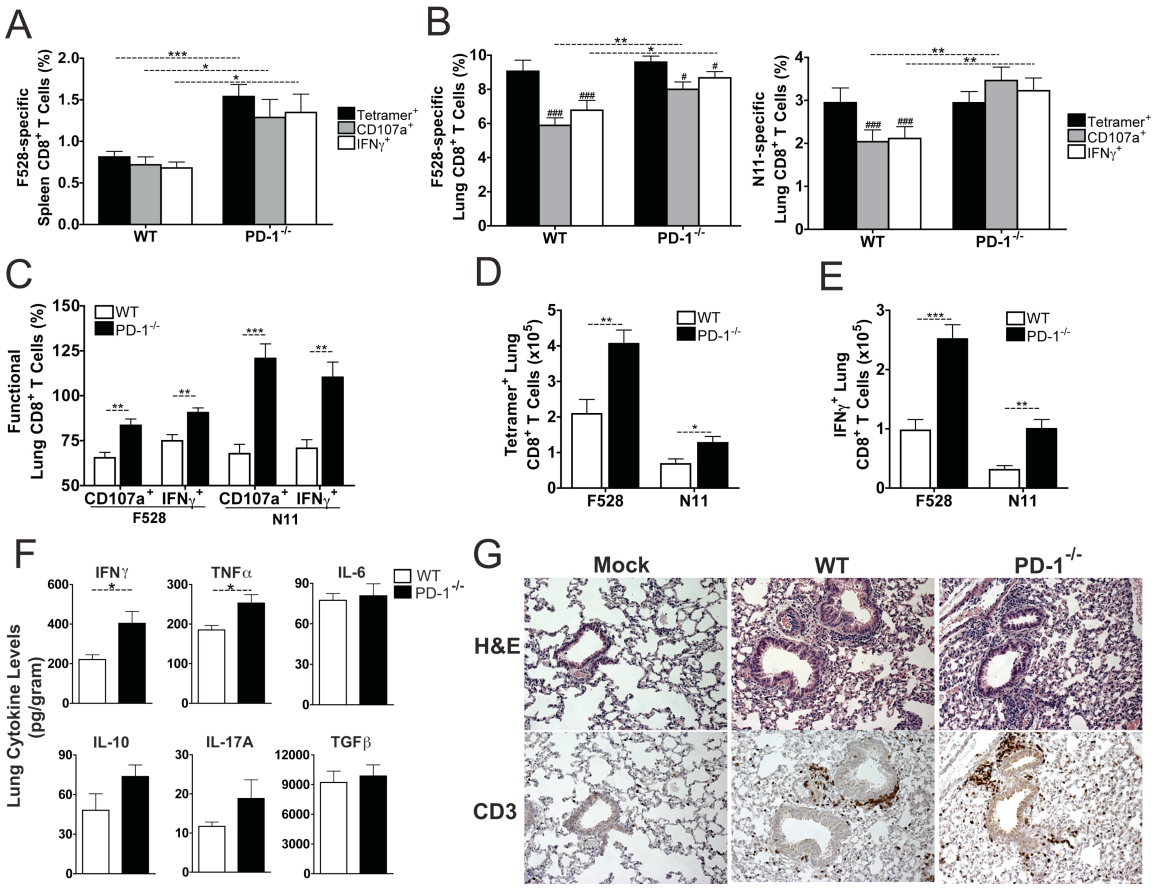

Figure 2-15. Pulmonary T_{CD8} impairment is prevented during HMPV LRI in *PD-1*$^{-/-}$ mice. Wildtype (WT) and *PD-1*$^{-/-}$ mice were infected with HMPV and 7 days later spleen and lung lymphocytes were harvested. (**A** and **B**) The spleen H2-D^b/$F_{528\text{-}536}$ (F528) specific T_{CD8} response (**A**) and the lung F528 and H2-K^b/$N_{11\text{-}19}$ (N11) specific T_{CD8} responses (**B**) were quantified. (**C-E**) The percentage of functional F528- or N11-specific lung T_{CD8} (**C**) as well as the absolute number of tetramer$^+$ (**D**) and IFNγ^+ (**E**) epitope-specific cells were calculated. (**F**) Lung cytokines were quantified by cytometric bead array at day 7 post-infection. (Note: IL-2 and IL-4 levels were below the limit of detection). (**G**) Lung sections from WT or *PD-1*$^{-/-}$ mice were either H&E or anti-CD3 stained. Images are representative of four individual mice per group. Original magnification = 200X. Data are combined from two (**F**) or three (**A-E**) independent experiments with 4-6 individual mice per group per experiment. $^{\#}$ p<0.05, $^{\#\#}$ p<0.005, $^{\#\#\#}$ p<0.0005 (two-tailed, paired t-test); * p<0.05, ** p<0.005, *** p<0.0005 (two-tailed, Student's t-test).

We then tested the effect of PD-1 ablation on influenza virus LRI. Because T_{CD8} were not impaired on day 7 (Figure 2-7A), we examined the T_{CD8} response at day 8 post-infection with IAV (strain HK/x31) in WT versus *PD-1*$^{-/-}$ mice. NP366-specific pulmonary T_{CD8} drastically upregulated PD-1 in WT mice (Figure 2-16A) and were impaired (Figure 2-16B). IFNγ^{+} and CD107a^{+} NP366-specific T_{CD8} were increased in the lungs of *PD-1*$^{-/-}$ mice compared to WT animals (Figure 2-16B,C). The IAV-specific *PD-1*$^{-/-}$ T_{CD8} did not contain more GzmB (Figure 2-16D), suggesting that increased supernatant GzmB levels found in some studies may be attributable to increased degranulation and not increased production (Telcian et al., 2011; Trautmann et al., 2006), while more prolonged blockade of the PD-1 pathway may be necessary to increase T_{CD8} granzyme expression (Velu et al., 2007; Velu et al., 2009). *PD-1*$^{-/-}$ mice took longer to recover from infection than WT mice as measured by weight loss (Figure 2-16E). Additionally, both WT and *PD-1*$^{-/-}$ animals exhibited increased breathing effort compared to mock infection, but, in contrast to anti-PD-L treatment of HMPV infected mice, lack of PD-1 signaling did not exacerbate airway dysfunction (Figure 2-16F). The results of these experiments suggest that PD-1 negatively regulates T_{CD8} during LRI caused by both HMPV and IAV, which may help to speed recovery by limiting adverse immune-mediated effects on respiratory physiology.

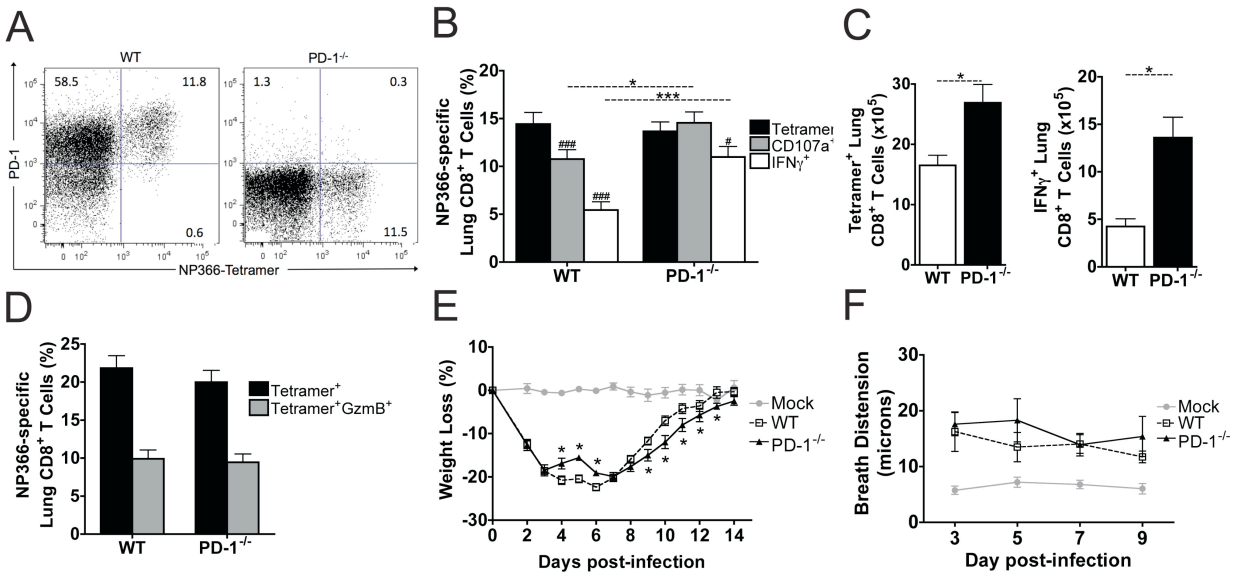

Figure 2-16. Pulmonary T_{CD8} impairment is improved but recovery is delayed in IAV-infected *PD-1*$^{-/-}$ mice**.** WT and *PD-1*$^{-/-}$ mice were infected with IAV (strain HK/x31) and 8 days later lung lymphocytes were isolated. (**A)** Representative flow cytometry plots showing PD-1 staining on NP366-specific T_{CD8} in WT versus *PD-1*$^{-/-}$ mice. Numbers in each quadrant indicate the percentage of $CD8^+$ T cells. (**B**) Quantification of the lung NP366-specific T_{CD8} response. (**C**) The absolute number of tetramer$^+$ (left) or IFNγ^+ (right) NP366-specific lung T_{CD8} was calculated. (**D**) NP366 tetramer-labeled cells were permeabilized and stained for intracellular granzyme B (GzmB). (**E**) Weight loss is shown as a percentage of initial body weight. (**F**) Breath distension was measured as described in Methods. Mock indicates mice that were mock infected. Data are combined from two (**F**) or three (**A-E**) independent experiment with 5 individual mice per group per experiment. $^{\#}$ p<0.05, $^{\#\#\#}$ p<0.0005 (two-tailed, paired t-test); * p<0.05, *** p<0.0005 (two-tailed, Student's t-test).

Anti-PD-L treatment improves secondary immune responses by overcoming T_{CD8} impairment during challenge infection

Given the large degree of impairment observed during secondary infection or DC challenge of previously infected mice, we sought to elucidate the role of PD-1 in inhibiting secondary immune responses. Since primary HMPV infection elicits sterilizing immunity, we employed intranasal DC immunization to elicit lung-infiltrating M195-specific T_{CD8} in the absence of infection. Mice were challenged with HMPV 18 days post-immunization and the M195-specific secondary immune response and viral titers were

quantified at day 5 post-challenge either in the presence or absence of anti-PD-L treatment (Figure 2-17A). Mice that were not DC immunized generated a small M195-specific response (1.3% tetramer$^+$, Figure 2-17B), consistent with previous results observed during primary infection (Figure 2-4D). Mice that were M195-DC immunized and isotype treated mounted a robust secondary M195-specific response (8% tetramer$^+$, Figure 2-17B). However, only half of these cells were functional as determined by CD107a mobilization (56%) or IFNγ production (45%) (Figure 2-17B,C). Anti-PD-L significantly restored both degranulation (87%) and IFNγ production (81%) to M195-specific cells during challenge infection (Figure 2-17B,C). Similarly to anti-PD-L treatment during primary infection, blocking PD-1 ligation resulted in PD-1 upregulation on M195-specific T_{CD8} (Figure 2-17D). Importantly, anti-PD-L reduced lung viral titers 5-fold more than isotype treated mice and greater than 20-fold compared to unimmunized HMPV-infected mice (Figure 2-17E). Taken together, these results indicate that pulmonary T_{CD8} impairment during both primary and secondary infection is mediated by the PD-1/PD-L1 pathway, and that this impairment can be prevented to maintain functional anti-viral T_{CD8} and enhance viral clearance.

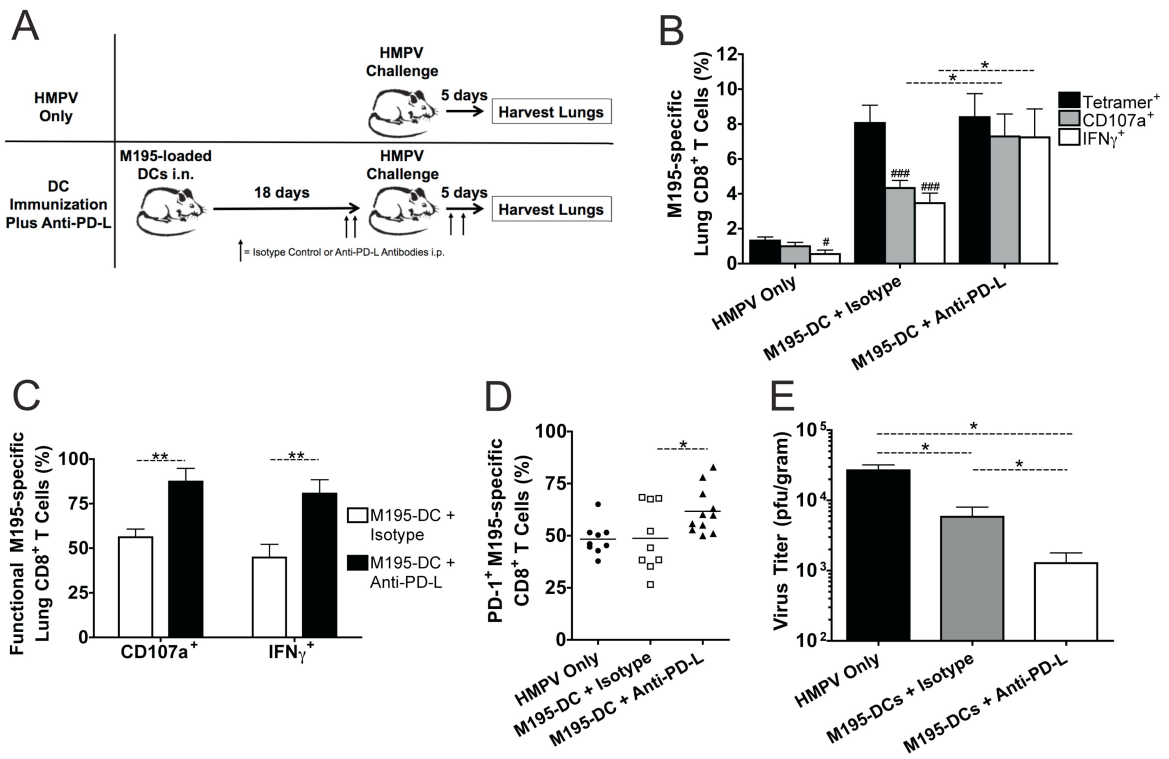

Figure 2-17. Anti-PD-L treatment improves secondary immune responses by overcoming T_{CD8} impairment during challenge infection. (**A**) Experimental strategy: mice were either not immunized (HMPV Only) or immunized i.n. with M195-loaded DCs. Eighteen days later, mice were challenged with HMPV. Immunized mice were injected i.p. with isotype control antibody (M195-DC + Isotype) or both anti-PD-L1 (250µg) and anti-PD-L2 (200µg) blocking antibodies (M195-DC + Anti-PD-L) for two days prior to infection and then on days 1 and 3 during HMPV infection. (**B** and **C**) Five days post-challenge, the lung M195-specific T_{CD8} response was quantified (**B**) and the functionality of these cells was calculated (**C**). (**D**) PD-1 expression on lung M195-specific T_{CD8}. (**E**) Lung viral titers were quantified by plaque assay. Data are combined from two independent experiments with 4-6 individual mice per group per experiment. $^{\#}$ $p<0.05$, $^{\#\#\#}$ $p<0.0005$ (two-tailed, paired t-test); * $p<0.05$, ** $p<0.005$ (two-tailed, Student's t-test).

PD-1 and PD-L1 are expressed in the lower airways of patients with severe 2009 H1N1 pandemic IAV, RSV or PIV-3 infection

To determine whether the PD-1/PD-L1 pathway is activated during acute viral LRI in humans, we obtained autopsy specimens from pediatric and adult patients with severe LRI or nonpulmonary disease as controls. Both 2009 H1N1 pandemic IAV and RSV caused pronounced lung pathology, including severe pneumonia (Figure 2-18B) and bronchiolitis (Figure 2-18C) with extensive T_{CD8} infiltration (Figure 2-18F,G). PD-1 was detected on small lymphocytes and macrophages present in the airway and interstitium (Figure 2-18J,K, Figure 2-19), while PD-L1 was expressed on alveolar and bronchiolar epithelial cells, as well as on airway and tissue macrophages (Figure 2-18N,O,R,S, Figure 2-19). In total, PD-1 was detected in 3/4 2009 H1N1 cases, 2/3 RSV cases and 1/1 PIV-3 case. PD-L1 was detected in 4/4 H1N1 cases, 3/3 RSV cases and 1/1 PIV-3 case. In control cases (4 total), PD-1 and PD-L1 expression was restricted to sparse airway macrophages (Figure 2-18 and Figure 2-19). These results suggest that the PD-1/PD-L1 pathway is engaged and may play a significant role in inhibiting adaptive immune responses during acute viral LRI in humans.

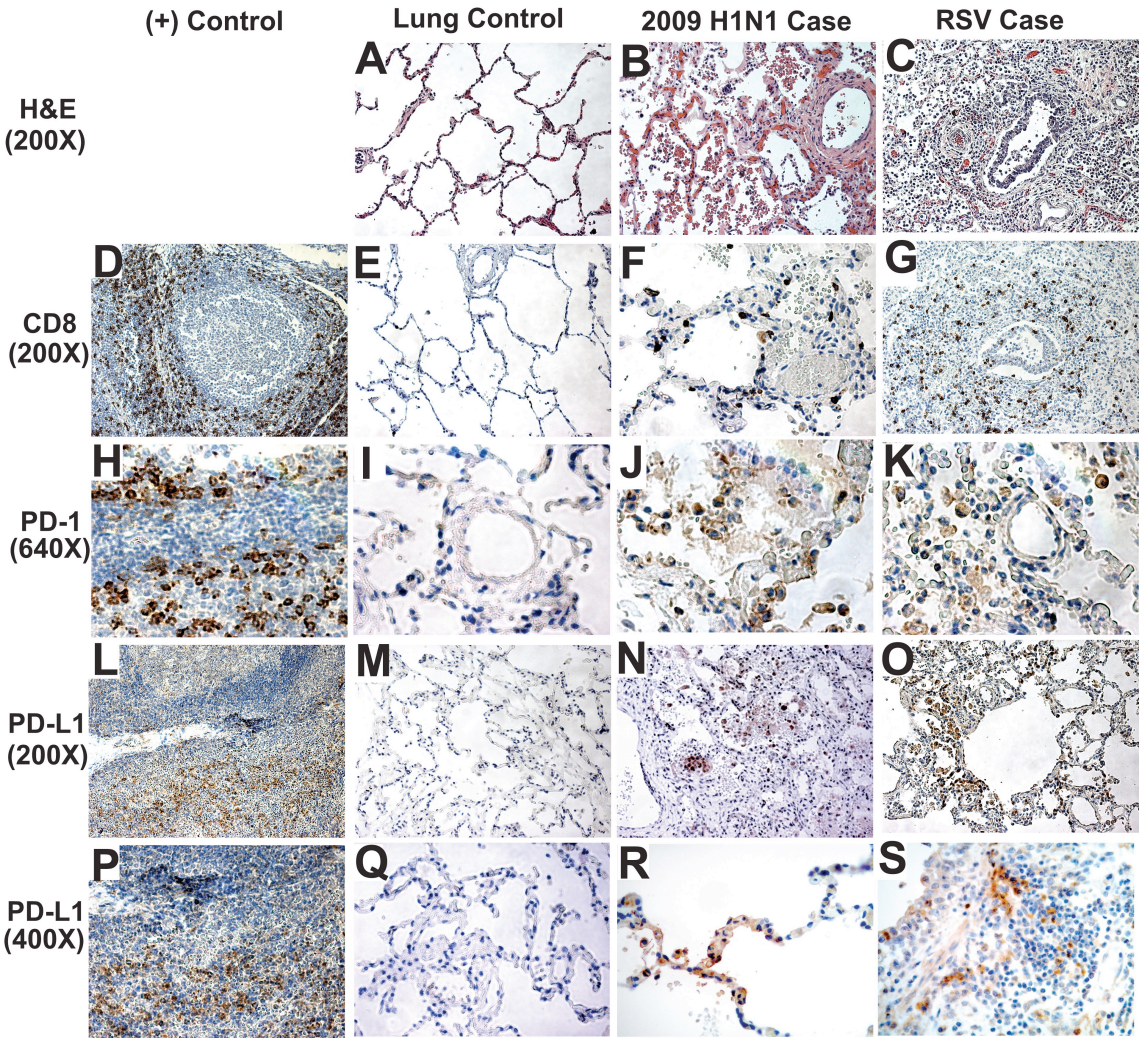

Figure 2-18. PD-1 and PD-L1 are expressed in the lower airways of pediatric patients with severe 2009 H1N1 pandemic IAV or RSV infection (See also Figure 2-19). Lung autopsy specimens were fixed and stained with H&E (**A-C**), anti-CD8 (**D-G**), anti-PD-1 (**H-K**) or anti-PD-L1 (**L-S**) antibodies. Tonsil (**D,H**) or spleen (**L,P**) tissue were used as positive controls. "Lung Control" (**A,E,I,M,Q**) is from a patient with non-pulmonary disease, while "2009 H1N1 Case" (**B,F,J,N,R**) is from a 12-year old patient with 2009 H1N1 pandemic IAV infection and "RSV Case" (**C,G,K,O,S**) is from an 18-month old child with RSV infection. Original magnifications as indicated.

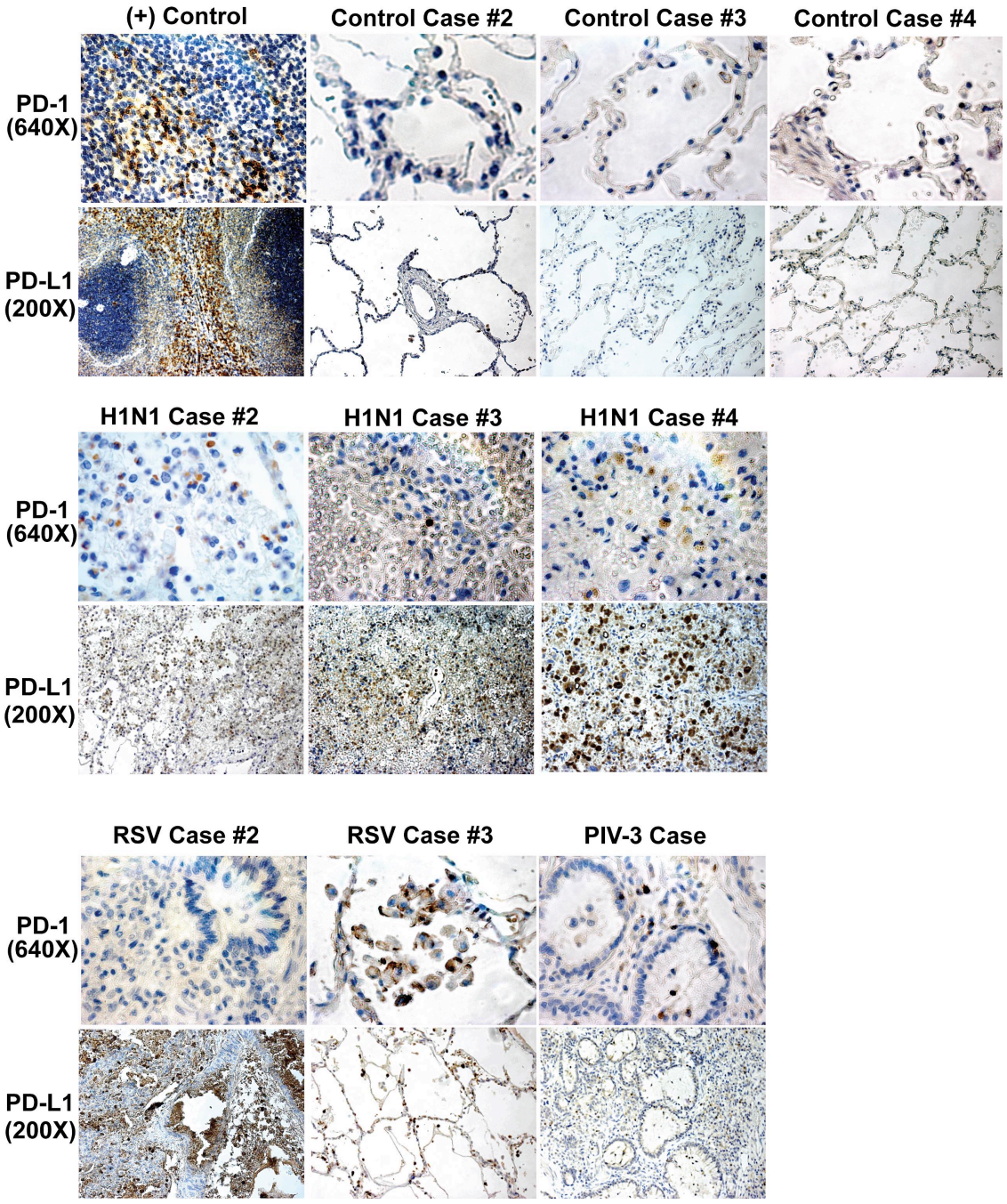

Figure 2-19. PD-1 and PD-L1 are expressed in the lower airways of adult and pediatric patients with severe 2009 H1N1 pandemic IAV, RSV or PIV-3 infection (see also Figure 2-18). Lung autopsy specimens were stained with anti-PD-1 or anti-PD-L1 antibodies. Tonsil or spleen tissues were used as positive controls for PD-1 or PD-L1, respectively. "Control Cases" are from patients with non-pulmonary disease (Case #2 – 33-year old male; Case #3 – 57-year old male; Case #4 – 37-year old male). "H1N1 Cases" are from patients infected with 2009 H1N1 pandemic IAV (Case #2 – 31-year old male; Case #3 – 41-year old male; Case #4 – 19-month old female). "RSV Cases" are from patients infected with seasonal RSV (Case #2 – 2-year old male; Case #3 – 63-year old male).

"PIV-3 Case" is from a 7-year old male infected with PIV-3. Original magnifications as indicated.

DISCUSSION

Pulmonary T_{CD8} impairment has been described during murine acute viral LRI (Chang and Braciale, 2002; DiNapoli et al., 2008; Gray et al., 2005; Lukens et al., 2006; Vallbracht et al., 2006), but the mechanism has not been elucidated. We show in two different mouse models and during both primary and secondary LRI that the PD-1/PD-L1 pathway mediates this impairment. Both dominant and subdominant epitope-specific T_{CD8} were impaired during HMPV, IAV or VACV infections, indicating that loss of pulmonary T_{CD8} function via PD-1 signaling is not restricted to a single virus family. Pulmonary T_{CD8} impairment resembles the exhaustion phenotype observed during chronic viral infections where T_{CD8} upregulate PD-1 and fail to respond when restimulated by viral antigen. T_{CD8} exhaustion occurs several weeks after infection, with the ability to produce IFNγ and TNF lost first, followed later by impaired degranulation and cytotoxic capabilities (Barber et al., 2006; Wherry et al., 2003). In contrast, we found that PD-1-mediated pulmonary T_{CD8} impairment occurred rapidly (by day 7 post-infection), with simultaneous loss of degranulation and IFNγ production that continued for several weeks after viral clearance.

Since PD-1 was upregulated early during acute viral LRI on T_{CD8} but also maintained for several weeks following clearance, it is unclear whether early exposure to viral antigen or persistent low-level TCR stimulation from residual antigen maintains PD-1-mediated impairment after viral clearance. DC (Figure 2-7C,D) and DNA immunization (Chang and Braciale, 2002) experiments suggest that it may be the former, as T_{CD8} elicited in these antigen-low environments maintain effector capabilities. In the current study, we could not detect infectious virus in the lung past day 10; nonetheless, we did

find trace amounts of viral genome via real-time RT-PCR up to 50 days post-infection, similar to genome persistence described for both RSV (Schwarze et al., 2004) and IAV (Kim et al., 2010). This result suggests that persistent viral genome may provide a source of viral antigen to maintain TCR signaling and PD-1 expression even after infectious virus has been eliminated. Additionally, we found that splenic T_{CD8} were unimpaired and down-regulated PD-1 over time, indicating that trafficking away from the infected lung and escape from antigen-driven TCR signaling may prevent impairment.

Additionally, cognate viral antigen in the context of active LRI was required for both pulmonary T_{CD8} impairment and PD-1 expression. Pulmonary T_{CD8} elicited by i.n. DC immunization, where antigen is only transiently presented by the immunizing DCs before MHC class I internalization (Paulsson and Wang, 2004), were unimpaired and PD-1^{lo}. Additionally, heterologous VACV-specific T_{CD8} remained unimpaired and PD-1^{lo} even during HMPV challenge, indicating that antigen-dependent TCR signaling is the primary driver of impairment and PD-1 expression in this setting. However, antigen alone was not sufficient to induce impairment at early time points, as providing cognate peptide to M195-specific T_{CD8} in the lungs of M195-DC immunized mice upregulated PD-1 but did not cause impairment. It is possible that more long term stimulation with antigen may eventually induce impairment. In one model system, chronic antigen stimulation achieved by repeated i.p, injections of IAV lead to T_{CD8} exhaustion, as shown by a severe proliferation defect (Bucks et al., 2009). However, impairment in this setting was not reversed by PD-L1 blockade and was more dependent on TRAIL signaling. During most LRI both antigen and inflammation are abundantly present, so determining the precise role of each in mediating impairment represents a challenge. Our results would suggest that antigen-dependent TCR signaling is an important determinant of PD-1 expression, but that inflammation is also required for the induction of PD-1 ligands and subsequent inhibitory signaling.

Therefore, we hypothesized that regulation and expression of PD-L1contributes significantly to impairment during acute viral LRI. In vitro, both HMPV and IAV infection of human bronchial epithelial cells resulted in PD-L1 upregulation, corroborating findings using RSV, where it was also shown that IFNγ alone is capable of increasing PD-L1 (Stanciu et al., 2006). In vivo, we found that PD-L1 expression correlated with viral replication and the induction of the adaptive immune response, as PD-L1 was upregulated 6-fold by day 5 post-infection (the peak of viral replication) and 10-fold by day 7. HMPV, RSV and IAV all infect respiratory tract epithelial cells. Anti-viral T_{CD8} must recognize and interact with these infected cells in order to clear each virus. Furthermore, it has been demonstrated that RSV infection of primary human bronchial epithelial cells induced PD-L1 upregulation, leading to impairment of human T_{CD8} in vitro (Telcian et al., 2011). Therefore, we propose a model whereby viral antigen signaling through the TCR leads to PD-1 upregulation on pulmonary T_{CD8}, while viral infection of airway epithelial cells induces PD-L1, leading to PD-1 ligation and inhibitory signaling when T_{CD8} interact with infected cells. This may represent a negative feedback loop designed to protect the lung against immune-mediated damage. Anti-viral T_{CD8} enter the lung at day 5 post-infection capable of degranulating and producing IFNγ, yet by day 7 show signs of impairment. IFNγ produced by either $CD8^+$ or $CD4^+$ T cells may then upregulate PD-L1 on respiratory epithelial cells, thereby initiating PD-1 signaling in anti-viral T_{CD8} and down-regulating their effector functions. This contrasts with chronic viral infections caused by LCMV (Mueller et al., 2010; Rodriguez-Garcia et al., 2011) and HIV (Rodriguez-Garcia et al., 2011), where myeloid cells have been shown to contribute more to impairment and exhaustion, suggesting that viral tropism may dictate which cell types mediate impairment. In the case of viral LRI, it could be infected lung epithelial

cells, adjacent cells exposed to type I or type II IFNs, or both of these cell populations that contribute to T_{CD8} impairment *in vivo*.

We show that pulmonary T_{CD8} impairment is preventable, indicating a novel therapeutic avenue for acute viral LRI, for which few specific treatments currently exist. Disruption of PD-1 signaling via therapeutic antibody blockade preserved T_{CD8} effector functions and decreased viral titers. As T_{CD8} functions also improved during both HMPV and IAV infections of *PD-1*$^{-/-}$ mice, targeting the PD-1/PD-L1 pathway may provide clinical utility by enhancing anti-viral T_{CD8} during a variety of acute LRI. Increasing T_{CD8} effector functions and the presence of proinflammatory cytokines did not exacerbate airway histopathology in either anti-PD-L treated or *PD-1*$^{-/-}$ mice. This contrasts with both chronic LCMV infection (Barber et al., 2006) and acute coronavirus CNS infection (Phares et al., 2009), where PD-L1$^{-/-}$ mice exhibited exacerbated pathology and increased mortality, indicating that PD-1 may play differential roles depending on the virus and site of infection. We observed differences even among LRI caused by different viruses, as anti-PD-L treatment of HMPV infected mice resulted in mildly increased breathing effort and pulsus paradoxus, whereas IAV infected *PD-1*$^{-/-}$ mice displayed no enhanced airway dysfunction compared to WT mice. Thus, a therapeutic “window” for PD-1/PD-L1 modulation during acute viral LRI may exist between enhanced protection and immunopathology. Direct manipulation of the PD-1/PD-L1 pathway has so far proven safe and at least partially effective against both hematologic malignancies (Berger et al., 2008) and solid tumors (Brahmer et al., 2010) in humans and against SIV in non-human primates (Velu et al., 2009). Cytokine therapies that indirectly overcome PD-1 signaling also hold therapeutic promise (Chang et al., 2004; Pellegrini et al., 2011).

DC challenge of HMPV primed mice was not capable of overcoming the impairment program set in motion during primary infection, adding to recent findings that high levels of viral antigen present during the initial infection mediate chromatin

remodeling around the PD-1 locus allowing for rapid expression in memory T_{CD8} upon re-exposure to antigen (Youngblood et al., 2011). Furthermore, our results and those from the LCMV chronic infection model (West et al., 2011) indicate that antigen-experienced T_{CD8} are highly susceptible to PD-1-mediated impairment. During challenge infection T_{CD8} rapidly upregulated PD-1 and were more severely impaired than during primary infection. Following DC immunization, we demonstrated that memory T_{CD8} provide some protection against viral challenge, which can be augmented by blocking PD-1 signaling. Therefore, modulation of the PD-1/PD-L1 pathway should be considered in the rational design of novel HMPV, RSV or IAV vaccines. Future experiments are needed to further uncover the role of PD-1 in inhibiting memory T_{CD8} responses.

Finally, we determined that PD-1 and PD-L1 are abundantly expressed in the lower airways during acute viral LRI in humans. Additional studies are needed to determine if PD-1 levels are associated with T_{CD8} impairment and poor clinical outcomes in patients with severe acute viral LRI. However, unlike in chronic infections with HIV and HCV, peripheral blood T_{CD8} may not exhibit functional impairment, and thus examination of pulmonary T_{CD8} will be required. Additionally, while our findings suggest that the PD-1/PD-L1 pathway may contribute to severe disease in humans, it will be interesting to determine what role this pathway plays in the ability of common respiratory viruses to continuously reinfect individuals. Human airway epithelial cells upregulate PD-L1 and PD-L2 in response to IFNγ and TNFα in vitro (Kim et al., 2005; Stanciu et al., 2006) and to human rhinovirus infection in vivo (Heinecke et al., 2008). Therefore, upon reinfection, upper and lower respiratory tract epithelial cell PD-L would be poised to impair airway resident memory T cells as well as newly recruited cells, thus preventing an effective early immune response to limit viral replication. Results from anti-PD-L treated mice that were DC immunized suggest that memory T_{CD8} may be similarly, if not more, affected by PD-1 signaling than naïve cells. Taken together, our results indicate

that antigen-dependent PD-1 upregulation and subsequent ligation by PD-L1 plays a prominent role in mediating pulmonary T_{CD8} impairment. These findings suggest that targeting the PD-1/PD-L1 pathway may provide therapeutic potential in patients with acute viral LRI and offer novel approaches for developing effective respiratory viral vaccines.

MATERIALS AND METHODS

Mice and Viruses

C57BL/6 (B6) mice were purchased from the Jackson Laboratory. B6-Kb^0Db^0;B7.2 transgenic (B7tg) mice were obtained with permission from Drs. Alexander Sette (La Jolla Institute for Allergy and Immunology, La Jolla, CA) and Francois Lemonnier (Institut Pasteur, Paris, France). *PD-1*$^{-/-}$ mice were obtained with permission from Dr. Tasuku Honjo (Kyoto University, Kyoto, Japan). All animals were bred and maintained in specific pathogen-free conditions in accordance with the Vanderbilt Institutional Animal Care and Use Committee. 6-12 week old age- and gender-matched animals were used in all experiments. HMPV (pathogenic clinical strain TN/94-49, genotype A2) was grown and titered in LLC-MK2 cells as previously described (Williams et al., 2005). Influenza virus strains A/34/PR/8 (PR8; H1N1; ATCC) and HK/x31 (x31; H3N2; kindly provided by Dr. Jon McCullers, St. Jude Children's Hospital, Memphis, TN) were grown in MDCK cells and titered on LLC-MK2 cells. The CR-19 strain of vaccinia virus was grown and titered on BSC-40 cells. For all experiments, mice were anesthetized with ketamine-xylazine and infected intranasally (i.n.) with $1.5x10^6$ PFU of HMPV, 10^2 PFU of PR8, $5x10^2$ PFU of x31, or 10^4 PFU of VACV in a 100uL volume. x31 was used in experiments with *PD-1*$^{-/-}$ mice because it induced a more robust $CD8^+$ T cell response than PR8.

Viral titration and quantification of total lung cytokines

Viral titers were measured by plaque titration as previously described (Williams et al., 2005). Cytometric Bead Array was used to quantify IFNγ, TNFα, IL-2, IL-4, IL-6, IL-10, IL-17A and TGFβ cytokine levels in undiluted lung homogenates according to the manufacturer's instructions (BD Biosystems).

Epitope prediction, synthetic peptides and IFNγ ELISPOT assays

The online prediction algorithms SYFPETHI, BIMAS and IEDB were used to generate HMPV epitope predictions for the HLA-B**0702* (Rock et al., 2011), H2-D^b and H2-K^b alleles. The top ~80 HLA-B**0702*-, ~40 H2-D^b- and ~40 H2-K^b-restricted 8-10 amino acid long predictopes were synthesized for HLA-B**0702* (by Mimotopes) or $H2^b$ (by Genscript) to >95% purity as determined by analytical high-performance liquid chromatography. ELISPOT analysis was performed as previously described (Rock and Crowe, 2003). The mitogen Concanavalin A (i.e. ConA, Sigma) was used as a positive control, while stimulation with an irrelevant peptide served as the negative control. The average number of spots in the negative control wells was subtracted from each experimental value, which was then expressed as spot forming cells (SFC) per 10^6 lymphocytes.

Generation of MHC class I tetramers

The construct encoding a hybrid heavy chain of the HLA-B**0702* molecule was designed by replacing amino acids 206-299 of the human α3 domain (NCBI RefSeq NM_002116.6 and NM_005514.6) with amino acids 203-296 from the mouse H2-K^b molecule (NCBI RefSeq NM_001001892.2). Constructs expressing H2-K^b and -D^b heavy chains were previously described (Choi et al., 2001). Recombinant heavy chains encoding a C-

terminal BirA recognition sequence and β2m were produced in *Escherichia coli* as described (Rodenko et al., 2006). MHC class I monomers were refolded with cognate conditional peptide ligands (Bakker et al., 2008), biotinylated and purified as described (Toebes et al., 2009). UV-mediated exchange of conditional peptide with viral-derived peptides and quantification of peptide exchange were conducted as previously described (Hadrup et al., 2009). MHC tetramer formation with PE- and APC-streptavidin conjugated fluorochromes (Invitrogen) was performed as previously described (Hadrup et al., 2009). Tetramers were generated for the following viral epitopes: **HMPV** (HLA-B*0702/$M_{195-203}$ [APYAGLIMI], HLA-B*0702/$N_{198-206}$ [YPRMDIPKI], H2-D^b/$F_{528-536}$ [SGVTNNGFI], H2-K^b/N_{11-19} [LSYKHAIL]), **influenza virus** (H2-D^b/$NP_{366-374}$ [ASNENMETM]), **vaccinia virus** (HLA-B*0702/$A34R_{82-90}$ [LPRPDTRHL], HLA-B*0702/$D1R_{808-817}$ [RPSTRNFFEL]).

Tetramer staining

Lymphocytes were isolated from spleens and lungs of infected animals as follows: lungs were rinsed in R10 media (RPMI-1640 [Mediatech] plus 10% FBS, 2mM glutamine, 50μg/mL gentamicin, 2.5μg/mL Amphotericin B and 50μM β-mercaptoethanol [Gibco]) to remove blood. The lungs were then minced with a scalpel and incubated with 2mg/mL Collagenase A (Roche) and 20μg/mL DNase (Roche) for 1hr at 37°C. Single cell suspensions of digested lungs or whole spleens were obtained by pressing through a steel screen (80 mesh) and then passing over a nylon cell strainer (70μm pore size). Erythrocytes were lysed using RBC Lysis Buffer (Sigma). 2-3x10^6 lymphocytes were added to each well of a 96-well round-bottom plate (Falcon). Lymphocytes were first stained with violet LIVE/DEAD dye (Invitrogen) according to the manufacturer's instructions, then Fc-blocked with 1μg per 10^6 cells anti-CD16/32 (BD Biosciences), and finally incubated with PE- or APC-labeled tetramers (0.1-1 μg/ml), anti-CD8α (clone 53-

6.7, BD Biosciences), and anti-CD19 (clone 1D3, eBioscience). In some experiments, cells were also stained for PD-1 (clone J43, BD Biosciences) or with an isotype control antibody (hamster IgG2κ). Surface/tetramer staining was performed for 1.5 hours at 4°C in PBS containing 1% FBS for HLA-B**0702* tetramers. For $H2^b$ tetramers, surface/tetramer staining was performed for 1 hour at RT in FACS buffer containing 50 nM Dasatinib (LC Laboratories) (Lissina et al., 2009) as preliminary experiments demonstrated enhanced tetramer staining under these conditions. Background staining levels with an irrelevant tetramer (typically 0.05-0.2% of $CD8^+$ T cells) were subtracted from each experimental value. For intracellular GzmB staining, cells were additionally surface stained for CD62L (clone MEL-14, BD Biosciences) and then fixed and permeabilized (BD Fix/Perm Reagent) and incubated with anti-GzmB (clone GB12, Invitrogen) for 30min at 4°C. $GzmB^+$ cells were identified by exclusionary gating from the $CD62L^+$ population as previously described (Yuen et al., 2010). Flow cytometric data were collected using an LSRII (BD Biosciences) and analyzed with FlowJo software (Tree Star).

Peptide restimulation and intracellular cytokine staining (ICS)

In parallel with tetramer staining, lung or spleen lymphocytes isolated from the same mice were restimulated *in vitro* for 6 hours at 37°C with the indicated synthetic peptide (10μM final concentration) in the presence of anti-CD107a antibody (clone 1D4B, BD Bioscience). The protein transport inhibitors brefeldin A and monensin (BD Bioscience) were added for the final 4 hours of restimulation. Stimulation with PMA/Ionomycin (50ng/mL PMA plus 2ug/mL ionomycin, Sigma) served as a positive control. After restimulation, cells were surface stained for CD3ε (clone 145-2C11), CD8α and CD19, followed by fixation/permeabilization and staining for intracellular IFNγ (clone XMG1.2),

TNFα (clone MP6-XT22) and/or IL-2 (clone JES6-5H4) (all from BD Bioscience) and analyzed by flow cytometry. Background CD107a/cytokine levels following restimulation with an irrelevant peptide were subtracted from each experimental value.

Generation of bone marrow-derived dendritic cells and immunizations

In preliminary experiments, we isolated primary pulmonary DCs from naïve mice using magnetic selection with anti-CD11c microbeads (Miltenyi Biotec) and then peptide-loaded/LPS-matured them before immunizing recipient mice i.n.. The purity of the isolated $CD11c^+$ DCs was 95-98% and approximately 8-10% were $CD103^+$ lung-resident DCs, which have been shown to efficiently home to draining LNs to prime naïve T cells during respiratory virus infection (Kim et al., 2010). Intranasal immunization with $3x10^5$ peptide-loaded, LPS-matured lung $CD11c^+$ DCs elicited unimpaired, PD-1^{lo} epitope-specific T_{CD8} (not shown). However, because of the need for large numbers of naïve mice to obtain a sufficient quantity of pulmonary DCs, bone marrow-derived DCs were employed for all immunization experiments. bmDCs were generated as previously described (Matheu et al., 2008) with slight modifications. Briefly, bone marrow was obtained from the femurs and tibiae of B7tg mice, lysed of erythrocytes, and resuspended at 10^6 cells/mL in DC Media (R10 plus 20ng/mL rmGM-CSF and 10ng/mL rmIL-4 [Peprotech]) in 10cm sterile tissue-culture dishes. After 3 days of culture, 75% of the media was replaced with fresh DC Media and at day 6 cells were counted and re-plated. On day seven,100ng/mL LPS (Sigma) and 10μM peptide were added overnight to mature and load the DCs with a particular epitope, respectively. The next day DCs were collected, counted and resuspended in PBS. By this time >85% of cells were $CD11c^{hi}$ as determine by flow cytometry, which is characteristic of murine DCs. Maturation status was determined by staining unmatured or LPS-matured DCs for HLA-B**0702* (clone sc-53304, Santa Cruz Biotechnology, Inc.), H2-IA^b (clone 25-9-17, BD

Bioscience), CD86 (clone GL-1, BD Bioscience), CCR7 (, eBioscience), CD11b (clone M1/70, BD Bioscience) and CD11c (clone HL3, BD Bioscience). For generation of lung-infiltrating epitope-specific T_{CD8}, mice were immunized i.n. with $2x10^6$ peptide-loaded, LPS-matured DCs. Some mice were then challenged as described in figure legends. Additionally, some mice immunized i.n. with M195-loaded DCs were treated daily i.n. with either 50µg of M195 peptide or an irrelevant HLA-B**0702*-restricted peptide. The same procedure was used to isolate lung lymphocytes from DC immunized mice and virus infected mice.

Real-time RT-PCR

Metal screens used for obtaining single-cell lymphocyte suspension from lungs (see above) were rinsed with 1mL of RLT lysis buffer (Qiagen) and the cell lysates were collected and frozen at -20°C. Samples were thawed and RNA was extracted using the MagNA Pure LC Total Nucleic Acid Isolation Kit (Roche Applied Sciences) on a MagNA Pure LC using the Total NA External Lysis protocol and stored at -80°C until further use. Real-time RT-PCR was performed in 25µL reaction mixtures containing 5µL of extracted RNA on an ABI StepOnePlus Real-Time PCR System (Life Technologies/Applied Biosystems) using the AgPath-ID One-Step RT-PCR kit (Applied Biosystems/Ambion). For HMPV genome detection, primers and probe targeting the HMPV N gene were previously published (Ali et al., 2011). Viral genome copy number was determined using a standard curve generated with RNA runoff transcripts of the target. For PD-L1 gene expression, exon-spanning primers and probes were obtained and used according to the manufacturer's instructions (Applied Biosystems/Ambion). All values were normalized to the housekeeping gene HPRT and experimental samples are reported as fold change in PD-L1 compared to mice that were mock infected (100µL i.n. of LLC-MK2 cell lysate) using the ΔΔCt method. Cycling conditions were 50°C for 30 min, followed by an

activation step at 95°C for 10 min and then 45 cycles of 15 sec at 95°C and 30 sec at 60°C. Samples with cycle threshold (Ct) values less than 40 were considered positive.

PD-L blocking antibodies

Mice were injected i.p. with rat isotype control antibody (Bio X-cell, clone LTF-2) or both rat anti-mouse PD-L1 (Bio X-cell, clone 10F.9G2) plus rat anti-mouse PD-L2 (Bio X-cell, clone TY-25) antibodies as described in figure legends.

PD-L1 expression on human bronchial epithelial cells

The human bronchial epithelial cell line BEAS-2b was either mock infected with LLC-MK2 cell lysate or infected at various multiplicities of infection (MOI) with either HMPV or PR8 in serum-free Opti-MEM containing trypsin. 48 hours later cells were collected, LIVE/DEAD stained (see above), and then incubated with mouse anti-human PD-L1 antibody (clone MIH1, BD Biosciences) or isotype control for 30min at 4°C. The fold-increase in PD-L1 expression over mock infection was determined by flow cytometry.

Immunohistochemistry of mouse and human lung specimens

Mouse. Mock- (i.e. LLC-MK2 cell lysate) or virus-infected lungs were inflated with 10% formalin and fixed overnight. Samples were then paraffin-embedded and sectioned 5μm in thickness before placing on charged slides and baked overnight at 50°C. The paraffin was removed from the slides, and the sections were placed in heated Target Retrieval Solution (DakoCytomation) for 20 min. After an additional 20 min of cooling, the slides were rinsed in Tris-buffered saline–Tween for 5 min immediately prior to being placed on an automated Leica Bond-Max IHC stainer. Endogenous peroxidase was neutralized with 0.03% hydrogen peroxide. Lungs were stained with anti-CD3 (Santa Cruz

Biotechnology, Inc.) for 60min at RT. The Bond Intense R detection system was used for visualization.

Human. Tissue blocks obtained at autopsy from patients with confirmed LRI were provided by the Vanderbilt Translational Pathology Shared Resource with approval from the Vanderbilt Institutional Review Board (#111350). Influenza virus was detected by nasal swab in most cases and confirmed by lung H1N1 viral probe at the time of death. RSV infection was confirmed by rapid antigen testing. PIV-3 was confirmed by viral culture. Control lung specimens were obtained from individuals who expired from non-pulmonary disease. Patient characteristics are provided in the relevant figure legends. Samples were prepared as described above for mouse lungs. Anti-PD-L1 (clone 29E.2A3, BioLegend Inc.), anti-PD-1 (clone 7A11B1, Sigma-Aldrich) and anti-CD8 antibodies (clone C8/144B, Thermo Scientific) were used as the primary antibodies. The Bond Refine Polymer detection system was used for visualization. The slides were counterstained lightly with Mayer's hematoxylin, dehydrated, and coverslipped.

Pulse Oximetry

A rodent pulse oximeter (MouseOx, Starr Life Sciences Corp.) was used to measure breath distension as previously described (Stokes et al., 2011).

Statistical analysis

Data analysis was performed using Prism v4.0 (GraphPad Software). Comparisons between tetramer staining and ICS within the same animals were performed using a paired two-tailed *t* test. Comparisons between two groups were performed using an unpaired two-tailed Student's *t* test. Multiple group comparisons were performed using a one-way ANOVA with a Bonferroni post-test for comparison of individual groups. $p<0.05$

was considered significant, with *p*-values of $p<0.005$ and $p<0.0005$ reported where applicable. Error bars on each graph represent standard error of the mean.

Study approval

All animals were maintained in accordance with the NIH Guide for the Care and Use of Laboratory Animals and were handled according to protocols approved by the Vanderbilt University subcommittee on animal care (IACUC). The study involving analysis of human autopsy specimens was approved by the Vanderbilt University Institutional Review Board.

CHAPTER III

PD-1 Impairs Secondary Effector Lung $CD8^+$ T Cells During Respiratory Virus Reinfection

INTRODUCTION

Respiratory viruses like human metapneumovirus (HMPV) and respiratory syncytial virus (RSV) are important causes of acute lower respiratory infections (LRI), which result in significant morbidity and mortality, especially in infants, the elderly and the immunocompromised. No effective vaccines or therapeutics exist for these viruses. The majority of LRI beyond infancy are actually reinfections, as nearly all individuals experience primary infection during early childhood (van den Hoogen et al., 2001a). HMPV reinfection in children causes illness at a rate that equals primary infection (Pavlin et al., 2008) and can occur with both genetically heterologous and homologous viruses (Yang et al., 2009). Despite a high frequency of infection and minimal antigenic drift, protective immunity is poorly established, as individuals can be repeatedly reinfected throughout life (Hall et al., 1991; Johnson et al., 1961; Kroll and Weinberg, 2011). High anti-HMPV antibody titer in serum is insufficient to prevent reinfection in adults (Okamoto et al., 2010). Reinfections with respiratory viruses cause important clinical disease, but the mechanisms promoting recurrent viral LRI are not well understood. While much attention has been placed on humoral immunity, the above evidence argues that antibodies are not always associated with protection. Indeed, in animal models, both arms of the adaptive immune response contribute (Kolli et al., 2008; Skiadopoulos et al., 2004; Wyde et al., 2005).

The $CD8^+$ T cell (T_{CD8}) response against HMPV (Erickson et al., 2012), like that of RSV (Chang and Braciale, 2002) and influenza virus (Erickson et al., 2012; Vallbracht et

al., 2006), is functionally impaired in the respiratory tract. Virus-specific lung T_{CD8} do not optimally respond to stimulation by releasing lytic granules or producing anti-viral cytokines such as IFNγ. We recently demonstrated that during primary infection the inhibitory receptor programmed death-1 (PD-1) significantly contributes to this impairment by repressing T_{CD8} effector functions (Erickson et al., 2012). Blockade of PD-1 signaling restored lung T_{CD8} functions and enhanced viral control. Although PD-1 has mainly been associated with T cell exhaustion during chronic infection and cancer (Wherry, 2011), it has an increasingly recognized role during acute infections (Brown et al., 2010), in particular LRI (Zdrenghea and Johnston, 2012). Additionally, several other inhibitory receptors have recently been identified that contribute to functional T_{CD8} impairment or exhaustion in a variety of settings (Odorizzi and Wherry, 2012). We hypothesized that inhibitory receptor signaling contributes to the propensity of respiratory viruses to cause recurrent infections by promoting lung T_{CD8} impairment. We sought to elucidate PD-1's contribution to HMPV reinfection and to determine whether PD-1 limits the effectiveness of potential vaccination strategies directed at the cellular immune response. Given the severity and frequency of reinfections by respiratory viruses and the lack of vaccines, these studies have important implications for future vaccines and therapeutic interventions.

RESULTS

μMT mice are susceptible to reinfection with HMPV

Rodents are normally protected against reinfection with respiratory viruses due to the presence of neutralizing antibodies (Graham et al., 1991; Prince et al., 1999; Williams et al., 2005). We therefore utilized the B cell-deficient mouse strain μMT, which has been used to model reinfection with influenza virus (Epstein et al., 1998; Graham and Braciale, 1997), to test whether they are susceptible to reinfection with HMPV.

HMPV demonstrated similar replication kinetics in the lungs and nasal turbinates during primary infection of μMT and WT mice (Figure 3-1A). There was a slight decrease in lung titers at day 7 in WT compared to μMT mice. Virus was cleared from the lungs by day 10 in both strains. Upon reinfection, WT mice were completely protected against viral replication, as expected (Figure 3-1B). However, HMPV replicated to similarly high titers as during primary infection in challenged μMT mice. Indeed, lung titers were indistinguishable between primary and secondary infection at day 5, the usual peak of viral replication. By day 7, μMT mice displayed enhanced clearance, with the majority of mice having no detectable lung viral titers. μMT mice were also better able to clear virus from the nasal epithelium during secondary infection, as most mice had no detectable titers at days 5 and 7 post-challenge. Thus, μMT mice are susceptible to reinfection with HMPV, although they clear the infection more rapidly than during primary infection.

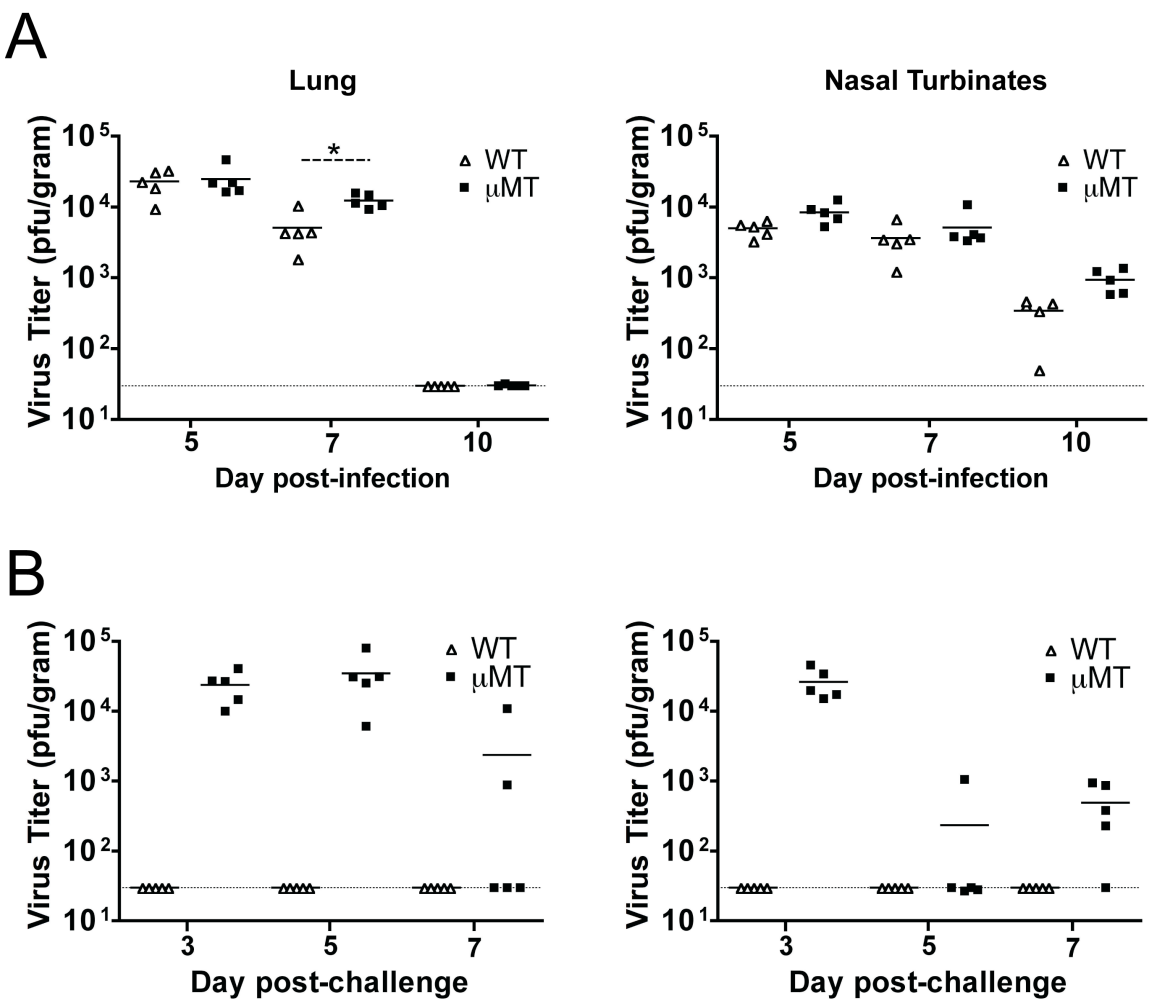

Figure 3-1. μMT mice are susceptible to reinfection with HMPV. (**A**) WT (open triangles) and μMT mice (closed squares) were infected with HMPV and viral titers were quantified for the lung (left) and nasal turbinates (right) in plaque forming units (pfu) per gram of tissue at the indicated days post-infection. (**B**) WT and μMT mice were infected with HMPV and then challenged 8 weeks later and viral titers were quantified. Each symbol represents and individual mouse and horizontal lines denote the group mean. The dotted line indicates the limit of detection for the plaque assay. Data are from a single experiment with 5 mice per group per time point. *p<0.05, student's t-test.

Secondary effector lung T_{CD8} express multiple inhibitory receptors

The ability of μMT mice to more rapidly clear HMPV during secondary infection is presumably due to cellular immunity, i.e., $CD4^+$ and $CD8^+$ T cells. As mentioned previously, the inhibitory receptor PD-1 contributes to T_{CD8} impairment during primary respiratory virus infection (Erickson et al., 2012). TIM-3 (Sharma et al., 2011) and LAG-3

(Workman et al., 2004) are additional inhibitory receptors that have been shown to negatively impact T_{CD8} during LRI. The NK cell receptor 2B4 can also deliver inhibitory signals, as it has been shown to exacerbate exhaustion of secondary effector T_{CD8} during chronic infections (West et al., 2011). We therefore characterized the co-expression of these inhibitory receptors at day 7 during both primary and secondary HMPV infection of μMT mice. The $D^b/F_{528\text{-}536}$ (F528) epitope (SGVTNNGFI) represents the dominant T_{CD8} epitope during primary HMPV infection (Erickson et al., 2012). Reinfected μMT mice generated a three-fold greater F528-specific response compared to primary infected mice (Figure 3-2A). PD-1, LAG-3 and 2B4 were more highly expressed on secondary F528-specific T_{CD8} (Figure 3-2B). The mechanisms regulating most of these receptors is not known, but it was recently shown that PD-1 is poised for rapid re-expression due to demethylation of its promoter during initial infection (Youngblood et al., 2011). Such epigenetic alterations could explain the higher expression of these receptors. Also, inhibitory receptor expression increases over time during primary infection (see Chapter IV), so the increased expression by secondary effector T_{CD8} could be due to more rapid differentiation from memory precursors compared to naïve $CD8^+$ T cells during primary infection.

Co-expression of inhibitory receptors is important in T_{CD8} exhaustion during chronic infection, as the number of receptors expressed on the cell surface corresponds to the degree of functional impairment (Blackburn et al., 2009). During HMPV LRI, most F528-specific lung T_{CD8} express ≥ 2 inhibitory receptors and a large fraction express ≥ 3 (Figure 3-2C). A greater proportion of lung T_{CD8} express 3 or 4 inhibitory receptors during secondary infection compared to primary infection. While the expression pattern of these receptors is similar during primary and secondary infection, the number of F528-specific T_{CD8} expressing all four receptors or PD-1, TIM-3 and LAG-3 is increased during reinfection (Figure 3-2D). Additionally, the fraction of cells that express PD-1 only or no

inhibitory receptors is decreased during secondary infection, confirming a skewing towards augmented inhibitory receptor expression.

Given the co-expression of numerous inhibitory receptors during reinfection, we next sought to determine their potential contribution to lung T_{CD8} impairment. To do so, we isolated lung cells from reinfected μMT mice and added them to an IFNγ-detecting ELISPOT assay. Cells were restimulated with F528-peptide and incubated with blocking monoclonal antibodies against each inhibitory receptors or its ligand(s). F528 peptide restimulation of lung cells plus PD-L1 or PD-1 blockade resulted in significantly more IFNγ-secreting cells than isotype-treated cells (i.e., more spots) (Figure 3-2E), confirming our previous *in vivo* results during primary infection (Erickson et al., 2012). Anti-PD-L1 and anti-PD-1 treatment also resulted in larger spots (Figure 3-3), indicating a greater amount of IFNγ secreted by each cell compared to isotype treatment. Blocking PD-L2, TIM-3, LAG-3, 2B4 or CD48 (the ligand for 2B4) alone did not result in any significant changes. There was a trend toward decreased responsiveness during 2B4 blockade, which could indicate a stimulatory role for this receptor during reinfection. Indeed, 2B4 has dual stimulatory/inhibitory functions depending on the isoform expressed (Chlewicki et al., 2008). Combined blockade of TIM-3, LAG-3 or 2B4 with PD-L1 did not result in greater responses than PD-L1 or PD-1 blockade alone. These results suggest that PD-1 is the dominant mediator of lung T_{CD8} impairment early during reinfection.

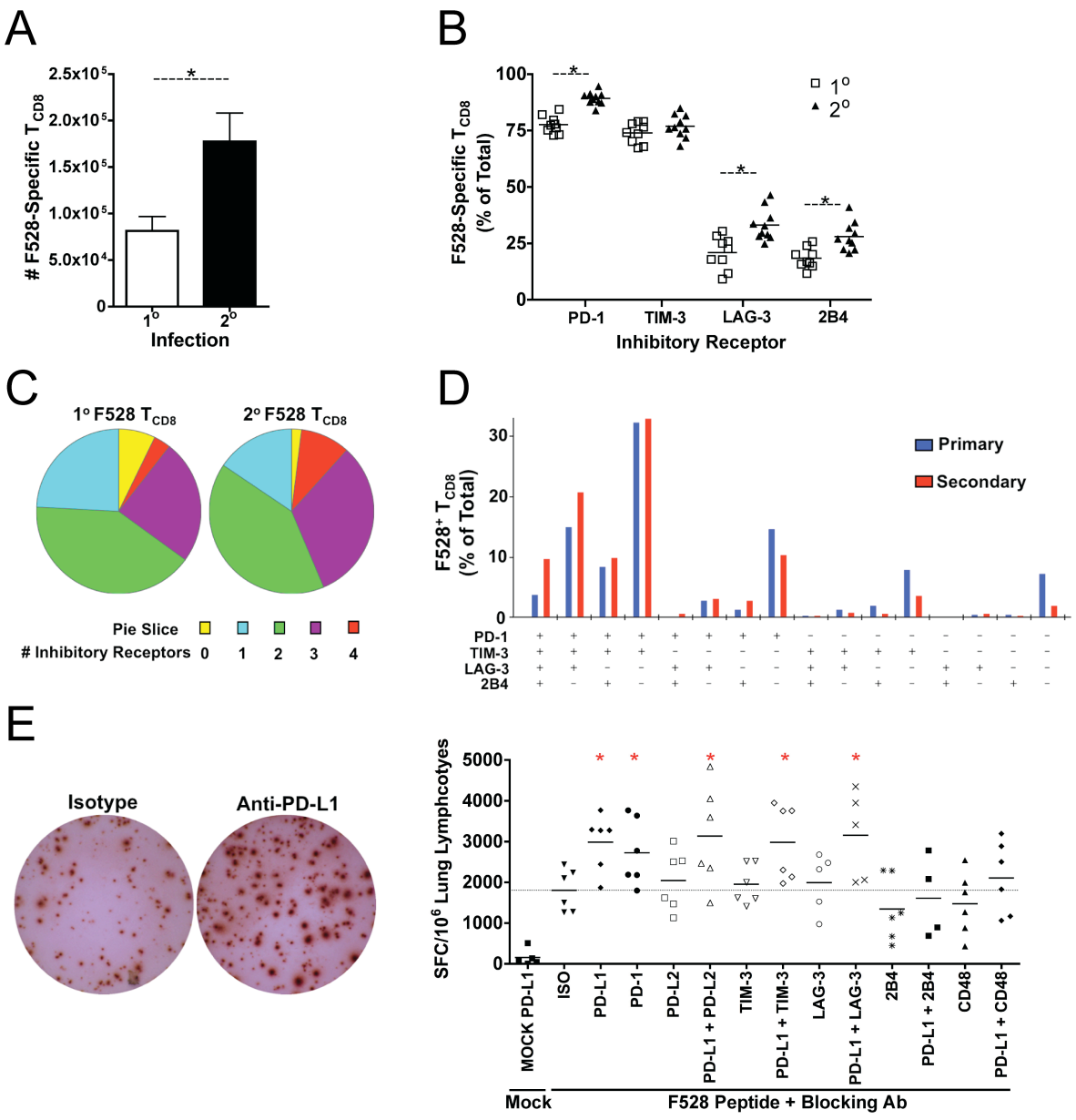

Figure 3-2. Secondary effector lung T_{CD8} express multiple inhibitory receptors. Lung lymphocytes were isolated at day 7 after primary HMPV infection of μMT mice (1^o) or reinfection of μMT mice infected with HMPV 10 weeks earlier (2^o). (**A**) The total number of D^b/F528-specific lung T_{CD8} was calculated based on tetramer staining. (**B**) Cell surface expression of the inhibitory receptors PD-1, TIM-3, LAG-3 and 2B4 was quantified on 1^o (open squares) or 2^o (closed triangles) F528 tetramer$^+$ lung T_{CD8}. (**C**) Co-expression of inhibitory receptors is displayed as the total # expressed by 1^o or 2^o F528 tetramer$^+$ lung T_{CD8}. (**D**) Patterns of inhibitory receptor expression are shown. Data in (A-D) are combined from two independent experiments with 4-5 mice per group per experiment. * $p<0.05$, student's t-test. (**E**) 2^o lung cells were isolated at day 6 post-reinfection of μMT mice, added to anti-IFNγ-coated ELISPOT plates and restimulated with F528 peptide in the presence of the indicated inhibitory receptor blocking antibodies. Each spot represents a single IFNγ–secreting cell. (Left) Representative wells are shown. (Right)

Data are expressed as the number of spot forming cells (SFC) per 10^6 lymphocytes. Each symbol represents the mean from one of 5 or 6 total independent experiments with 2-3 mice per experiment. Mock indicates wells stimulated with an irrelevant peptide. Dotted line indicates the mean number of spots from F528-stimulated, isotype control antibody treated cells as a reference. * $p<0.05$, student's t-test compared to isotype treatment.

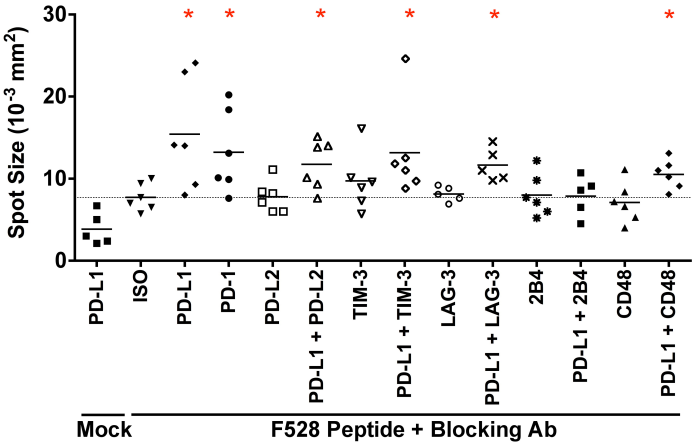

Figure 3-3. *In vitro* blockade of PD-1 signaling results in more IFNγ secretion by HMPV-specific T_{CD8}. Continuation of Figure 3-2E (see corresponding legend). Spot size is directly related to the amount of IFNγ secreted by restimulated cells.

Therapeutic PD-1 blockade restores function to impaired secondary lung T_{CD8} and enhances virus clearance

To directly test whether PD-1 signaling contributes to lung T_{CD8} impairment during HMPV reinfection, we therapeutically blocked this pathway by injecting μMT mice undergoing secondary infection with blocking antibodies directed against PD-1 ligands or with isotype control antibody. Naïve μMT mice were also infected for comparison of T_{CD8} responses and viral titers. We examined both the F528-and N11-specific T_{CD8} responses. Primary infected μMT mice possessed F528-specific T_{CD8} that were mostly functional (Figure 3-4A,B), as previously described for early times p.i. (see Chapter II). Secondary lung T_{CD8} in isotype-treated, reinfected mice were more impaired than

primary T_{CD8} (Figure 3-4A,B), indicating that elevated inhibitory receptor co-expression during reinfection (Figure 3-2) is correlated with decreased functionality. Anti-PD-L treatment resulted in enhanced degranulation ability and greater IFNγ production for N11-specifc T_{CD8} compared to isotype-treated mice (Figure 3-4A). Treatment also resulted in a greater percentage of functional F528- and N11-specific T_{CD8} (Figure 3-4B). TNF production was significantly enhanced for F528-specific T_{CD8} and trended higher for N11-specific cells. PD-1 was more highly expressed during secondary infection and PD-L blockade further increased PD-1 expression (Figure 3-4C). Surprisingly, at day 6 p.i., isotype-treated, reinfected mice still possessed indistinguishable lung viral titers compared to primary infected μMT mice (Figure 3-4D). Anti-PD-L treatment reduced lung viral titers ~4-fold in reinfected mice, suggesting that PD-1 signaling impairs the ability of secondary effector lung T_{CD8} to effectively reduce viral replication. These results indicate that PD-1 signaling impairs the T cell response during reinfection and may therefore contribute to respiratory virus reinfection.

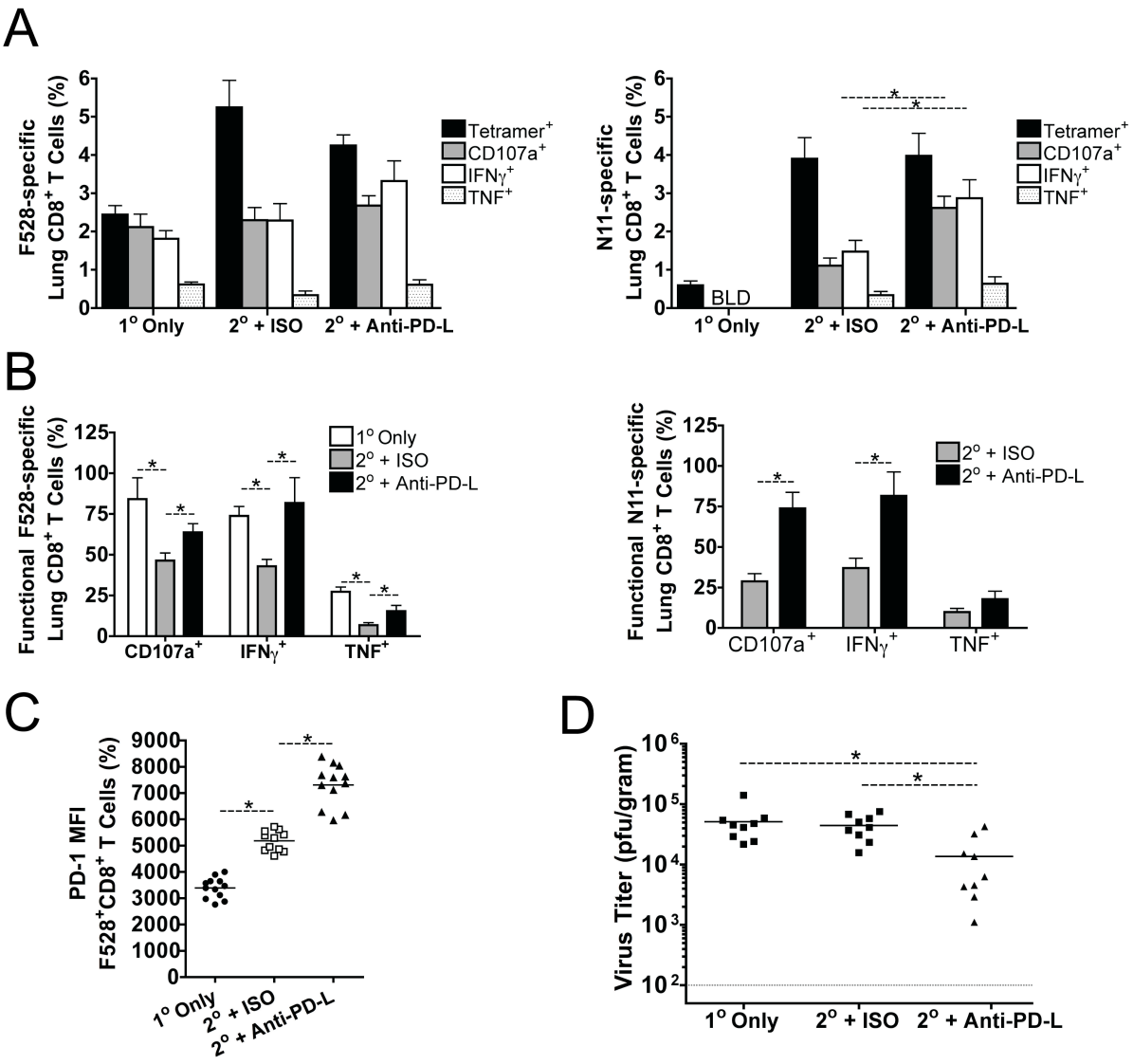

Figure 3-4. Therapeutic PD-1 blockade restores function to impaired secondary lung T_{CD8} and enhances virus clearance. μMT mice either underwent primary infection (1^o Only) or were infected with HMPV and then reinfected 16 weeks later. Of the reinfected mice, one group received 200μg of anti-PD-L1 and anti-PD-L2 antibodies i.p. (2^o + Anti-PD-L) while another group received the same amount of isotype control antibody (2^o + ISO). (**A**) The lung D^b/F528 and K^b/N11-specific T_{CD8} responses were quantified via tetramer staining (black bars), CD107a mobilization (gray bars) and intracellular IFNγ (white bars) or TNF production (white dotted bars) at day 6 p.i. BLD = below limit of detection. (**B**) The percentage of functional HMPV-specific T_{CD8} was calculated by dividing the percentage that degranulate or make IFNγ by the percentage that stain tetramer$^+$. (**C**) PD-1 MFI for F528-specific T_{CD8} is shown. (**D**) Lung viral titers were quantified by plaque assay. The dotted line indicates the limit of detection for the plaque assay. Data are combined from three independent experiments with 3-5 mice per group per experiment. Error bars, s.e.m. * $p<0.05$, student's t-test.

PD-1 limits the effectiveness of vaccine-elicited anti-viral T_{CD8}

Vaccine strategies that only elicit humoral immune responses against the related virus RSV have thus far proven unsuccessful and potentially hazardous (Collins and Melero, 2011), highlighting the need for better understanding of the contribution of T cells to protective immunity against RSV and HMPV. Recently, a peptide vaccination strategy proved highly effective against RSV, especially when given close to the time of challenge infection (Lee et al., 2012). However, the efficacy waned when mice were challenged several weeks later. For a vaccine to be effective, it must induce immune responses that remain protective after several months or years. We therefore tested whether PD-1 was responsible for the decreased effectiveness of T_{CD8}-directed peptide vaccination. WT and *PD-1*$^{-/-}$ mice were immunized i.v. with F528 TriVax (F528 peptide + Anti-CD40 Ab + Poly[I:C]) and the T_{CD8} response was monitored in peripheral blood. *PD-1*$^{-/-}$ mice were employed to ensure PD-1 signaling did not occur throughout the entire experiment, from vaccine prime to the end of viral challenge. We found that WT mice generated more F528-specific T_{CD8} than *PD-1*$^{-/-}$ mice, which was true in three independent experiments (Figure 3-5A). Five days post-HMPV challenge, we detected a greater overall F528-response in the WT mice compared to *PD-1*$^{-/-}$ mice as determined by tetramer staining (Figure 3-5B), which corresponded to the greater magnitude of the initial immunization. There were similar percentages of degranulating or IFNγ-producing F528-specific T_{CD8} in both groups. However, calculation of the percentage of functional lung T_{CD8} (which takes into account the different magnitude of tetramer response) revealed that F528-specific T_{CD8} were more functional in *PD-1*$^{-/-}$ mice (Figure 3-5C).

To determine whether PD-1 affects the ability of the vaccine-elicited T_{CD8} to control viral replication, we measured viral titers in vaccinated WT and *PD-1*$^{-/-}$ mice, as well as in unvaccinated or control vaccinated mice (Figure 3-5D). We found that in all the groups examined, only *PD-1*$^{-/-}$ mice receiving F528 TriVax had decreased viral titers at

day 5 post-challenge. These results suggest that PD-1 limits the effectiveness of anti-viral T_{CD8} elicited by peptide vaccination. Interestingly, F528 was not protective at all in WT mice, unlike an immunodominant RSV epitope tested using TriVax in BALB/c mice (Lee et al., 2012). However, when PD-1 signaling was removed, we found that HMPV-specific T_{CD8} were more functional and viral replication was reduced. This suggests that the effect on viral titers might be even more pronounced if the *PD-1*$^{-/-}$ mice generated a similar immune response to F528 TriVax. It is unclear why the WT mice responded with a higher number of epitope-specific cells. TriVax is a potent vaccination strategy that elicits a very robust T_{CD8} response (Cho and Celis, 2009). PD-1 may temper some of the strong stimulatory signals received during priming that potentially cause activation-induced cell death (Green et al., 2003).

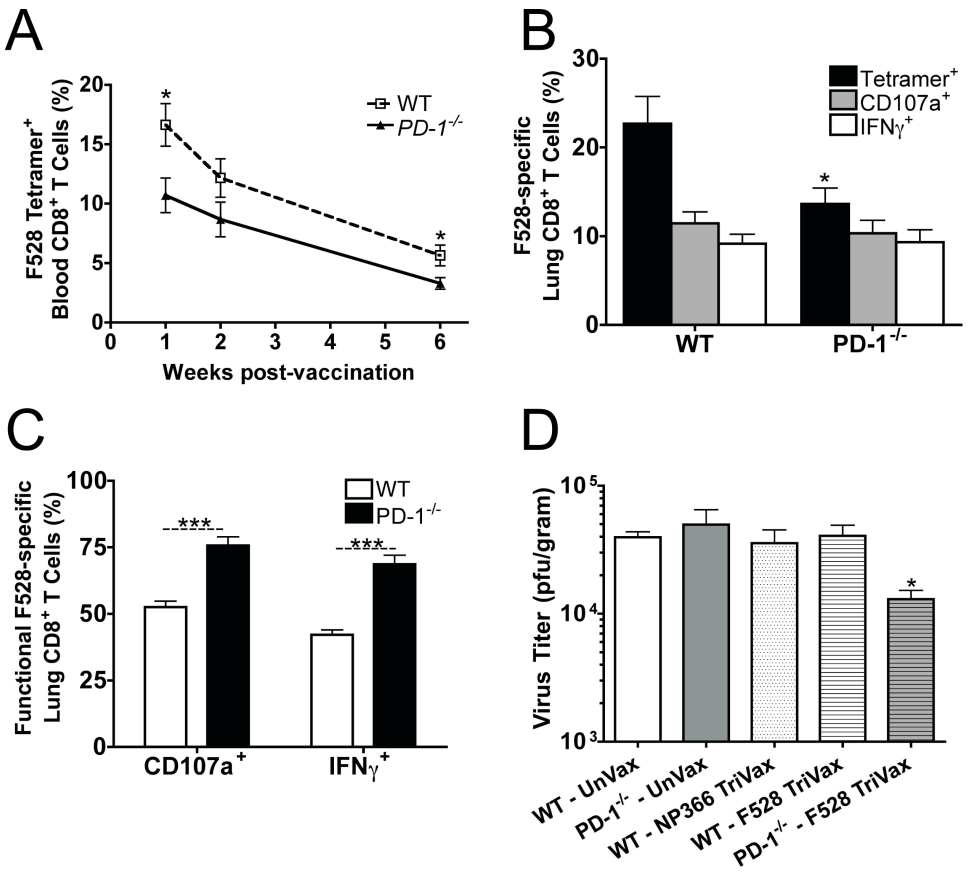

Figure 3-5. PD-1 limits the effectiveness of vaccine-elicited anti-viral T_{CD8}. WT or *PD-1*$^{-/-}$ mice were immunized i.v. with F528 TriVax (see Materials and Methods). (**A**) The F528-specific response to immunization was measured in the peripheral blood via tetramer staining in WT (open squares) and *PD-1*$^{-/-}$ mice (closed triangles). (**B**) The lung F528-specific T_{CD8} response was quantified via tetramer staining (black bars), CD107a mobilization (gray bars) and intracellular IFNγ production (white bars) at day 5 p.i. (**C**) The percentage of functional F528-specific T_{CD8} was calculated. (**D**) Lung viral titers were quantified by plaque assay. UnVax indicates mice that were not immunized with TriVax. NP366 is the immunodominant epitope for influenza virus. Data are combined from three independent experiments with 5 mice per group per experiment. Error bars, s.e.m. * $p<0.05$, *** $p<0.0005$, student's t-test.

DISCUSSION

Taken together, our findings indicate that PD-1 inhibits secondary effector lung T_{CD8} during respiratory virus reinfection. μMT mice were permissive to reinfection by HMPV, overcoming the major drawback of rodent models for the analysis of a productive secondary infection. The exact mechanisms allowing respiratory viruses to repeatedly reinfect individuals throughout life has been unclear. We provide data to suggest that rapid re-expression of multiple inhibitory receptors contributes to the functional impairment of secondary effector T_{CD8} in the respiratory tract. *In vitro* studies only uncovered a role for PD-1 in impairing these cells; thus it remains to be determined if TIM-3, LAG-3 and 2B4 play a role *in vivo*. We focused on the dominant inhibitory receptor PD-1, and found that, as during primary infection (Erickson et al., 2012), PD-1 potently inhibits T_{CD8} effector functions. Therapeutic blockade of this pathway restored T_{CD8} functionality and allowed for better virus control in secondarily infected lungs. PD-1 signaling also limited the efficacy of a peptide vaccination formula (TriVax). These results highlight the importance of better understanding the role of PD-1 and other inhibitory receptors in modulating lung T_{CD8} effector functions in order to design more effective vaccines and therapeutics against respiratory viruses. Further work is warranted to explore whether PD-1-mediated T_{CD8} impairment contributes to respiratory virus reinfection in humans.

MATERIALS AND METHODS

Mice and Infections

C57BL/6 (B6) were purchased from the Jackson Laboratory. μMT mice were a kindly provided by Dr. Mark Boothby (Vanderbilt University, Nashville, TN). *PD-1*$^{-/-}$ mice were obtained with permission from Dr. Tasuku Honjo (Kyoto University, Kyoto, Japan). All animals were bred and maintained in specific pathogen-free conditions in accordance with the Vanderbilt Institutional Animal Care and Use Committee. Age- and gender-matched animals were used in all experiments. HMPV (pathogenic clinical strain TN/94-49, genotype A2) was grown and titered in LLC-MK2 cells as previously described (Williams et al., 2005). Mice were anesthetized with ketamine-xylazine and infected intranasally (i.n.) with $1x10^6$ plaque forming units (PFU) of HMPV. Viral titers in infected mouse lungs and nasal turbinates were measured by plaque titration as previously described (Williams et al., 2005).

Flow Cytometry Staining

Lung lymphocytes were tetramer-stained or restimulated for intracellular cytokine staining (ICS) in parallel as previously described (Erickson et al., 2012). Lung cells were stained for the inhibitory receptors PD-1 (clone RMP1-30), TIM-3 (clone RMT3-23), LAG-3 (clone C9B7W) and 2B4 (clone m2B4 (B6)458.1) or with appropriate isotype control antibodies (all from Biolegend). Flow cytometric data were collected using an LSRII or Fortessa (BD Biosciences) and analyzed with FlowJo software (Tree Star). The Boolean gating function in FlowJo was used to assess inhibitory receptor co-expression and patterns were visualized using the SPICE program (NIAID).

IFNγ ELISPOT

ELISPOT assays were performed as previously described (Rock and Crowe, 2003) with slight modifications. $5x10^4$ lung cells were added to triplicate wells. Peptides were then added (10μM final concentration) followed by inhibitory receptor blocking antibodies (10μg/mL final concentration). The following blocking antibodies were used: isotype control (clone LTF-2, Bio X-cell), anti-PD-L1 (clone 10F.9G2, Bio X-cell), anti-PD-L2 (clone TY-25, Bio X-cell), anti-PD-1 (clone J43, Bio X-cell), anti-TIM-3 (clone RMT3-23, Bio X-cell), anti-LAG-3 (clone C9B7W, Bio X-cell), anti-2B4 (clone m2B4 (B6)458.1, Biolegend), and anti-CD48 (clone HM48-1, Bio X-cell). Plates were incubated at 37C for 42-48 hours, developed, and then counted using an ImmunoSpot Micro Analyzer (Cellular Technology Limited). The average number of spots in wells stimulated with an irrelevant peptide was subtracted from each experimental value, which was then expressed as spot forming cells (SFC) per 10^6 lymphocytes.

***In vivo* Antibody Blockade**

Mice were injected i.p. with 200μg of rat isotype control antibody (clone LTF-2, Bio X-cell) or 200μg of both rat anti-mouse PD-L1 (clone 10F.9G2, Bio X-cell) plus rat anti-mouse PD-L2 (clone TY-25, Bio X-cell) to block PD-1 signaling.

Peptide Vaccination (TriVax)

Mice were injected intravenously with a mixture of 200μg D^b/F528 peptide, 50μg anti-CD40 antibody (clone FGK4.5, Bio X-cell) and 50μg poly(I:C) (Invivogen, San Diego, CA). Peripheral blood was obtained to check immune responses in all vaccinated animals.

Statistical Analysis

Data analysis was performed using Prism v4.0 (GraphPad Software). Comparisons between tetramer staining and ICS within the same animals were performed using a paired, two-tailed *t* test. Comparisons between two groups were performed using an unpaired, two-tailed Student's *t* test. Multiple group comparisons were performed using a one-way ANOVA with a Bonferroni post-test. Error bars on each graph represent standard error of the mean unless otherwise noted.

CHAPTER IV

$CD8^+$ T Cells During Viral Acute Respiratory Infection Are Uniquely Differentiated and Regulated by Multiple Inhibitory Receptors

INTRODUCTION

$CD8^+$ T cells possess critical functions that protect against intracellular pathogens and cancer, including cytotoxicity, cytokine production and long-lived memory potential (Kaech and Cui, 2012; Zhang and Bevan, 2011). During acute infection, naïve T_{CD8} encounter Ag, acquire effector functions and proliferate to clear the infection, after which 90-95% die while the remaining few become memory cells (Zhang and Bevan, 2011). Memory T_{CD8} can rapidly reactivate their effector functions and proliferate upon pathogen re-encounter, contributing to protective immunity (Kaech and Wherry, 2007). During chronic infection, a different sequence of events occurs: pathogen-specific T_{CD8} initially acquire effector functions, but gradually become dysfunctional and fail to eliminate the infection (Shin and Wherry, 2007). 'Exhaustion' is the term used to describe this hierarchical loss of T_{CD8} functions. Proliferative ability and IL-2 production are lost early, followed next by TNF, with IFNγ production failing only late in exhaustion (Wherry, 2011). Prolonged TCR stimulation by persistent viral or tumor antigens is thought to transcriptionally reprogram exhausted T_{CD8}, resulting in these functional changes (Youngblood et al., 2012).

The paradigm that acute infection generates functional effector T cells followed by memory development, while chronic infection causes T cell exhaustion, is not generalizable to all infections. During acute viral LRI in mice, T_{CD8} become functionally impaired, rapidly losing cytotoxicity and cytokine production (Chang and Braciale, 2002; DiNapoli et al., 2008; Gray et al., 2005; Lukens et al., 2006; Vallbracht et al., 2006). In

contrast to exhaustion, lung T_{CD8} impairment during LRI occurs rapidly, with IFNγ production waning as early as day seven (Chang and Braciale, 2002). Additionally, only T_{CD8} in the respiratory tract become impaired; T_{CD8} in lymphoid organs maintain their effector functions, suggesting that the infected lung environment is critical for the development of impairment (Erickson et al., 2012). LRI are cleared within 7-12 days even in the face of T_{CD8} impairment, but disease severity may be affected and generation of protective immunity may be compromised. Failure to generate a quality memory T_{CD8} response may partially explain the ability of respiratory viruses to repeatedly reinfect individuals despite minimal antigenic drift (Hall et al., 1991; Johnson et al., 1961; Kroll and Weinberg, 2011). A better understanding of the phenotype, functions and mechanisms controlling lung T_{CD8} activity during LRI is needed to design new and effective therapeutics and vaccines.

We previously uncovered a role for the inhibitory receptor programmed death-1 (PD-1) in mediating lung T_{CD8} impairment during human metapneumovirus (HMPV) and influenza virus infection (Erickson et al., 2012). Blocking PD-1 during acute viral LRI resulted in increased T_{CD8} degranulation, IFNγ production and ability to clear the infection. PD-1 blockade also restores function to exhausted T_{CD8} during HIV infection (Trautmann et al., 2006) and LCMV clone 13 infection of mice (Barber et al., 2006) and has shown promise in recent cancer clinical trials (Berger et al., 2008; Brahmer et al., 2010). These results suggest that similar inhibitory pathways may be activated during T_{CD8} exhaustion in the setting of chronic infection and lung T_{CD8} impairment during acute infection. Exhausted T_{CD8} express numerous inhibitory receptors, including TIM-3 (Jin et al., 2010b), LAG-3 (Blackburn et al., 2009), 2B4 (West et al., 2011), and others (Nakamoto et al., 2009). The role of these receptors and their cooperation with PD-1 to cause lung T_{CD8} functional impairment during pulmonary infection is unexplored.

We addressed this issue by comparing the global gene expression profiles of impaired lung T_{CD8} to unimpaired spleen T_{CD8} in the same HMPV-infected mice. Gene expression analysis has uncovered numerous pathways regulating effector and memory T_{CD8} development after acute infection (Kaech et al., 2002) and exhaustion during chronic infection (Doering et al., 2012; Wherry et al., 2007). Furthermore, given the functional differences that exist between effector T_{CD8} present during most acute infections, exhausted T_{CD8} during chronic infections, and impaired lung T_{CD8} during LRI, we hypothesized that each population would possess a unique gene expression profile that may provide insights into the mechanisms governing each functional state. We found that impaired lung T_{CD8} co-express numerous inhibitory receptors that are regulated by Ag and TCR signaling. Viral infection induced greater expression of the ligands for each receptor. We found that LAG-3 can compensate for PD-1 deficiency and rapidly reinstate impairment, uncovering an overlapping, redundant system of inhibitory receptor regulation of lung T_{CD8} dysfunction. We conclude that lung T_{CD8} possess a unique gene expression profile sharing some qualities of both acute effector T_{CD8} and exhausted T_{CD8} present in chronic infection. Further investigation of this unique state of T_{CD8} differentiation may yield novel therapeutics and vaccination strategies.

RESULTS

Lung T_{CD8} Impairment Is Cell-intrinsically Regulated by PD-1

To determine if lung T_{CD8} impairment occurs through direct PD-1 signaling on the T_{CD8} surface or if other cell types are involved, we generated WT:*PD-1*$^{-/-}$ bone marrow chimeric mice. After reconstitution of irradiated recipients with either 1:1 WT (Thy1.1^{+}):*PD-1*$^{-/-}$ (Thy1.2^{+}) donor bone marrow cells (Figure 4-1A) or 4:1 WT:*PD-1*$^{-/-}$ cells (not shown), the T_{CD8} compartment consisted of approximately twice as many *PD-1*$^{-/-}$ as WT cells (Figure 4-1A). HMPV infection resulted in additional recruitment of *PD-1*$^{-/-}$ T_{CD8} to the lung as compared to WT cells (Figure 4-1A). We quantified the total $D^b/F_{528\text{-}536}$ (F528) and $K^b/N_{11\text{-}19}$ (N11) epitope-specific T_{CD8} levels via tetramer staining, and in parallel their effector functions via brief peptide restimulation followed by intracellular cytokine staining (ICS). The overall F528 and N11 T_{CD8} responses were greater amongst *PD-1*$^{-/-}$ cells (Figure 4-1B), likely reflecting increased precursor frequencies due to increased overall numbers of cells. More importantly, we observed greater frequencies of degranulating (i.e., CD107a^{+}) or IFNγ-producing *PD-1*$^{-/-}$ versus WT T_{CD8}. To control for the greater overall T_{CD8} response by *PD-1*$^{-/-}$ cells, we calculated the percentage of T_{CD8} capable of degranulating or making IFNγ and compared WT and *PD-1*$^{-/-}$ cells within the same mouse. Lung T_{CD8} were more functional in *PD-1*$^{-/-}$ compared to WT cells for both epitopes and both effector functions measured (Figure 4-1C). Impairment in WT lung T_{CD8} despite increased relative levels of *PD-1*$^{-/-}$ cells, plus increased functionality of *PD-1*$^{-/-}$ T_{CD8}, lead us to conclude that PD-1 functions in a cell-intrinsic manner to impair T_{CD8} during LRI.

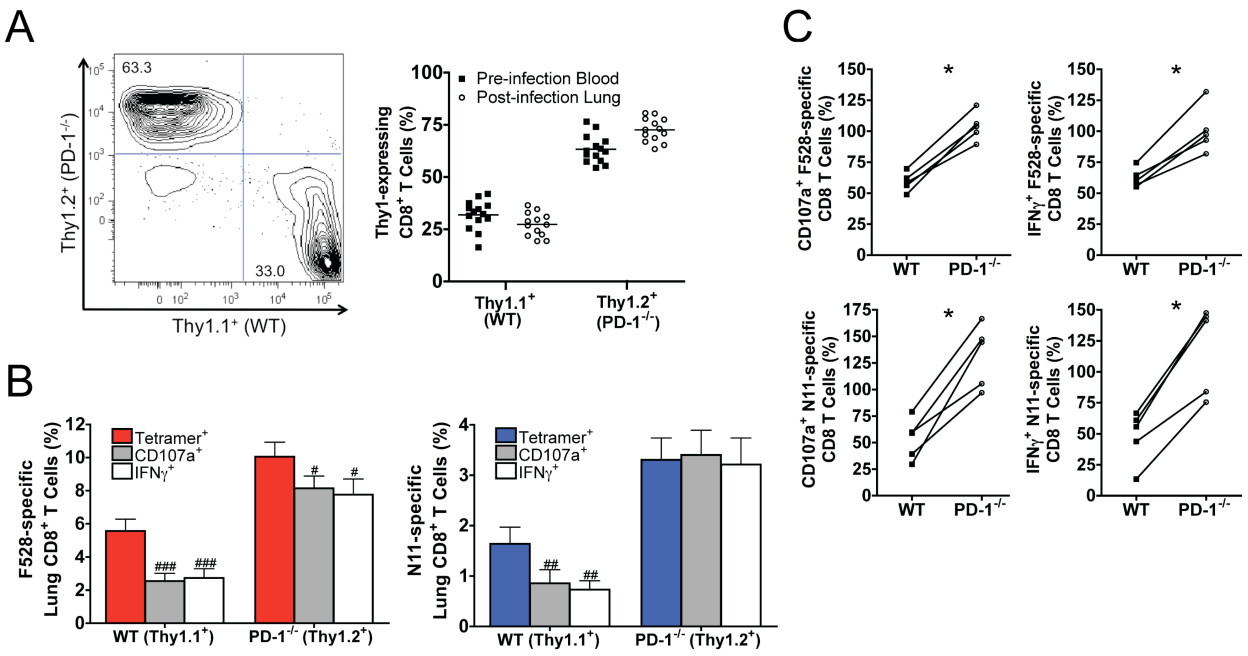

Figure 4-1. Lung T_{CD8} impairment is cell-intrinsically regulated by PD-1. (**A**) WT:*PD-1*$^{-/-}$ mixed bone marrow chimeric mice were checked for reconstitution in the blood before and in the lung after HMPV infection. Each symbol represents and individual mouse and the horizontal bar indicates the mean. (**B**) Mixed bone marrow chimeric mice were infected with HMPV and the lung D^b/F528 and K^b/N11-specific T_{CD8} responses were quantified via tetramer staining (colored bars), CD107a mobilization (gray bars) and intracellular IFNγ production (white bars) at day 7 post-infection (p.i.). Error bars, s.e.m. Data are combined from three independent experiments with 4-5 mice per experiment. # p<0.05, ## p<0.005, ### p<0.0005, paired t-test. (**C**) The percentage of functional HMPV-specific T_{CD8} was calculated by dividing the percentage that degranulate or make IFNγ by the percentage that stain tetramer$^+$. Lines connect data points from WT and *PD-1*$^{-/-}$ T_{CD8} within the same mouse. Data are representative of one out of three independent experiments. * p<0.05, paired t-test.

Gene Expression Analysis of Impaired Lung T_{CD8} and Unimpaired Spleen T_{CD8}

Given the cell-intrinsic nature of PD-1-mediated lung T_{CD8} impairment, we reasoned that a more thorough examination of impaired anti-viral T_{CD8} might reveal other mechanisms regulating their function in the respiratory tract. We previously showed that HMPV-specific T_{CD8} in different environments within the same infected mouse have very different functional capacities (Erickson et al., 2012). HMPV-specific T_{CD8} in the lung rapidly lose the ability to produce IFNγ (Figure 4-2A) or degranulate (not shown) while these effector functions are maintained in the spleen over time. Secondary lung T_{CD8}

following challenge of previously infected mice or mice immunized with HMPV-specific class I-restricted epitopes are also highly impaired in their ability to degranulate or make cytokines (Erickson et al., 2012).

We therefore compared global gene expression differences between impaired pulmonary T_{CD8} and functional splenic T_{CD8} from the same HMPV-infected mice. To do so, we infected B6-Kb^0Db^0;B7.2 transgenic (B7tg) mice, in which T_{CD8} only recognize epitopes restricted by the human MHC class I molecule HLA-B**0702* (Rohrlich et al., 2003a). The T_{CD8} response in B7tg mice is dominated by the $M_{195–203}$ (M195) epitope, which accounts for approximately 60% of anti-viral T_{CD8} (Erickson et al., 2012). At day 7 p.i. we sorted spleen and lung M195-specific T_{CD8} as well as secondary lung M195-specific T_{CD8} from mice primed with M195-loaded DCs then challenged with HMPV (see Materials and Methods). M195-specific T_{CD8} were sorted to high purity (Figure 4-2B) and gene expression analysis was performed. Two samples (one spleen [#5] and one secondary lung [#17]) were deemed outliers based upon per-component analysis and excluded from further study (Figure 4-3).

We quantified the gene expression differences of these populations and compared them to naïve T_{CD8} in order to make direct comparisons between the three groups. Approximately 900 genes were up or down-regulated by all three populations of M195-specific T_{CD8} compared to naïve T_{CD8} (Figure 4-2C), which reflect many genes associated with T cell activation and differentiation (Supplementary Table 1). Over 1,300 genes were differentially expressed by both primary and secondary lung T_{CD8}. Despite large numbers of overlapping genes between these groups, each population contained numerous genes uniquely identifying them: 173 for spleen, 319 for lung and 652 for secondary lung T_{CD8}. A total of 370 genes differed between the impaired lung T_{CD8} and unimpaired spleen T_{CD8} from the same infected mice, indicating that lung anti-viral T_{CD8} adopt a unique gene expression profile while combating infection.

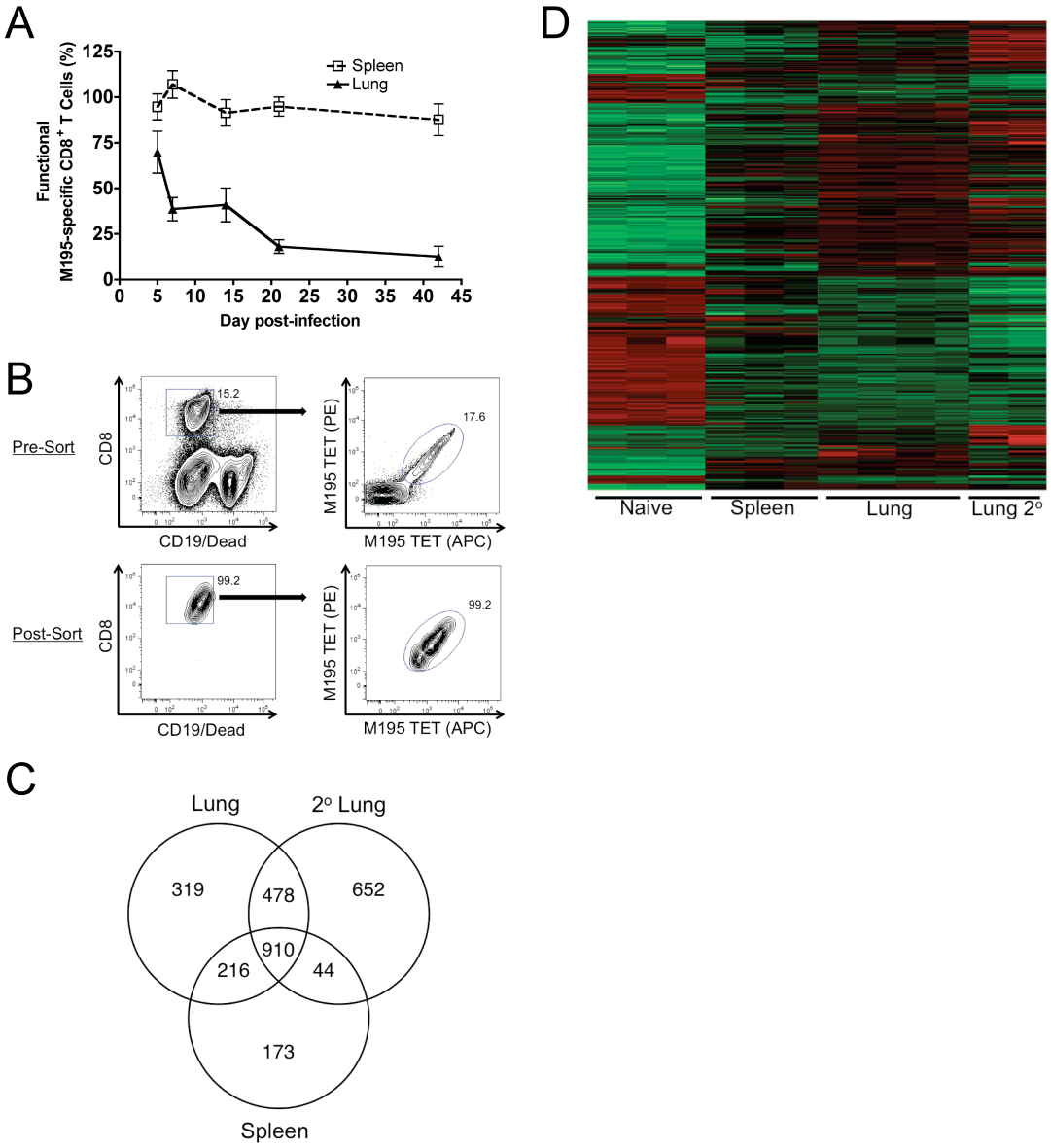

Figure 4-2. Gene expression analysis of impaired lung T_{CD8} and unimpaired spleen T_{CD8}. (**A**) Time course of HMPV M195-specific T_{CD8} functionality in the lung and the spleen calculated from data in (Erickson et al., 2012). (**B**) Pre- and post-sort analysis of lung M195-specific T_{CD8} at day 7 p.i. Cells were sorted based on dual staining with APC- and PE-conjugated M195-specific tetramers. Numbers indicate the percentage of cells staining positive in the indicated gates. (**C**) The total number of genes found differentially expressed for the indicated M195-specific T_{CD8} populations compared to naïve T_{CD8} from microarray analysis. Secondary lung T_{CD8} were generated as described in Materials and Methods. (**D**) Heatmap resulting from ANOVA analysis of the gene-expression profiles of naive, spleen, lung, and secondary lung M195-specific T_{CD8} showing the relatedness of individual samples. Each row represents a unique gene while each column is an individual sample.

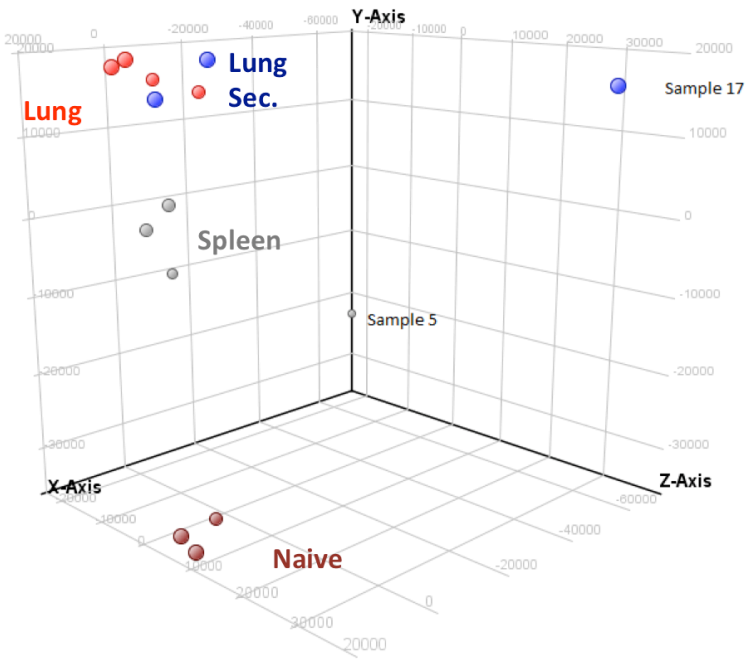

Figure 4-3. Per-component analysis of gene expression data. Gene expression data is plotted on three principal component axes. Sample #5 (spleen M195-specific T_{CD8}) and Sample #17 (secondary lung M195-specific T_{CD8}) were excluded from further analysis.

Numerous IFN-Regulated Genes Are Expressed by Lung T_{CD8} Which Support T_{CD8} Expansion But Not Function

We noted that numerous IFN-regulated genes were upregulated by lung T_{CD8}, including IRF7, MX1, MX2, OAS2, RSAD2, SOCS1, CXCL9/10 and others. Lung T_{CD8} are exposed to type I IFN generated by infected respiratory epithelial cells. To determine whether these interferon-stimulated genes play a role in T_{CD8} impairment, we infected IFNAR$^{-/-}$ mice (which are unable to respond to type I IFN) and quantified the T_{CD8} response (Figure 4-4). We found a significant decrease in the percentage and number of HMPV-specific T_{CD8} in the IFNAR$^{-/-}$ mice as compared to WT controls (Figure 4-4A and 4-4B). The percentage of functional T_{CD8} was not changed (Figure 4-4C), but the amount of IFNγ made by virus-specific T_{CD8} as determined by MFI was significantly decreased (Figure 4-4D). From this, we confirm that type I IFN is a key third signal for T_{CD8}

proliferation (Curtsinger and Mescher, 2010), but that it does not play a role in enforcing early T_{CD8} functional impairment.

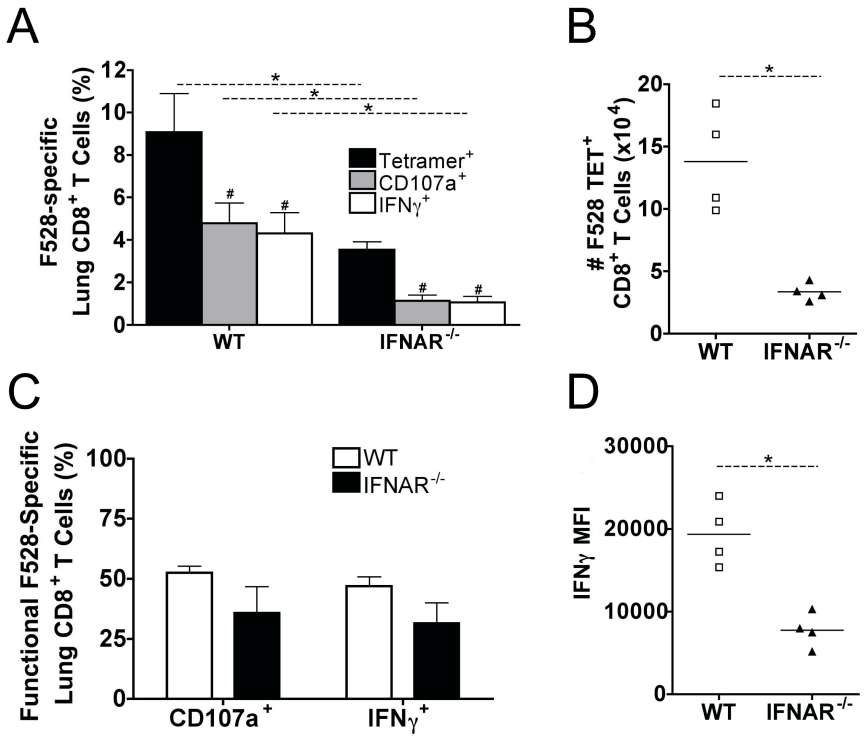

Figure 4-4. Type I IFN signaling affects T_{CD8} expansion but not functional impairment. *IFNAR*$^{-/-}$ and control WT mice were infected with HMPV and the lung T_{CD8} response was quantified at day 7 p.i. (**A**) Tetramer staining and ICS were performed for F528-specific T_{CD8}. (**B**) The total number of F528-specific T_{CD8} was calculated. (**C**) The percentage of functional F528-specific T_{CD8} was calculated. (**D**) Mean fluorescence intensity (MFI) of IFNγ. Error bars, s.e.m. Data are combined from two independent experiments with 4-5 mice per experiment. # p<0.05, paired student's t-test. * p<0.05, unpaired student's t-test.

Genes Encoding Several Inhibitory Receptors and Pathways Are Upregulated in Impaired Lung T_{CD8}

Lung T_{CD8} impairment during acute viral LRI resembles the T cell exhaustion state observed during chronic infections (Wherry, 2011) and cancer (Baitsch et al., 2012). We were therefore interested to find that several genes encoding inhibitory

receptors with known roles during exhaustion are also upregulated in impaired lung T_{CD8}. The genes encoding TIM-3 (HAVCR2), LAG-3 (CD233) and 2B4 (CD244) were all more highly expressed by lung T_{CD8}. Of note, *Pdcd1,* the gene that encodes PD-1, was not differentially expressed between spleen and lung T_{CD8}, which may reflect either recent activation of spleen T_{CD8} or migration from the infected lung where they had encountered Ag. Other known inhibitory receptors, such as CTLA-4, CD160 and BTLA, were not different between any of the three groups we analyzed. In summary, impaired lung T_{CD8} displayed coordinated upregulation of several genes associated with T cell exhaustion.

Kinetics of T_{CD8} Inhibitory Receptor and Ligand Expression

To confirm that increased gene expression of these inhibitory receptors corresponds to increased cell surface expression, we performed flow cytometic analysis of HMPV-specific T_{CD8}. At days 7, 10 and 14 after HMPV infection we quantified their expression on spleen and lung M195-specific T_{CD8}. Despite similar *Pdcd1* mRNA levels between lung and spleen T_{CD8}, surface PD-1 expression was greater in lung T_{CD8} at day 7 and remained elevated over spleen PD-1 expression at all time points (Figure 4-5A,B). The same was true for TIM-3 and LAG-3, with LAG-3 expression being at least 4-fold greater in the lung. 2B4 expression was similar at day 7, but increased steadily in the lung over time. We quantified the co-expression of inhibitory receptors and found spleen M195-specifc T_{CD8} mainly express 0 or 1 inhibitory receptor at each time point (Figure 4-5C). By day 14, ~50% express none of the analyzed receptors. In contrast, only ~30% of lung T_{CD8} express 0 or 1 inhibitory receptor at day 7, with many expressing 2, a large population expressing 3 and a significant portion expressing all 4. At day 14 p.i., lung T_{CD8} still co-express many inhibitory receptors. Analysis of the actual combinations of inhibitory receptors expressed by lung T_{CD8} over time revealed a shifting landscape (Figure 4-5D). PD-1 was consistently high and co-expressed with TIM-3 and LAG-3 at

day 7, but shifted to co-expression with TIM-3 and 2B4 by day 10. Also, by day 14, PD-1^{neg} populations emerged that were characterized by expression of TIM-3 and 2B4, only 2B4 or no inhibitory receptors. PD-1 was the most commonly expressed inhibitory receptor in the spleen, but lack of expression of these markers dominated (Figure 4-6). Thus, impaired lung T_{CD8} are associated with the co-expression of multiple inhibitory receptors.

We previously demonstrated that PD-1 upregulation without a concomitant increase in its ligand did not result in rapid T_{CD8} impairment (Erickson et al., 2012). We therefore stained lung epithelial cells (Ep-CAM$^+$) and antigen presenting cells (CD11c$^+$) for each of the identified inhibitory receptors' ligand. Ep-CAM expression was restricted to CD45$^-$ cells while CD11c$^+$ cells were CD45$^+$ (not shown). PD-L1 was upregulated on both cell types at day 7 p.i. compared to mock-infected animals (though with much higher overall expression on CD11c$^+$ cells), decreased on day 10, and returned to near baseline by day 14 (Figure 4-5E). PD-L2 was undetectable on both cell types (not shown). MHC-II, the ligand for LAG-3, was highly expressed at baseline, upregulated by infection and remained elevated. CD48, the ligand for 2B4, was only expressed by CD11c$^+$ cells and was not altered by infection. Finally, we stained for intracellular galectin-9, the soluble ligand for TIM-3 (Sakuishi et al., 2011), and found it to be upregulated by infection and remained elevated. These results indicate that the ligands for each inhibitory receptor are expressed at steady-state in mouse lungs and are increased by HMPV infection.

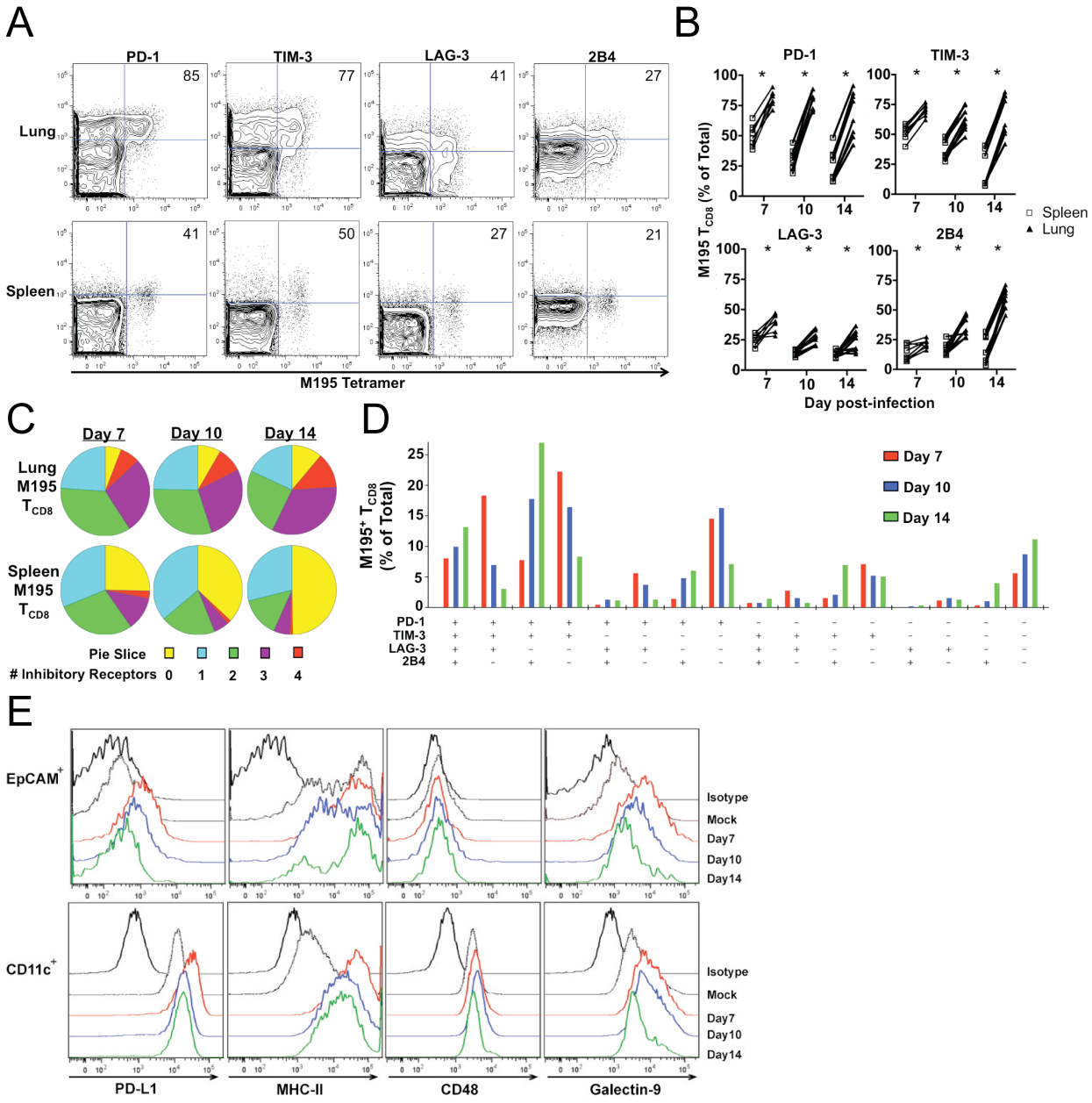

Figure 4-5. Kinetics of T_{CD8} inhibitory receptor and ligand expression. (**A**) Multi-parameter flow cytometry was used to quantify expression of the inhibitory receptors PD-1, TIM-3, LAG-3 and 2B4 on M195-specific T_{CD8} at day 7 p.i. Numbers indicate % tetramer^{+} T_{CD8} expressing the receptor in the lung or spleen. Data are representative of two independent experiments with 4-5 mice per time point. (**B**) Expression of individual inhibitory receptors on M195-specific T_{CD8} from the lung and spleen at indicated times p.i. Lines connect lung and spleen samples from the same mouse. Data are combined from two independent experiments. * $p<0.05$, paired t-test. (**C**) Boolean gating analysis for the co-expression of inhibitory receptors on M195-specific T_{CD8} at indicated times p.i.

(**D**) Relative expression of possible inhibitory receptor combinations. (**E**) Expression of the ligands for each inhibitory receptor on lung epithelial cells (Ep-CAM^{+}) or antigen presenting cells (CD11c^{+}) at the indicated times p.i. Ligand:Recetor pairs are PD-L1:PD-1, MHC-II:LAG-3, CD48:2B4, Galectin-9:TIM-3. Representative data from two independent experiments with 4-5 mice per time point are shown. Mock indicates mock-infection with cell lysate.

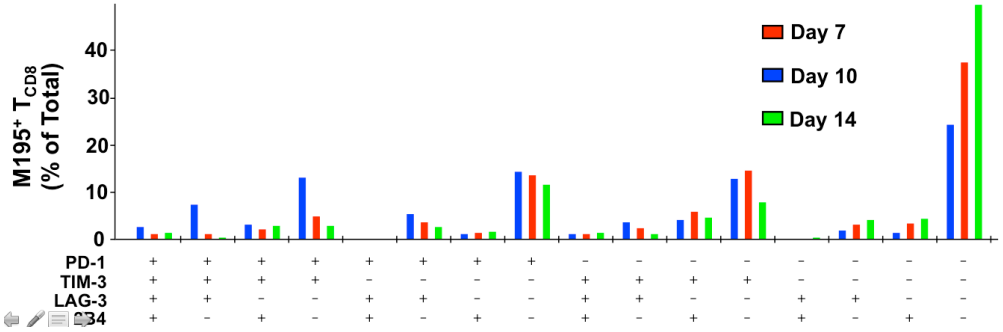

Figure 4-6. Kinetics of spleen T_{CD8} inhibitory receptor co-expression**.** Boolean gating analysis was performed for the co-expression of inhibitory receptors on splenic M195^{+} T_{CD8} at indicated times p.i. The expression of possible inhibitory receptor expression combinations is shown.

Cognate Antigen Drives Impairment and Inhibitory Receptor Upregulation

Ag-induced TCR signaling is associated with PD-1 upregulation during chronic infections (Barber et al., 2006; Blattman et al., 2009; Trautmann et al., 2006; Zhang et al., 2007). To determine whether viral Ag is necessary for pulmonary T_{CD8} impairment and inhibitory receptor upregulation, we took advantage of the fact that i.n. dendritic cell (DC) immunization elicits unimpaired PD-1^{low} T_{CD8} directly in the lung (Erickson et al., 2012). We immunized mice i.n. with DCs loaded with the vaccinia virus epitope $A34R_{82-90}$ (A34R), challenged them with HMPV a week later, and either gave cognate peptide or a control HLA-B*0702-restricted peptide i.n. during the infection (Figure 4-7A). Of note, mice receiving mock peptide did not lose weight during the infection (HMPV does not cause clinical disease in mice), while those receiving A34R peptide lost nearly 25% of

their body weight (Figure 4-7B). Additionally, the endogenous M195-response was diminished in A34R-treated mice (not shown) and so was not included in the following analysis. Heterologous A34R-specific T_{CD8} in mice receiving control peptide were minimally impaired, while M195-specific T_{CD8} in the same infected lungs were more impaired (Figure 4-7C). In contrast, A34R-specific T_{CD8} in mice receiving cognate peptide expanded in number and were severely impaired. Compared to M195-specific cells, A34R-specific T_{CD8} in mock-treated mice expressed far less PD-1, TIM-3, LAG-3 (Figure 4-7D) and 2B4 (not shown). Furthermore, inhibitory receptor co-expression was greatly reduced in A34R-specifc T_{CD8} (Figure 4-7E), closely resembling the expression profile of unimpaired spleen T_{CD8} (Figure 4-5C). The large degree of functional impairment observed in A34R-specific T_{CD8} in A34R peptide-treated mice was associated with a dramatic increase in inhibitory receptor co-expression (Figure 4-7D,E). Thus, cognate Ag-induced TCR signaling contributes to lung T_{CD8} impairment and drives inhibitory receptor expression.

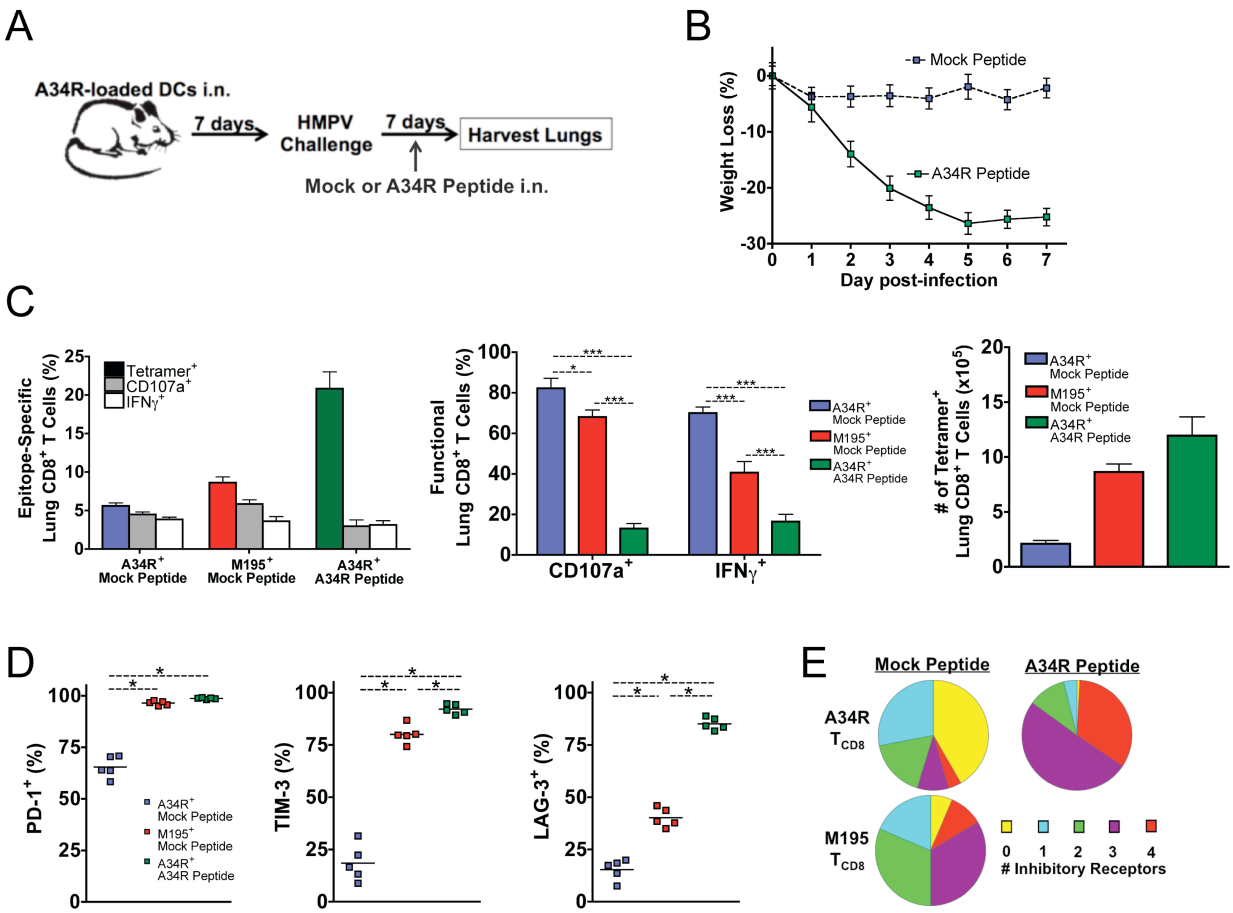

Figure 4-7. Cognate antigen drives impairment and inhibitory receptor upregulation. (**A**) Experimental design: mice were immunized i.n. with A34R-loaded DCs (see Materials and Methods) and challenged 7 days later with HMPV. During the infection, mice were given either cognate or mock peptide i.n. daily. At day 7 p.i., the lung A34R- and M195-specific T_{CD8} response in mock peptide-treated mice and the A34R-specific T_{CD8} response in A34R peptide-treated mice was quantified. (**B**) Weight loss during HMPV infection of DC-immunized, peptide-treated mice. (**C**) Tetramer staining and ICS for the A34R and M195 T_{CD8} epitopes at day 7 p.i. (left graph). The percentage of functional epitope-specific T_{CD8} (middle graph) and the total number of tetramer$^+$ T_{CD8} were calculated (right graph). For each bar, the epitope analyzed is given with the treatment written directly below. (**D**) Inhibitory receptor expression on A34R- and M195-specific T_{CD8}. (**E**) Inhibitory receptor co-expression was determined for both epitopes as in Figure 3. Results are combined from three independent experiments (B,C) or are representative of one such experiment (D,E) with 5 mice per group. Error bars, s.e.m. * $p<0.05$, student's t-test.

In Vitro Blockade of Inhibitory Receptors

To determine whether inhibitory receptor co-expression identifies all epitope-specific T_{CD8} or just the subset that are impaired, we performed ICS for IFNγ and TNF after peptide stimulation and then stained for inhibitory receptors. We found that the functional subset of $IFN\gamma^+$ (Figure 4-8A) or $IFN\gamma^+TNF^+$ (not shown) M195-specific lung T_{CD8} express a similar number and pattern of inhibitory receptors as those identified by tetramer staining. These results suggest that the functional subset of lung T_{CD8} may be susceptible to impairment due to continued inhibitory receptor expression. Collectively, the data presented so far suggest that lung T_{CD8} functional decline is associated with the substantial co-expression of multiple inhibitory receptors on HMPV-specific T_{CD8}.

To screen inhibitory receptors for functional relevance to T_{CD8} impairment, we developed an *in vitro* method to block individual or combinations of receptors. Lung suspension cells (Figure 4-8B,D) or splenocytes (Figure 4-8C) from HMPV-infected mice were added to an IFNγ detecting ELISPOT assay, restimulated with M195-peptide and incubated with monoclonal antibodies against various inhibitory receptors or their ligands. M195 restimulation of lung cells plus PD-L1 blockade resulted in significantly more IFNγ-secreting cells (i.e. more spots; see Figure 4-8B), confirming our previous *in vivo* results (Erickson et al., 2012). Importantly, PD-L1 blockade of restimulated splenocytes (which are unimpaired *in vivo*, Figure 4-2A) had no effect (Figure 4-8C). Blockade of TIM-3 and LAG-3 resulted in more spots in restimulated lung cells at both day 7 (Figure 4-8C) and day 10 p.i. (Figure 4-8D). Blocking 2B4 had no effect at day 7 but a significant effect at day 10 p.i. Combining PD-L1 blockade with TIM-3, LAG-3 or PD-L2 blockade resulted in even greater numbers of spots. Combination blockade also resulted in larger spots (i.e. more IFNγ production per cell) (Figure 4-9). Taken together,

these results indicate that lung T_{CD8} expressing multiple inhibitory receptors are impaired and that blockade of these receptors enhances cytokine production *in vitro*.

Additionally, PD-1 signaling impairs T_{CD8} during primary influenza virus infection of mice (Erickson et al., 2012), but we found less of a role for PD-1 on the secondary NP366-specific T_{CD8} response during heterologous challenge infection (Figure 4-10A). *PD-1*$^{-/-}$ mice showed a slight restoration of T_{CD8} functions, as well as a greater number of IFNγ-producing cells (Figure 4-10B,C). We harvested lung cells from these mice and tested blocking antibodies against the four inhibitory receptors and discovered that blocking TIM-3 had the greatest effect (Figure 4-10D), which was more than PD-1 blockade (Figure 4-10E). A role for TIM-3 in impairing influenza-specific T_{CD8} is consistent with a previous report (Sharma et al., 2011). LAG-3 blockade also resulted in a greater response, while 2B4 had no effect. These results demonstrate that a high-throughput ELISPOT assay can be used to identify functional inhibitory receptors in multiple settings.

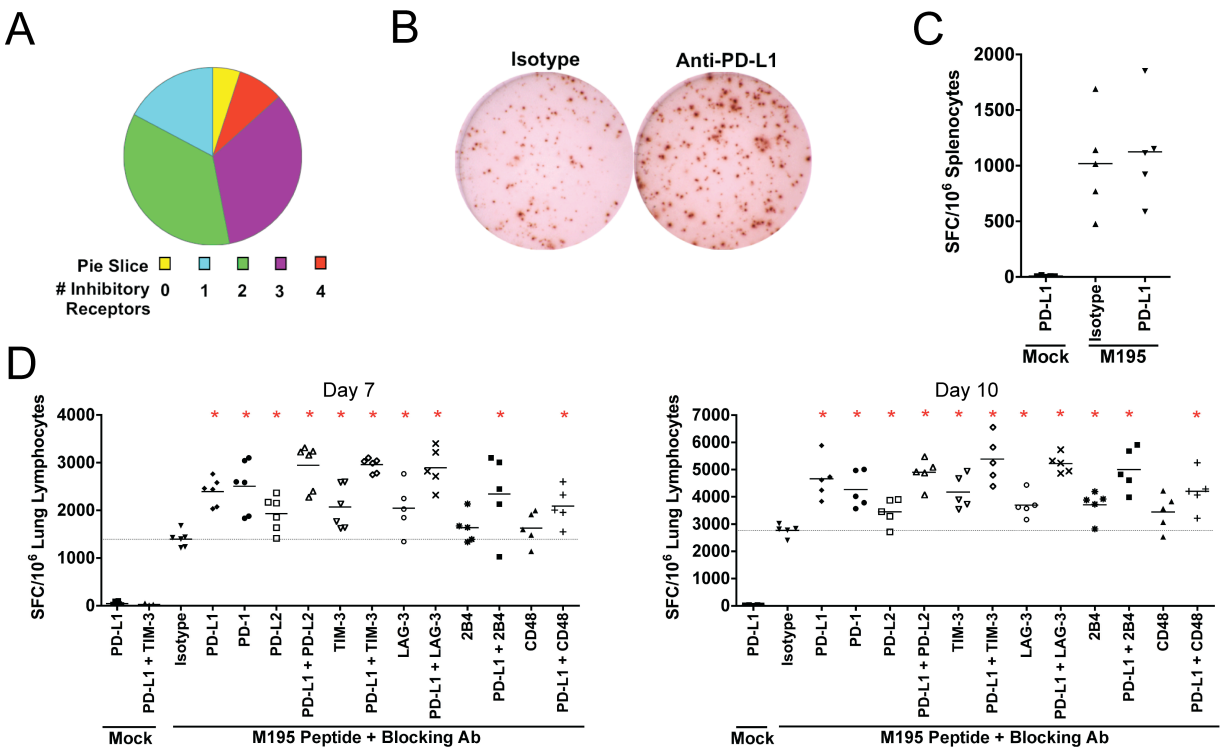

Figure 4-8. *In vitro* blockade of inhibitory receptors. (**A**) ICS and inhibitory receptor staining following brief M195 peptide stimulation of lung T_{CD8} at day 10 p.i. The percentage of M195-specific T_{CD8} that produce IFNγ was quantified and populations were grouped based on the total number of inhibitory receptors expressed. M195-specific T_{CD8} inhibitory receptor expression did not change during the stimulation (not shown). Data are combined from two experiments with 5 mice per experiment. (**B**) Lung cells were added to anti-IFNγ-coated ELISPOT plates and restimulated with M195 peptide in the presence of anti-PD-L1 blocking antibody or isotype control antibody for 48 hours. Each spot represents a single IFNγ-secreting cell. Representative wells are shown. (**C**) Splenocytes were stimulated as in (B). (**D**) Lung cells were stimulated with M195 peptide in the presence of the indicated inhibitory receptor blocking antibodies at day 7 or day 10 p.i. Mock indicates wells stimulated with an irrelevant peptide. Data are expressed as the number of spot forming cells (SFC) per 10^6 lymphocytes. Each symbol represents the mean from one of five or six total independent experiments with 2-3 mice per experiment. Dotted line indicates the mean number of spots from M195-stimulated, isotype control antibody treated cells as a reference. * $p<0.05$, student's t-test.

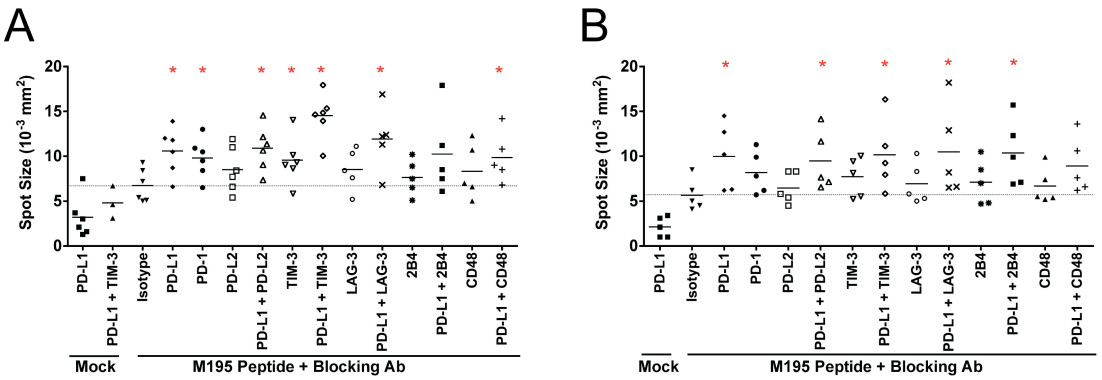

Figure 4-9. *In vitro* blockade of inhibitory receptors (continued). The mean spot size is shown for M195 restimulated lung T_{CD8} at days 7 (**A**) and 10 p.i. (**B**) in the presence of the indicated inhibitory receptor blocking antibodies. Each symbol represents the mean from one of five or six total independent experiments with 2-3 mice per experiment. Dotted line indicates the mean spot size from M195-stimulated, isotype control antibody treated cells as a reference.

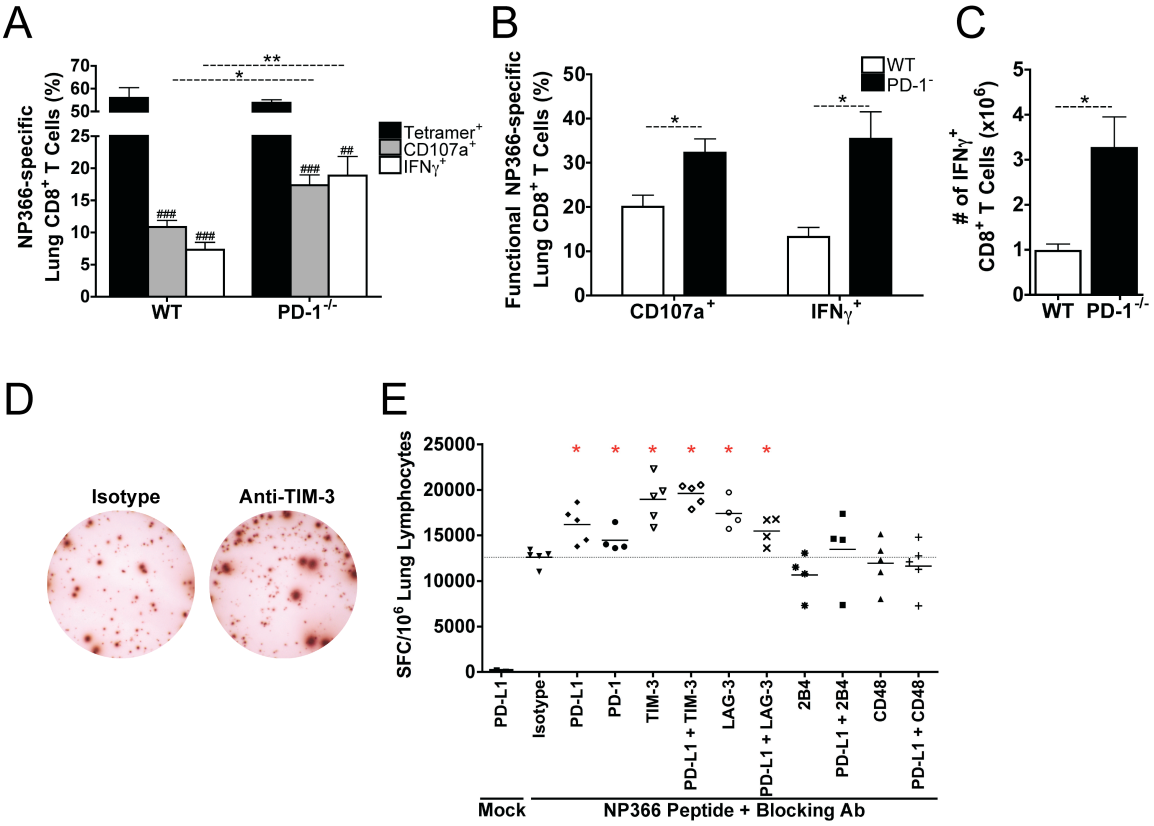

Figure 4-10. Lack of PD-1 signaling minimally restores function to secondary lung T_{CD8} during influenza virus heterologous challenge *in vivo* but blocking TIM-3 restores function *in vitro*. *PD-1*$^{-/-}$ and control WT mice were primed i.p. with influenza virus strain PR8 (H1N1) and then challenged i.n. with strain x31 (H3N2). The lung and spleen T_{CD8} responses were quantified at day 7 post-challenge. (**A**) Tetramer staining and ICS were

performed for NP366-specific lung and spleen T_{CD8}. (**B**) The percentage of functional NP366-specific lung T_{CD8} was calculated. (**C**) The total number of IFNγ^+ NP366-specific T_{CD8} was calculated. Error bars, s.e.m. Data are representative of one out of two independent experiments with 5 mice per experiment. # $p<0.05$, paired student's t-test. * $p<0.05$, unpaired student's t-test. (**D**) Lung cells were added to anti-IFNγ-coated ELISPOT plates and restimulated with NP366 peptide in the presence of TIM-3 blocking antibody or isotype control antibody for 42-48 hours. Representative wells are shown. Each spot represents a single IFNγ-secreting cell. (**E**) NP366 restimulation with incubation of indicated inhibitory receptor blocking monoclonal antibodies. Mock indicates wells stimulated with an irrelevant peptide. Data are expressed as the number of spot forming cells (SFC) per 10^6 lymphocytes. Each symbol represents the mean from one of four or five total independent experiments with 2-3 mice per experiment. Dotted line indicates the mean number of spots from NP366-stimulated, isotype control antibody treated cells as a reference. * $p<005$, student's t-test.

LAG-3 Compensates for PD-1 *in vivo* to Impair Lung T_{CD8}

T_{CD8} effector functions wane over time (Figure 4-2A), so we hypothesized that inhibitory receptor signaling might play an even greater role at later time points. However, we were surprised to find only a marginal effect when PD-1 signaling was absent on day 10 (not shown) or day 14 p.i.(Figure 4-11). Thus, we thought alternate inhibitory pathways may function in the absence or blockade of PD-1 signaling. Such compensatory impairment has the ability to undermine potential therapeutic interventions. Both TIM-3 and LAG-3 can collaborate with PD-1 to cause T cell exhaustion. However, neither have been described to compensate for PD-1 once it is blocked. Since blockade of both receptors enhanced the *in vitro* response of virus-specific lung T_{CD8}, we first tested TIM-3 blockade *in vivo*, but did not find any change in T_{CD8} functions (not shown). We then tested LAG-3 and found that HMPV-specific lung T_{CD8} better degranulated or made the cytokines IFNγ and TNF in *PD-1*$^{-/-}$ mice treated with anti-LAG-3 versus control treated animals (Figure 4-12A). This corresponded to more functional T_{CD8} compared to isotype-treated mice (Figure 4-12B). Thus, LAG-3 can compensate for the loss of PD-1 signaling just days after PD-1 is the primary driver of impairment, returning lung T_{CD8} to an impaired state.

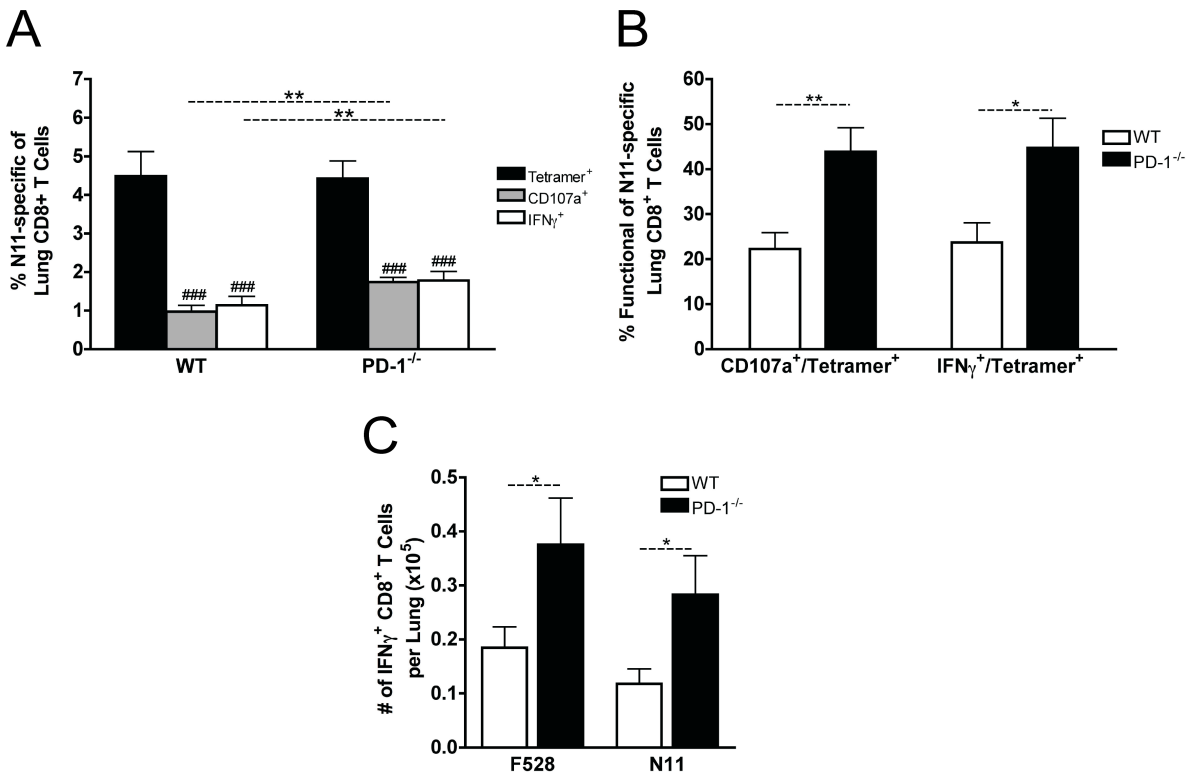

Figure 4-11. The effects of blocking PD-1 signaling in Lung T_{CD8} are minimized at later time points. *PD-1*$^{-/-}$ and control WT mice were infected with HMPV and the lung T_{CD8} response was quantified at day 14 p.i. (**A**) Tetramer staining and ICS were performed for N11-specific T_{CD8}. (**B**) The percentage of functional N11-specific T_{CD8} was calculated. (**C**) The total number of IFNγ^+ F528- and N11-specific T_{CD8} was calculated. Error bars, s.e.m. Data are combined from two independent experiments with 5 mice per experiment. # $p<0.05$, paired student's t-test. * $p<0.05$, unpaired student's t-test.

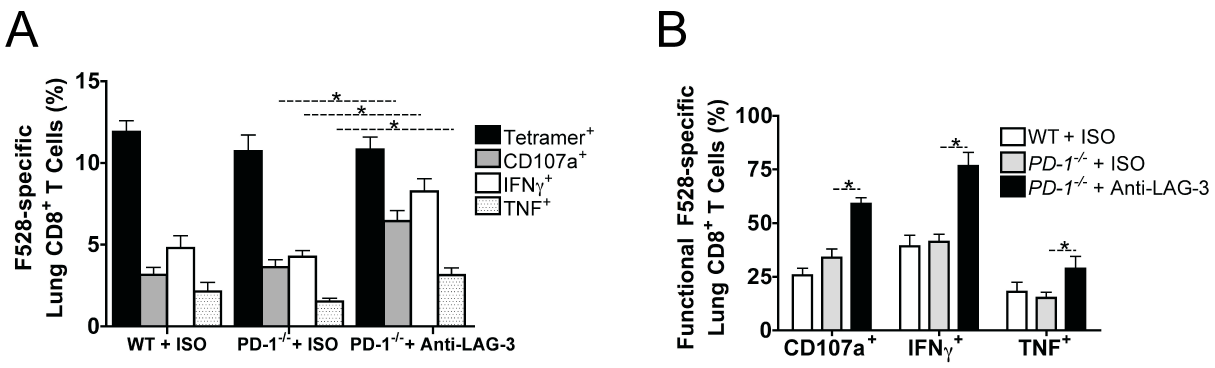

Figure 4-12. LAG-3 compensates for lack of PD-1 signaling *in vivo* to impair lung T_{CD8}. *PD-1*$^{-/-}$ mice were infected with HMPV and treated with isotype control or anti-LAG-3 antibody. (**A**) The lung F528- and N11-specific T_{CD8} responses were quantified on day 10 p.i. (**B**) The percentage of functional F528- and N11-specific T_{CD8} was calculated. Results are combined from two independent experiments with 5-7 mice per group. Error bars, s.e.m. * p<0.05, student's t-test.

Gene Expression Profile of Impaired Lung T_{CD8} Is Unique Compared to Effector or Exhausted T_{CD8} During LCMV Infection

Thus far, our data have indicated numerous similarities between impaired lung T_{CD8} during acute viral LRI and exhausted T_{CD8} during chronic infection; in particular, functional impairment is associated with expression of multiple inhibitory receptors. However, important differences exist concerning lung T_{CD8} impairment, including the speed with which impairment develops and the ability of additional inhibitory receptors to quickly compensate for loss of PD-1 signaling. We were therefore interested in more thoroughly comparing the gene expression profiles of impaired lung T_{CD8} to exhausted T_{CD8}. To do so, we compared our dataset to previously published data analyzing the gene expression of functional effector T_{CD8} generated by acute LCMV Armstrong infection and exhausted T_{CD8} during chronic LCMV clone13 infection (Doering et al., 2012). Clustering based on gene expression differences revealed that impaired lung T_{CD8} most closely resemble T_{CD8} early during chronic infection (day 8 p.i.), followed by functional effectors during acute infection (Figure 4-13). Lung T_{CD8} were more distantly related to T_{CD8} later during chronic infection (day30 p.i.). However, numerous genes

were uniquely up- or down-regulated by lung T_{CD8} versus the other groups. These results indicate that lung T_{CD8} during acute viral LRI are most closely related to T_{CD8} early during the exhaustion process, but that they also possess a unique gene expression profile.

DISCUSSION

In this study we examined the global gene expression profile of impaired lung T_{CD8} and determined the role of various inhibitory receptors during acute viral LRI. We first determined that lung T_{CD8} impairment is regulated by PD-1 in a cell-intrinsic manner. Importantly, this excluded a role for other PD-1-expressing cell types and focused our attention on additional T_{CD8}-intrinsic mechanisms of impairment. PD-1 signaling affects other immune cells during some acute infections. PD-1 impairs macrophage function and limits survival during sepsis (Huang et al., 2009), while it restrains DC innate immune functions during bacterial infection (Yao et al., 2009). Blocking PD-1 during rabies infection enhances survival (Lafon et al., 2008), but whether T_{CD8} are involved in this process is unclear. A T_{CD8}-intrinsic role for PD-1 was suggested by *in vitro* studies showing that blocking PD-L1 on epithelial cells during RSV infection (Telcian et al., 2011) or microglial cells during coronavirus infection (Phares et al., 2009) resulted in increased IFNγ production by memory T_{CD8}. Bone marrow chimeric experiments confirmed an intrinsic role for PD-1 in impairing T_{CD8} memory development and secondary responses after VACV infection (Allie et al., 2011). Here we used bone marrow chimeric mice to show that PD-1 cell-intrinsically regulates T_{CD8} functions during acute viral LRI. The contribution of T_{CD8}-intrinsic PD-1 signaling to viral clearance cannot be assessed using this model, so the possibility exists that PD-1 expression by other immune cells may further limit viral clearance.

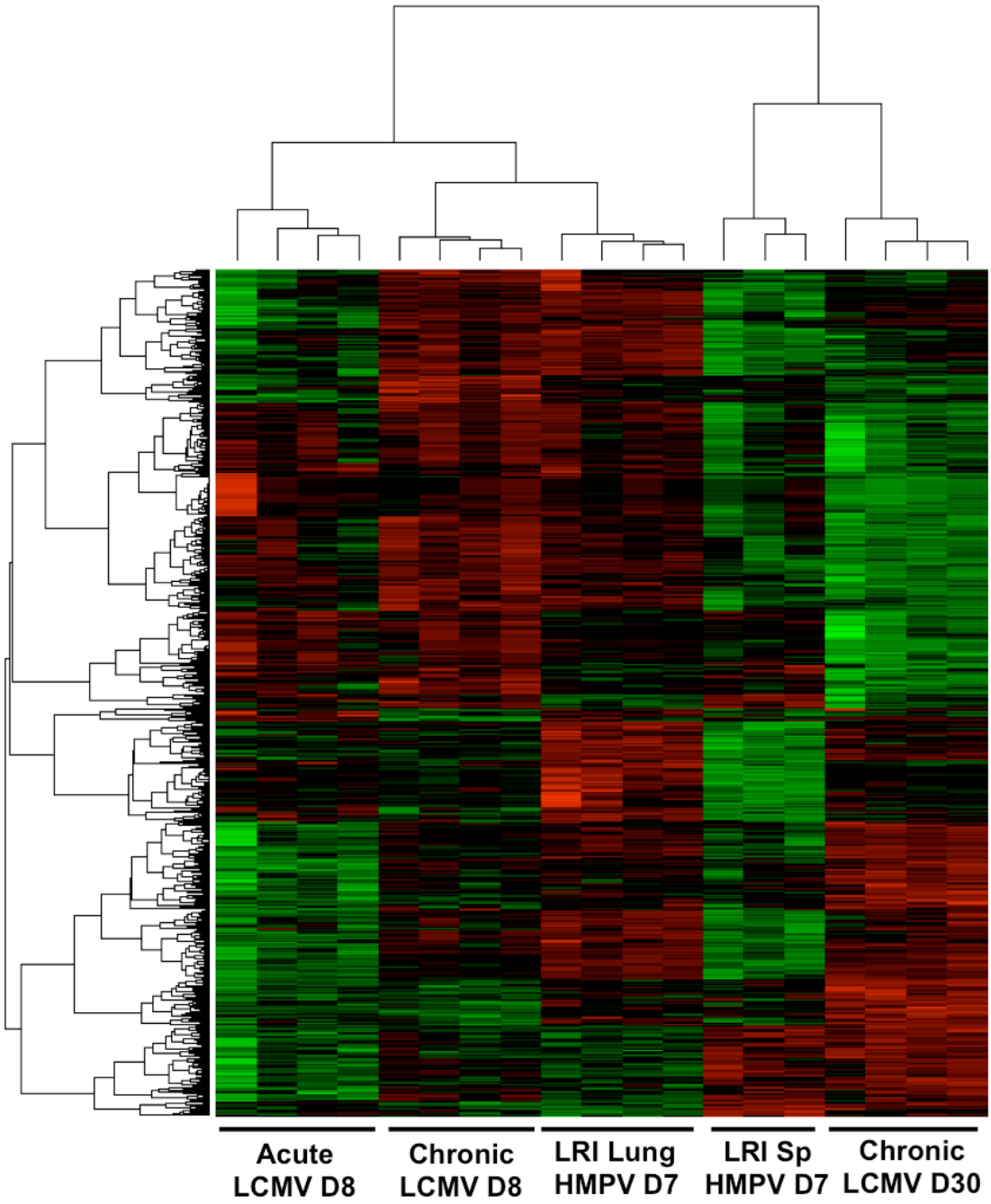

Figure 4-13. Gene expression profile of impaired lung T_{CD8} is unique compared to functional effector or exhausted T_{CD8} during LCMV infection. Lung and spleen (Sp) M195-specific T_{CD8} gene expression was directly compared to that of splenic gp33-specific T_{CD8} during acute (Armstrong strain) or chronic (clone 13 strain) LCMV infection (from Doering et al., 2012). LCMV samples include early acute (day 8), early chronic (day 8) and late chronic (day 30). Batch effect was compensated for before further analysis. Heatmap resulting from ANOVA analysis of the gene-expression profiles of each T_{CD8} population showing the relatedness of individual samples is shown.

Our data challenge the paradigm that acute infections generate functional effector T_{CD8} that transition to memory T_{CD8}. We observed rapid impairment of lung T_{CD8} under the control of PD-1, which until recently was thought to operate only under conditions of prolonged Ag stimulation. However, by day 7 post-HMPV infection, lung T_{CD8} have lost most of their ability to make IL-2 and TNF and less than half retain he ability to make IFNγ or degranulate (Erickson et al., 2012). Not only are lung T_{CD8} dysfunctional during acute viral LRI, but surface markers commonly used to distinguish between terminal effectors and memory precursors do not correspond to other described acute infections. It is thought that T_{CD8} with greater effector activity (termed short-lived effector cells or SLECs) are KLRG1^{hi}IL-7R^{low}, while T_{CD8} with memory potential (memory precursor effector cells or MPECs) are KLRG1^{low}IL-7R^{hi} (Kaech and Cui, 2012). Impaired lung T_{CD8} are KLRG1^{low}IL-7R^{mid}, suggesting a memory phenotype (Figure 4-14). However, unlike memory cells, impaired lung T_{CD8} gradually decline in number, lose functionality and exhibit a severely impaired phenotype when challenged (Erickson et al., 2012).

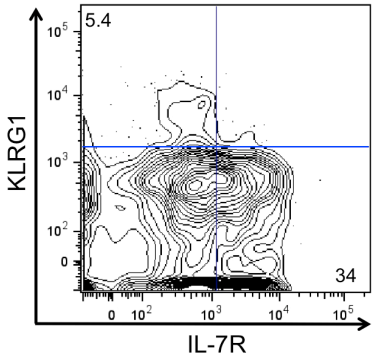

Figure 4-14. KLRG1 and IL-7R expression on impaired lung T_{CD8}. The expression of KLRG-1 versus IL-7R is shown for M195-specific T_{CD8} in B7tg mice at day 7 p.i. Numbers in each quadrant are the percentage of cells staining positive in that gate. Data are representative of two independent experiments with 3-5 mice per experiment.

Where do lung T_{CD8} during acute viral LRI exist on the spectrum of T cell differentiation? To answer this, we globally profiled gene expression in impaired lung

versus unimpaired spleen epitope-specific T_{CD8} to identify pathways that might explain the stark difference in functionality observed between these two T_{CD8} populations. Lung T_{CD8} exhibited a more diverse pattern of gene expression, differentially expressing 319 genes compared to spleen T_{CD8}. Many of these were attributable to type I IFN signaling, but experiments using $IFNAR^{-/-}$ mice showed that type I IFNs do not account for the functional differences we observed. Lung T_{CD8} upregulated the expression of numerous genes encoding chemokines, including CCL1, CCL3, CCL4, CXCL9 and CXCL15, suggesting a role for lung T_{CD8} in recruiting other inflammatory cells to the infected lung. Lung T_{CD8} transcribed more *Ifng, Tnfa* and *Il2* mRNA despite a decreased ability to produce these proteins, suggesting post-transcriptional regulation exists for these cytokines, a phenotype also observed during exhaustion (Wherry et al., 2007).

Recently the transcriptional circuitry that regulates effector, memory and exhausted T_{CD8} has been defined (reviewed by Kaech and Cui, 2012). T-bet, which supports effector T_{CD8} function and prevents exhaustion (Kao et al., 2011), and Eomes, which promotes exhaustion (Paley et al., 2012), were not differentially expressed between spleen and lung T_{CD8} during acute viral LRI. Fos and Jun, two proteins that form the heterodimeric transcription factor AP-1, were both more highly expressed in lung T_{CD8}. AP-1 was recently described as a transcriptional activator of PD-1 (Xiao et al., 2012) and so may represent a link between Ag-induced TCR signaling and PD-1. The genes encoding transcription factors *Id2* and *Id3* were more highly expressed in lung T_{CD8}. ID2 supports development of terminal effectors (Cannarile et al., 2006) while ID3 promotes survival of long-lived memory cells (Ji et al., 2011). ID2 would likely contribute more early during effector differentiation of lung T_{CD8} but the contribution of each of these transcriptional regulators to impairment remains to be defined. Additionally, the *Prdm1* gene, which encodes the transcriptional repressor BLIMP-1, is upregulated in lung T_{CD8}, while BCL-6, which opposes BLIMP-1 activity, is down-regulated in both lung

and spleen T_{CD8}. During acute infections, high BLIMP-1 expression enhances T cell functions and the formation of KLRG1^{hi}IL-7R^{low} terminal effectors (Rutishauser et al., 2009). During chronic infection, BLIMP-1 is highly expressed in association with the upregulation of inhibitory receptors (Shin et al., 2009). During viral LRI, a role for BLIMP-1 has been described in the generation of IL-10-producing effector T_{CD8} (Sun et al., 2011b). In our analysis, BLIMP-1 expression was not different between exhausted T_{CD8} from chronic LCMV infection and impaired lung T_{CD8}. Given the high expression of inhibitory receptors on lung T_{CD8}, BLIMP-1 may favor functional impairment, but further experiments are necessary to explore this possibility.

Lung T_{CD8} expression of Tbet, BLIMP-1, AP-1 and ID2 during acute viral LRI all imply an effector phenotype. Indeed, lung T_{CD8} are effectors that produce cytokines, degranulate and kill infected cells. However, they rapidly lose these effector functions in conjunction with coordinated upregulation of several inhibitory receptors. These inhibitory receptors temper immune responses in a number of settings (Odorizzi and Wherry, 2012) and their roles in LRI are not well understood. TIM-3, which is co-expressed by PD-1^{+} T cells during chronic infections (Jin et al., 2010a) and cancer (Sakuishi et al., 2010a), also impairs T cell responses during acute viral infections (Sehrawat et al., 2010; Sharma et al., 2011). Here we found that TIM-3 was expressed by lung T_{CD8} and *in vitro* blockade resulted in more IFNγ-secreting cells. 2B4 can be either inhibitory or stimulatory (Chlewicki et al., 2008), but in the setting of chronic infection it contributes to the rapid impairment of memory T_{CD8} (West et al., 2011). Interestingly, we found higher expression of 2B4 on secondary compared to primary T_{CD8}, suggesting 2B4 may preferentially regulate secondary effector T_{CD8}. We were unable to test this hypothesis *in vivo*, however, as 2B4 blocking antibodies also deplete when used in animals. Lung T_{CD8} also expressed higher levels of *Il10* and *Il10ra* mRNA. T cells are the primary producers of IL-10 during LRI (Sun et al., 2009) and it has been

proposed that their expression of IL-10R facilitates an intrinsic T_{CD8} counter-regulatory mechanism (Sun et al., 2011a), suggesting that IL-10 may also be a key mediator of T_{CD8} impairment. However, unlike during chronic infection where IL-10 blockade enables clearance of an established infection (Ejrnaes et al., 2006), blocking IL-10 during acute infection only serves to increase inflammation and not accelerate viral clearance (Sun et al., 2011a) so its application in therapeutic approaches may be limited.

We found that LAG-3 is capable of compensating for PD-1 to impair lung T_{CD8} during HMPV infection. LAG-3 shares homology with CD4 and also binds MHC-II (Baixeras et al., 1992), impairing T cell activation and proliferation (Hannier et al., 1998). Combined blockade of PD-1 and LAG-3 restores T_{CD8} functions during chronic viral infection (Blackburn et al., 2009) and boosts T follicular helper cell function during malaria (Butler et al., 2012b). The mechanism of how LAG-3 impairs T_{CD8} is unclear, but we found that its ligand, MHC-II, was abundantly expressed by lung epithelial cells and APCs. We found that lung T_{CD8} returned to a functionally impaired state by day 10 p.i. The rapidity with which lung T_{CD8} become impaired is striking and separates this process from T cell exhaustion, which occurs over several weeks. We found that additional blockade of LAG-3 enhanced T_{CD8} effector functions. This finding suggests that lung T_{CD8} functions are tightly regulated by a layered system of inhibitory receptors. PD-1 appears to be a master regulator that down-regulates T_{CD8} functionality early, while LAG-3 plays a prominent role in impairing cells even in the absence of PD-1. In addition, blocking LAG-3 or TIM-3 *in vitro* restored function to lung T_{CD8}, although not to the degree of PD-1. This suggests redundancy in inhibitory pathways for impairing effector functions, especially since T_{CD8} remain impaired despite a complete lack of PD-1 signaling *in vivo*. These results have important implications for the deployment of any future therapeutic interventions targeting the PD-1 pathway during acute viral LRI. If other inhibitory receptors can quickly compensate for a blocked PD-1 pathway, then a

combination approach might be more effective. Further elucidation of the mechanisms utilized by TIM-3 and LAG-3 to impair T cells may identify a common downstream molecule that can be effectively targeted.

In summary, we have defined the gene expression profile of impaired lung T_{CD8} and determined that their differentiation state comprises elements of both effector and exhausted T cells. We validated the expression and function of four inhibitory receptors. LAG-3 collaborated with PD-1 to impair lung T_{CD8} and could compensate for a lack of PD-1 signaling just a few days after PD-1 signaling blockade effectively restored T_{CD8} functions. The approach of identifying inhibitory receptors expressed by impaired T_{CD8} followed by *in vitro* and *in vivo* screening could lead to the identification of additional novel therapeutic targets. Our results suggest that an overlapping system of inhibitory receptors keeps lung T_{CD8} in check, and that therapeutically it may be necessary to target multiple pathways, or an upstream regulator of these pathways, to achieve durable clinical outcomes.

MATERIALS AND METHODS

Mice

C57BL/6 (B6) and congenic Thy1.1^{+} mice were purchased from the Jackson Laboratory. B6-Kb^{0}Db^{0};B7.2 transgenic (B7tg) mice were obtained with permission from Drs. Alexander Sette (La Jolla Institute for Allergy and Immunology, La Jolla, CA) and Francois Lemonnier (Institut Pasteur, Paris, France). *PD-1*$^{-/-}$ mice were obtained with permission from Dr. Tasuku Honjo (Kyoto University, Kyoto, Japan). All animals were bred and maintained in specific pathogen-free conditions in accordance with the Vanderbilt Institutional Animal Care and Use Committee. 6-12 week old age- and gender-matched animals were used in all experiments. Mixed bone-marrow chimeric mice were generated by irradiating Thy1.1^{+} recipients with 2 doses of 5 Gy, 4 hours apart, followed by reconstitution with 1x10^{6} WT (Thy1.1^{+}) and 1x10^{6} *PD-1*$^{-/-}$ (Thy1.2^{+}) bone-marrow cells 24 hours later. Mice were rested for 8 weeks and then bled to check reconstitution before use in experiments.

Viruses and Infections

HMPV (pathogenic clinical strain TN/94-49, genotype A2) was grown and titered in LLC-MK2 cells as previously described (Williams et al., 2005). Influenza virus strains A/34/PR/8 (PR8; H1N1; ATCC) and HK/x31 (x31; H3N2; kindly provided by Dr. Jon McCullers, St. Jude Children's Hospital, Memphis, TN) were grown in MDCK cells and titered on LLC-MK2 cells. For all experiments, mice were anesthetized with ketamine-xylazine and infected intranasally (i.n.) with 1x10^{6} PFU of HMPV. For influenza virus challenge experiments, mice were primed i.p. with 2x10^{5} PFU of PR8 and challenged i.n. with 5x10^{2} PFU of x31 at least 15 weeks later.

Flow Cytometry Staining

Tetramers were generated for the following viral epitopes as previously described (Erickson et al., 2012): HMPV (HLA-B*0702/$M_{195-203}$ [APYAGLIMI], H2-D^b/$F_{528-536}$ [SGVTNNGFI], H2-K^b/N_{11-19} [LSYKHAIL]), influenza virus (H2-D^b/$NP_{366-374}$ [ASNENMETM]), vaccinia virus (HLA-B*0702/$A34R_{82-90}$ [LPRPDTRHL]). Lymphocytes were isolated from spleens and lungs of infected animals and stained as previously described (Erickson et al., 2012). Cells were stained with PE- or APC-labeled tetramers (0.1-1 µg/ml), anti-CD8α (clone 53-6.7, BD Biosciences), and anti-CD19 (clone 1D3, iCyt). In some experiments, cells were also stained for the inhibitory receptors PD-1 (clone RMP1-30), TIM-3 (clone RMT3-23), LAG-3 (clone C9B7W) and 2B4 (clone m2B4 (B6)458.1) or with appropriate isotype controls (all from Biolegend). For mixed bone marrow chimera experiments, cells were stained for Thy1.1 (clone OX-7, BD Biosciences) and Thy1.2 (clone 53-2.1, BD Biosciences). Surface/tetramer staining was performed for 1 hour at RT in PBS containing 1% FBS and 50nM dasatinib. To stain for the ligands of each inhibitory receptor, lung cell suspensions were stained with LIVE/DEAD dye and Fc blocked in the presence of 20% mouse serum followed by surface staining for Ep-CAM (clone G8.8, Biolegend), CD11c (clone HL3, BD Biosciences), PD-L1 (clone MIH5, BD Biosciences), PD-L2 (clone TY25, Abcam), MHC-II (clone M5/114.15.2, eBiosciences) and CD48 (clone HM48-1, Biolegend). Some cells were also fixed and permeabilized to stain for intracellular Galectin-9 (clone 108A2, Biolegend). Intracellular cytokine staining was performed in parallel with tetramer staining as previously described (Erickson et al., 2012). Flow cytometric data were collected using an LSRII or Fortessa (BD Biosciences) and analyzed with FlowJo software (Tree Star). The Boolean gating function in FlowJo was used to assess inhibitory receptor co-expression and patterns were visualized using the SPICE program (NIAID).

Cell Sorting

To obtain sufficient quantities of primary epitope-specific T_{CD8}, on day 7 after HMPV infection the spleens and lungs from three mice were pooled together after processing to form one sample. Samples were stained, sorted and RNA purified on separate days in independent experiments. Cells were processed in ice-cold R10 media containing 10nM dasatinib to prevent activation and TCR signaling. Lung cells were processed as before. Splenocytes were depleted of B cells by incubation on goat anti-mouse IgG and IgM (100µg/mL) (Southern Biotechnology) coated T-75 flasks at 10^6 cells/mL for 1hr at 37C and then processed as before. Both lung and spleen cells were stained for viability, CD19, CD8 and M195-tetramers (both PE- and APC-conjugated). Splenocytes were also stained for CD44 (clone IM-7; BD Biosciences) and CD62L (MEL-14; BD Biosciences) to obtain control naïve cells. Dual-tetramer positive T_{CD8} were sorted using a BD FACSAria III. Samples were maintained at 4C for the entirety of the sort and purity was 97%–99% for all populations.

RNA Amplification and Hybridization

Total RNA was isolated from sorted naive, spleen, lung and secondary lung M195-specific T_{CD8} using a RNeasy kit (QIAGEN) according to the manufacturer's instructions. On-column DNase digestion was peformed and eluted RNA was quantified and checked for integrity using an Agilent 2100 Bioanalyzer. RNA was amplified using a WT Ovation Pico kit (NuGen) and then converted to cDNA. Amplified samples were again checked for integrity and then hybridized to Mouse Gene 1.1 ST microarrays (Affymetrix) and scanned on the GeneTitan Instrument (Affymetrix).

Microarray Data Analysis

HMPV T_{CD8} data analysis - Microarray data were processed using the oligo package implementation of rma in R software (Carvalho et al., 2007). Four groups (naïve, spleen, lung, and secondary lung) were compared using Limma Package (Smyth, 2004). Significantly changed probes were identified by ANOVA. p-values were adjusted for multiple comparisons using the false discovery rate (FDR) method (Benjamini, 1995). The thresholds for significance were set to control the expected FDR at values <10% and the fold-change at 2.

HMPV data versus LCMV data - GSE41867 data (Blackburn et al., 2009) was downloaded from the NCBI GEO database. The microarray data files from the current study and GSE41867 were processed separately using the oligo package implementation of rma in R software. The batch effect of two data sets was corrected using ComBat package (Johnson et al., 2007). Five groups (spleen and lung are from the HMPV data set and three spleen groups from GSE41867) were compared using Limma package and significantly changed probes were identified as before.

Generation of Bone Marrow-Derived Dendritic Cells and Immunizations

Bone marrow-derived DCs were generated as previously described (Erickson et al., 2012). To obtain secondary M195-specific T_{CD8}, mice were primed i.n. with $2x10^6$ M195-loaded, LPS-matured DCs and then challenged with HMPV three weeks later. For generation of lung-infiltrating vaccinia virus $A34R_{82-90}$-specific T_{CD8}, mice were immunized i.n. with A34R-DCs and then challenged seven days later with HMPV and were treated daily i.n. during the infection with either 50µg A34R peptide or an irrelevant HLA-B**0702*-restricted peptide.

IFNγ ELISPOT

ELISPOT assays were performed as previously described (Rock and Crowe, 2003) with slight modifications. $5x10^4$ lung cells or $2x10^5$ spleen cells were added to triplicate wells. Peptides were then added (10μM final concentration) followed by inhibitory receptor blocking antibodies (10μg/mL final concentration). The following blocking antibodies were used: isotype control (clone LTF-2, Bio X-cell), anti-PD-L1 (clone 10F.9G2, Bio X-cell), anti-PD-L2 (clone TY-25, Bio X-cell), anti-PD-1 (clone J43, Bio X-cell), anti-TIM-3 (clone RMT3-23, Bio X-cell), anti-LAG-3 (clone C9B7W, Bio X-cell), anti-2B4 (clone m2B4 (B6)458.1, Biolegend), and anti-CD48 (clone HM48-1, Bio X-cell). Plates were incubated at 37C for 42-48 hours, developed, and then counted using the ImmunoSpot Micro Analyzer (Cellular Technology Limited). The average number of spots in wells stimulated with an irrelevant peptide was subtracted from each experimental value, which was then expressed as spot forming cells (SFC) per 10^6 lymphocytes.

In vivo LAG-3 Antibody Blockade

To block LAG-3 signaling, mice were injected i.p. with 200μg of rat anti-mouse LAG-3 antibody (clone C9B7W, Bio X-cell) on day 3 p.i. On days 5, 7 and 9 p.i.,100μg of anti-LAG-3 or isotype control antibody were given i.n. and 100μg were given i.p. We found that i.p. administration alone was insufficient to block LAG-3 signaling (not shown).

Statistical Analysis

Data analysis was performed using Prism v4.0 (GraphPad Software). Comparisons between tetramer staining and ICS within the same animals were performed using a paired two-tailed *t* test. Comparisons between two groups were performed using an unpaired two-tailed Student's *t* test. Multiple group comparisons were performed using a one-way ANOVA with a Bonferroni post-test for comparison of individual groups. $p<0.05$

was considered significant, with *p*-values of $p<0.005$ and $p<0.0005$ reported where applicable. Error bars on each graph represent standard error of the mean unless otherwise noted.

CHAPTER V

Summary and Future Directions

Thesis Summary

The data presented in this thesis elucidate mechanisms by which virus-specific lung T_{CD8} become functionally impaired during viral acute lower respiratory infection. I showed that lung T_{CD8} are significantly impaired during HMPV and IAV infections of mice and this dysfunction was associated with upregulation of the inhibitory receptor PD-1. Viral replication and, more specifically, viral Ag were necessary for PD-1 upregulation and impairment. Blockade of the PD-1 pathway using either therapeutic antibody treatment or genetic ablation restored lung T_{CD8} functions and blockade also resulted in enhanced viral clearance. I used blockade of PD-1 signaling during secondary infection of B cell deficient mice to show that PD-1 contributes to the capacity of respiratory viruses to cause reinfection. PD-1 blockade also substantially improved T_{CD8} effector functions during challenge infection of mice that were vaccinated against HMPV-specific viral T_{CD8} epitopes. Importantly, I showed that the PD-1/PD-L1 pathway is activated in humans during serious viral LRI, suggesting a potentially novel therapeutic intervention in clinically ill patients. Finally, I examined the global gene expression changes that occur during lung T_{CD8} impairment. I found that lung T_{CD8} possess a unique gene expression profile that resembles early exhaustion and is characterized by the expression of numerous inhibitory receptors plus their corresponding ligands on lung parenchymal cells. LAG-3, in particular, was able to compensate for a lack of PD-1 signaling and reinstate impairment.

The phenomenon of lung T_{CD8} impairment was first described over a decade ago by Chang and Braciale (2002) in RSV-infected mice. Subsequently, a handful of other papers recapitulated these findings for PIV-5, RSV and IAV (DiNapoli et al., 2008; Gray et al., 2005; Lukens et al., 2006; Vallbracht et al., 2006). In Chapter II, I described my initial experiments to characterize HMPV infection of C57BL/6 mice and the subsequent T_{CD8} response. I confirmed that HMPV-specific lung T_{CD8} were also impaired. This impairment began as early as day 7 p.i. and became more pronounced over time. Impairment occurred in both dominant and subdominant epitopes and during both primary and challenge infection. To explain this phenomenon, I researched causes of T cell dysfunction and found three main categories: anergy, senescence and exhaustion. Anergy is caused by insufficient activation signals during priming, which I suspected was not the case for LRI since HMPV-specific T_{CD8} were generated at high frequency and were initially completely functional. Senescence occurs after terminal differentiation, so I reasoned that what I observed in the lung was occurring too early to be senescence. The third possibility, exhaustion, also takes time to develop (several weeks), but has a well-defined role in impairing T_{CD8} during other viral infections.

Therefore, I stained lung T_{CD8} for the exhaustion marker PD-1 and found it to be highly expressed. Additionally, in contrast to previously published data showing that PD-1 is rapidly down-regulated during acute infection, I found that PD-1 expression was maintained on lung T_{CD8} for several weeks post-infection, long after viral clearance. Splenic virus-specific T_{CD8}, on the other hand, down-regulate PD-1 as expected after resolution of acute infection. I next turned my attention to the regulation of PD-1 expression on the cell surface of lung T_{CD8}. To address this question, I first infected mice with a different respiratory virus and found that IAV infection also caused high PD-1 expression on impaired virus-specific T_{CD8}. To determine if all T_{CD8} that traffic to the lung nonspecifically upregulate PD-1, I needed a method of eliciting epitope-specific T_{CD8} in

the absence of infection or overt inflammation. I utilized bone marrow-derived DCs for this purpose and found that HMPV-specific T_{CD8} elicited by DC immunization were fully functional and expressed low levels of PD-1. Heterologous T_{CD8} elicited in this manner were also unimpaired and PD-1^{lo} during HMPV infection, indicating that TCR signaling was the primary driver of PD-1 upregulation and impairment.

I then determined that PD-1 was not just associated with lung T_{CD8} impairment, but that impairment was caused by PD-1 signaling. During chronic infections and cancer, blockade of the PD-1 pathway results in partial reversal of T cell exhaustion (Wu et al., 2012). I therefore injected HMPV-infected mice with blocking antibodies directed against the PD-1 ligands, PD-L1 and PD-L2, and found that lung T_{CD8} effector functions were restored. This corresponded to a greater ability to control viral infection as well. These results were recapitulated in *PD-$1^{-/-}$* mice infected with HMPV or IAV. I also showed that PD-1 blockade during challenge infection of mice that were DC immunized also resulted in enhanced T_{CD8} functions and lower viral titers. To conclude this chapter, I showed that PD-1 and PD-L1 were abundantly expressed in the lungs of pediatric and adult patients with severe viral LRI caused by RSV, PIV-3 or IAV. These results were important to extend our findings to humans and support the notion that PD-1-directed therapies or vaccination approaches could prove beneficial in infected patients.

In Chapter III, I expanded on the work in Chapter II concerning PD-1 and reinfection: secondary effector lung T_{CD8} generated by reinfection of WT mice or challenge of DC immunized mice were severely impaired and expressed high levels of PD-1. Additionally, PD-1 blockade in the latter case restored T_{CD8} functionality. I therefore was curious whether PD-1 signaling prevents effective immunity against respiratory viruses, predisposing individuals to reinfection. Reinfections are extremely common with respiratory viruses, despite minimal antigenic drift on the part of HMPV or RSV, the presence of high titers of serum neutralizing antibodies and even a vaccine

against IAV. I first needed a model in which to study reinfection. WT mice are completely protected against viral replication during secondary infection due to the antibody response. I found that HMPV replicated to high titers during reinfection of B cell deficient μMT mice. There was a greater anti-HMPV T_{CD8} response during reinfection compared to primary infection and these cells expressed even higher levels of PD-1. Additionally, they co-expressed other inhibitory receptors (TIM-3, LAG-3 and 2B4). Importantly, I found that therapeutic PD-1 blockade restored functionality to secondary effector anti-viral T_{CD8} in the lung and decreased viral titers, suggesting that PD-1-mediated pulmonary T_{CD8} impairment might contribute to reinfection susceptibility. I also showed that PD-1 limits the effectiveness of a peptide vaccination strategy, highlighting the importance of better understanding lung T_{CD8} impairment to improve future vaccines.

In Chapter IV, I characterized the global gene expression changes that occur during lung T_{CD8} impairment. I first showed that PD-1 acts cell-intrinsically to impair T_{CD8} during HMPV infection by using bone marrow chimeric mice. This result suggested that additional mechanisms might exist that regulate T_{CD8} functions at the level of the T cell itself. To broadly investigate this potential, I used flow cytometry to sort lung and spleen T_{CD8} to high purity and then performed microarray analysis to determine differences in gene expression. We were surprised to find nearly 400 genes upregulated in lung compared to spleen T_{CD8} specific for the same viral epitope. The environment that the T_{CD8} exists in therefore seems very important for the phenotype and function of that cell. An analogy would be two human identical twins that are separated at birth: while genetically indistinguishable, they may have very different personalities and attitudes that reflect being raised in different environments. Additionally, we looked at the gene expression of secondary lung T_{CD8} generated by DC immunizing mice and then challenging with HMPV. There was a strong overlap between the gene expression pattern of primary and secondary lung T_{CD8}, but secondary effectors also uniquely

expressed over 650 genes. Despite these differences, a core gene signature of ~900 genes were differentially expressed by lung and spleen T_{CD8} compared to naïve cells. These results highlight the profound gene expression differences that can occur in clonally similar T_{CD8} present in different environments or with different stimulation histories.

Many of the genes we identified as upregulated in lung T_{CD8} have known immune functions, but I was particularly interested in the high expression of several inhibitory receptors. TIM-3, LAG-3 and 2B4 were all upregulated by impaired lung T_{CD8} compared to unimpaired spleen T_{CD8}. Each of these receptors has been described to enforce some aspect of T cell exhaustion during chronic infection or cancer. I used multi-parameter flow cytometry staining to confirm increased co-expression of these inhibitory receptors by lung $T_{CD8.}$ Splenic T_{CD8} expressed 0 or 1 receptor, while lung T_{CD8} co-expressed mainly 2 or 3. Importantly, these receptors do not function in a vacuum, as they require stimulation through their specific ligands. I found that HMPV infection upregulated each ligand on both epithelial cells and APCs.

To explore the regulation of these inhibitory receptors, I took advantage of an experimental approach I developed in Chapter II, namely DC immunization. This time, however, I DC immunized mice, reinfected all of them and then either provided mock peptide or cognate peptide i.n. This allowed me to specifically add back what I previously determined was the major stimulus for PD-1 expression: TCR stimulation. Again, heterologous T_{CD8} that did not perceive Ag were less impaired than endogenous HMPV-specific T_{CD8} or heterologous T_{CD8} in mice receiving cognate peptide treatment. All four inhibitory receptors were much more highly expressed by T_{CD8} in the presence of cognate Ag. These results demonstrated that not just PD-1 expression is controlled by TCR signaling, but also additional inhibitory receptors.

I then adapted an old assay for a new purpose to determine if each inhibitory receptor was actually functional on virus-specific $T_{CD8.}$ Lung cells were restimulated with peptide in the presence of inhibitory receptor blocking antibodies and IFNγ secretion was measured by ELISPOT assay. I confirmed that PD-1 plays a strong role in enforcing lung T_{CD8} impairment, as many more spots were observed when either PD-1 or PD-L1 were blocked. Both TIM-3 and LAG-3 also were found to be functional inhibitory receptors and combining these two with PD-L1 resulted in increased spots when compared to PD-L1 blockade alone. I therefore next explored if LAG-3 played a role in lung T_{CD8} impairment *in vivo*. Since PD-1 blockade effectively restored function early during infection, I chose to look at day 10 p.i. when PD-1 blockade begins to fail and impairment returns. I hypothesized that the rapid return to impairment was due to other inhibitory receptors. Indeed this was the case, as blocking LAG-3 resulted in restored T_{CD8} effector functions. These results suggested that inhibitory receptors can compensate for one another during acute viral LRI and so combined blockade approaches might work better than singly targeting these pathways.

Lung T_{CD8} share many similarities with exhausted T cells during chronic infection: they fail to respond when restimulated, express PD-1 and other inhibitory receptors and are regulated by TCR stimulation. I was therefore curious about the full extent of similarities and differences between lung T_{CD8} impairment and T cell exhaustion during chronic infection. Therefore, I downloaded a microarray dataset from a recently published paper exploring the differences in transcriptional nodes during acute or chronic LCMV infection. After normalizing the data, we were able to directly make comparisons between the groups. I found that lung T_{CD8} during acute viral LRI are most closely related to T_{CD8} early during chronic infection (i.e. in cells that are just starting to become functionally impaired but that are not yet fully exhausted). The next closest

population in terms of gene expression was T_{CD8} early during acute infection, followed by exhausted T_{CD8} late during chronic infection. Impaired lung T_{CD8} still shared numerous genes with exhausted T_{CD8}, but they were most closely related to cells early in the process, indicating they are in a state of early, or premature, exhaustion. They also expressed many genes that were not seen in any of the populations present during acute or chronic LCMV infection, indicating that they exist in a unique state compared to other known T_{CD8} populations.

Lung T_{CD8} impairment occurs in response to recognition of viral Ag in the lung as T_{CD8} are recruited there to battle the infection. Ag consists of an immunogenic peptide fragment from a viral protein expressed on the cell surface by MHC class I molecules. TCR recognize the peptide:MHC complex, which normally initiates cytokine production and degranulation by the T_{CD8}, but also upregulates PD-1 and other inhibitory receptors. Inflammatory cytokines elicited by the infection upregulate the expression of the ligands for these receptors, driving inhibitory signaling in the T_{CD8} and loss of effector functions. This model is summarized in Figure 5-1. Additionally, my data suggests that lung T_{CD8} are a heterogeneous population consisting of functional effector T_{CD8} and impaired cells (Figure 5-2). The impaired T_{CD8} persist for several weeks following virus clearance. Despite this, memory T_{CD8} must also develop, as reinfection results in a more robust secondary response. Unfortunately, these re-expanded cells are also impaired, limiting their ability to clear the infection.

Lung T_{CD8} impairment during acute viral LRI is an important phenomenon that contributes to respiratory virus pathogenesis, severity and reinfection. Although impairment was first described in 2002, we were the first to idenfity a molecular mechanism controlling impairment. I saw similarities between impairment and T cell exhaustion, which lead to the discovery that PD-1 mediates lung T_{CD8} impairment during LRI. Despite similarities with exhaustion in chronic infection, numerous important

differences exist, including the rapidity with which lung T_{CD8} become impaired and a unique gene expression signature that includes several genes not normally associated with T cells. My research has contributed to our knowledge of T cell biology, especially in the areas of effector function and immunoregulatory receptors. My data reveal an important role for PD-1 in controlling T_{CD8} impairment during both primary LRI and reinfection. Additionally, I identified other inhibitory receptors that contribute to this process. Thus, while much has been learned concerning the T cell response to acute and chronic infections, my research studies have uncovered a new area of investigation surrounding regulation of effector functions at sites of active infection. The results of this work have important implications for human health and therapeutic intervention during viral infections.

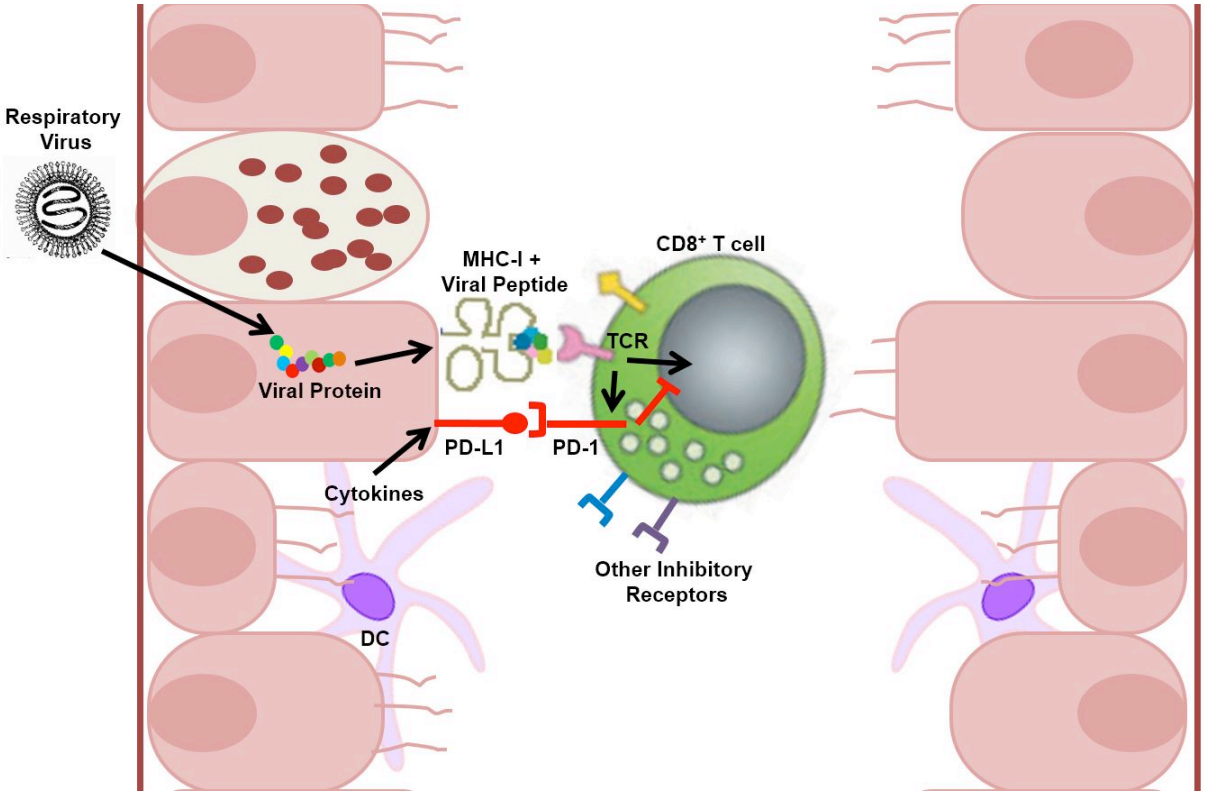

Figure 5-1. Model of lung T_{CD8} impairment during acute viral LRI. A respiratory bronchiole in the lower airway is depicted. A respiratory virus, such as HMPV, infects an

epithelial cell. Viral proteins are translated, some of which become processed by the cellular proteasome into antigenic peptides, which are then transported into the endoplasmic reticulum and loaded onto MHC class I molecules (not shown), and then trafficked to the cell surface. The peptide:MHC complex is then recognized by the TCR on a virus-specific T_{CD8}. TCR signaling is necessary for activation, cytotoxicity and cytokine production, but it also causes PD-1 upregulation, as well as expression of other known inhibitory receptors. PD-1 can then interact with its ligand PD-L1, which is expressed on both epithelial cells and APCs (such as DCs) in the lung. One or both of these cell types could deliver the signal to T_{CD8}. PD-L1 ligation activates PD-1 signaling, which opposes TCR stimulation, resulting in T_{CD8} functional impairment.

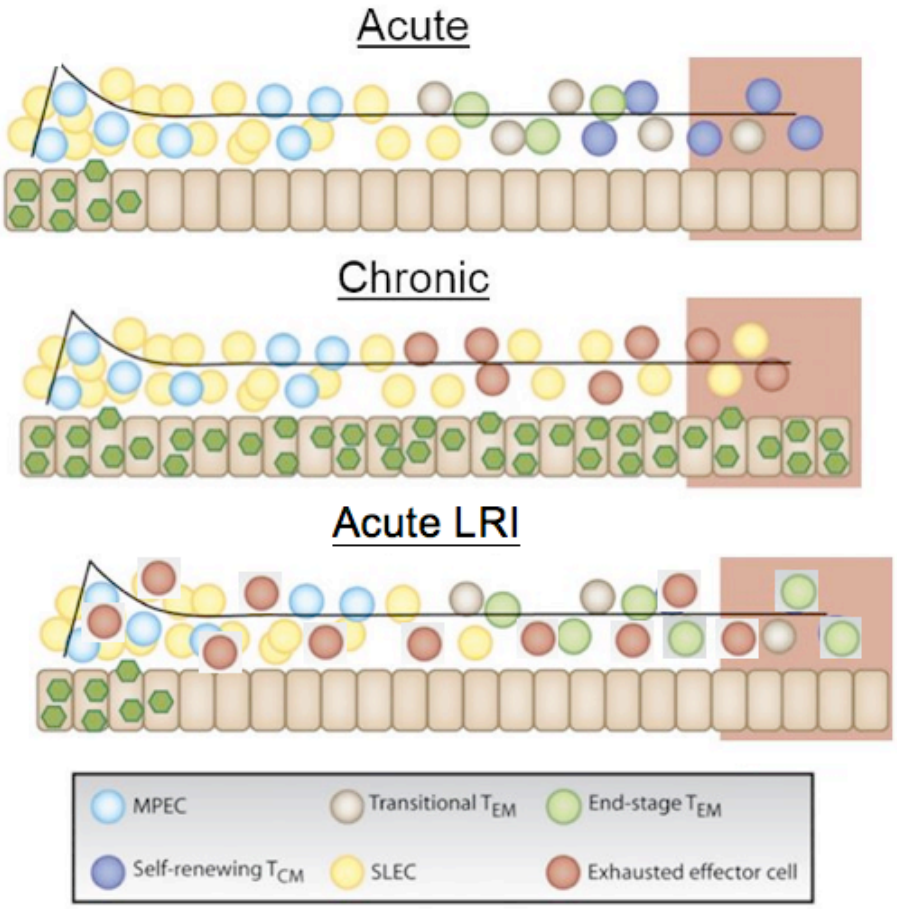

Figure 5-2. Heterogeneous T_{CD8} populations during acute viral LRI. During acute infections, SLEC (yellow cells) and MPEC (aqua cells) develop early, with SLEC dying soon after viral clearance, while MPEC transition into functional memory cells (purple cells) over time. During chronic infections, this same process takes place early. However, Ag persistence and high inflammation lead to T cell exhaustion (maroon cells). My data suggests that during acute viral LRI, the appearance of highly impaired T_{CD8} coincides with SLEC and MPEC. Impaired cells persist for several weeks following viral clearance. Memory T cells do develop, as reinfection of mice results in a greater secondary response. However, these secondary effector T_{CD8} are also impaired (not shown). Modified from (Kaech and Wherry, 2007).

Future Directions

Other mechanisms causing lung T_{CD8} impairment

My thesis research revealed that PD-1 significantly contributes to lung T_{CD8} impairment during acute viral LRI. Undoubtedly, other molecules are also involved in this process. For instance, LAG-3, TIM-3 and 2B4 are other inhibitory receptors expressed by impaired lung T_{CD8}. I found a role for LAG-3 in compensating for PD-1 as early as day 10 p.i. It will be interesting to determine if blocking LAG-3 alone has any effect or whether PD-1 must be blocked as well. I chose to only block LAG-3 in the absence of PD-1 signaling since PD-1 is such a dominant regulator of T_{CD8} impairment. I reasoned that leaving PD-1 unchecked would still result in impairment. LAG-3 could function independently of PD-1, but this is not the case during chronic infection, as LAG-3 blockade alone had no effect and only worked in conjunction with PD-1 blockade (Blackburn et al., 2009). Still, others have found a role for LAG-3 alone in limiting T_{CD8} expansion during LRI (Workman et al., 2004), so the possibility that LAG-3 blockade alone could affect T_{CD8} impairment should be examined.

TIM-3 is another inhibitory receptor that cooperates with PD-1 to cause T cell exhaustion (Jin et al., 2010b) and also has independent effects on T cell proliferation and function during acute viral LRI (Sharma et al., 2011). Blockade of TIM-3 alone, or in combination with PD-1, should be performed using our mouse model of HMPV infection. 2B4 is a receptor that can function as either an inhibitor or a stimulator (Chlewicki et al., 2008). During chronic LCMV infection, 2B4 has a specialized role in enforcing exhaustion of secondary effector T_{CD8} (West et al., 2011). In my studies, I found 2B4 to be more highly expressed on lung compared to spleen T_{CD8} and its expression rose from day 7 to 14 p.i. in the lung only. Additionally, 2B4 expression was higher on secondary compared to primary lung T_{CD8} after reinfection of μMT mice. These results suggest that

2B4 may play a late role in impairment during primary infection and may regulate secondary T_{CD8} to a larger degree. I observed no effect on T_{CD8} functions by blocking this receptor *in vitro*, which could be explained by either a non-function blocking anti-2B4 antibody or use of a ligand other than CD48 (since anti-CD48 treatment also had no effect.) Currently all anti-2B4 antibodies cause depletion *in vivo,* so the only remaining option for studying this pathway is to obtain *Cd244*$^{-/-}$ mice (2B4 knockout), which could yield valuable insights into the role of this pathway in T_{CD8} during viral infection.

It is interesting that almost all of the TIM-3^{+} or LAG-3^{+} lung T_{CD8} are present within the PD-1^{+} subset, suggesting a possible hierarchy of inhibitory receptors that function to impair T_{CD8} functions in a layered manner. Indeed, PD-1^{hi} T_{CD8} may be more prone to impairment due to co-expression of other inhibitory receptors and not necessarily due to more PD-1 on the cell surface (Wherry, 2011). First, not all cells expressing high amounts of PD-1 are impaired (Duraiswamy et al., 2011), especially during acute infection (Zelinskyy et al., 2011). Second, some human T cell functions are restored by PD-1 blockade while others are not (Day et al., 2006; Trautmann et al., 2006). Third, PD-1^{mid} T_{CD8} respond the best to PD-1 blockade, while PD-1^{hi} T_{CD8} remain impaired (Blackburn et al., 2008). The latter result suggests that either a more advanced, non-reversible state of exhaustion exists in the PD-1^{hi} population or that additional inhibitory receptors maintain T cell dysfunction. From *in vitro* studies of human T cells, it seems that PD-1 alone is capable of controlling all T cell functions (proliferation, cytotoxicity and cytokine production) depending on the amount expressed on the cell surface (Wei et al., 2013), but the reality is likely that other receptors play a part as well based on the *in vivo* work. My studies showed that LAG-3 compensates for a lack of PD-1 signaling, suggesting these pathways do cooperate in some manner to maintain impairment. It is unclear if all of the inhibitory receptors function to block all T_{CD8} functions or if some are tuned to block specific functions. Blockade of each inhibitory

receptor could be pursued to parse out which receptors affect which T cell functions. Differentiating their individual contributions will help guide future therapeutics.

Transcriptional regulation of lung T_{CD8} impairment and PD-1 expression

A fundamental question surrounding lung T_{CD8} impairment is what are the upstream controllers of this process? In other words, if inhibitory receptors are the enforcers of impairment, what regulates the enforcers? Again, there is little data concerning this in the acute LRI field. However, significant progress has been made in the realm of T cell exhaustion. Several transcription factors have been identified that control various aspects of exhaustion. For example, Eomes drives T cells into terminal differentiation and then exhaustion via high PD-1 expression (Paley et al., 2012), whereas T-bet prevents exhaustion by repressing PD-1 (Doering et al., 2012; Kao et al., 2011). Furthermore, the transcription factor AP-1 directly binds to the PD-1 promoter and enhances expression (Xiao et al., 2012), suggesting a key link between TCR signaling and PD-1 expression.

The transcriptional regulator BLIMP-1 promotes T cell effector differentiation, but higher levels lead to functional exhaustion (Shin et al., 2009). This suggests that BLIMP-1 may act as a rheostat directly controlling T cell functionality versus impairment based upon environmental cues like inflammation and Ag levels. During acute infection, a role for BLIMP-1 has been described in promoting T_{CD8} accumulation in the lung during IAV infection by upregulation of chemokine receptors (Kallies et al., 2009). However, its role in lung T_{CD8} impairment has not been explored. Importantly, my microarray analysis found AP-1 and BLIMP-1 to be more highly expressed by lung T_{CD8} compared to spleen T_{CD8}. Given the known evidence linking BLIMP-1 to T cell exhaustion plus its role during acute viral LRI, further investigation of this transcriptional regulator is warranted to determine the contribution of BLIMP-1 to lung T_{CD8} impairment.

Contribution of PD-L1 expressed by different cell types

Aside from inhibitory receptor expression, other important lines of investigation exist concerning how the lung's immunosuppressive environment for T_{CD8} is established. In Chapter IV, I described the upregulation of the known ligands for several inhibitory receptors by lung epithelial cells and also $CD11c^+$ cells. However, it is not known which cell type actually delivers the inhibitory signal to T_{CD8}. In general, APCs are thought to be the primary displayers of stimulatory or inhibitory signals to T cells. However, for PD-1 signaling, the protection of peripheral tissues is the main goal (Keir et al., 2008; Keir et al., 2007), and so most parenchymal cells can upregulate PD-L1. For the lung, this means respiratory epithelial cells, which are the cells primarily infected with HMPV (Cox and Williams, 2013). Others have shown that respiratory virus infection of primary human epithelial cells results in PD-L1 upregulation (Telcian et al., 2011) and I demonstrated by IHC in Chapter II that PD-L1 is expressed in the lungs of infected human patients. Epithelial cells have previously been demonstrated to be capable of Ag presentation and stimulation of T cells through CD80 and CD86 expression (Zdrenghea and Johnston, 2012). Surprisingly, these cells also express MHC-II and so are capable of presentinf Ag to $CD4^+$ T cells as well (Wilkinson et al., 2012). Since epithelial cells are the targets of respiratory virus infection, T_{CD8} must interact closely with them to fulfill their cytotoxic functions. Therefore coming into close proximity is necessary for their function and so epithelial cells are capable of delivering both inhibitory and stimulatory signals to anti-viral T_{CD8}.

To test the hypothesis that respiratory epithelial cell PD-L1 expression is necessary for PD-1-mediated impairment, reciprocal bone marrow chimeric mice could be constructed using a combination of WT and *PD-L1*$^{-/-}$ mice. In particular, mice where PD-L1 is lacking in only non-hematopoietic cells would be informative regarding the idea

that epithelial cell expression of PD-L1 is the most important for T_{CD8} impairment. I set out to test this hypothesis myself but ran into a major roadblock. We obtained *PD-L1*$^{-/-}$ mice and infected them with HMPV, but they did not recapitulate our findings with *PD-1*$^{-/-}$ mice or with PD-L blockade. I tested if PD-L2 might compensate for lack of PD-L1, but addition of PD-L2 blockade to *PD-L1*$^{-/-}$ mice also did not result in restored lung T_{CD8} functions. There is evidence that this particular strain of *PD-L1*$^{-/-}$ mice possess a T_{CD8} priming defect during IAV infection (Talay et al., 2009). We subsequently obtained a different strain of *PD-L1*$^{-/-}$ mice and so an important future direction is to characterize these mice and perform the necessary bone marrow chimeric experiments to differentiate between the contributions of PD-L1 expressed by epithelial cells versus hematopoietic cells.

PD-L1 reverse signaling

An important observation that warrants further investigation is a difference I noticed between blocking PD-1 signaling therapeutically with antibodies versus *PD-1*$^{-/-}$ mice. With PD-L blockade, I observed a reduction in lung viral titers, especially at day 7 p.i. (Chapter II), while I saw no difference in titers in *PD-1*$^{-/-}$ mice (not shown). One possible explanation lies in the fact that two slightly different strains were used for these experiments: PD-L blockade was performed in B7tg mice, where the T_{CD8} response is restricted by the HLA-B**0702* allele, whereas *PD-1*$^{-/-}$ mice are on the normal C57BL/6 background, where the T_{CD8} response is restricted by the endogenous murine MHC molecules H2-D^b and H2-K^b. The T_{CD8} response in B7tg mice is dominated by a single immunodominant epitope (M195), while the response in WT mice is more broadly distributed amongst at least three dominant epitopes (F528, N11 and M222). The degree of T_{CD8} impairment was higher for M195-specific T_{CD8}, so restoration of T_{CD8} function in B7tg mice may have allowed for enhanced viral clearance due to increased

functionality of the single dominant epitope in that background. Also in support of this idea is that viral titers at day 7 in B7tg are higher than what is normally observed in WT mice, suggesting a slight delay in viral clearance from the adaptive immune response (i.e. the M195-specific T_{CD8}).

However, alternative explanations exist that warrant further investigation. While PD-L1 is thought of primarily as a ligand for PD-1, evidence also exists suggesting that PD-L1 acts as a receptor and signals into the cell expressing it. This signal can come from PD-1 ligation (Kuipers et al., 2006), but can also come from the costimulatory molecule B7-1 (Butte et al., 2007). PD-1 can signal through PD-L1 on DCs to suppress their activation and increase IL-10 production (Kuipers et al., 2006). PD-L1 can also inhibit T cells, as B7-1 interacting with PD-L1 on the T cell delivers a functionally significant inhibitory signal (Keir et al., 2008). Blockade of PD-1, PD-L1 and PD-L2 has yielded different results in various disease models, which could be explained by the reverse or bidirectional signaling described above. In general, anti-PD-L1 therapy has achieved the most success. Indeed, I also found this to be the case, as PD-1 antibody blockade had no effect *in vivo* (data not shown). I attributed this to poor access to lung parenchymal T_{CD8} since *in vitro* blockade with this antibody worked as well as anti-PD-L1 (Chapter IV). Another explanation though, is that anti-PD-L therapy also overcame PD-L1-mediated inhibitory effects on lung T_{CD8} that are superior to blocking PD-1 alone.

Four categories of PD-L1 blocking antibodies exist that can be used to tease apart the independent contributions of PD-1 and PD-L1 to impaired immunity (Table 5-1). There are antibodies that block only PD-1, those that block only B7-1, those that block both, and those that block neither PD-1 nor B7-1 interactions. Of note, the anti-PD-L1 blocking antibody I used in my studies blocks PD-L1's interaction with both PD-1 and B7-1. *In vitro* testing of these antibodies using the ELISPOT assay described in

Chapter IV or *in vivo* in HMPV-infected mice could yield valuable insights into the nuances of the PD-1/PD-L1 pathway during acute viral LRI.

Anti-PD-L1	Blocks PD-1:PD-L1	Blocks B7-1:PD-L1
10F.9G2	++	+
10F.2H11	-	+

Anti-B7-1	Blocks CD28,CTLA-4:B7-1	Blocks B7-1:PD-L1
1G10	+	+
16-10A1	++	-

Table 5-1. Commonly used antibodies that block PD-L1:PD-1, PD-L1:B7-1 or B7-1:CTLA-4/CD28 interactions. Note that the 10F.9G2 Ab was used in experiments described in this work.

Additionally, in the experiments where I blocked PD-L in B7tg mice, I also noticed a key difference in the cytokine response compared to *PD-1*$^{-/-}$ mice: PD-L blockade resulted in a large increase in the IL-6 concentration in the lung. IL-6 is an acute phase protein with myriad functions and could be responsible for the decreased viral titers in B7tg mice. These data also suggests that PD-L1 blockade may enhance macrophage functions, as these cells are key producers of IL-6. If so, identification of the specific factor elicited by IL-6 that reduced viral replication could reveal an additional avenue for therapeutic intervention.

CD4$^+$ T cell help (or lack thereof)

CD4$^+$ T cells possess numerous functions that catalyze the adaptive immune response. A key function is providing help to T_{CD8}, which allows for more robust expansion, survival, acquisition of effector functions and memory development (Wiesel and Oxenius, 2012). T_{CD8} during chronic infection develop even more severe exhaustion when CD4$^+$ T cells are depleted (Blackburn et al., 2009; Wherry et al., 2003), suggesting that CD4$^+$ T cells can help prevent functional impairment. Indeed, the cytokine IL-21 is

produced by $CD4^+$ T cells and specifically maintains T_{CD8} during chronic infection (Yi et al., 2009). Additionally, help through the co-stimulatory receptor CD40 can restore T_{CD8} cytolytic effector differentiation in the liver during experimental HBV infection, which is normally suppressed by PD-1 (Isogawa et al., 2013). During PD-1 blockade and restoration of T_{CD8} from exhaustion, CD40 is necessary for optimal polyfunctionality, proliferation and IL-21 signaling (Bhadra et al., 2011). During acute infections, $CD4^+$ T cell help through CD40 enhances T_{CD8} functions and improves memory T cell development (Fuse et al., 2009). Importantly, T_{CD8} that lack proper CD4+ T cell help during priming overexpress PD-1 during challenge infection and do not optimally expand (Fuse et al., 2009).

The contribution of $CD4^+$ T cells to HMPV immunity is poorly understood. $CD4^+$ T cells contribute to lung pathology and the antibody response (Kolli et al., 2008), but not much else is known. The contribution of $CD4^+$ T cell help to T_{CD8} impairment during acute viral LRI is unknown. I hypothesize that a suboptimal $CD4^+$ T cell response contributes to lung T_{CD8} impairment by failure to provide adequate co-stimulation through IL-2 production and CD40 costimulation. To test this, several approaches can be used. First, I would deplete $CD4^+$ T cells and monitor for exacerbation of T_{CD8} impairment. Since $CD4^+$ T cell depletion during chronic infection accelerates and worsens T cell exhaustion I would expect a similar result here. Next, I would provide exogenous help through treatment with IL-2 or anti-CD40. Others have previously described a benefit regarding T_{CD8} functionality with IL-2 treatment during RSV infection (Chang et al., 2004) and anti-CD40 therapy during chronic infection (Isogawa et al., 2013). Finally, I would characterize the $CD4^+$ T cell response to HMPV to determine the quantity of epitope-specific cells, their phenotype and the cytokines produced by these cells. Further differentiation of the $CD4^+$ T cells into T_h1, T_h2 and T_{reg} populations will be important to understand the overall effect on T_{CD8} impairment. Some evidence suggests that T_{reg} may

suppress T_{CD8} during RSV infection (Ruckwardt et al., 2009), but further studies are necessary that more specifically target induced T_{reg}. These studies will help clarify whether $CD4^+$ T cell help, or a lack of it, contributes to lung T_{CD8} impairment during acute viral LRI.

Vaccination approaches designed to prevent PD-1-mediated T_{CD8} impairment

My thesis work has implications for new vaccination strategies against respiratory viruses. I showed in Chapter II and III that secondary lung T_{CD8} are even more impaired than primary T_{CD8} and this coincides with significant upregulation of inhibitory receptors. Furthermore, PD-1 signaling limited the effectiveness of a peptide-based vaccine against RSV (Lee et al., 2012) and cancer (Barrios and Celis, 2012). A key question moving forward is how can T_{CD8} impairment be avoided to enhance the effectiveness of vaccines? Inhibitory receptor signaling can limit the effectiveness of secondary T_{CD8} responses. In addition, having to block PD-1 or other receptors during reinfection defeats the purpose of a prophylactic vaccination strategy. Therefore, further work is required to elucidate strategies that prevent T_{CD8} impairment during challenge infection that can be imprinted during priming.

Currently there is limited knowledge for how this can be accomplished, but a few lines of evidence do exist. As mentioned in the previous section, $CD4^+$ T cell help might be a critical factor in preventing impairment. Current HIV vaccination approaches attempt to elicit both anti-HIV $CD4^+$ and $CD8^+$ T cells (O'Connell et al., 2012). Data I presented in Chapter III, however, might argue against this alone being effective. Although we did not measure $CD4^+$ T cells, these cells are likely elicited during primary infection of B-cell deficient μMT mice and therefore memory $CD4^+$ T cells are present at the time of reinfection. Despite the presence of a $CD4^+$ T cell response, the T_{CD8} were still highly impaired during reinfection. Therefore, $CD4^+$ T cells alone might be

insufficient to prevent impairment. However, whether or not $CD4^+$ T cells are impaired themselves by respiratory virus infection is unknown, and could offer an explanation. If only impaired $CD4^+$ T cells are elicited by primary infection, then they may be ineffective at providing T_{CD8} help during challenge infection. DNA or protein-based vaccinations that elicit unimpaired $CD4^+$ T cells could overcome this potential issue.

IL-12 and type I IFN differentially programmed *in vitro* generated anti-cancer T_{CD8} for PD-1 expression and functional impairment after injection into a tumor model (Gerner et al., 2013). IL-12 stimulated cells were more functional, expressed less PD-1 and were better able to control tumor growth than IFNα-stimulated cells. PD-L1 blockade allowed IFNα-stimulated T_{CD8} to control tumor growth to comparable levels as IL-12-stimulated cells. Therefore, the cytokine environment during T_{CD8} priming plays a critical role in programming these cells for impairment upon challenge. During paramyxovirus infection, type I IFN is the primary innate cytokine that is produced (Guerrero-Plata et al., 2005a; Guerrero-Plata et al., 2005b). High levels of IFN during primary infection may therefore program T_{CD8} for later impairment.

I demonstrated in Chapter IV that IFN signaling through IFNAR was not responsible for impairment during primary infection. It would be interesting to analyze the secondary T_{CD8} response in these mice to see if IFN signaling during priming promotes impairment and PD-1 upregulation during reinfection. To allow for reinfection, IFNAR mice could be bred with μMT mice or anti-CD20 treatment could be used to deplete B cells. Additionally, in Chapter III, I immunized mice with TriVax, which contains poly(I:C) as an adjuvant to elicit type I IFN due to signaling through TLR3 (Alexopoulou et al., 2001). A more effective peptide vaccine might utilize a different adjuvant for priming, such as CpG, which elicits IL-12 (Ishii et al., 2004). A gene expression study revealed that 100-200 genes were differentially expressed between IL-12 and IFNα-stimulated cells (Agarwal et al., 2009), and so have the potential to

dramatically affect the T_{CD8} recall response. In the original paper describing TriVax, the authors used CpG and elicited equivalent levels of epitope-specific T_{CD8} during priming as poly(I:C) stimulation (Cho and Celis, 2009). However, the poly(I:C) allowed for a better booster response, so they proceeded with that adjuvant. The success of TriVax may lie in its ability to generate relatively huge numbers of epitope-specific T_{CD8}, a strategy that is not feasible in humans. Therefore, priming of a smaller response that is better able to re-expand and remain functional during challenge may be a better goal for peptide vaccination and should be followed up on with additional experimentation.

Lung T_{CD8} impairment in humans and PD-1's contribution

The vast majority of studies describing T_{CD8} responses to respiratory viruses have been performed using mice. A growing body of data suggests that T_{CD8} are impaired in the respiratory tract in murine models of human infections, which includes the data presented in this thesis. Currently the only evidence for impairment actually occurring in humans is shown in Figures 2-18 and 2-19. Here, we showed that PD-1 and PD-L1 are expressed in the lower airways of patients with severe LRI leading. The association between PD-1, T_{CD8} impairment, and mortality is very important and needs to be further explored in humans. Human studies are challenging, so care must be taken to elucidate this point without risk to patients and waste of resources. Therefore, the following experiments exploring T_{CD8} impairment in humans are given in order of least to most invasive and cumbersome.

First, further IHC analysis of PD-1/PD-L1 expression can be performed in additional patients to validate the results presented in Chapter II. There, I showed staining for ten patients, so additional data would be helpful in validating this point. Additionally, lung pathology specimens exist in the Vanderbilt Tissue and Pathology Shared Resource with no known virus causing LRI that could be identified using

immunostaining. Likely some of these cases are caused by HMPV, which, unlike RSV and IAV, has no rapid test for detection in the clinic. Second, it will be helpful to identify PD-1 staining in live, acutely infected patients. Specimens from patients undergoing a lung biopsy could be stained for PD-1/PD-L1, especially if rapid staining identifies an active viral infection. Third, nasal washes can be obtained from individuals with confirmed upper respiratory infection. The resulting epithelial cells could be stained for PD-L1 expression, while any T_{CD8} present could be stained for PD-1 and analyzed by flow cytometry. Third, it should be determined if polymorphisms in the PD-1 gene are associated with more severe disease. Patients presenting to the hospital with confirmed LRI could be enrolled in the study, their PD-1 gene sequenced and then monitored for outcomes. Additionally, patients with less severe LRI presenting to outpatient clinics could also be enrolled. Risk-associated polymorphisms in the PD-1 gene could then be identified, which would provide an association suggesting a functional role for PD-1 in human respiratory infection. To date, PD-1 polymorphisms have been associated with multiple sclerosis (Kroner et al., 2005), breast cancer (Hua et al., 2011), subacute sclerosing panencephalitis (Piskin et al., 2013) and ankylosing spondylitis (Yang et al., 2011).

If all of these studies yielded additional evidence suggesting activation of the PD-1/PD-L1 pathway, then a more invasive study could be performed in intubated ICU patients with serious LRI. Lung washes could be performed and the airway T cells then stained for PD-1 expression as well as restimulated and stained for intracelluar IFNγ. If PD-1 is indeed upregulated, then PD-1 blockade could be performed during restimulation to determine if it impairs human T_{CD8} during viral LRI. While our studies in mice focused on epitope-specific T_{CD8}, human studies may require looking at non-specific markers of activated cells unless HMPV epitopes are identified in humans with common HLA supertypes. Some human epitopes are known for influenza virus that

could be utilized. Analysis of peripheral blood T cells is unlikely to yield valuable results as us and others have repeatedly shown that T_{CD8} outside of the lung environment are not impaired and rapidly down-regulate inhibitory receptors. These studies will provide valuable insights into the existence of T_{CD8} impairment and the mechanisms controlling it in humans.

Conclusions

My thesis provides a framework to investigate further mechanisms of T_{CD8} impairment during respiratory virus infection. I have developed flow cytometry assays that will allow others to study additional mechanisms controlling T_{CD8} impairment and the contribution of other cell types to this process. Further, data from the microarray analysis of lung versus spleen HMPV-specific T_{CD8} can be used to generate additional hypotheses and confirm findings that arise at later times. The future directions described in this study will enhance our understanding of how inhibitory receptors shape the T_{CD8} response to acute infection. Additionally, these studies will elucidate the contribution of the ligands for these receptors, $CD4^+$ T cell help and the inflammatory milieu to T_{CD8} impairment and effective immunity. Further, I present studies that could potentially have direct implications for the development of more effective vaccines against respiratory viruses. These results will be especially important in the context of additional knowledge about lung T_{CD8} impairment in infected humans. This work will improve our understanding of protective immunity against respiratory viruses and therefore may lead to the development of novel vaccines or therapeutics.

Significance of Lung T_{CD8} Impairment

Does PD-1 mediate impairment during other acute, non-respiratory infections?

Initially, it appeared as though PD-1 only functioned during chronic Ag stimulation to prevent excess immunopathology. However, this idea has been revised to include some acute infections, particularly of the respiratory tract (Erickson et al., 2012; Lazar-Molnar et al., 2008; Yao et al., 2009). It is interesting to speculate whether PD-1 may serve to impair T cells present at other sites of acute infection. For instance, T_{CD8} are important for the control of viruses in the liver, CNS, gastrointestinal tract and skin. PD-1 may impair T_{CD8} during hepatitis A virus infection of the liver or rotavirus infection of the intestines. There is evidence to suggest that PD-1 impairs T_{CD8} in the liver during chronic HBV and HCV infection (Bowen and Walker, 2005; Isogawa et al., 2013; Nakamoto et al., 2009), but this has been hard to prove since mice are not readily infected by these viruses. PD-1 signaling has been associated with survival during acute viral CNS infection (Phares et al., 2009), suggesting it limits potentially fatal immunopathology. However, if it specifically impairs T_{CD8} in that setting is not known.

Viruses also commonly infect the skin and genital tract (herpes viruses) and the role of PD-1 in these settings is not known. While playing a broad role in protection against pathogens and environmental insult, the skin is not necessarily a critical organ. PD-1 may more preferentially protect organs like the lung, heart and CNS that are necessary for survival. In support of this, PD-1 has been shown to limit autoimmume damage of the kidneys, heart and pancreas, all of which are critical organs. Protection of critical organs would imply more selective pressure on the PD-1 gene, and indeed there is evidence to suggest this has been the case during mammalian evolution (Forni et al., 2013). The differentiation of these possibilities and the role of PD-1 during other acute infections have important implications for settings where PD-1-mediated therapy would be appropriate and safe.

What is the purpose of inhibitory receptor signaling in lung T_{CD8}?

PD-1 is thought to primarily function to promote peripheral tolerance (Fife and Pauken, 2011). *PD-1*$^{-/-}$ mice spontaneously develop a lupus-like illness or cardiomyopathy, depending on the background strain (Nishimura et al., 1998; Nishimura et al., 2001). Studies in diabetic mice have found a critical role for PD-1 in not just early phases of T cell activation, but also in regulating effector functions and tolerance at later time points (Ansari et al., 2003). PD-1 regulation is unique from that provided by CTLA-4, which functions early during T cell activation (Ansari et al., 2003; Fife et al., 2009). PD-1 has been shown to maintain tolerance for the prevention of many autoimmune diseases, such as experimental autoimmune encephalitis (a model of multiple sclerosis) (Salama et al., 2003) and collagen-induced arthritis (Wang et al., 2011). In the setting of tolerance, PD-L1 expression in the target organ is critically important. Like our findings during LRI, PD-L1 is upregulated during autoimmune inflammation (Fife and Pauken, 2011). It has been speculated that autoreactive T cells are continuously regulated by intrinsic inhibitory receptor signaling due to interaction with ligands present on target tissues (Fife and Pauken, 2011).

We found no role for PD-1 in limiting overt immunopathology during acute viral LRI (Figure 2-14). However, this may be a result of the subclinical illness caused by HMPV in rodents. A virus causing more serious pathology may have a more discernible effect. We did observe increased breathing effort in HMPV-infected mice receiving PD-L blockade, suggesting that some form of airway dysfunction is induced by subversion of PD-1 signaling. Based on the cumulative evidence surrounding PD-1, it seems most likely that PD-1 functions to prevent peripheral tissue damage due to over-exuberant or self-directed immune responses. PD-1 likely does not specifically exist to protect the lung from bystander damage, but that it exists to protect all tissues.

Why does lung T_{CD8} impairment develop so rapidly during acute viral LRI?

We infected mice with HMPV, IAV and VACV and all three of them lead to T_{CD8} impairment and PD-1 upregulation. Given that these three viruses are each from different families, it appears unlikely that all viruses have evolved to specifically target the PD-1 pathway. It would be very interesting if a virus was found that did *not* cause lung T_{CD8} impairment. Other viruses that could be tested include VSV, Sendai virus, pneumonia virus of mouse (PVM) and LCMV (Armstrong strain). In particular, the latter virus would be very interesting to test since systemic infection with acute LCMV does not cause T_{CD8} impairment and PD-1 is rapidly down-regulated following viral clearance. LCMV can be inoculated through the intranasal route (Rajini et al., 2010), so this would be feasible to test after generating LCMV-specific tetramers. If impairment does occur following intranasal LCMV infection, this would suggest that intrinsic mechanisms exist in the lung that specifically enforce the T_{CD8} impairment program during acute pulmonary infections.

The fact that lung T_{CD8} impairment occurs so rapidly suggests this may be the case, as functional exhaustion that occurs in other organs, such as the spleen during chronic infection, takes much longer to develop. The other potential contributors to impairment I mentioned previously (lack of CD4+ T cell help or cytokine environment) also contribute to T cell exhaustion during chronic infection, so alone cannot account for the speed with which impairment occurs during acute viral LRI. It is important to note that infection is required for impairment, since DC-elicited T_{CD8} in the lung are functional and express low levels of PD-1. Therefore, infection-induced factor(s) appear to be necessary.

I hypothesize that lung parenchymal cells are primarily responsible, then, for inducing rapid impairment of lung $T_{CD8,}$ through either direct or indirect mechanisms. Since DC-elicited T_{CD8} are functional, infection of lung cells must change their phenotype

in a way that is immunosuppressive to T_{CD8}. Respiratory epithelial cells, like Clara cells, secrete a variety of proteins, some of which have known immunomodulatory roles (Reynolds and Malkinson, 2010), like the secretoglobin-family members (Mukherjee et al., 2007). Interestingly, I found that the gene expression of one of these proteins, uteroglobin, was highly expressed in lung T_{CD8}. It is tempting to speculate that lung T_{CD8} acquire the ability to secrete cytokines that are not secreted by T_{CD8} located in other locations and that this regulates their ultimate function in a cell-intrinsic manner in the lung. What would be the cue for lung T_{CD8} to increase expression of such genes? This would be a fascinating question to explore and answers may provide evidence for organ-specific mechanisms of immune regulation.

These immunomodulatory molecules need not be T_{CD8}-derived, and could come from other cell types, like uteroglobin from Clara cells. Airway epithelial cells are known to be immunomodulatory as well. I described their expression of numerous ligands for inhibitory receptors in Chapter IV. Others have shown these ligands to be able to functionally impair human T_{CD8} (Telcian et al., 2011). They also constitutively express other immune molecules, such as MHC-I, B7-1, B7-2 and ICAM-1, which can be increased by infection (Papi and Johnston, 1999; Papi et al., 2000). Additionally, infection of human alveolar epithelial cells upregulates PD-L1 expression, indicating that infection of respiratory epithelial cells is capable of altering the immunomodulatory environment in the lung (Stanciu et al., 2006; Telcian et al., 2011). Furthermore, damage or death of these cells may lead to the release of alarmins, a family of endogenous molecules that are constitutively available and liberated upon tissue damage to activate an immune response. Such molecules could shape the function of lung T_{CD8} as well. These data suggest that lung epithelial cells express numerous molecules that are capable of modulating the immune response. Given that they also constitutively express many of them, they may be primed to impair T_{CD8} as they arrive in

the lung. Regardless of the cell type responsible for impairment, the lung is a portal of entry for numerous pathogens and so lung-specific mechanisms of immune inhibition represents a very important area of future investigation.

REFERENCES

Agarwal, P., Raghavan, A., Nandiwada, S.L., Curtsinger, J.M., Bohjanen, P.R., Mueller, D.L., and Mescher, M.F. (2009). Gene regulation and chromatin remodeling by IL-12 and type I IFN in programming for CD8 T cell effector function and memory. Journal of immunology *183*, 1695-1704.

Agata, Y., Kawasaki, A., Nishimura, H., Ishida, Y., Tsubata, T., Yagita, H., and Honjo, T. (1996a). Expression of the PD-1 antigen on the surface of stimulated mouse T and B lymphocytes. International immunology *8*, 765-772.

Agata, Y., Kawasaki, A., Nishimura, H., Ishida, Y., Tsubata, T., Yagita, H., and Honjo, T. (1996b). Expression of the PD-1 antigen on the surface of stimulated mouse T and B lymphocytes. Int Immunol *8*, 765-772.

Ahmed, R., and Gray, D. (1996). Immunological memory and protective immunity: understanding their relation. Science *272*, 54-60.

Alexopoulou, L., Holt, A.C., Medzhitov, R., and Flavell, R.A. (2001). Recognition of double-stranded RNA and activation of NF-kappaB by Toll-like receptor 3. Nature *413*, 732-738.

Ali, S.A., Gern, J.E., Hartert, T.V., Edwards, K.M., Griffin, M.R., Miller, E.K., Gebretsadik, T., Pappas, T., Lee, W.M., and Williams, J.V. (2011). Real-world comparison of two molecular methods for detection of respiratory viruses. Virol J *8*, 332.

Allie, S.R., Zhang, W., Fuse, S., and Usherwood, E.J. (2011). Programmed death 1 regulates development of central memory CD8 T cells after acute viral infection. Journal of immunology *186*, 6280-6286.

Alvarez, R., and Tripp, R.A. (2005). The immune response to human metapneumovirus is associated with aberrant immunity and impaired virus clearance in BALB/c mice. J Virol *79*, 5971-5978.

Angelosanto, J.M., Blackburn, S.D., Crawford, A., and Wherry, E.J. (2012). Progressive loss of memory T cell potential and commitment to exhaustion during chronic viral infection. Journal of virology *86*, 8161-8170.

Ansari, M.J., Salama, A.D., Chitnis, T., Smith, R.N., Yagita, H., Akiba, H., Yamazaki, T., Azuma, M., Iwai, H., Khoury, S.J.*, et al.* (2003). The programmed death-1 (PD-1) pathway regulates autoimmune diabetes in nonobese diabetic (NOD) mice. The Journal of experimental medicine *198*, 63-69.

Badovinac, V.P., and Harty, J.T. (2007). Manipulating the rate of memory CD8+ T cell generation after acute infection. Journal of immunology *179*, 53-63.

Badovinac, V.P., Messingham, K.A., Jabbari, A., Haring, J.S., and Harty, J.T. (2005a). Accelerated CD8+ T-cell memory and prime-boost response after dendritic-cell vaccination. Nature medicine *11*, 748-756.

Badovinac, V.P., Messingham, K.A., Jabbari, A., Haring, J.S., and Harty, J.T. (2005b). Accelerated CD8+ T-cell memory and prime-boost response after dendritic-cell vaccination. Nat Med *11*, 748-756.

Baitsch, L., Fuertes-Marraco, S.A., Legat, A., Meyer, C., and Speiser, D.E. (2012). The three main stumbling blocks for anticancer T cells. Trends Immunol *33*, 364-372.

Baixeras, E., Huard, B., Miossec, C., Jitsukawa, S., Martin, M., Hercend, T., Auffray, C., Triebel, F., and Piatier-Tonneau, D. (1992). Characterization of the lymphocyte activation gene 3-encoded protein. A new ligand for human leukocyte antigen class II antigens. The Journal of experimental medicine *176*, 327-337.

Bakker, A.H., Hoppes, R., Linnemann, C., Toebes, M., Rodenko, B., Berkers, C.R., Hadrup, S.R., van Esch, W.J., Heemskerk, M.H., Ovaa, H., and Schumacher, T.N. (2008). Conditional MHC class I ligands and peptide exchange technology for the human MHC gene products HLA-A1, -A3, -A11, and -B7. Proc Natl Acad Sci U S A *105*, 3825-3830.

Bannard, O., Kraman, M., and Fearon, D.T. (2009). Secondary replicative function of CD8+ T cells that had developed an effector phenotype. Science *323*, 505-509.

Barber, D.L., Wherry, E.J., Masopust, D., Zhu, B., Allison, J.P., Sharpe, A.H., Freeman, G.J., and Ahmed, R. (2006). Restoring function in exhausted CD8 T cells during chronic viral infection. Nature *439*, 682-687.

Barrios, K., and Celis, E. (2012). TriVax-HPV: an improved peptide-based therapeutic vaccination strategy against human papillomavirus-induced cancers. Cancer Immunol Immunother *61*, 1307-1317.

Benjamini, Y.a.H., Y. (1995). Controlling the False Discovery Rate: A Practical and Powerful Approach to Multiple Testing. Journal of the Royal Statistical Society. Series B (Methodological) *57*, 289-300.

Berger, R., Rotem-Yehudar, R., Slama, G., Landes, S., Kneller, A., Leiba, M., Koren-Michowitz, M., Shimoni, A., and Nagler, A. (2008). Phase I safety and pharmacokinetic study of CT-011, a humanized antibody interacting with PD-1, in patients with advanced hematologic malignancies. Clin Cancer Res *14*, 3044-3051.

Berkhoff, E.G., de Wit, E., Geelhoed-Mieras, M.M., Boon, A.C., Symons, J., Fouchier, R.A., Osterhaus, A.D., and Rimmelzwaan, G.F. (2005). Functional constraints of influenza A virus epitopes limit escape from cytotoxic T lymphocytes. Journal of virology *79*, 11239-11246.

Bertram, E.M., Lau, P., and Watts, T.H. (2002). Temporal segregation of 4-1BB versus CD28-mediated costimulation: 4-1BB ligand influences T cell numbers late in the primary response and regulates the size of the T cell memory response following influenza infection. Journal of immunology *168*, 3777-3785.

Betts, M.R., Brenchley, J.M., Price, D.A., De Rosa, S.C., Douek, D.C., Roederer, M., and Koup, R.A. (2003). Sensitive and viable identification of antigen-specific CD8+ T cells by a flow cytometric assay for degranulation. J Immunol Methods *281*, 65-78.

Betts, M.R., Nason, M.C., West, S.M., De Rosa, S.C., Migueles, S.A., Abraham, J., Lederman, M.M., Benito, J.M., Goepfert, P.A., Connors, M.*, et al.* (2006). HIV nonprogressors preferentially maintain highly functional HIV-specific CD8+ T cells. Blood *107*, 4781-4789.

Bhadra, R., Gigley, J.P., and Khan, I.A. (2011). Cutting edge: CD40-CD40 ligand pathway plays a critical CD8-intrinsic and -extrinsic role during rescue of exhausted CD8 T cells. Journal of immunology *187*, 4421-4425.

Blackburn, S.D., Shin, H., Freeman, G.J., and Wherry, E.J. (2008). Selective expansion of a subset of exhausted CD8 T cells by alphaPD-L1 blockade. Proceedings of the National Academy of Sciences of the United States of America *105*, 15016-15021.

Blackburn, S.D., Shin, H., Haining, W.N., Zou, T., Workman, C.J., Polley, A., Betts, M.R., Freeman, G.J., Vignali, D.A., and Wherry, E.J. (2009). Coregulation of CD8+ T cell exhaustion by multiple inhibitory receptors during chronic viral infection. Nat Immunol *10*, 29-37.

Blackburn, S.D., and Wherry, E.J. (2007). IL-10, T cell exhaustion and viral persistence. Trends Microbiol *15*, 143-146.

Blattman, J.N., Antia, R., Sourdive, D.J., Wang, X., Kaech, S.M., Murali-Krishna, K., Altman, J.D., and Ahmed, R. (2002). Estimating the precursor frequency of naive antigen-specific CD8 T cells. The Journal of experimental medicine *195*, 657-664.

Blattman, J.N., Grayson, J.M., Wherry, E.J., Kaech, S.M., Smith, K.A., and Ahmed, R. (2003). Therapeutic use of IL-2 to enhance antiviral T-cell responses in vivo. Nature medicine *9*, 540-547.

Blattman, J.N., Wherry, E.J., Ha, S.J., van der Most, R.G., and Ahmed, R. (2009). Impact of epitope escape on PD-1 expression and CD8 T-cell exhaustion during chronic infection. J Virol *83*, 4386-4394.

Bowen, D.G., and Walker, C.M. (2005). Adaptive immune responses in acute and chronic hepatitis C virus infection. Nature *436*, 946-952.

Brahmer, J.R., Drake, C.G., Wollner, I., Powderly, J.D., Picus, J., Sharfman, W.H., Stankevich, E., Pons, A., Salay, T.M., McMiller, T.L.*, et al.* (2010). Phase I study of single-agent anti-programmed death-1 (MDX-1106) in refractory solid tumors: safety, clinical activity, pharmacodynamics, and immunologic correlates. J Clin Oncol *28*, 3167-3175.

Brooks, D.G., Trifilo, M.J., Edelmann, K.H., Teyton, L., McGavern, D.B., and Oldstone, M.B. (2006). Interleukin-10 determines viral clearance or persistence in vivo. Nature medicine *12*, 1301-1309.

Brown, K.E., Freeman, G.J., Wherry, E.J., and Sharpe, A.H. (2010). Role of PD-1 in regulating acute infections. Current opinion in immunology *22*, 397-401.

Bruder, D., Srikiatkhachorn, A., and Enelow, R.I. (2006). Cellular immunity and lung injury in respiratory virus infection. Viral Immunol *19*, 147-155.

Bucks, C.M., Norton, J.A., Boesteanu, A.C., Mueller, Y.M., and Katsikis, P.D. (2009). Chronic antigen stimulation alone is sufficient to drive CD8+ T cell exhaustion. J Immunol *182*, 6697-6708.

Bueno, S.M., Gonzalez, P.A., Pacheco, R., Leiva, E.D., Cautivo, K.M., Tobar, H.E., Mora, J.E., Prado, C.E., Zuniga, J.P., Jimenez, J.*, et al.* (2008). Host immunity during RSV pathogenesis. Int Immunopharmacol *8*, 1320-1329.

Butler, N.S., Moebius, J., Pewe, L.L., Traore, B., Doumbo, O.K., Tygrett, L.T., Waldschmidt, T.J., Crompton, P.D., and Harty, J.T. (2012a). Therapeutic blockade of PD-L1 and LAG-3 rapidly clears established blood-stage Plasmodium infection. Nature immunology *13*, 188-195.

Butler, N.S., Vaughan, A.M., Harty, J.T., and Kappe, S.H. (2012b). Whole parasite vaccination approaches for prevention of malaria infection. Trends Immunol *33*, 247-254.

Butte, M.J., Keir, M.E., Phamduy, T.B., Sharpe, A.H., and Freeman, G.J. (2007). Programmed death-1 ligand 1 interacts specifically with the B7-1 costimulatory molecule to inhibit T cell responses. Immunity *27*, 111-122.

Cannarile, M.A., Lind, N.A., Rivera, R., Sheridan, A.D., Camfield, K.A., Wu, B.B., Cheung, K.P., Ding, Z., and Goldrath, A.W. (2006). Transcriptional regulator Id2 mediates CD8+ T cell immunity. Nature immunology *7*, 1317-1325.

Carvalho, B., Bengtsson, H., Speed, T.P., and Irizarry, R.A. (2007). Exploration, normalization, and genotype calls of high-density oligonucleotide SNP array data. Biostatistics *8*, 485-499.

Chang, J., and Braciale, T.J. (2002). Respiratory syncytial virus infection suppresses lung CD8+ T-cell effector activity and peripheral CD8+ T-cell memory in the respiratory tract. Nat Med *8*, 54-60.

Chang, J., Choi, S.Y., Jin, H.T., Sung, Y.C., and Braciale, T.J. (2004). Improved effector activity and memory CD8 T cell development by IL-2 expression during experimental respiratory syncytial virus infection. J Immunol *172*, 503-508.

Chang, J.T., Ciocca, M.L., Kinjyo, I., Palanivel, V.R., McClurkin, C.E., Dejong, C.S., Mooney, E.C., Kim, J.S., Steinel, N.C., Oliaro, J.*, et al.* (2011). Asymmetric proteasome segregation as a mechanism for unequal partitioning of the transcription factor T-bet during T lymphocyte division. Immunity *34*, 492-504.

Chemnitz, J.M., Parry, R.V., Nichols, K.E., June, C.H., and Riley, J.L. (2004a). SHP-1 and SHP-2 associate with immunoreceptor tyrosine-based switch motif of programmed death 1 upon primary human T cell stimulation, but only receptor ligation prevents T cell activation. J Immunol *173*, 945-954.

Chemnitz, J.M., Parry, R.V., Nichols, K.E., June, C.H., and Riley, J.L. (2004b). SHP-1 and SHP-2 associate with immunoreceptor tyrosine-based switch motif of programmed death 1 upon primary human T cell stimulation, but only receptor ligation prevents T cell activation. Journal of immunology *173*, 945-954.

Chen, L., and Flies, D.B. (2013). Molecular mechanisms of T cell co-stimulation and co-inhibition. Nat Rev Immunol *13*, 227-242.

Cheng, X., Zhao, Z., Ventura, E., Gran, B., Shindler, K.S., and Rostami, A. (2007). The PD-1/PD-L pathway is up-regulated during IL-12-induced suppression of EAE mediated by IFN-gamma. J Neuroimmunol *185*, 75-86.

Chlewicki, L.K., Velikovsky, C.A., Balakrishnan, V., Mariuzza, R.A., and Kumar, V. (2008). Molecular basis of the dual functions of 2B4 (CD244). Journal of immunology *180*, 8159-8167.

Cho, H.I., and Celis, E. (2009). Optimized peptide vaccines eliciting extensive CD8 T-cell responses with therapeutic antitumor effects. Cancer Res *69*, 9012-9019.

Choi, E.Y., Yoshimura, Y., Christianson, G.J., Sproule, T.J., Malarkannan, S., Shastri, N., Joyce, S., and Roopenian, D.C. (2001). Quantitative analysis of the immune response to mouse non-MHC transplantation antigens in vivo: the H60 histocompatibility antigen dominates over all others. J Immunol *166*, 4370-4379.

Collins, P.L., and Melero, J.A. (2011). Progress in understanding and controlling respiratory syncytial virus: still crazy after all these years. Virus Res *162*, 80-99.

Cox, R.G., and Williams, J.V. (2013). Breaking in: human metapneumovirus fusion and entry. Viruses *5*, 192-210.

Crawford, A., and Wherry, E.J. (2009a). The diversity of costimulatory and inhibitory receptor pathways and the regulation of antiviral T cell responses. Curr Opin Immunol *21*, 179-186.

Crawford, A., and Wherry, E.J. (2009b). The diversity of costimulatory and inhibitory receptor pathways and the regulation of antiviral T cell responses. Current opinion in immunology *21*, 179-186.

Croom, H.A., Denton, A.E., Valkenburg, S.A., Swan, N.G., Olson, M.R., Turner, S.J., Doherty, P.C., and Kedzierska, K. (2011). Memory precursor phenotype of CD8+ T cells reflects early antigenic experience rather than memory numbers in a model of localized acute influenza infection. European journal of immunology *41*, 682-693.

Crotty, S., Johnston, R.J., and Schoenberger, S.P. (2010). Effectors and memories: Bcl-6 and Blimp-1 in T and B lymphocyte differentiation. Nature immunology *11*, 114-120.

Cruz-Guilloty, F., Pipkin, M.E., Djuretic, I.M., Levanon, D., Lotem, J., Lichtenheld, M.G., Groner, Y., and Rao, A. (2009). Runx3 and T-box proteins cooperate to establish the transcriptional program of effector CTLs. The Journal of experimental medicine *206*, 51-59.

Curiel, T.J., Wei, S., Dong, H., Alvarez, X., Cheng, P., Mottram, P., Krzysiek, R., Knutson, K.L., Daniel, B., Zimmermann, M.C*., et al.* (2003). Blockade of B7-H1 improves myeloid dendritic cell-mediated antitumor immunity. Nat Med *9*, 562-567.

Curtsinger, J.M., and Mescher, M.F. (2010). Inflammatory cytokines as a third signal for T cell activation. Current opinion in immunology *22*, 333-340.

Day, C.L., Kaufmann, D.E., Kiepiela, P., Brown, J.A., Moodley, E.S., Reddy, S., Mackey, E.W., Miller, J.D., Leslie, A.J., DePierres, C*., et al.* (2006). PD-1 expression on HIV-specific T cells is associated with T-cell exhaustion and disease progression. Nature *443*, 350-354.

Deffrasnes, C., Hamelin, M.E., and Boivin, G. (2007). Human metapneumovirus. Semin Respir Crit Care Med *28*, 213-221.

DiNapoli, J.M., Murphy, B.R., Collins, P.L., and Bukreyev, A. (2008). Impairment of the CD8+ T cell response in lungs following infection with human respiratory syncytial virus is specific to the anatomical site rather than the virus, antigen, or route of infection. Virol J *5*, 105.

Doering, T.A., Crawford, A., Angelosanto, J.M., Paley, M.A., Ziegler, C.G., and Wherry, E.J. (2012). Network analysis reveals centrally connected genes and pathways involved in CD8+ T cell exhaustion versus memory. Immunity *37*, 1130-1144.

Dong, H., Strome, S.E., Salomao, D.R., Tamura, H., Hirano, F., Flies, D.B., Roche, P.C., Lu, J., Zhu, G., Tamada, K*., et al.* (2002). Tumor-associated B7-H1 promotes T-cell apoptosis: a potential mechanism of immune evasion. Nat Med *8*, 793-800.

Duraiswamy, J., Ibegbu, C.C., Masopust, D., Miller, J.D., Araki, K., Doho, G.H., Tata, P., Gupta, S., Zilliox, M.J., Nakaya, H.I*., et al.* (2011). Phenotype, function, and gene expression profiles of programmed death-1(hi) CD8 T cells in healthy human adults. Journal of immunology *186*, 4200-4212.

Edwards, K.M., Zhu, Y., Griffin, M.R., Weinberg, G.A., Hall, C.B., Szilagyi, P.G., Staat, M.A., Iwane, M., Prill, M.M., and Williams, J.V. (2013). Burden of human metapneumovirus infection in young children. The New England journal of medicine *368*, 633-643.

Ejrnaes, M., Filippi, C.M., Martinic, M.M., Ling, E.M., Togher, L.M., Crotty, S., and von Herrath, M.G. (2006). Resolution of a chronic viral infection after interleukin-10 receptor blockade. The Journal of experimental medicine *203*, 2461-2472.

Eppihimer, M.J., Gunn, J., Freeman, G.J., Greenfield, E.A., Chernova, T., Erickson, J., and Leonard, J.P. (2002). Expression and regulation of the PD-L1 immunoinhibitory molecule on microvascular endothelial cells. Microcirculation *9*, 133-145.

Epstein, S.L., Lo, C.Y., Misplon, J.A., and Bennink, J.R. (1998). Mechanism of protective immunity against influenza virus infection in mice without antibodies. Journal of immunology *160*, 322-327.

Erickson, J.J., Gilchuk, P., Hastings, A.K., Tollefson, S.J., Johnson, M., Downing, M.B., Boyd, K.L., Johnson, J.E., Kim, A.S., Joyce, S., and Williams, J.V. (2012). Viral acute lower respiratory infections impair CD8+ T cells through PD-1. The Journal of clinical investigation *122*, 2967-2982.

Fife, B.T., and Pauken, K.E. (2011). The role of the PD-1 pathway in autoimmunity and peripheral tolerance. Ann N Y Acad Sci *1217*, 45-59.

Fife, B.T., Pauken, K.E., Eagar, T.N., Obu, T., Wu, J., Tang, Q., Azuma, M., Krummel, M.F., and Bluestone, J.A. (2009). Interactions between PD-1 and PD-L1 promote tolerance by blocking the TCR-induced stop signal. Nature immunology *10*, 1185-1192.

Flynn, K.J., Belz, G.T., Altman, J.D., Ahmed, R., Woodland, D.L., and Doherty, P.C. (1998). Virus-specific CD8+ T cells in primary and secondary influenza pneumonia. Immunity *8*, 683-691.

Forni, D., Cagliani, R., Pozzoli, U., Colleoni, M., Riva, S., Biasin, M., Filippi, G., De Gioia, L., Gnudi, F., Comi, G.P.*, et al.* (2013). A 175 million year history of T cell regulatory molecules reveals widespread selection, with adaptive evolution of disease alleles. Immunity *38*, 1129-1141.

Francisco, L.M., Sage, P.T., and Sharpe, A.H. (2010). The PD-1 pathway in tolerance and autoimmunity. Immunol Rev *236*, 219-242.

Freeman, G.J., Long, A.J., Iwai, Y., Bourque, K., Chernova, T., Nishimura, H., Fitz, L.J., Malenkovich, N., Okazaki, T., Byrne, M.C.*, et al.* (2000). Engagement of the PD-1 immunoinhibitory receptor by a novel B7 family member leads to negative regulation of lymphocyte activation. J Exp Med *192*, 1027-1034.

Freeman, G.J., Wherry, E.J., Ahmed, R., and Sharpe, A.H. (2006). Reinvigorating exhausted HIV-specific T cells via PD-1-PD-1 ligand blockade. The Journal of experimental medicine *203*, 2223-2227.

Fuse, S., Tsai, C.Y., Molloy, M.J., Allie, S.R., Zhang, W., Yagita, H., and Usherwood, E.J. (2009). Recall responses by helpless memory CD8+ T cells are restricted by the up-regulation of PD-1. Journal of immunology *182*, 4244-4254.

Gallimore, A., Glithero, A., Godkin, A., Tissot, A.C., Pluckthun, A., Elliott, T., Hengartner, H., and Zinkernagel, R. (1998). Induction and exhaustion of lymphocytic choriomeningitis virus-specific cytotoxic T lymphocytes visualized using soluble tetrameric major histocompatibility complex class I-peptide complexes. The Journal of experimental medicine *187*, 1383-1393.

Gerlach, C., van Heijst, J.W., Swart, E., Sie, D., Armstrong, N., Kerkhoven, R.M., Zehn, D., Bevan, M.J., Schepers, K., and Schumacher, T.N. (2010). One naive T cell, multiple fates in CD8+ T cell differentiation. The Journal of experimental medicine *207*, 1235-1246.

Gerner, M.Y., Heltemes-Harris, L.M., Fife, B.T., and Mescher, M.F. (2013). Cutting Edge: IL-12 and Type I IFN Differentially Program CD8 T Cells for Programmed Death 1 Re-expression Levels and Tumor Control. Journal of immunology.

Gong, A.Y., Zhou, R., Hu, G., Li, X., Splinter, P.L., O'Hara, S.P., LaRusso, N.F., Soukup, G.A., Dong, H., and Chen, X.M. (2009). MicroRNA-513 regulates B7-H1 translation and is involved in IFN-gamma-induced B7-H1 expression in cholangiocytes. J Immunol *182*, 1325-1333.

Graham, B.S., Bunton, L.A., Wright, P.F., and Karzon, D.T. (1991). Reinfection of mice with respiratory syncytial virus. J Med Virol *34*, 7-13.

Graham, M.B., and Braciale, T.J. (1997). Resistance to and recovery from lethal influenza virus infection in B lymphocyte-deficient mice. The Journal of experimental medicine *186*, 2063-2068.

Gray, P.M., Arimilli, S., Palmer, E.M., Parks, G.D., and Alexander-Miller, M.A. (2005). Altered function in CD8+ T cells following paramyxovirus infection of the respiratory tract. J Virol *79*, 3339-3349.

Green, D.R., Droin, N., and Pinkoski, M. (2003). Activation-induced cell death in T cells. Immunological reviews *193*, 70-81.

Greenwald, R.J., Freeman, G.J., and Sharpe, A.H. (2005). The B7 family revisited. Annu Rev Immunol *23*, 515-548.

Griffin, D.E. (2010). Measles virus-induced suppression of immune responses. Immunol Rev *236*, 176-189.

Groschel, S., Piggott, K.D., Vaglio, A., Ma-Krupa, W., Singh, K., Goronzy, J.J., and Weyand, C.M. (2008). TLR-mediated induction of negative regulatory ligands on dendritic cells. J Mol Med *86*, 443-455.

Guerrero-Plata, A., Baron, S., Poast, J.S., Adegboyega, P.A., Casola, A., and Garofalo, R.P. (2005a). Activity and regulation of alpha interferon in respiratory syncytial virus and human metapneumovirus experimental infections. Journal of virology *79*, 10190-10199.

Guerrero-Plata, A., Casola, A., and Garofalo, R.P. (2005b). Human metapneumovirus induces a profile of lung cytokines distinct from that of respiratory syncytial virus. Journal of virology *79*, 14992-14997.

Hadrup, S.R., Toebes, M., Rodenko, B., Bakker, A.H., Egan, D.A., Ovaa, H., and Schumacher, T.N. (2009). High-throughput T-cell epitope discovery through MHC peptide exchange. Methods Mol Biol *524*, 383-405.

Hall, C.B. (2001). Respiratory syncytial virus and parainfluenza virus. N Engl J Med *344*, 1917-1928.

Hall, C.B., Walsh, E.E., Long, C.E., and Schnabel, K.C. (1991). Immunity to and frequency of reinfection with respiratory syncytial virus. J Infect Dis *163*, 693-698.

Hamilton, S.E., and Harty, J.T. (2002). Quantitation of CD8+ T cell expansion, memory, and protective immunity after immunization with peptide-coated dendritic cells. J Immunol *169*, 4936-4944.

Hand, T.W., Morre, M., and Kaech, S.M. (2007). Expression of IL-7 receptor alpha is necessary but not sufficient for the formation of memory CD8 T cells during viral infection. Proceedings of the National Academy of Sciences of the United States of America *104*, 11730-11735.

Hannier, S., Tournier, M., Bismuth, G., and Triebel, F. (1998). CD3/TCR complex-associated lymphocyte activation gene-3 molecules inhibit CD3/TCR signaling. Journal of immunology *161*, 4058-4065.

Hartert, T.V., Wheeler, A.P., and Sheller, J.R. (1999). Use of pulse oximetry to recognize severity of airflow obstruction in obstructive airway disease: correlation with pulsus paradoxus. Chest *115*, 475-481.

Heinecke, L., Proud, D., Sanders, S., Schleimer, R.P., and Kim, J. (2008). Induction of B7-H1 and B7-DC expression on airway epithelial cells by the Toll-like receptor 3 agonist double-stranded RNA and human rhinovirus infection: In vivo and in vitro studies. J Allergy Clin Immunol *121*, 1155-1160.

Hendriks, J., Xiao, Y., Rossen, J.W., van der Sluijs, K.F., Sugamura, K., Ishii, N., and Borst, J. (2005). During viral infection of the respiratory tract, CD27, 4-1BB, and OX40 collectively determine formation of CD8+ memory T cells and their capacity for secondary expansion. Journal of immunology *175*, 1665-1676.

Hogan, R.J., Cauley, L.S., Ely, K.H., Cookenham, T., Roberts, A.D., Brennan, J.W., Monard, S., and Woodland, D.L. (2002). Long-term maintenance of virus-specific effector memory CD8+ T cells in the lung airways depends on proliferation. Journal of immunology *169*, 4976-4981.

Hogan, R.J., Usherwood, E.J., Zhong, W., Roberts, A.A., Dutton, R.W., Harmsen, A.G., and Woodland, D.L. (2001). Activated antigen-specific CD8+ T cells persist in the lungs following recovery from respiratory virus infections. Journal of immunology *166*, 1813-1822.

Horton, H., Russell, N., Moore, E., Frank, I., Baydo, R., Havenar-Daughton, C., Lee, D., Deers, M., Hudgens, M., Weinhold, K., and McElrath, M.J. (2004). Correlation between interferon- gamma secretion and cytotoxicity, in virus-specific memory T cells. J Infect Dis *190*, 1692-1696.

Horvath, C.M. (2004). Silencing STATs: lessons from paramyxovirus interferon evasion. Cytokine Growth Factor Rev *15*, 117-127.

Hoves, S., Trapani, J.A., and Voskoboinik, I. (2010). The battlefield of perforin/granzyme cell death pathways. J Leukoc Biol *87*, 237-243.

Hua, Z., Li, D., Xiang, G., Xu, F., Jie, G., Fu, Z., Jie, Z., and Da, P. (2011). PD-1 polymorphisms are associated with sporadic breast cancer in Chinese Han population of Northeast China. Breast Cancer Res Treat *129*, 195-201.

Huang, X., Venet, F., Wang, Y.L., Lepape, A., Yuan, Z., Chen, Y., Swan, R., Kherouf, H., Monneret, G., Chung, C.S., and Ayala, A. (2009). PD-1 expression by macrophages plays a pathologic role in altering microbial clearance and the innate inflammatory response to sepsis. Proc Natl Acad Sci U S A *106*, 6303-6308.

Ichii, H., Sakamoto, A., Arima, M., Hatano, M., Kuroda, Y., and Tokuhisa, T. (2007). Bcl6 is essential for the generation of long-term memory CD4+ T cells. International immunology *19*, 427-433.

Ichii, H., Sakamoto, A., Hatano, M., Okada, S., Toyama, H., Taki, S., Arima, M., Kuroda, Y., and Tokuhisa, T. (2002). Role for Bcl-6 in the generation and maintenance of memory CD8+ T cells. Nature immunology *3*, 558-563.

Inman, B.A., Frigola, X., Dong, H., and Kwon, E.D. (2007). Costimulation, coinhibition and cancer. Curr Cancer Drug Targets *7*, 15-30.

Ishida, Y., Agata, Y., Shibahara, K., and Honjo, T. (1992). Induced expression of PD-1, a novel member of the immunoglobulin gene superfamily, upon programmed cell death. Embo J *11*, 3887-3895.

Ishii, K.J., Gursel, I., Gursel, M., and Klinman, D.M. (2004). Immunotherapeutic utility of stimulatory and suppressive oligodeoxynucleotides. Curr Opin Mol Ther *6*, 166-174.

Isogawa, M., Chung, J., Murata, Y., Kakimi, K., and Chisari, F.V. (2013). CD40 Activation Rescues Antiviral CD8(+) T Cells from PD-1-Mediated Exhaustion. PLoS Pathog *9*, e1003490.

Iwai, Y., Ishida, M., Tanaka, Y., Okazaki, T., Honjo, T., and Minato, N. (2002). Involvement of PD-L1 on tumor cells in the escape from host immune system and tumor immunotherapy by PD-L1 blockade. Proc Natl Acad Sci U S A *99*, 12293-12297.

Jackson, S.R., Berrien-Elliott, M.M., Meyer, J.M., Wherry, E.J., and Teague, R.M. (2013). CD8+ T cell exhaustion during persistent viral infection is regulated independently of the virus-specific T cell receptor. Immunol Invest *42*, 204-220.

Jeannet, G., Boudousquie, C., Gardiol, N., Kang, J., Huelsken, J., and Held, W. (2010). Essential role of the Wnt pathway effector Tcf-1 for the establishment of functional CD8 T cell memory. Proceedings of the National Academy of Sciences of the United States of America *107*, 9777-9782.

Ji, Y., Pos, Z., Rao, M., Klebanoff, C.A., Yu, Z., Sukumar, M., Reger, R.N., Palmer, D.C., Borman, Z.A., Muranski, P*., et al.* (2011). Repression of the DNA-binding inhibitor Id3 by Blimp-1 limits the formation of memory CD8+ T cells. Nature immunology *12*, 1230-1237.

Jin, H.T., Anderson, A.C., Tan, W.G., West, E.E., Ha, S.J., Araki, K., Freeman, G.J., Kuchroo, V.K., and Ahmed, R. (2010a). Cooperation of Tim-3 and PD-1 in CD8 T-cell exhaustion during chronic viral infection. Proceedings of the National Academy of Sciences of the United States of America *107*, 14733-14738.

Jin, H.T., Anderson, A.C., Tan, W.G., West, E.E., Ha, S.J., Araki, K., Freeman, G.J., Kuchroo, V.K., and Ahmed, R. (2010b). Cooperation of Tim-3 and PD-1 in CD8 T-cell exhaustion during chronic viral infection. Proc Natl Acad Sci U S A *107*, 14733-14738.

Johnson, K.M., Chanock, R.M., Rifkind, D., Kravetz, H.M., and Knight, V. (1961). Respiratory syncytial virus. IV. Correlation of virus shedding, serologic response, and illness in adult volunteers. JAMA *176*, 663-667.

Johnson, W.E., Li, C., and Rabinovic, A. (2007). Adjusting batch effects in microarray expression data using empirical Bayes methods. Biostatistics *8*, 118-127.

Joshi, N.S., Cui, W., Chandele, A., Lee, H.K., Urso, D.R., Hagman, J., Gapin, L., and Kaech, S.M. (2007). Inflammation directs memory precursor and short-lived effector CD8(+) T cell fates via the graded expression of T-bet transcription factor. Immunity *27*, 281-295.

Jung, H.W., Son, H.Y., Jin, G.Z., and Park, Y.K. (2010). Preventive role of PD-1 on MPTP-induced dopamine depletion in mice. Cell Biochem Funct *28*, 217-223.

Kaech, S.M., and Cui, W. (2012). Transcriptional control of effector and memory CD8+ T cell differentiation. Nat Rev Immunol *12*, 749-761.

Kaech, S.M., Hemby, S., Kersh, E., and Ahmed, R. (2002). Molecular and functional profiling of memory CD8 T cell differentiation. Cell *111*, 837-851.

Kaech, S.M., and Wherry, E.J. (2007). Heterogeneity and cell-fate decisions in effector and memory CD8+ T cell differentiation during viral infection. Immunity *27*, 393-405.

Kallies, A., Xin, A., Belz, G.T., and Nutt, S.L. (2009). Blimp-1 transcription factor is required for the differentiation of effector CD8(+) T cells and memory responses. Immunity *31*, 283-295.

Kao, C., Oestreich, K.J., Paley, M.A., Crawford, A., Angelosanto, J.M., Ali, M.A., Intlekofer, A.M., Boss, J.M., Reiner, S.L., Weinmann, A.S., and Wherry, E.J. (2011). Transcription factor T-bet represses expression of the inhibitory receptor PD-1 and sustains virus-specific CD8+ T cell responses during chronic infection. Nature immunology *12*, 663-671.

Kasagi, S., Kawano, S., and Kumagai, S. (2011). PD-1 and autoimmunity. Crit Rev Immunol *31*, 265-295.

Kaufmann, D.E., Kavanagh, D.G., Pereyra, F., Zaunders, J.J., Mackey, E.W., Miura, T., Palmer, S., Brockman, M., Rathod, A., Piechocka-Trocha, A*., et al.* (2007). Upregulation of CTLA-4 by HIV-specific CD4+ T cells correlates with disease progression and defines a reversible immune dysfunction. Nature immunology *8*, 1246-1254.

Keir, M.E., Butte, M.J., Freeman, G.J., and Sharpe, A.H. (2008). PD-1 and its ligands in tolerance and immunity. Annu Rev Immunol *26*, 677-704.

Keir, M.E., Freeman, G.J., and Sharpe, A.H. (2007). PD-1 regulates self-reactive CD8+ T cell responses to antigen in lymph nodes and tissues. Journal of immunology *179*, 5064-5070.

Kim, J., Myers, A.C., Chen, L., Pardoll, D.M., Truong-Tran, Q.A., Lane, A.P., McDyer, J.F., Fortuno, L., and Schleimer, R.P. (2005). Constitutive and inducible expression of b7 family of ligands by human airway epithelial cells. Am J Respir Cell Mol Biol *33*, 280-289.

Kim, T.S., Hufford, M.M., Sun, J., Fu, Y.X., and Braciale, T.J. (2010). Antigen persistence and the control of local T cell memory by migrant respiratory dendritic cells after acute virus infection. J Exp Med *207*, 1161-1172.

Kinter, A.L., Godbout, E.J., McNally, J.P., Sereti, I., Roby, G.A., O'Shea, M.A., and Fauci, A.S. (2008). The common gamma-chain cytokines IL-2, IL-7, IL-15, and IL-21 induce the expression of programmed death-1 and its ligands. J Immunol *181*, 6738-6746.

Kohlmeier, J.E., Cookenham, T., Roberts, A.D., Miller, S.C., and Woodland, D.L. (2010). Type I interferons regulate cytolytic activity of memory CD8(+) T cells in the lung airways during respiratory virus challenge. Immunity *33*, 96-105.

Kohlmeier, J.E., Miller, S.C., Smith, J., Lu, B., Gerard, C., Cookenham, T., Roberts, A.D., and Woodland, D.L. (2008). The chemokine receptor CCR5 plays a key role in the early memory CD8+ T cell response to respiratory virus infections. Immunity *29*, 101-113.

Kohlmeier, J.E., Miller, S.C., and Woodland, D.L. (2007). Cutting edge: Antigen is not required for the activation and maintenance of virus-specific memory CD8+ T cells in the lung airways. Journal of immunology *178*, 4721-4725.

Kolli, D., Bataki, E.L., Spetch, L., Guerrero-Plata, A., Jewell, A.M., Piedra, P.A., Milligan, G.N., Garofalo, R.P., and Casola, A. (2008). T lymphocytes contribute to antiviral immunity and pathogenesis in experimental human metapneumovirus infection. Journal of virology *82*, 8560-8569.

Kotelkin, A., Belyakov, I.M., Yang, L., Berzofsky, J.A., Collins, P.L., and Bukreyev, A. (2006). The NS2 protein of human respiratory syncytial virus suppresses the cytotoxic T-cell response as a consequence of suppressing the type I interferon response. J Virol *80*, 5958-5967.

Kroll, J.L., and Weinberg, A. (2011). Human metapneumovirus. Semin Respir Crit Care Med *32*, 447-453.

Kroner, A., Mehling, M., Hemmer, B., Rieckmann, P., Toyka, K.V., Maurer, M., and Wiendl, H. (2005). A PD-1 polymorphism is associated with disease progression in multiple sclerosis. Ann Neurol *58*, 50-57.

Kuipers, H., Muskens, F., Willart, M., Hijdra, D., van Assema, F.B., Coyle, A.J., Hoogsteden, H.C., and Lambrecht, B.N. (2006). Contribution of the PD-1 ligands/PD-1 signaling pathway to dendritic cell-mediated CD4+ T cell activation. European journal of immunology *36*, 2472-2482.

Lafon, M., Megret, F., Meuth, S.G., Simon, O., Velandia Romero, M.L., Lafage, M., Chen, L., Alexopoulou, L., Flavell, R.A., Prehaud, C., and Wiendl, H. (2008). Detrimental contribution of the immuno-inhibitor B7-H1 to rabies virus encephalitis. J Immunol *180*, 7506-7515.

Langley, G.F., and Anderson, L.J. (2011). Epidemiology and prevention of respiratory syncytial virus infections among infants and young children. Pediatr Infect Dis J *30*, 510-517.

Latchman, Y., Wood, C.R., Chernova, T., Chaudhary, D., Borde, M., Chernova, I., Iwai, Y., Long, A.J., Brown, J.A., Nunes, R.*, et al.* (2001). PD-L2 is a second ligand for PD-1 and inhibits T cell activation. Nat Immunol *2*, 261-268.

Lazar-Molnar, E., Gacser, A., Freeman, G.J., Almo, S.C., Nathenson, S.G., and Nosanchuk, J.D. (2008). The PD-1/PD-L costimulatory pathway critically affects host resistance to the pathogenic fungus Histoplasma capsulatum. Proc Natl Acad Sci U S A *105*, 2658-2663.

Lechner, F., Wong, D.K., Dunbar, P.R., Chapman, R., Chung, R.T., Dohrenwend, P., Robbins, G., Phillips, R., Klenerman, P., and Walker, B.D. (2000). Analysis of successful immune responses in persons infected with hepatitis C virus. The Journal of experimental medicine *191*, 1499-1512.

Lee, S., Stokes, K.L., Currier, M.G., Sakamoto, K., Lukacs, N.W., Celis, E., and Moore, M.L. (2012). Vaccine-elicited CD8+ T cells protect against respiratory syncytial virus strain A2-line19F-induced pathogenesis in BALB/c mice. Journal of virology *86*, 13016-13024.

Lee, S.J., Jang, B.C., Lee, S.W., Yang, Y.I., Suh, S.I., Park, Y.M., Oh, S., Shin, J.G., Yao, S., Chen, L., and Choi, I.H. (2006). Interferon regulatory factor-1 is prerequisite to the constitutive expression and IFN-gamma-induced upregulation of B7-H1 (CD274). FEBS Lett *580*, 755-762.

Lefrancois, L., and Obar, J.J. (2010). Once a killer, always a killer: from cytotoxic T cell to memory cell. Immunological reviews *235*, 206-218.

Liang, S., Mozdzanowska, K., Palladino, G., and Gerhard, W. (1994). Heterosubtypic immunity to influenza type A virus in mice. Effector mechanisms and their longevity. Journal of immunology *152*, 1653-1661.

Lin, D.Y., Tanaka, Y., Iwasaki, M., Gittis, A.G., Su, H.P., Mikami, B., Okazaki, T., Honjo, T., Minato, N., and Garboczi, D.N. (2008). The PD-1/PD-L1 complex resembles the antigen-binding Fv domains of antibodies and T cell receptors. Proc Natl Acad Sci U S A *105*, 3011-3016.

Ling, Z., Tran, K.C., and Teng, M.N. (2009). Human respiratory syncytial virus nonstructural protein NS2 antagonizes the activation of beta interferon transcription by interacting with RIG-I. J Virol *83*, 3734-3742.

Lissina, A., Ladell, K., Skowera, A., Clement, M., Edwards, E., Seggewiss, R., van den Berg, H.A., Gostick, E., Gallagher, K., Jones, E.*, et al.* (2009). Protein kinase inhibitors substantially improve the physical detection of T-cells with peptide-MHC tetramers. J Immunol Methods *340*, 11-24.

Lukens, M.V., Claassen, E.A., de Graaff, P.M., van Dijk, M.E., Hoogerhout, P., Toebes, M., Schumacher, T.N., van der Most, R.G., Kimpen, J.L., and van Bleek, G.M. (2006). Characterization of the CD8+ T cell responses directed against respiratory syncytial virus during primary and secondary infection in C57BL/6 mice. Virology *352*, 157-168.

Maekawa, Y., Minato, Y., Ishifune, C., Kurihara, T., Kitamura, A., Kojima, H., Yagita, H., Sakata-Yanagimoto, M., Saito, T., Taniuchi, I.*, et al.* (2008). Notch2 integrates signaling by the transcription factors RBP-J and CREB1 to promote T cell cytotoxicity. Nature immunology *9*, 1140-1147.

Malek, T.R., and Castro, I. (2010). Interleukin-2 receptor signaling: at the interface between tolerance and immunity. Immunity *33*, 153-165.

Matheu, M.P., Sen, D., Cahalan, M.D., and Parker, I. (2008). Generation of bone marrow derived murine dendritic cells for use in 2-photon imaging. J Vis Exp.

Melendi, G.A., Zavala, F., Buchholz, U.J., Boivin, G., Collins, P.L., Kleeberger, S.R., and Polack, F.P. (2007). Mapping and characterization of the primary and anamnestic H-2(d)-restricted cytotoxic T-lymphocyte response in mice against human metapneumovirus. J Virol *81*, 11461-11467.

Mousavi, S.F., Soroosh, P., Takahashi, T., Yoshikai, Y., Shen, H., Lefrancois, L., Borst, J., Sugamura, K., and Ishii, N. (2008). OX40 costimulatory signals potentiate the memory commitment of effector CD8+ T cells. Journal of immunology *181*, 5990-6001.

Mueller, S.N., and Ahmed, R. (2009). High antigen levels are the cause of T cell exhaustion during chronic viral infection. Proc Natl Acad Sci U S A *106*, 8623-8628.

Mueller, S.N., Vanguri, V.K., Ha, S.J., West, E.E., Keir, M.E., Glickman, J.N., Sharpe, A.H., and Ahmed, R. (2010). PD-L1 has distinct functions in hematopoietic and nonhematopoietic cells in regulating T cell responses during chronic infection in mice. J Clin Invest *120*, 2508-2515.

Mukherjee, A.B., Zhang, Z., and Chilton, B.S. (2007). Uteroglobin: a steroid-inducible immunomodulatory protein that founded the Secretoglobin superfamily. Endocr Rev *28*, 707-725.

Naito, T., Tanaka, H., Naoe, Y., and Taniuchi, I. (2011). Transcriptional control of T-cell development. International immunology *23*, 661-668.

Nakamoto, N., Cho, H., Shaked, A., Olthoff, K., Valiga, M.E., Kaminski, M., Gostick, E., Price, D.A., Freeman, G.J., Wherry, E.J., and Chang, K.M. (2009). Synergistic reversal of intrahepatic HCV-specific CD8 T cell exhaustion by combined PD-1/CTLA-4 blockade. PLoS Pathog *5*, e1000313.

Nishimura, H., Minato, N., Nakano, T., and Honjo, T. (1998). Immunological studies on PD-1 deficient mice: implication of PD-1 as a negative regulator for B cell responses. Int Immunol *10*, 1563-1572.

Nishimura, H., Okazaki, T., Tanaka, Y., Nakatani, K., Hara, M., Matsumori, A., Sasayama, S., Mizoguchi, A., Hiai, H., Minato, N., and Honjo, T. (2001). Autoimmune dilated cardiomyopathy in PD-1 receptor-deficient mice. Science *291*, 319-322.

Nolz, J.C., and Harty, J.T. (2011). Protective capacity of memory CD8+ T cells is dictated by antigen exposure history and nature of the infection. Immunity *34*, 781-793.

Nurieva, R., Thomas, S., Nguyen, T., Martin-Orozco, N., Wang, Y., Kaja, M.K., Yu, X.Z., and Dong, C. (2006). T-cell tolerance or function is determined by combinatorial costimulatory signals. EMBO J *25*, 2623-2633.

O'Connell, R.J., Kim, J.H., Corey, L., and Michael, N.L. (2012). Human immunodeficiency virus vaccine trials. Cold Spring Harb Perspect Med *2*, a007351.

Obar, J.J., Jellison, E.R., Sheridan, B.S., Blair, D.A., Pham, Q.M., Zickovich, J.M., and Lefrancois, L. (2011). Pathogen-induced inflammatory environment controls effector and memory CD8+ T cell differentiation. Journal of immunology *187*, 4967-4978.

Odorizzi, P.M., and Wherry, E.J. (2012). Inhibitory receptors on lymphocytes: insights from infections. Journal of immunology *188*, 2957-2965.

Okamoto, M., Sugawara, K., Takashita, E., Muraki, Y., Hongo, S., Nishimura, H., and Matsuzaki, Y. (2010). Longitudinal course of human metapneumovirus antibody titers and reinfection in healthy adults. J Med Virol *82*, 2092-2096.

Okazaki, T., Maeda, A., Nishimura, H., Kurosaki, T., and Honjo, T. (2001). PD-1 immunoreceptor inhibits B cell receptor-mediated signaling by recruiting src homology 2-domain-containing tyrosine phosphatase 2 to phosphotyrosine. Proc Natl Acad Sci U S A *98*, 13866-13871.

Pages, F., Ragueneau, M., Rottapel, R., Truneh, A., Nunes, J., Imbert, J., and Olive, D. (1994). Binding of phosphatidylinositol-3-OH kinase to CD28 is required for T-cell signalling. Nature *369*, 327-329.

Paley, M.A., Kroy, D.C., Odorizzi, P.M., Johnnidis, J.B., Dolfi, D.V., Barnett, B.E., Bikoff, E.K., Robertson, E.J., Lauer, G.M., Reiner, S.L., and Wherry, E.J. (2012). Progenitor and terminal subsets of CD8+ T cells cooperate to contain chronic viral infection. Science *338*, 1220-1225.

Palmer, E.M., Holbrook, B.C., Arimilli, S., Parks, G.D., and Alexander-Miller, M.A. (2010). IFNgamma-producing, virus-specific CD8+ effector cells acquire the ability to produce IL-10 as a result of entry into the infected lung environment. Virology *404*, 225-230.

Papi, A., and Johnston, S.L. (1999). Respiratory epithelial cell expression of vascular cell adhesion molecule-1 and its up-regulation by rhinovirus infection via NF-kappaB and GATA transcription factors. J Biol Chem *274*, 30041-30051.

Papi, A., Stanciu, L.A., Papadopoulos, N.G., Teran, L.M., Holgate, S.T., and Johnston, S.L. (2000). Rhinovirus infection induces major histocompatibility complex class I and costimulatory molecule upregulation on respiratory epithelial cells. The Journal of infectious diseases *181*, 1780-1784.

Parish, I.A., and Kaech, S.M. (2009). Diversity in CD8(+) T cell differentiation. Current opinion in immunology *21*, 291-297.

Paulsson, K.M., and Wang, P. (2004). Quality control of MHC class I maturation. FASEB J *18*, 31-38.

Pavia, A.T. (2011). Viral infections of the lower respiratory tract: old viruses, new viruses, and the role of diagnosis. Clin Infect Dis *52 Suppl 4*, S284-289.

Pavlin, J.A., Hickey, A.C., Ulbrandt, N., Chan, Y.P., Endy, T.P., Boukhvalova, M.S., Chunsuttiwat, S., Nisalak, A., Libraty, D.H., Green, S.*, et al.* (2008). Human metapneumovirus reinfection among children in Thailand determined by ELISA using purified soluble fusion protein. The Journal of infectious diseases *198*, 836-842.

Pellegrini, M., Calzascia, T., Toe, J.G., Preston, S.P., Lin, A.E., Elford, A.R., Shahinian, A., Lang, P.A., Lang, K.S., Morre, M.*, et al.* (2011). IL-7 engages multiple mechanisms to overcome chronic viral infection and limit organ pathology. Cell *144*, 601-613.

Pham, N.L., Badovinac, V.P., and Harty, J.T. (2009). A default pathway of memory CD8 T cell differentiation after dendritic cell immunization is deflected by encounter with inflammatory cytokines during antigen-driven proliferation. Journal of immunology *183*, 2337-2348.

Phares, T.W., Ramakrishna, C., Parra, G.I., Epstein, A., Chen, L., Atkinson, R., Stohlman, S.A., and Bergmann, C.C. (2009). Target-dependent B7-H1 regulation contributes to clearance of central nervous system infection and dampens morbidity. J Immunol *182*, 5430-5438.

Pipkin, M.E., Sacks, J.A., Cruz-Guilloty, F., Lichtenheld, M.G., Bevan, M.J., and Rao, A. (2010). Interleukin-2 and inflammation induce distinct transcriptional programs that promote the differentiation of effector cytolytic T cells. Immunity *32*, 79-90.

Piskin, I.E., Calik, M., Abuhandan, M., Kolsal, E., Celik, S.K., and Iscan, A. (2013). PD-1 Gene Polymorphism in Children with Subacute Sclerosing Panencephalitis. Neuropediatrics *44*, 187-190.

Prince, G.A., Prieels, J.P., Slaoui, M., and Porter, D.D. (1999). Pulmonary lesions in primary respiratory syncytial virus infection, reinfection, and vaccine-enhanced disease in the cotton rat (Sigmodon hispidus). Lab Invest *79*, 1385-1392.

Quigley, M., Pereyra, F., Nilsson, B., Porichis, F., Fonseca, C., Eichbaum, Q., Julg, B., Jesneck, J.L., Brosnahan, K., Imam, S.*, et al.* (2010). Transcriptional analysis of HIV-specific CD8+ T cells shows that PD-1 inhibits T cell function by upregulating BATF. Nature medicine *16*, 1147-1151.

Rajini, B., Zeng, J., Suvas, P.K., Dech, H.M., and Onami, T.M. (2010). Both systemic and mucosal LCMV immunization generate robust viral-specific IgG in mucosal secretions, but elicit poor LCMV-specific IgA. Viral immunology *23*, 377-384.

Rao, R.R., Li, Q., Odunsi, K., and Shrikant, P.A. (2010). The mTOR kinase determines effector versus memory CD8+ T cell fate by regulating the expression of transcription factors T-bet and Eomesodermin. Immunity *32*, 67-78.

Rebuck, A.S., and Pengelly, L.D. (1973). Development of pulsus paradoxus in the presence of airways obstruction. N Engl J Med *288*, 66-69.

Reynolds, S.D., and Malkinson, A.M. (2010). Clara cell: progenitor for the bronchiolar epithelium. Int J Biochem Cell Biol *42*, 1-4.

Roberts, A.D., and Woodland, D.L. (2004). Cutting edge: effector memory CD8+ T cells play a prominent role in recall responses to secondary viral infection in the lung. J Immunol *172*, 6533-6537.

Rock, M.T., and Crowe, J.E., Jr. (2003). Identification of a novel human leucocyte antigen-A*01-restricted cytotoxic T-lymphocyte epitope in the respiratory syncytial virus fusion protein. Immunology *108*, 474-480.

Rock, M.T., McKinney, B.A., Yoder, S.M., Prudom, C.E., Wright, D.W., and Crowe, J.E., Jr. (2011). Identification of potential human respiratory syncytial virus and metapneumovirus T cell epitopes using computational prediction and MHC binding assays. J Immunol Methods.

Rodenko, B., Toebes, M., Hadrup, S.R., van Esch, W.J., Molenaar, A.M., Schumacher, T.N., and Ovaa, H. (2006). Generation of peptide-MHC class I complexes through UV-mediated ligand exchange. Nat Protoc *1*, 1120-1132.

Rodriguez-Garcia, M., Porichis, F., de Jong, O.G., Levi, K., Diefenbach, T.J., Lifson, J.D., Freeman, G.J., Walker, B.D., Kaufmann, D.E., and Kavanagh, D.G. (2011). Expression of PD-L1 and PD-L2 on human macrophages is up-regulated by HIV-1 and differentially modulated by IL-10. J Leukoc Biol *89*, 507-515.

Rohrlich, P.S., Cardinaud, S., Firat, H., Lamari, M., Briand, P., Escriou, N., and Lemonnier, F.A. (2003a). HLA-B*0702 transgenic, H-2KbDb double-knockout mice: phenotypical and functional characterization in response to influenza virus. International immunology *15*, 765-772.

Rohrlich, P.S., Cardinaud, S., Firat, H., Lamari, M., Briand, P., Escriou, N., and Lemonnier, F.A. (2003b). HLA-B*0702 transgenic, H-2KbDb double-knockout mice: phenotypical and functional characterization in response to influenza virus. Int Immunol *15*, 765-772.

Ruckwardt, T.J., Bonaparte, K.L., Nason, M.C., and Graham, B.S. (2009). Regulatory T cells promote early influx of CD8+ T cells in the lungs of respiratory syncytial virus-infected mice and diminish immunodominance disparities. Journal of virology *83*, 3019-3028.

Rutebemberwa, A., Ray, S.C., Astemborski, J., Levine, J., Liu, L., Dowd, K.A., Clute, S., Wang, C., Korman, A., Sette, A.*, et al.* (2008). High-programmed death-1 levels on hepatitis C virus-specific T cells during acute infection are associated with viral persistence and require preservation of cognate antigen during chronic infection. J Immunol *181*, 8215-8225.

Rutishauser, R.L., Martins, G.A., Kalachikov, S., Chandele, A., Parish, I.A., Meffre, E., Jacob, J., Calame, K., and Kaech, S.M. (2009). Transcriptional repressor Blimp-1 promotes CD8(+) T cell terminal differentiation and represses the acquisition of central memory T cell properties. Immunity *31*, 296-308.

Sad, S., Kagi, D., and Mosmann, T.R. (1996). Perforin and Fas killing by CD8+ T cells limits their cytokine synthesis and proliferation. J Exp Med *184*, 1543-1547.

Sakuishi, K., Apetoh, L., Sullivan, J.M., Blazar, B.R., Kuchroo, V.K., and Anderson, A.C. (2010a). Targeting Tim-3 and PD-1 pathways to reverse T cell exhaustion and restore anti-tumor immunity. The Journal of experimental medicine *207*, 2187-2194.

Sakuishi, K., Apetoh, L., Sullivan, J.M., Blazar, B.R., Kuchroo, V.K., and Anderson, A.C. (2010b). Targeting Tim-3 and PD-1 pathways to reverse T cell exhaustion and restore anti-tumor immunity. J Exp Med *207*, 2187-2194.

Sakuishi, K., Jayaraman, P., Behar, S.M., Anderson, A.C., and Kuchroo, V.K. (2011). Emerging Tim-3 functions in antimicrobial and tumor immunity. Trends Immunol *32*, 345-349.

Salama, A.D., Chitnis, T., Imitola, J., Ansari, M.J., Akiba, H., Tushima, F., Azuma, M., Yagita, H., Sayegh, M.H., and Khoury, S.J. (2003). Critical role of the programmed death-1 (PD-1) pathway in regulation of experimental autoimmune encephalomyelitis. The Journal of experimental medicine *198*, 71-78.

Salmond, R.J., Emery, J., Okkenhaug, K., and Zamoyska, R. (2009). MAPK, phosphatidylinositol 3-kinase, and mammalian target of rapamycin pathways converge at the level of ribosomal protein S6 phosphorylation to control metabolic signaling in CD8 T cells. Journal of immunology *183*, 7388-7397.

Schreiner, B., Mitsdoerffer, M., Kieseier, B.C., Chen, L., Hartung, H.P., Weller, M., and Wiendl, H. (2004). Interferon-beta enhances monocyte and dendritic cell expression of B7-H1 (PD-L1), a strong inhibitor of autologous T-cell activation: relevance for the immune modulatory effect in multiple sclerosis. J Neuroimmunol *155*, 172-182.

Schwartz, R.H. (2003). T cell anergy. Annual review of immunology *21*, 305-334.

Schwarze, J., O'Donnell, D.R., Rohwedder, A., and Openshaw, P.J. (2004). Latency and persistence of respiratory syncytial virus despite T cell immunity. Am J Respir Crit Care Med *169*, 801-805.

Sehrawat, S., Reddy, P.B., Rajasagi, N., Suryawanshi, A., Hirashima, M., and Rouse, B.T. (2010). Galectin-9/TIM-3 interaction regulates virus-specific primary and memory CD8 T cell response. PLoS Pathog *6*, e1000882.

Sharma, S., Sundararajan, A., Suryawanshi, A., Kumar, N., Veiga-Parga, T., Kuchroo, V.K., Thomas, P.G., Sangster, M.Y., and Rouse, B.T. (2011). T cell immunoglobulin and mucin protein-3 (Tim-3)/Galectin-9 interaction regulates influenza A virus-specific humoral and CD8 T-cell responses. Proceedings of the National Academy of Sciences of the United States of America *108*, 19001-19006.

Sharpe, A.H., Wherry, E.J., Ahmed, R., and Freeman, G.J. (2007). The function of programmed cell death 1 and its ligands in regulating autoimmunity and infection. Nature immunology *8*, 239-245.

Sheppard, K.A., Fitz, L.J., Lee, J.M., Benander, C., George, J.A., Wooters, J., Qiu, Y., Jussif, J.M., Carter, L.L., Wood, C.R., and Chaudhary, D. (2004). PD-1 inhibits T-cell receptor induced phosphorylation of the ZAP70/CD3zeta signalosome and downstream signaling to PKCtheta. FEBS Lett *574*, 37-41.

Shin, H., Blackburn, S.D., Intlekofer, A.M., Kao, C., Angelosanto, J.M., Reiner, S.L., and Wherry, E.J. (2009). A role for the transcriptional repressor Blimp-1 in CD8(+) T cell exhaustion during chronic viral infection. Immunity *31*, 309-320.

Shin, H., and Wherry, E.J. (2007). CD8 T cell dysfunction during chronic viral infection. Current opinion in immunology *19*, 408-415.

Skiadopoulos, M.H., Biacchesi, S., Buchholz, U.J., Riggs, J.M., Surman, S.R., Amaro-Carambot, E., McAuliffe, J.M., Elkins, W.R., St Claire, M., Collins, P.L., and Murphy, B.R. (2004). The two major human metapneumovirus genetic lineages are highly related antigenically, and the fusion (F) protein is a major contributor to this antigenic relatedness. Journal of virology *78*, 6927-6937.

Smyth, G.K. (2004). Linear models and empirical bayes methods for assessing differential expression in microarray experiments. Stat Appl Genet Mol Biol *3*, Article3.

Stanciu, L.A., Bellettato, C.M., Laza-Stanca, V., Coyle, A.J., Papi, A., and Johnston, S.L. (2006). Expression of programmed death-1 ligand (PD-L) 1, PD-L2, B7-H3, and inducible costimulator ligand on human respiratory tract epithelial cells and regulation by respiratory syncytial virus and type 1 and 2 cytokines. J Infect Dis *193*, 404-412.

Stokes, K.L., Chi, M.H., Sakamoto, K., Newcomb, D.C., Currier, M.G., Huckabee, M.M., Lee, S., Goleniewska, K., Pretto, C., Williams, J.V.*, et al.* (2011). Differential pathogenesis of respiratory syncytial virus clinical isolates in BALB/c mice. J Virol *85*, 5782-5793.

Sun, J., Cardani, A., Sharma, A.K., Laubach, V.E., Jack, R.S., Muller, W., and Braciale, T.J. (2011a). Autocrine regulation of pulmonary inflammation by effector T-cell derived IL-10 during infection with respiratory syncytial virus. PLoS Pathog *7*, e1002173.

Sun, J., Dodd, H., Moser, E.K., Sharma, R., and Braciale, T.J. (2011b). CD4+ T cell help and innate-derived IL-27 induce Blimp-1-dependent IL-10 production by antiviral CTLs. Nature immunology *12*, 327-334.

Sun, J., Madan, R., Karp, C.L., and Braciale, T.J. (2009). Effector T cells control lung inflammation during acute influenza virus infection by producing IL-10. Nature medicine *15*, 277-284.

Sun, J.C., Lehar, S.M., and Bevan, M.J. (2006). Augmented IL-7 signaling during viral infection drives greater expansion of effector T cells but does not enhance memory. Journal of immunology *177*, 4458-4463.

Surh, C.D., Boyman, O., Purton, J.F., and Sprent, J. (2006). Homeostasis of memory T cells. Immunological reviews *211*, 154-163.

Talay, O., Shen, C.H., Chen, L., and Chen, J. (2009). B7-H1 (PD-L1) on T cells is required for T-cell-mediated conditioning of dendritic cell maturation. Proceedings of the National Academy of Sciences of the United States of America *106*, 2741-2746.

Teague, R.M., Greenberg, P.D., Fowler, C., Huang, M.Z., Tan, X., Morimoto, J., Dossett, M.L., Huseby, E.S., and Ohlen, C. (2008). Peripheral CD8+ T cell tolerance to self-proteins is regulated proximally at the T cell receptor. Immunity *28*, 662-674.

Telcian, A.G., Laza-Stanca, V., Edwards, M.R., Harker, J.A., Wang, H., Bartlett, N.W., Mallia, P., Zdrenghea, M.T., Kebadze, T., Coyle, A.J.*, et al.* (2011). RSV-induced bronchial epithelial cell PD-L1 expression inhibits CD8+ T cell nonspecific antiviral activity. J Infect Dis *203*, 85-94.

Tinoco, R., Alcalde, V., Yang, Y., Sauer, K., and Zuniga, E.I. (2009). Cell-intrinsic transforming growth factor-beta signaling mediates virus-specific CD8+ T cell deletion and viral persistence in vivo. Immunity *31*, 145-157.

Toebes, M., Rodenko, B., Ovaa, H., and Schumacher, T.N. (2009). Generation of peptide MHC class I monomers and multimers through ligand exchange. Curr Protoc Immunol *Chapter 18*, Unit 18 16.

Trautmann, L., Janbazian, L., Chomont, N., Said, E.A., Gimmig, S., Bessette, B., Boulassel, M.R., Delwart, E., Sepulveda, H., Balderas, R.S.*, et al.* (2006). Upregulation of PD-1 expression on HIV-specific CD8+ T cells leads to reversible immune dysfunction. Nat Med *12*, 1198-1202.

Utzschneider, D.T., Legat, A., Fuertes Marraco, S.A., Carrie, L., Luescher, I., Speiser, D.E., and Zehn, D. (2013). T cells maintain an exhausted phenotype after antigen withdrawal and population reexpansion. Nature immunology *14*, 603-610.

Vallbracht, S., Unsold, H., and Ehl, S. (2006). Functional impairment of cytotoxic T cells in the lung airways following respiratory virus infections. Eur J Immunol *36*, 1434-1442.

van de Sandt, C.E., Kreijtz, J.H., and Rimmelzwaan, G.F. (2012). Evasion of influenza A viruses from innate and adaptive immune responses. Viruses *4*, 1438-1476.

van den Hoogen, B.G., de Jong, J.C., Groen, J., Kuiken, T., de Groot, R., Fouchier, R.A., and Osterhaus, A.D. (2001a). A newly discovered human pneumovirus isolated from young children with respiratory tract disease. Nature medicine *7*, 719-724.

van den Hoogen, B.G., de Jong, J.C., Groen, J., Kuiken, T., de Groot, R., Fouchier, R.A., and Osterhaus, A.D. (2001b). A newly discovered human pneumovirus isolated from young children with respiratory tract disease. Nat Med *7*, 719-724.

Velu, V., Kannanganat, S., Ibegbu, C., Chennareddi, L., Villinger, F., Freeman, G.J., Ahmed, R., and Amara, R.R. (2007). Elevated expression levels of inhibitory receptor programmed death 1 on simian immunodeficiency virus-specific CD8 T cells during chronic infection but not after vaccination. J Virol *81*, 5819-5828.

Velu, V., Titanji, K., Zhu, B., Husain, S., Pladevega, A., Lai, L., Vanderford, T.H., Chennareddi, L., Silvestri, G., Freeman, G.J.*, et al.* (2009). Enhancing SIV-specific immunity in vivo by PD-1 blockade. Nature *458*, 206-210.

Virgin, H.W., Wherry, E.J., and Ahmed, R. (2009). Redefining chronic viral infection. Cell *138*, 30-50.

Wang, G., Hu, P., Yang, J., Shen, G., and Wu, X. (2011). The effects of PDL-Ig on collagen-induced arthritis. Rheumatol Int *31*, 513-519.

Wei, F., Zhong, S., Ma, Z., Kong, H., Medvec, A., Ahmed, R., Freeman, G.J., Krogsgaard, M., and Riley, J.L. (2013). Strength of PD-1 signaling differentially affects T-cell effector functions. Proceedings of the National Academy of Sciences of the United States of America.

West, E.E., Youngblood, B., Tan, W.G., Jin, H.T., Araki, K., Alexe, G., Konieczny, B.T., Calpe, S., Freeman, G.J., Terhorst, C.*, et al.* (2011). Tight regulation of memory CD8(+) T cells limits their effectiveness during sustained high viral load. Immunity *35*, 285-298.

Wherry, E.J. (2011). T cell exhaustion. Nature immunology *12*, 492-499.

Wherry, E.J., Barber, D.L., Kaech, S.M., Blattman, J.N., and Ahmed, R. (2004). Antigen-independent memory CD8 T cells do not develop during chronic viral infection. Proceedings of the National Academy of Sciences of the United States of America *101*, 16004-16009.

Wherry, E.J., Blattman, J.N., Murali-Krishna, K., van der Most, R., and Ahmed, R. (2003). Viral persistence alters CD8 T-cell immunodominance and tissue distribution and results in distinct stages of functional impairment. J Virol *77*, 4911-4927.

Wherry, E.J., Ha, S.J., Kaech, S.M., Haining, W.N., Sarkar, S., Kalia, V., Subramaniam, S., Blattman, J.N., Barber, D.L., and Ahmed, R. (2007). Molecular signature of CD8+ T cell exhaustion during chronic viral infection. Immunity *27*, 670-684.

WHO (2012). Influenza (seasonal) fact sheet No. 211. Available online: http://www.who.int/mediacentre/factsheets/fs211/en/index.html (accessed 15 June 2013).

Wiesel, M., and Oxenius, A. (2012). From crucial to negligible: functional CD8(+) T-cell responses and their dependence on CD4(+) T-cell help. European journal of immunology *42*, 1080-1088.

Wilkinson, T.M., Li, C.K., Chui, C.S., Huang, A.K., Perkins, M., Liebner, J.C., Lambkin-Williams, R., Gilbert, A., Oxford, J., Nicholas, B.*, et al.* (2012). Preexisting influenza-specific CD4+ T cells correlate with disease protection against influenza challenge in humans. Nature medicine *18*, 274-280.

Williams, J.V., Harris, P.A., Tollefson, S.J., Halburnt-Rush, L.L., Pingsterhaus, J.M., Edwards, K.M., Wright, P.F., and Crowe, J.E., Jr. (2004). Human metapneumovirus and lower respiratory tract disease in otherwise healthy infants and children. N Engl J Med *350*, 443-450.

Williams, J.V., Tollefson, S.J., Johnson, J.E., and Crowe, J.E., Jr. (2005). The cotton rat (Sigmodon hispidus) is a permissive small animal model of human metapneumovirus infection, pathogenesis, and protective immunity. J Virol *79*, 10944-10951.

Williams, J.V., Wang, C.K., Yang, C.F., Tollefson, S.J., House, F.S., Heck, J.M., Chu, M., Brown, J.B., Lintao, L.D., Quinto, J.D.*, et al.* (2006). The role of human metapneumovirus in upper respiratory tract infections in children: a 20-year experience. J Infect Dis *193*, 387-395.

Wilson, E.B., Kidani, Y., Elsaesser, H., Barnard, J., Raff, L., Karp, C.L., Bensinger, S., and Brooks, D.G. (2012). Emergence of distinct multiarmed immunoregulatory antigen-presenting cells during persistent viral infection. Cell Host Microbe *11*, 481-491.

Wirth, T.C., Xue, H.H., Rai, D., Sabel, J.T., Bair, T., Harty, J.T., and Badovinac, V.P. (2010). Repetitive antigen stimulation induces stepwise transcriptome diversification but preserves a core signature of memory CD8(+) T cell differentiation. Immunity *33*, 128-140.

Workman, C.J., Cauley, L.S., Kim, I.J., Blackman, M.A., Woodland, D.L., and Vignali, D.A. (2004). Lymphocyte activation gene-3 (CD223) regulates the size of the expanding T cell population following antigen activation in vivo. Journal of immunology *172*, 5450-5455.

Wu, Y.L., Liang, J., Zhang, W., Tanaka, Y., and Sugiyama, H. (2012). Immunotherapies: the blockade of inhibitory signals. Int J Biol Sci *8*, 1420-1430.

Wyde, P.R., Chetty, S.N., Jewell, A.M., Schoonover, S.L., and Piedra, P.A. (2005). Development of a cotton rat-human metapneumovirus (hMPV) model for identifying and evaluating potential hMPV antivirals and vaccines. Antiviral Res *66*, 57-66.

Xiao, G., Deng, A., Liu, H., Ge, G., and Liu, X. (2012). Activator protein 1 suppresses antitumor T-cell function via the induction of programmed death 1. Proceedings of the National Academy of Sciences of the United States of America *109*, 15419-15424.

Yamazaki, T., Akiba, H., Iwai, H., Matsuda, H., Aoki, M., Tanno, Y., Shin, T., Tsuchiya, H., Pardoll, D.M., Okumura, K.*, et al.* (2002). Expression of programmed death 1 ligands by murine T cells and APC. J Immunol *169*, 5538-5545.

Yang, C.F., Wang, C.K., Tollefson, S.J., Piyaratna, R., Lintao, L.D., Chu, M., Liem, A., Mark, M., Spaete, R.R., Crowe, J.E., Jr., and Williams, J.V. (2009). Genetic diversity and evolution of human metapneumovirus fusion protein over twenty years. Virology journal *6*, 138.

Yang, Q., Liu, Y., Liu, D., Zhang, Y., and Mu, K. (2011). Association of polymorphisms in the programmed cell death 1 (PD-1) and PD-1 ligand genes with ankylosing spondylitis in a Chinese population. Clin Exp Rheumatol *29*, 13-18.

Yao, S., Wang, S., Zhu, Y., Luo, L., Zhu, G., Flies, S., Xu, H., Ruff, W., Broadwater, M., Choi, I.H.*, et al.* (2009). PD-1 on dendritic cells impedes innate immunity against bacterial infection. Blood *113*, 5811-5818.

Ye, F., Turner, J., and Flano, E. (2012). Contribution of pulmonary KLRG1(high) and KLRG1(low) CD8 T cells to effector and memory responses during influenza virus infection. Journal of immunology *189*, 5206-5211.

Yi, J.S., Du, M., and Zajac, A.J. (2009). A vital role for interleukin-21 in the control of a chronic viral infection. Science *324*, 1572-1576.

Youngblood, B., Oestreich, K.J., Ha, S.J., Duraiswamy, J., Akondy, R.S., West, E.E., Wei, Z., Lu, P., Austin, J.W., Riley, J.L.*, et al.* (2011). Chronic Virus Infection Enforces Demethylation of the Locus that Encodes PD-1 in Antigen-Specific CD8(+) T Cells. Immunity *35*, 400-412.

Youngblood, B., Wherry, E.J., and Ahmed, R. (2012). Acquired transcriptional programming in functional and exhausted virus-specific CD8 T cells. Curr Opin HIV AIDS *7*, 50-57.

Yuen, T.J., Flesch, I.E., Hollett, N.A., Dobson, B.M., Russell, T.A., Fahrer, A.M., and Tscharke, D.C. (2010). Analysis of A47, an immunoprevalent protein of vaccinia virus, leads to a reevaluation of the total antiviral CD8+ T cell response. J Virol *84*, 10220-10229.

Zdrenghea, M.T., and Johnston, S.L. (2012). Role of PD-L1/PD-1 in the immune response to respiratory viral infections. Microbes Infect *14*, 495-499.

Zelinskyy, G., Myers, L., Dietze, K.K., Gibbert, K., Roggendorf, M., Liu, J., Lu, M., Kraft, A.R., Teichgraber, V., Hasenkrug, K.J., and Dittmer, U. (2011). Virus-specific CD8+ T cells upregulate programmed death-1 expression during acute friend retrovirus infection but are highly cytotoxic and control virus replication. J Immunol *187*, 3730-3737.

Zhang, J.Y., Zhang, Z., Wang, X., Fu, J.L., Yao, J., Jiao, Y., Chen, L., Zhang, H., Wei, J., Jin, L.*, et al.* (2007). PD-1 up-regulation is correlated with HIV-specific memory CD8+ T-cell exhaustion in typical progressors but not in long-term nonprogressors. Blood *109*, 4671-4678.

Zhang, N., and Bevan, M.J. (2011). CD8(+) T cells: foot soldiers of the immune system. Immunity *35*, 161-168.

Zhang, Z., Zhang, J.Y., Wherry, E.J., Jin, B., Xu, B., Zou, Z.S., Zhang, S.Y., Li, B.S., Wang, H.F., Wu, H.*, et al.* (2008). Dynamic programmed death 1 expression by virus-specific CD8 T cells correlates with the outcome of acute hepatitis B. Gastroenterology *134*, 1938-1949, 1949 e1931-1933.

Zhou, Q., Munger, M.E., Veenstra, R.G., Weigel, B.J., Hirashima, M., Munn, D.H., Murphy, W.J., Azuma, M., Anderson, A.C., Kuchroo, V.K., and Blazar, B.R. (2011). Coexpression of Tim-3 and PD-1 identifies a CD8+ T-cell exhaustion phenotype in mice with disseminated acute myelogenous leukemia. Blood *117*, 4501-4510.

Zhou, X., Yu, S., Zhao, D.M., Harty, J.T., Badovinac, V.P., and Xue, H.H. (2010). Differentiation and persistence of memory CD8(+) T cells depend on T cell factor 1. Immunity *33*, 229-240.